



**NTNU – Trondheim**  
Norwegian University of  
Science and Technology

# Electromagnetic Interference in Dwnhole Applications

**Tigist Atnafseged Adamu**

Master of Science in Electric Power Engineering

Submission date: July 2012

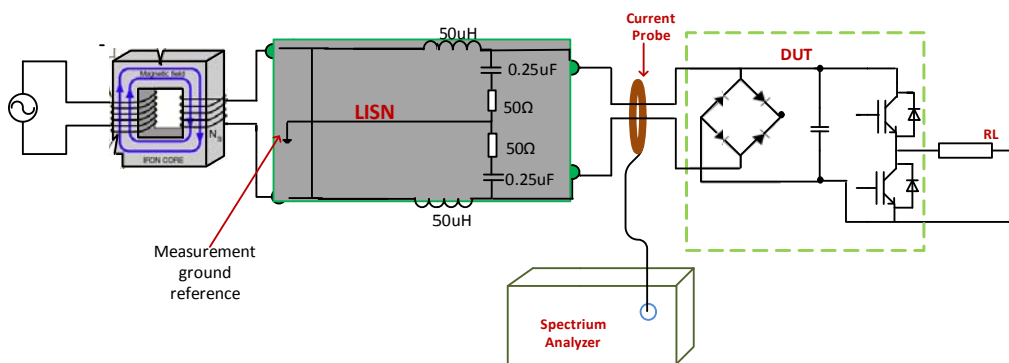
Supervisor: Tore Marvin Undeland, ELKRAFT

Norwegian University of Science and Technology  
Department of Electric Power Engineering





# Electromagnetic Interference in Downhole Applications



**Tigist Atnafseged Adamu**

Master of Science in Electric Power Engineering

Submission date: July 2012

Supervisor: Professor. Tore Marvin Undeland, ELKRAFT

Co-supervisors: Dr. Richard Lund, SmartMotor

Dr. Supratim Basu, Bose Research, Bangalore, India

Dr. Alexey Matveev, SmartMotor

Norwegian University of Science and Technology  
Department of Electric Power Engineering



## **Problem description**

This master thesis work will be a continuation of the specialization project performed in the autumn 2011. The goal of the project was to study and provide an overview of the theoretical background of electromagnetic interference (EMI) and electromagnetic compatibility (EMC) and to see how EMI phenomena can affect various real world environments like drive train system commonly used for many applications, wind power system, tidal turbine, downhole drive in oil well and subsea drive in oil well.

High-frequency switching in modern frequency converters creates EMI, overvoltages, bearing currents and interference in the control system. The concrete application of this project should be to analyse origins and mechanisms of propagation of the noise and choose appropriate means of mitigation for downhole drive.

The main tasks should be:

- Study about EMI/EMC
- Study and compare different filter types by their performance, size, power loss and cost
- Simulation model for different filter topologies, simulation tool will be Matlab
- Conducted EMI laboratory test

Assignment given: 27. January 2012

Supervisor: Professor Tore Marvin Undeland, ELKRAFT



## **Acknowledgement**

First and foremost, I would like to express my deep gratitude to Prof. Tore M. Undeland for giving me this chance to do this thesis and his support during the project work has been very much appreciated.

I am particularly grateful for the assistance all service laboratory staff for their support from the day the project started. Especially the project would not have been possible without the support of Vladimir Klubicka.

My special thanks are extended to the staff of SmartMotor AS for Dr. Alexey Matveev and Dr. Richard Lund dedicated their time so generously enabling me to visit their office offering valuable material resource, showing me the right track and new ideas have been very much appreciated.

I would like to thank also Dr. Supratim Basu and Dr. Salvatore D'Arco their guidance and valuable support and gave me a new knowledge has been very much appreciated.

Tigist Atnafseged Adamu  
Trondheim, Norway  
July 2012





## Summary

Electromagnetic compatibility (EMC) and electromagnetic interference (EMI) are topics which have been of concern to electrical industry for many years. Excessive generation of electromagnetic noise and interference, resulting inadequate EMC, is one potential source of interaction and performance degradation which may reduce operational effectiveness of the devices. Because of this, EMC testing services and regulation imposed by governments have forced product designer to pay close attention electromagnetic interference level of their products.

For improving oil and gas production recovery, from mature fields and for exploitation of deep and ultra-deep offshore reservoirs new downhole technologies are required. Electrification of downhole applications has proven to be very promising and the technologies are designed for deployment in harsh environments.

This master thesis deals with the study of EMI problems for downhole drive train system especially caused by EMI phenomena.

The two aspects of EMI and EMC are studied, the manner in which how EMI can generate and propagate then affect receptor or victim intentionally and unintentionally are discussed. Followed by types of EMI phenomena (voltage dip, electrostatic discharge (ESD), surge, fast transient and rapid voltage change ( $dv/dt$ )) their occurrence and adverse effects of them are studied.

$dv/dt$ , overvoltage and EMI filter types are studied and designed. Comparisons are made by their performance, size, power loss and cost. To verify their performance simulation model are made for downhole drive system to filter  $dv/dt$  and overvoltage at the motor terminals.

After having the theoretical base, practical pre-compliance conducted EMI measurements are made for single phase chopper and three phase inverter.

The influence of EMI such as reverse recovery current of diode, stray or leakage inductance, gate drive resistance, heat sink grounding, duty cycle and switching frequency are investigated on the single phase chopper.

An  $L_f C_f$  harmonic filter is designed and placed between the inverter and motor terminals and differential mode EMI noise is measured in the system.



## Table of content

<b>Problem description</b> .....	<b>i</b>
<b>Acknowledgement</b> .....	<b>ii</b>
<b>Summary</b> .....	<b>iv</b>
<b>List of figures</b> .....	<b>ix</b>
<b>List of tables</b> .....	<b>xiv</b>
<b>Nomenclature</b> .....	<b>xv</b>
<b>1. Introduction</b> .....	<b>1</b>
1.1 Background and Scope .....	1
1.2 Downhole drive systems .....	2
1.3 Task description.....	2
1.4 Structure of the thesis .....	3
<b>2 Introduction to EMI and EMC</b> .....	<b>4</b>
2.1 EMI: its source, coupling path and receptor .....	5
2.1.1 How EMI is generated (source) .....	5
2.1.2 What EMI affects (receptor).....	6
2.1.3 How EMI propagates (coupling path).....	7
2.1.4 Conducted noise coupling mode .....	10
2.2 EMC .....	11
2.2.1 EMC standards, applicability and regulation.....	12
2.2.2 Types of equipment in EMC categories.....	14
2.2.3 CE marking for EMC.....	14
<b>3 Types of EMI phenomena</b> .....	<b>16</b>
3.1 Conducted RF .....	16
3.2 Radiated RF.....	16
3.3 Magnetic fields .....	16
3.4 Voltage dips .....	17
3.5 Electrostatic discharge (ESD).....	17
3.6 Surges and fast transients .....	18
3.7 Interferences caused by inverters that drive electric machines .....	19
3.7.1 Bearing currents .....	19
3.7.2 Noise due to dv/dt.....	21
<b>4 Types of filters</b> .....	<b>22</b>
4.1 Introduction to filters .....	22

4.2	The use of filters .....	22
4.2.1	Protection of motor insulation .....	22
4.2.2	Reduction of motor acoustic noise .....	26
4.2.3	Reduction of high frequency EM noise in the motor cable.....	26
4.3	Filter types .....	27
4.4	Harmonic and overvoltage filter types.....	27
4.4.1	Reactor ( $L_f$ ) filter at the inverter terminal .....	27
4.4.2	$R_fC_f$ filter at the motor terminal .....	28
4.4.3	$R_fL_fC_f$ filter at the inverter terminal .....	32
4.4.4	$R_fL_fC_f$ split RC to +/- DC link filter at the inverter terminal .....	33
4.4.5	$L_fC_f$ filter at the inverter terminal .....	37
4.5	Filters for EMI .....	38
4.5.1	High frequency EM noise filter .....	38
<b>5</b>	<b>Downhole system and EMI consideration .....</b>	<b>40</b>
5.1	Downhole systems .....	41
5.2	EMI consideration .....	42
<b>6</b>	<b>Simulation results .....</b>	<b>45</b>
6.1	System simulation for reactor ( $L_f$ ) filter.....	46
6.2	System simulation for $R_fC_f$ filter .....	50
6.3	System simulation for $R_fL_fC_f$ filter .....	53
6.4	System simulation for $R_fL_fC_f$ split RC to +/- DC link filter .....	56
6.5	System simulation for $L_fC_f$ filter.....	60
6.6	The tool (GUI environment) .....	62
6.7	Summary of comparison filter types .....	64
<b>7</b>	<b>Introduction to conducted EMI measurement.....</b>	<b>67</b>
7.1	Measurement instrumentation.....	68
7.2	Test circuit one .....	72
7.3	Experimental results.....	75
7.3.1	The influence of reverse recovery on EMI .....	75
7.3.2	The influence of stray or leakage inductance on EMI .....	78
7.3.3	The influence of gate drive resistance ( $R_g$ ) on EMI.....	80
7.3.4	The influence of heat sink grounding on EMI.....	82
7.3.5	The influence of duty cycle on EMI .....	83
7.3.6	The influence of switching frequency on EMI .....	84

7.4	Test circuit two .....	85
7.5	The influence of PWM-inverter-fed motors on EMI .....	87
7.5.1	LISN filter between the inverter and motor terminal .....	87
7.5.2	$L_f C_f$ filter between the inverter and motor terminal .....	91
7.6	Test circuit three .....	101
<b>8</b>	<b>Conclusion and further work.....</b>	<b>103</b>
	<b>Bibliography.....</b>	<b>105</b>
	<b>Appendix.....</b>	<b>108</b>
<b>A</b>	<b>Zoomed out view filter results .....</b>	<b>108</b>
A1	When $R_f C_f$ filter at the motor terminals .....	108
A2	When $R_f L_f C_f$ filter at the inverter terminals .....	109
A3	When $R_f L_f C_f$ split RC to +/- DC link filter at the inverter terminals .....	111
A4	CM noise voltage at inverter and motor terminals using $R_f C_f$ filter .....	114
A5	CM noise voltage at inverter and motor terminals using $R_f L_f C_f$ filter.....	115
A6	CM noise voltage at inverter and motor terminals using $R_f L_f C_f$ split filter .....	117
A7	CM noise voltage at inverter and motor terminals using $L_f C_f$ filter.....	118
<b>B</b>	<b>Matlab GUI code.....</b>	<b>119</b>
<b>C</b>	<b>Specification of instruments .....</b>	<b>135</b>
<b>D</b>	<b>Pictures of laboratory test setup.....</b>	<b>137</b>

## List of figures

Figure 1.1 Downhole offshore template .....	1
Figure 1.2 Proposed downhole system topology .....	2
Figure 2.1 Radio frequency range .....	4
Figure 2.2 Three basic elements of any EMI problem.....	5
Figure 2.3 Taxonomy of EMI sources .....	5
Figure 2.4 Taxonomy of EMI receptors .....	7
Figure 2.5 Electrical coupling.....	8
Figure 2.6 Electrical coupling solution.....	8
Figure 2.7 Magnetic coupling .....	9
Figure 2.8 Magnetic coupling solution .....	9
Figure 2.9 Capacitive coupling.....	10
Figure 2.10 Capacitive coupling solution.....	10
Figure 2.11 Conducted interference .....	11
Figure 2.12 CE marking.....	15
Figure 3.1 Voltage dip, brownout and blackout.....	17
Figure 3.2 Circulating current caused by ESD.....	18
Figure 3.3 Charge built up for different material .....	18
Figure 3.4 Typical wave profile of fast transients and surges [14].....	19
Figure 3.5 Showing flow of circulating current .....	20
Figure 3.6 Shaft grounding current .....	21
Figure 3.7 Capacitive discharge current .....	21
Figure 4.1 Converter output voltage (dotted line) and motor terminal voltage (solid line).....	23
Figure 4.2 Cable impedance as a set of RLC circuits.....	23
Figure 4.3 Definition of dv/dt IEC standard.....	25
Figure 4.4 Definition of dv/dt NEMA standard .....	25
Figure 4.5 Limit lines for $V_{peak}$ and rise time $t_r$ [14].....	26
Figure 4.6 Typical output reactor configuration .....	27
Figure 4.7 $R_f C_f$ filter at the motor terminal.....	29
Figure 4.8 Equivalent circuit of the cable with $R_f C_f$ filter .....	29
Figure 4.9 Repeated wave reflection with $R_f C_f$ motor terminal filter where $R_f = Z_c$ .....	30
Figure 4.10 $R_f L_f C_f$ filter at the inverter terminal .....	33
Figure 4.11 $R_f L_f C_f$ split RC to +/- DC link configuration filter .....	33
Figure 4.12 $R_f L_f C_f$ split RC to +/- DC link filter at the inverter terminal filter .....	34
Figure 4.13 Frequency response curve .....	36
Figure 4.14 $L_f C_f$ filter at the inverter terminal .....	37
Figure 4.15 EMI filter .....	38
Figure 4.16 Common mode filter .....	39
Figure 4.17 Differential mode filter.....	39
Figure 5.1 Two possible configurations of the converters .....	40
Figure 5.2 Downhole system topology.....	41
Figure 5.3 Conducted emission from 150 kHz-30 MHz $I > 1000A$ .....	43
Figure 5.4 Conducted emission from 150 kHz-30 MHz $I < 1000A$ .....	44
Figure 5.5 Radiated emission from 30 MHz-1 GHz .....	44

Figure 6.1 System model for reactor ( $L_f$ ) filter using two level inverter .....	46
Figure 6.2 Motor terminal voltage without a filter .....	46
Figure 6.3 Zoomed out view for 100 m $V_{ab}$ inverter vs time with the calculated $L_f$ filter .....	47
Figure 6.4 Zoomed out view for 100 m $V_{ab}$ filter vs time with the calculated $L_f$ filter.....	47
Figure 6.5 Zoomed out view for 100 m $V_{ab}$ motor vs time with the calculated $L_f$ filter .....	47
Figure 6.6 Zoomed out view for 300 m $V_{ab}$ inverter vs time with the calculated $L_f$ filter.....	47
Figure 6.7 Zoomed out view for 300 m $V_{ab}$ filter vs time with the calculated $L_f$ filter.....	48
Figure 6.8 Zoomed out view for 300 m $V_{ab}$ motor vs time with the calculated $L_f$ filter.....	48
Figure 6.9 Zoomed out view for 600 m $V_{ab}$ inverter vs time with the calculated $L_f$ filter .....	48
Figure 6.10 Zoomed out view for 600 m $V_{ab}$ filter vs time with the calculated $L_f$ filter.....	48
Figure 6.11 Zoomed out view for 600 m $V_{ab}$ motor vs time with the calculated $L_f$ filter .....	49
Figure 6.12 THD for inverter, filter and motor when the cable length is 100 m.....	49
Figure 6.13 THD for inverter, filter and motor when the cable length is 300 m.....	49
Figure 6.14 THD for inverter, filter and motor when the cable length is 600 m.....	50
Figure 6.15 System model for $R_f C_f$ filter using two level inverter .....	50
Figure 6.16 Result representation for $R_f C_f$ filter.....	51
Figure 6.17 Zoomed in view for 100 m $V_{ab}$ inverter & motor vs time with calculated $R_f C_f$ filter .....	51
Figure 6.18 Zoomed in view for 300 m $V_{ab}$ inverter & motor vs time with calculated $R_f C_f$ filter .....	52
Figure 6.19 Zoomed in view for 600 m $V_{ab}$ inverter & motor vs time with calculated $R_f C_f$ filter .....	52
Figure 6.20 THD for inverter, filter and motor when the cable length is 100 m.....	52
Figure 6.21 THD for inverter, filter and motor when the cable length is 300 m.....	52
Figure 6.22 THD for inverter, filter and motor when the cable length is 600 m.....	53
Figure 6.23 System model for $R_f L_f C_f$ filter using two level inverter .....	53
Figure 6.24 Result representation for $R_f L_f C_f$ filter .....	54
Figure 6.25 Zoomed in view for 100 m $V_{ab}$ inverter, filer & motor vs time with calculated $R_f L_f C_f$ filter	54
Figure 6.26 Zoomed in view for 300 m $V_{ab}$ inverter, filer & motor vs time with calculated $R_f L_f C_f$ filter	55
Figure 6.27 Zoomed in view for 600 m $V_{ab}$ inverter, filer & motor vs time with calculated $R_f L_f C_f$ filter	55
Figure 6.28 THD for inverter, filter and motor when the cable length is 100 m.....	55
Figure 6.29 THD for inverter, filter and motor when the cable length is 300 m.....	56
Figure 6.30 THD for inverter, filter and motor when the cable length is 600 m.....	56
Figure 6.31 System model for $R_f L_f C_f$ split filter using two level inverter .....	57
Figure 6.32 Zoomed in view for 100 m $V_{ab}$ inverter, filer & motor vs time with calculated $R_f L_f C_f$ split filter .....	58
Figure 6.33 Zoomed in view for 300 m $V_{ab}$ inverter, filer & motor vs time with calculated $R_f L_f C_f$ split filter .....	58
Figure 6.34 Zoomed in view for a 600 m $V_{ab}$ inverter, filer & motor vs time with calculated $R_f L_f C_f$ split .....	58
Figure 6.35 THD for inverter, filter and motor when the cable length is 100 m.....	59
Figure 6.36 THD for inverter, filter and motor when the cable length is 300 m.....	59
Figure 6.37 THD for inverter, filter and motor when the cable length is 600 m.....	59
Figure 6.38 System model for $L_f C_f$ filter using two level inverter.....	60
Figure 6.39 Zoomed out view for 600m $V_{ab}$ inverter vs time with calculated $L_f C_f$ filter.....	60
Figure 6.40 Zoomed out view for 600 m $V_{ab}$ filter vs time with calculated $L_f C_f$ filter .....	61
Figure 6.41 Zoomed out view for 600 m $V_{ab}$ motor vs time with calculated $L_f C_f$ filter.....	61
Figure 6.42 THD for inverter, filter and motor when the cable length is 600 m.....	61

Figure 6.43 GUI user interface tool .....	62
Figure 7.1 Conducted limits [39] .....	68
Figure 7.2 Agilent spectrum analyzer N9000A series CXA signal analyzer.....	69
Figure 7.3 Agilent 41800A series active Probe .....	69
Figure 7.4 Pearson current Probe .....	70
Figure 7.5 Internal circuit of LISN-50-50-4 .....	70
Figure 7.6 LISN impedance versus frequency .....	71
Figure 7.7 FCC-LISN-50-50-4.....	71
Figure 7.8 Typical conducted emission measuring lab set-up .....	72
Figure 7.9 EMI measurement laboratory setup .....	72
Figure 7.10 Line and neutral inserted into the probe for CM noise measurement .....	73
Figure 7.11 Line and neutral inserted into the probe for DM noise measurement.....	74
Figure 7.12 Measurement by using current probe and 50 $\Omega$ receiver point of LISN .....	74
Figure 7.13 Switching properties of a diode voltage and current vs time .....	75
Figure 7.14 Reverse recovery current waveforms .....	76
Figure 7.15 Voltage output vs time for hard and soft recovery current.....	77
Figure 7.16 Current output vs time for hard and soft recovery current.....	77
Figure 7.17 Differential mode noise level for hard and soft recovery current .....	77
Figure 7.18 Stray inductance in the circuit.....	78
Figure 7.19 Front and top view of copper plate strip .....	79
Figure 7.20 Example of copper plate strip .....	79
Figure 7.21 Voltage output vs time with regular cable of wire and with copper strip .....	79
Figure 7.22 Current output vs time with regular cable of wire and with copper strip .....	79
Figure 7.23 DM EMI noise level with regular cable of wire and with copper strip .....	80
Figure 7.24 Turn on and turn off gate resistance.....	80
Figure 7.25 Voltage output vs time for different $R_g$ .....	81
Figure 7.26 Current output vs time for different $R_g$ .....	81
Figure 7.27 DM EMI noise level for different $R_g$ .....	81
Figure 7.28 Parasitic capacitance between the DUT and the heat sink.....	82
Figure 7.29 Voltage output vs time by connecting and disconnecting of the heat sink to ground .....	83
Figure 7.30 Current output vs time by connecting and disconnecting of the heat sink to ground .....	83
Figure 7.31 CM EMI noise level connecting and disconnecting of the heat sink to ground .....	83
Figure 7.32 Voltage output vs time for different duty cycle .....	84
Figure 7.33 Current output vs time for different duty cycle .....	84
Figure 7.34 DM EMI noise level for different duty cycle.....	84
Figure 7.35 Voltage output vs time for different switching frequency.....	85
Figure 7.36 Current output vs time for different switching frequency.....	85
Figure 7.37 DM EMI noise level for different switching frequency.....	85
Figure 7.38 Motor equivalent circuit [51] .....	86
Figure 7.39 Laboratory setup .....	87
Figure 7.40 Low-pass filter .....	88
Figure 7.41 Second order frequency when $\xi=1.76$ .....	89
Figure 7.42 Inverter terminal output voltage.....	89
Figure 7.43 Motor terminal output voltage .....	90
Figure 7.44 Inverter terminal output current .....	90



Figure 7.45 Motor terminal output current .....	90
Figure 7.46 LISN as a filter .....	90
Figure 7.47 $L_f C_f$ filter between the inverter and the motor .....	91
Figure 7.48 $L_f C_f$ filter arrangement .....	91
Figure 7.49 $L_f C_f$ passive filter .....	92
Figure 7.50 Second order frequency response when $\xi = 1$ .....	93
Figure 7.51 Second order frequency response when $\xi = 0.5$ .....	94
Figure 7.52 Inverter terminal output voltage without load .....	95
Figure 7.53 Motor terminal voltage without load .....	95
Figure 7.54 Inverter terminal output current without load .....	95
Figure 7.55 Motor terminal current without load .....	96
Figure 7.56 Reduction of DM noise after adding the filter .....	96
Figure 7.57 Inverter terminal output voltage with load .....	96
Figure 7.58 Motor terminal voltage with load .....	97
Figure 7.59 Inverter terminal output current with load .....	97
Figure 7.60 Motor terminal current with load .....	97
Figure 7.61 Reduction of DM noise after adding the filter .....	97
Figure 7.62 Inverter terminal output voltage without load .....	98
Figure 7.63 Motor terminal voltage without load .....	98
Figure 7.64 Inverter terminal output current without load .....	98
Figure 7.65 Motor terminal current without load .....	98
Figure 7.66 Reduction of DM noise after adding the filter .....	99
Figure 7.67 Inverter output voltage with load .....	99
Figure 7.68 Motor terminal voltage with load .....	99
Figure 7.69 Inverter output current with load .....	100
Figure 7.70 Motor terminal current with load .....	100
Figure 7.71 Reduction of DM noise after adding the filter .....	100
Figure 7.72 Isolated gate driver schematic [54] .....	101
Figure A. 1 Zoomed out view 100 m $V_{ab}$ inverter vs time with calculated $R_f C_f$ filter .....	108
Figure A. 2 Zoomed out view 100 m $V_{ab}$ motor vs time with calculated $R_f C_f$ filter .....	108
Figure A. 3 Zoomed out view 300 m $V_{ab}$ inverter vs time with calculated $R_f C_f$ filter .....	108
Figure A. 4 Zoomed out view 300 m $V_{ab}$ motor vs time with calculated $R_f C_f$ filter .....	108
Figure A. 5 Zoomed out view 600 m $V_{ab}$ inverter vs time with calculated $R_f C_f$ filter .....	109
Figure A. 6 Zoomed out view 600 m $V_{ab}$ motor vs time with calculated $R_f C_f$ filter .....	109
Figure A. 7 Zoomed out view 100 m $V_{ab}$ inverter vs time with calculated $R_f L_f C_f$ filter .....	109
Figure A. 8 Zoomed out view 100 m $V_{ab}$ filter vs time with calculated $R_f L_f C_f$ filter .....	109
Figure A. 9 Zoomed out view 100 m $V_{ab}$ motor vs time with calculated $R_f L_f C_f$ filter .....	110
Figure A. 10 Zoomed out view 300 m $V_{ab}$ inverter vs time with calculated $R_f L_f C_f$ filter .....	110
Figure A. 11 Zoomed out view 300 m $V_{ab}$ filter vs time with calculated $R_f L_f C_f$ filter .....	110
Figure A. 12 Zoomed out view 300 m $V_{ab}$ motor vs time with calculated $R_f L_f C_f$ filter .....	110
Figure A. 13 Zoomed out view 600 m $V_{ab}$ inverter vs time with calculated $R_f L_f C_f$ filter .....	111
Figure A. 14 Zoomed out view 600 m $V_{ab}$ filter vs time with calculated $R_f L_f C_f$ filter .....	111
Figure A. 15 Zoomed out view 600 m $V_{ab}$ motor vs time with calculated $R_f L_f C_f$ filter .....	111

---

Figure A. 16 Zoomed out view 100 m $V_{ab}$ inverter vs time with calculated $R_fL_fC_f$ split filter .....	111
Figure A. 17 Zoomed out view 100m $V_{ab}$ filter vs time with calculated $R_fL_fC_f$ split filter .....	112
Figure A. 18 Zoomed out view 100 m $V_{ab}$ motor vs time with calculated $R_fL_fC_f$ split filter .....	112
Figure A. 19 Zoomed out view 300 m $V_{ab}$ inverter vs time with calculated $R_fL_fC_f$ split filter .....	112
Figure A. 20 Zoomed out view 300 m $V_{ab}$ filter vs time with calculated $R_fL_fC_f$ split filter .....	112
Figure A. 21 Zoomed out view 300 m $V_{ab}$ motor vs time with calculated $R_fL_fC_f$ split filter .....	113
Figure A. 22 Zoomed out view 600 m $V_{ab}$ inverter vs time with calculated $R_fL_fC_f$ split filter .....	113
Figure A. 23 Zoomed out view 600 m $V_{ab}$ filter vs time with calculated $R_fL_fC_f$ split filter .....	113
Figure A. 24 Zoomed out view 600 m $V_{ab}$ motor vs time with calculated $R_fL_fC_f$ split filter .....	113
Figure A. 25 For 100 m $V_{cm}$ inverter and motor terminal vs time with calculated $R_fC_f$ filter.....	114
Figure A. 26 For 300 m $V_{cm}$ inverter and motor terminal vs time with calculated $R_fC_f$ filter.....	114
Figure A. 27 For 600 m $V_{cm}$ inverter and motor terminal vs time with calculated $R_fC_f$ filter .....	115
Figure A. 28 For 100 m $V_{cm}$ inverter and motor terminal vs time with calculated $R_fL_fC_f$ filter.....	115
Figure A. 29 For 300 m $V_{cm}$ inverter and motor terminal vs time with calculated $R_fL_fC_f$ filter.....	116
Figure A. 30 For 600 m $V_{cm}$ inverter and motor terminal vs time with calculated $R_fL_fC_f$ filter.....	116
Figure A. 31 For 100 m $V_{cm}$ inverter and motor terminal vs time with calculated $R_fL_fC_f$ split filter ....	117
Figure A. 32 For 300 m $V_{cm}$ inverter and motor terminal vs time with calculated $R_fL_fC_f$ split filter ....	117
Figure A. 33 For 600 m $V_{cm}$ inverter and motor terminal vs time with calculated $R_fL_fC_f$ split filter ....	118
Figure A. 34 For 600 m $V_{cm}$ inverter and motor terminal vs time with calculated $L_fC_f$ filter.....	118
Figure D.1 EMI measurement laboratory setup for the chopper test circuit .....	137
Figure D.2 EMI measurement lab setup when LISN filter between the inverter & motor terminal...	137
Figure D.3 SiC test drive circuit .....	138

## List of tables

Table 1.1 Downhole drive specification .....	3
Table 2.1 Types of immunity and emission .....	12
Table 2.2 Standards setting institutions .....	13
Table 2.3 Important immunity standards .....	13
Table 2.4 Important emission standards.....	14
Table 4.1 Reflection coefficients for different motor size [20] .....	25
Table 4.2 Filter parameter of $R_f C_f$ .....	32
Table 4.3 Filter parameter of $R_f L_f C_f$ .....	36
Table 5.1 EMI effects to consider for downhole .....	42
Table 5.2 Applicable EMC standards for downhole .....	42
Table 6.1 Cable parameters .....	45
Table 6.2 Cable parameters values in the positive and zero system .....	45
Table 6.3 Calculated filter parameters for 100 m, 300 m and 600 m cable length .....	46
Table 6.4 Calculated filter parameter for 100 m, 300 m and 600 m cable length .....	51
Table 6.5 Calculated filter parameter for 100 m, 300 m and 600 m cable length .....	54
Table 6.6 Calculated filter parameter for 100 m, 300 m and 600 m cable length .....	57
Table 6.7 Calculated filter parameter for 100 m, 300 m and 600 m cable length .....	60
Table 6.8 Summary results of filters when motor fed by 100 m cable length .....	65
Table 6.9 Summary results of filters when motor fed by 300 m cable length .....	65
Table 6.10 Summary results of filters when motor fed by 600 m cable length .....	65
Table 7.1 Data sheet.....	76
Table 7.2 Electrical cable parameter .....	93
Table C. 1 Key Features & specifications for N9000A series CXA signal analyzer .....	135
Table C. 2 Key Features & specifications Agilent 41800A series active Probe .....	135
Table C. 3 Key Features & specifications PEARSON current probe model 110.....	136
Table C. 4 Key Features & Specifications of FCC-LISN-50-50-4 .....	136

## Nomenclature

### List of abbreviations

AC	alternating current
ASD	adjustable speed drive
AWG	American wire gauge
CAN	controller area network
CISPR	International Special Committee on Radio Interference
CE	conducted emission
CEN	European Committee for Standardization
CENELEC	European Committee for Electro technical Standardization
CM	common mode
CMOS	Complementary Metal-Oxide Semiconductor
CISPR	International Special Committee on Radio Interference
DC	direct current
DM	differential mode
DSP	digital signal processing
DUT	device under test
EM	electromagnetic
EMC	electromagnetic compatibility
ESD	electrostatic discharge
EMI	electromagnetic interference
ETSI	European Telecommunications Standards Institute
HF	high frequency
GSM	global system mobile
IEC	International Electro technical Commission
IEEE	Institute of Electrical and Electronics Engineers
IGBT	insulated gate bipolar transistor
LISN	line impedance stabilization network
MOSFET	metal-oxide semiconductor field-effect transistor
MOS	metal-oxide semiconductor
NEMA	National Electrical Manufacturer Association
PCB	printed circuit board
PV	photovoltaic
PWM	pulse width modulation
RF	radio frequency
RFI	radio frequency interference
SiC	Silicon carbide
SMSP	switched mode power supply
THD	total harmonic distortion

### List of Roman symbols

$C_c$	capacitance of the cable
$C_f$	capacitance filter
$C_x$	X capacitor
$C_y$	Y capacitor
$dv/dt$	rapid voltage change

$e_1$	the first incident voltage across the cable
$e_2$	the first reflected voltage across the cable
$e_f$	the total voltage across R <sub>f</sub> -C <sub>f</sub>
$E$	supply voltage
$f$	supply frequency
$f_{co}$	cutoff frequency
$f_{sw}$	switching frequency
$f_1$	fundamental frequency
$G_c$	characteristic conductance of the insulation
$i_1$	the first incident current through the cable
$i_2$	the first reflected current through the cable
$I$	fundamental load current demanded from AC line
$I_g$	gate current
$I_1$	the rms Dc-link voltage
$I_C$	collector current
$l_c$	length of the cable
$I_{cm}$	common mode current
$I_{dm}$	differential mode current
$l_{cr}$	critical cable length
$I_{rr}$	reverse recovery current
$L$	inductance
$L_c$	inductance of the cable
$L_f$	inductance filter
$Q_{rr}$	electric charge
$R_c$	resistance of the cable
$R_f$	resistance filter
$R_g$	gate resistance of the drive
$t_{rr}$	reverse recovery time
$T_{amb}$	downhole ambient temperature
$t_r$	rise time
$V$	supply voltage line to line
$V_{peak}$	peak voltage
$V_{dc}$	DC- link voltage
$V_1$	the voltage induced in the victim
$Z_c$	cable characteristics of impedance
$Z_m$	motor surge impedance
$Z\%$	percent impedance desired

### List of Greek symbols

$L\sigma$	stray inductance
$\lambda$	wavelength
$\omega$	angular frequency
$\xi$	damping coefficient
$\Gamma$	reflection coefficient



## 1. Introduction

### 1.1 Background and Scope

For economically and environmentally acceptable solutions for improving oil and gas recovery from mature fields, and for exploitation of deep and ultra-deep offshore reservoirs new downhole technologies are required.

Before this technology, many of the downhole application processes were mechanically or hydraulically powered, now it is starting to be electrified. Electrification of downhole applications has proven to be very promising and the technologies are designed for deployment in harsh environments characterized by high temperature, pressure and salt water.

Downhole drive systems are used for drilling motors, subsurface valves, progressive cavity pumps and intervention tools. The following figure shows the possibility of downhole template.

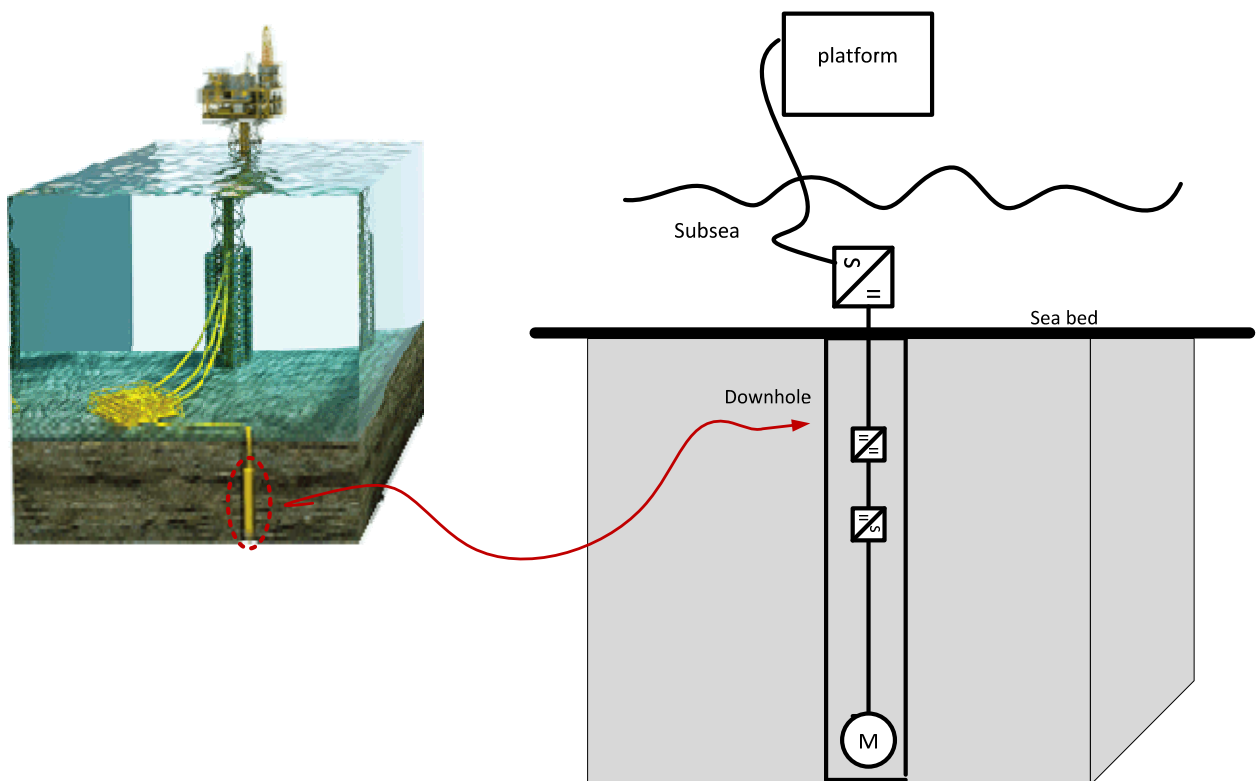


Figure 1.1 Downhole offshore template

Figure 1.1[1] shows promising new technologies of downhole that is designed to extract a higher percentage of oil, the seabed while sealing the hole behind itself, when the job is finished the cable is cut and the tool is left buried.

## 1.2 Downhole drive systems

The use of adjustable speed drive (ASD's) for oil and gas technologies has improved the production level, but due to switching frequency characteristics of converter, it creates high EMI and  $dv/dt$  in power distribution system. Another problem on the ASD's is the cable. The long cable length between the motor and the converter contributes on high-frequency ringing at the motor terminal or a voltage drop when the motor is starting.

Downhole drive systems will have comprehensive key design features of a silicon carbide (SiC) technology with tolerable characteristics of high frequency, high temperature and cooling efforts, including new downhole cables technologies which makes the motor much easier to run and long trouble free operational life in the system.

## 1.3 Task description

The electrification of downhole applications has proven to be very promising, but the high-frequency switching characteristics of frequency converters create high EMI, and this EMI leads to malfunction of devices as well as degrading its performance like creating interference, disturbance in the control system, overvoltage and bearing currents in the motor.

Therefore, the first step should be a comprehensive study needed for EMI, including the motor and long cable impedance mismatch characteristics, since this is the most likely difficult technical problem which degrade not only downhole technologies but also any power drive systems (PDS). Figure 1.2 shows the proposed downhole system topology.

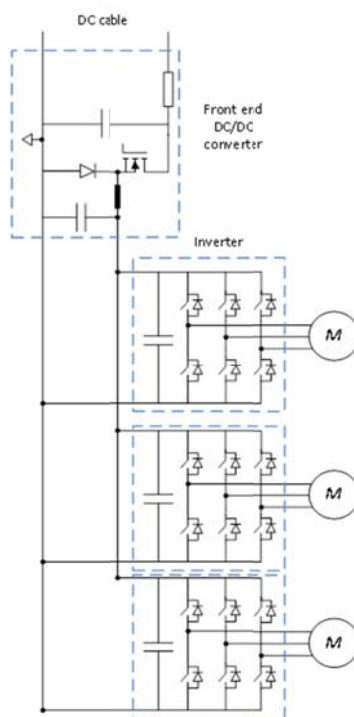


Figure 1.2 Proposed downhole system topology



The required specifications of the drive are given in the following table [2]

Table 1.1 Downhole drive specification

<b>Downhole drive specification</b>	
$V_{DC}$	500 V
$I_1$	5-10 A
$f_{sw}$	15 kHz
$T_{amb}$	175 <sup>0</sup> C
<b>Where</b>	<i>V<sub>DC</sub> is the DC-link voltage</i> <i>I<sub>1</sub> is the rms DC-link voltage</i> <i>f<sub>sw</sub> is the switching frequency</i> <i>T<sub>amb</sub> is the downhole ambient temperature</i>

The objective of this thesis is to analyse the negative aspects of EMI phenomena due to fast switching power devices (high dv/dt and di/dt) used in power electronic converters, and to explore mitigation techniques to reduce EMI noise and dv/dt effectively.

It is quite evident that the high rate switching characteristics of frequency converter will cause a voltage rise and stress the motor insulation; in addition also the long cable that is employed between the frequency converter and the motor is the major source for a large voltage spike and/or a voltage drop at the motor terminals.

Due to these effects, is seen that, it is important to develop the simulation models to design and filter high dv/dt and EMI at motor terminal, and to do practical conducted EMI measurements so that the worst case could be avoidable.

## 1.4 Structure of the thesis

This thesis organized as follows:

- Chapter 1 defines the scope, problem description and structure of the thesis.
- Chapter 2 gives short introduction of theoretical background of EMI and EMC, EMI coupling mechanism form source to victim and EMC standards setting institution, applicability and regulation.
- Chapter 3 reviews EMI phenomena like conducted and radiated emissions from the drive systems, bearing current in the motors, surge and fast transients, voltage dips and dv/dt.
- Chapter 4 introduces different filter types that are used to mitigate overvoltage and EMI at the motor terminal.
- Chapter 5 focused on downhole system study its applicability, system review, level of interference.
- Chapter 6 simulation results for different filter types.
- Chapter 7 laboratory experiments for single phase, three phase inverter and the method that was used to drive SiC.
- Chapter 8 summarizes the conclusions and further work.

## 2 Introduction to EMI and EMC

EMI is electromagnetic disturbance that degrades and demotes the normal operation of electronic devices. This unwanted disturbance in the electrical system is due to electromagnetic radiation and/or electromagnetic conduction [3, 4].

Electromagnetic radiation and electromagnetic conduction are differentiated by the way in which an electromagnetic field propagates. Conducted EMI requires a physical electrical connection between the affected devices and the noise signal source for its transmission while radiated EMI propagates through air or space without the need for any physical electrical connection between the noise signal source and the affected devices [4]. Conducted EMI causes in the affected devices skin effect, proximity effect, hysteresis losses, transients, voltage drops, electromagnetic disturbances, eddy current losses and harmonic distortion.

EMI is often caused by a steady stream of radio frequency (RF) energy propagated by EM (electromagnetic) waves that extends from a few kHz to GHz range. Conducted RFI is most often found in the low frequency range of several kHz to 30 MHz. Radiated RFI is most often found in the frequency range from 30 MHz to 1 GHz. Figure 2.1, represents these showing of radio frequency range.

Examples of such RF sources include energy emanating from man-made sources like computers, refrigerator, compact disc players, phones, TV, shavers, washing machine, electric motors, arc welding machine, air craft navigation and military equipment's. Examples of natural sources are solar flares and lightning.

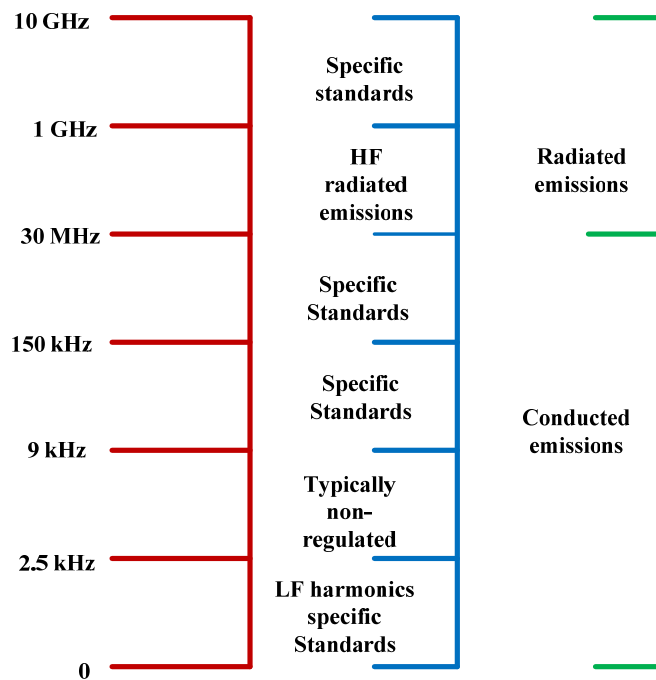


Figure 2.1 Radio frequency range

## 2.1 EMI: its source, coupling path and receptor

The three basic elements of any EMI problems are source, coupling path and receptor.

A **source** is a high frequency component that generates the noise. It is any device that transmits, distributes, processes or utilizes any form of electrical energy, where some aspect of its operation generates conducted or radiated signals that can cause equipment performance degradation to another equipment [4, 5].

A **receptor** is the victim or the exposed device affected by the conducted or radiated electromagnetic energy from the source element [5].

A **coupling path** is the propagation medium that transmits EMI from source to the receptor. Usually below 30 MHz propagation of EMI occurs from source to victim by conducted emission and above 30 MHz by radiated emission. There is no clear transition frequency boundary [5].

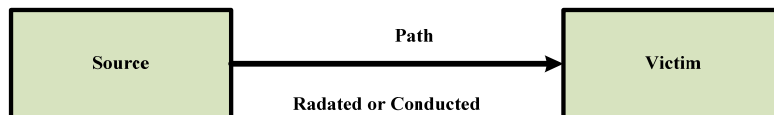


Figure 2.2 Three basic elements of any EMI problem

A brief description is made for source, receptor and coupling path in the next section.

### 2.1.1 How EMI is generated (source)

Figure 2.3 shows taxonomy of the different sources of EMI. Those sources can be divided in two to parts, **man-made** and **natural**. A brief description of each category is given below [5].

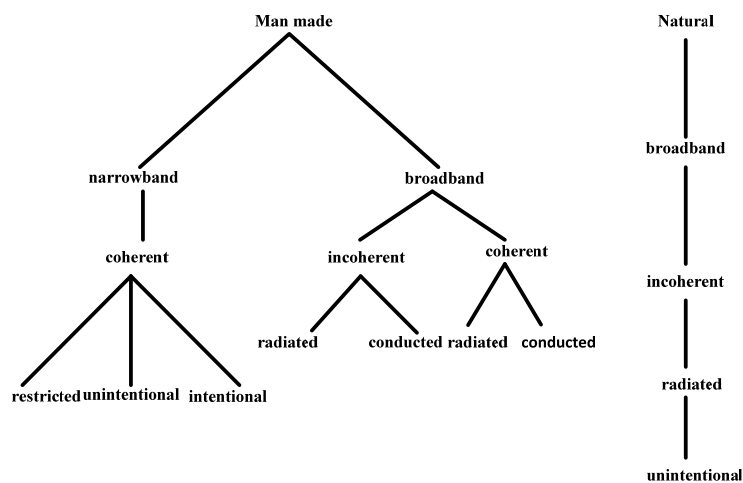


Figure 2.3 Taxonomy of EMI sources

- **Natural EMI sources** - these sources are associated with natural phenomena. They include atmospheric charge/discharge phenomena such as lightning and precipitation static radiation, from the sun and galactic sources such as radio stars, galaxies, and other cosmic sources. As shown in the above diagram, all natural sources are classified as broadband, incoherent, radiated, and unintentional.
- **Man-made EMI sources** - these sources are associated with man-made devices such as power lines, auto ignition and fluorescent lights.
- **Broadband EMI** - electromagnetic conducted and radiated signals whose amplitude vary as a function of frequency and extends over a frequency range greater than the bandwidth of the receptor.
- **Narrowband EMI** - electromagnetic conducted and radiated signals whose amplitude vary as a function of frequency and extends over a frequency range narrower than the bandwidth of the receptor.
- **Coherent broadband signals** - neighbouring components of the signal (in the frequency domain) that has a well-defined amplitude, frequency and phase relationship.
- **Incoherent broadband signals** - neighbouring components of the signal (in the frequency domain) that are random or pseudorandom (bandwidth limited) in phase or amplitude.
- **Conducted EMI** - noise signals transmitted via electrical conduction paths (i.e. wires, ground planes), etc.
- **Radiated EMI** - electric and magnetic fields transmitted through space from source to receptor. As these traverse further, after a distance greater than wavelength ( $\lambda$ )/ $2\pi$ , they combine and propagate as EM fields.
- **Intentional radiating emitters** - emitters whose primary function depends their ability to radiate/receive EM waves. Examples include electronic licensed communication systems. These include communication, navigation and radar systems.
- **Unintentional (incidental) radiating devices**- devices that radiate radio frequencies but is not considered their primary function.
- **Restricted radiating devices**- devices that intentionally use electromagnetic radiation for purposes other than communication or data transfer. Examples include garage door operating systems, wireless microphones, etc.

### 2.1.2 What EMI affects (receptor)

Any EMI situation requires not only an emission source but also a receptor. A receptor is also called a "victim" and consists of any devices when exposed to conducted or radiated electromagnetic energy from emitting sources. Many devices can be emission sources and receptors simultaneously. For example, most communication electronic systems can be emission and receptor sources because they contain transmitters and receivers. Figure 2.4, shows taxonomy of different receptors that are susceptible to EMI. Similar to the emission source taxonomy, receptors can be divided into **natural** and **man-made** receptors. A brief description of each category is given below [5].

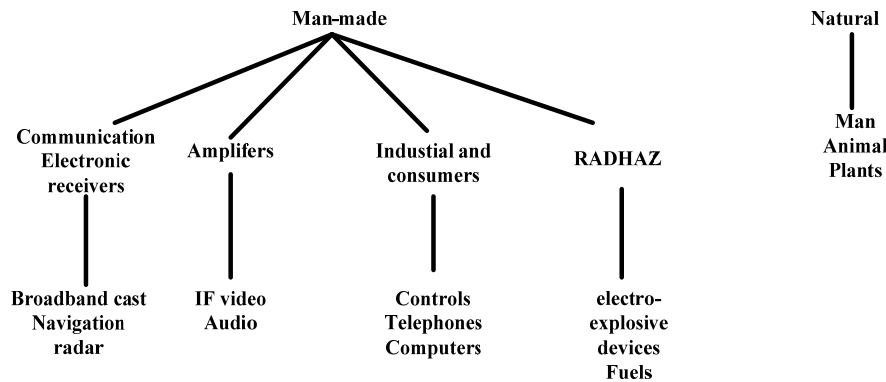


Figure 2.4 Taxonomy of EMI receptors

- **Natural EMI receptors** - natural receptors include humans, animals and plants.
- **Man-made EMI receptors** - man-made receptors can be categorized into 4 categories: communication electronic receivers, amplifiers, industrial, RADHAZ is an acronym for RADiation HAZards, etc.
- **Communication electronic receivers** - these receivers include broadcast receivers, communication receivers, relay communication receivers and radar receivers.
- **Amplifiers** - audio amplifiers.
- **Industrial and consumer receptors** - industrial receptors include digital computers, industrial process controls, electronic test equipment's, biomedical instruments and public address systems. Consumer receptors include radio and TV receivers, electronic musical instruments, climate control systems, etc.
- **RADHAZ** - This category includes radiation hazards to electro-explosive devices and fuels. (RADHAZ) the name given by the U.S. Department of Defense to the program that determines the extent of radiation hazards and methods for controlling them.

### 2.1.3 How EMI propagates (coupling path)

There are different EMI coupling mechanisms for the interference to pass/traverse from source to the receptor. These include common impedance coupling and radiated coupling. These phenomena are described in detail below [4].

#### Common impedance coupling

There are three principal impedance coupling mechanism when the interference passes through from source to victim. These are electrical coupling, magnetic coupling and capacitive coupling. Common impedance coupling routes are those which are due to circuit impedance which the source shares with the victim. The most obvious common impedances are those in which the impedance is physically present, as with a shared conductor (electrical coupling); but the common impedance may also be due to mutual inductive coupling between two current loops (magnetic coupling), or to mutual capacitive coupling between two voltage nodes (capacitive coupling). The following sections describe the common impedance coupling mechanisms and methods to mitigate them [4].

## Electrical coupling

When the source (output of equipment A in Figure 2.5) shares a common path/connection with a victim (input of equipment B), then any current that flows from A's output will pass through this common impedance this in turn will develop a voltage in series with B's input. This common impedance could be even a small length of wire or a PCB track. The voltage developed across an inductor as a result of current flow through, it is given by equation (2.1). The output and input may be part of the same system; in this case there is a spurious feedback path occurs through the common impedance, which can cause oscillations/interference [4].

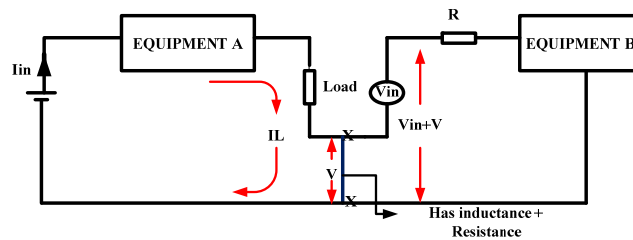


Figure 2.5 Electrical coupling

$$V = -L \frac{dI_L}{dt} \quad 2.1$$

Where

$V$  is the voltage induced on the victim

$L$  is the self-inductance

$I_L$  is the current through the conductor

The solution for this noise is, to separate the connections so that there is no common current path and hence no common impedance between the two circuits (figure 2.6). The only “penalty” for doing this is the need for extra wiring or track to separate the common paths and a clear understanding on how each current loop is generated. This applies to any circuit, which requires common impedance such as power rail connections or grounds. Grounds are the most usual source of common impedance because the ground connection, often not shown on circuit diagrams, is taken for granted [4].

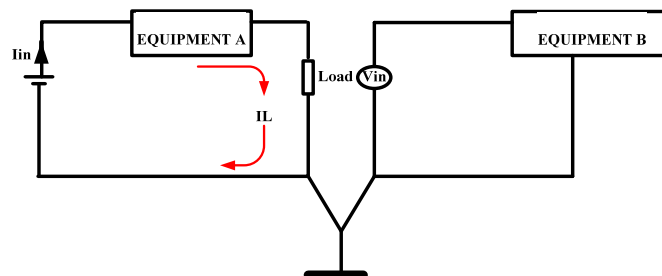


Figure 2.6 Electrical coupling solution

## Magnetic coupling

Alternating current flowing in a conductor creates a magnetic field which will couple with a nearby conductor and induce a voltage in it (Figure 2.7).

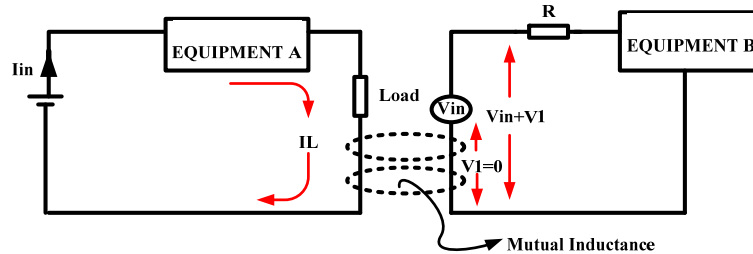


Figure 2.7 Magnetic coupling

The voltage induced in the victim conductor is now given by equation (2.2).

$$V_1 = -M \frac{dI_L}{dt} \quad 2.2$$

Where

$M$  is the mutual inductance

$V_1$  is the voltage induced in the victim

Notice the similarity between this and equation (2.1).  $M$  depends on the areas of the source and victim current loops, their orientation and separation distance and the presence of any magnetic screening.

The solution for this noise is to add shield for the circuit, adding a shield helps reduce the mutual inductance and reduce induced noise. The shield must enclose the protected circuit and seams/apertures should not allow leakages. This is shown in figure 2.8.

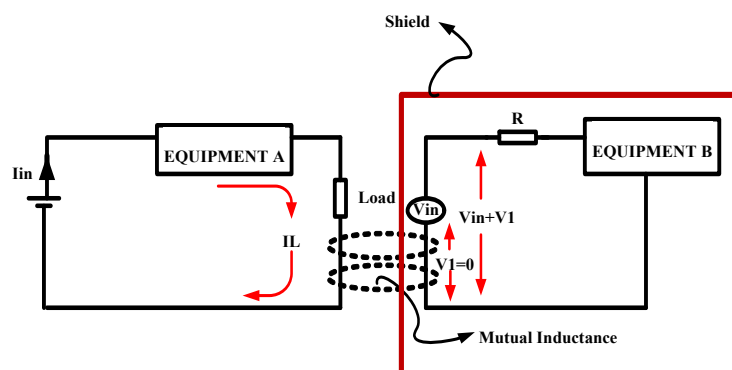


Figure 2.8 Magnetic coupling solution

## Capacitive coupling

Changing voltage on one conductor creates an electric field which may couple with a nearby conductor and induce a voltage on it. This induced voltage is unwanted and it creates a noise in the circuit. The induced voltage becomes:

$$V_1 = R_s C \frac{dv}{dt} \quad 2.3$$

Where  $C$  is the capacitance coupling between the source and the nearby conductor, this is shown in figure 2.9.

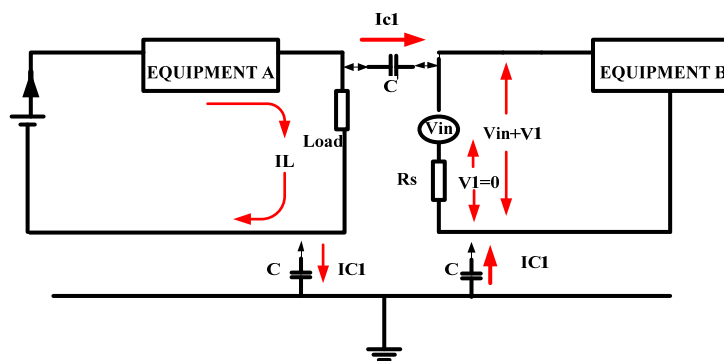


Figure 2.9 Capacitive coupling

The solution for this noise is, to add a shield that is grounded to the noise source, not to the earth. The method is shown in figure 2.10.

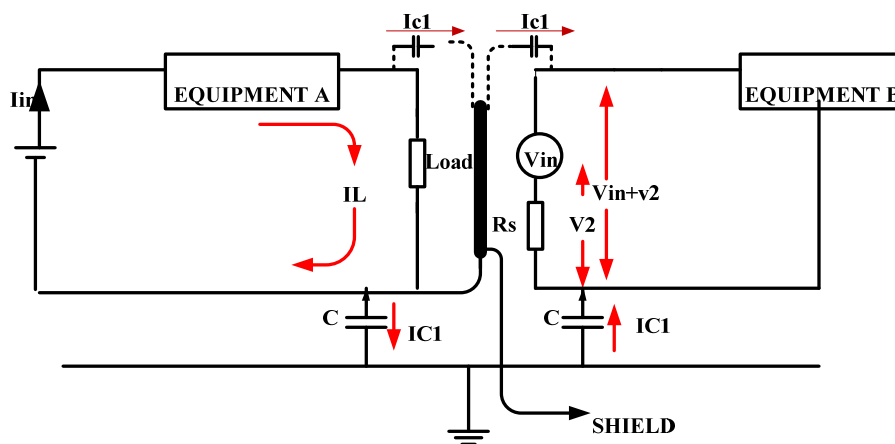


Figure 2.10 Capacitive coupling solution

### 2.1.4 Conducted noise coupling mode

There are two conducted noise coupling mode mechanism when the interference passes through from source to receptor. These are differential mode (DM) and common mode (CM) noise. The following section describes these phenomena [6].



## Differential mode

The DM noise is a current or a voltage measured between the lines of the source that is a line to line voltage or the line current  $I_{dm}$  in figure 2.11.

The transmission of the differential mode noise is through the input line to the utility system and through the DC-side network to the load on the power converter. Moreover, the conducted paths through stray capacitance between components due to magnetic coupling between circuits must be considered [6].

## Common mode

The CM noise is a voltage or a current measured between the power lines and ground, such as  $I_{cm}$  in figure 2.11.

The transmission of the common mode noise is entirely through parasitic capacitor or stray capacitor. These stray capacitances exist between various components. For safety reason, the most power electronic equipment has grounded cabinet the noise appearing on the ground line contributes significantly to the EMI [6].

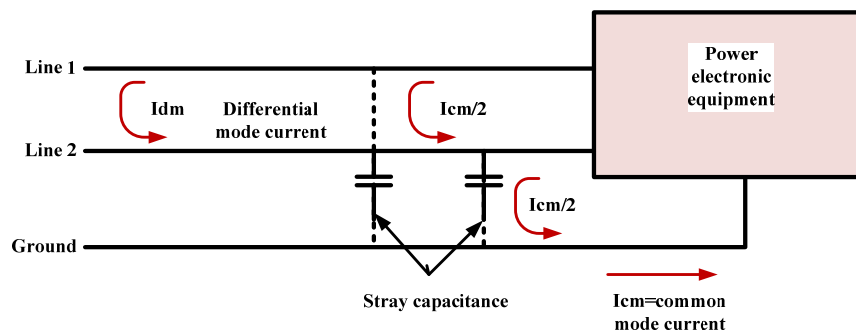


Figure 2.11 Conducted interference

## 2.2 EMC

### Broader definition of EMC

*Electromagnetic compatibility (EMC) refers to the ability of the device, equipment or system to function satisfactory in its electromagnetic environment without introducing intolerable electromagnetic disturbance to anything in that environment [7].* It is important to ensure that the equipment designed has an acceptable degree of electromagnetic compatibility.

Since poor EMC performance of the product can be extremely costly in terms of losing customer's satisfaction and quality, today product designers will test their products to possible noise ambient conditions, before releasing them to the market.

EMC regulation would split in to two areas. These are Emission and Immunity [4].

## Emission

The aim of EMC on the emission side is to ensure the equipment does not disturb other equipment from the high frequency to low frequency noise it generates [4, 8]. The source of high frequency emission is the fast switching of power components such as IGBTs and control electronics including digital circuits. This high frequency emission can propagate by conduction and radiation. The source of low-frequency emission is input current harmonics or radiation from transformers. Various existing EMC regulations set the limit to the level of noise an equipment can generate for a given application environment.

## Immunity

Susceptibility or immunity is the ability of the receptor or victim equipment to operate correctly in the presence of EMI. But susceptibility and immunity are opposite in nature - the device which has high immunity has low susceptibility, and vice versa. The aim of EMC on the immunity side is, the equipment is not disturbed by noise generated by nearby other equipment and is also immune to external high frequency and to low frequency noise that can possibly attack the equipment [4, 8].

**Table 2.1 Types of immunity and emission**

Types of immunity	Types of emission
Mains voltage drop-outs, dips, surges and distortion	Mains distortion, mains voltage and current distortion transients or RFI generated within the equipment and conducted out via the mains supply
Transients and radio frequency interference (RFI) conducted into the equipment via the mains or signal leads	Transients or RFI, generated within the equipment and conducted out via the mains or signal leads
Radiated transient or RFI picked and conducted into the equipment via the mains or signal leads	RFI radiated directly from the equipment circuitry, enclosure and cables
RFI picked up directly by the equipment circuitry	
Electrostatic discharge on the equipment	
Magnetic fields up directly by the equipment circuitry	

### 2.2.1 EMC standards, applicability and regulation

The European standards bodies (CEN, CENELEC and ETSI) define any standard as a document, established by consensus and approved by a recognized body that provides, for common and repeated use, rules, guidelines or characteristics for activities or their results, aimed at the achievement of the optimum degree of order in a given context. Standards are based on consolidated results of science, technology and experience, and aimed at the promotion of optimum community benefits [9].

## EMC standards

The objective of EMC standards is, to provide EM spectrum protection, adequate power quality and to make compatibility between the devices and also have trouble free operation of the system [4]. EMC standards also addresses the countermeasures, such as control regimes, design and measurement, which should be taken in order to prevent emissions from causing any adverse effect in the system.

### Scope and coverage

For any equipment there are two essential requirements [4]:

1. Equipment shall not generate electromagnetic disturbance exceeding a level allowing radio and telecommunications equipment and other apparatus to operate as intended.
2. Equipment shall have an adequate level of intrinsic immunity from electromagnetic disturbance.

Many firms will not be able to assess whether their product is able to meet the two essential requirements and so one has to read the EMC directive to choose and undertake their own technical assessment.

### Standards setting institutions

Table 2.2 Standards setting institutions

DOD	Department of Defense (USA)	Immunity & Emission standards
IEC	International Electro Technical Commission(USA)	Immunity standards
CISPR	International Special Committee on Radio Interference Operating under IEC (USA)	Emission Standards
FCC	Federal Communication Commission (USA)	Emission standards
BSI	British Standard Institution (UK )	Emission standards
VDE	Verband Deutscher Elektrotechniker (Germany)	Emission standards

Table 2.3 Important immunity standards

IEC 61000-4-2	Electrostatic discharge immunity test
IEC 61000-4-3	Radiated radio frequency EM field immunity test
IEC 61000-4-4	Electrical fast transient
IEC 61000-4-5	Surge immunity test
IEC 61000-4-6	Conducted radio frequency EM field immunity test
IEC 61000-4-8	Power frequency magnetic field immunity test
IEC 61000-4-11	Voltage dips, short interruptions and voltage variations immunity test

Table 2.4 Important emission standards

CISPR 11	Industrial, scientific and medical equipment's
CISPR 12	Automobiles
CISPR 13	Audio visual and similar apparatus
CISPR 14	Household and similar electrical appliances
CISPR 15	Electrical lighting and similar equipment's
CISPR 22	Information technology equipment's
FCC Part 15	Radio frequency devices
IEC 61000-3-2	Limits of harmonic current emission (< 16A per phase)

### 2.2.2 Types of equipment in EMC categories

The equipment covered by EMC divided into two categories: apparatus and fixed installations [10].

**Apparatus** - means any finished appliance or combination thereof made commercially available (i.e., placed on the market) as a single functional unit, intended for the end-user, and liable to generate electromagnetic disturbance, or the performance of which is liable to be affected by such disturbance. (For example, an inverter) [8].

- Finished appliance or combination
- Commercially available
- As a single functional unit
- For the end-user

**Fixed installation** - a particular combination of several types of apparatus, equipment and/or components, which are assembled, installed and intended to be used permanently at a predefined location. (For example, a wind turbine or a PV (photovoltaic) installation) [8].

- Particular combination of apparatus and/or other devices
- Assembled, installed and intended to be permanently used at a predefined location
- Includes also large machines and networks

### 2.2.3 CE marking for EMC

Components or sub-assemblies intended for incorporation into an apparatus by the end users need to carry the European CE marking for EMC. This means the equipment meets the requirements of the European EMC directive for the given type of equipment.

Components or sub-assemblies intended for incorporation into an apparatus by another manufacturer or assembler do not need to carry the CE marking for EMC and the complete finished equipment needs to meet the EMC directive. On a similar argument, if all the internal components are individually CE marked it will not make the whole equipment to be eligible for CE marking automatically [8].

Further the products may carry the CE marking for other directives than EMC.

Apparatus and systems must be CE marked. Fixed installations are required to satisfy various parts of the directives, but are not required to be CE marked. Figure 2.12 shows the representation of the CE mark [8].



Figure 2.12 CE marking

### 3 Types of EMI phenomena

As described in Chapter 2, sources for conducted and radiated emissions are mainly noise switching circuits that propagate as differential mode (DM) and common mode (CM) noise. These can cause inference in other nearby equipment.

EMI is caused by conducted and radiated electromagnetic emissions and is often globally called as emission and interference from external disturbances like lightning, surges, electro static discharge etc., is often globally termed as immunity. Some such common phenomena are detailed below.

#### 3.1 Conducted RF

When the RF energy couples to a circuit by induction, it is a case of conducted RF disturbance. Coupling can occur in the input/output cables or a common path. Signal levels as high as  $30 V_{rms}$  are practical and usually are within the frequency range between 150 kHz to 80 MHz that are common in the real world.

The **IEC/EN 61000-4-6** is the international standard that describes methods for testing for immunity to conducted RF. In the standard, various test levels and test methods are described.

#### 3.2 Radiated RF

When the RF energy couples to a circuit by radiation, it is a case of radiated RF disturbance. Coupling can occur directly into the circuit or equipment. Signal levels as high as 30 V/m are practical and usually are within the frequency range between 80 MHz to 2000 MHz that are common in the real world. For example disturbances from GSM phones work between 800 MHz or 1900 MHz are common.

The **IEC/EN 61000-4-3** is the international standard that describes methods for testing for immunity to radiated RF. In the standard, various test levels and test methods are described.

#### 3.3 Magnetic fields

Electric fields are created by differences in voltage: the higher the voltage, the stronger will be the resultant field. Magnetic fields are created when electric current flows: the greater the current, the stronger the magnetic field. An electric field will exist even when there is no current flowing. If current does flow, the strength of the magnetic field will vary with power consumption but the electric field strength will be constant.

Electronic products are often subjected to magnetic fields at AC mains frequencies. These fields are frequently produced in the vicinity of power transformers and can cause problems with video displays and other electronic products having sensitivity to magnetic fields. Continuous field levels up to 30 A/m are practical.

The **IEC/EN 61000-4-8** is the international standard that describes methods for testing for immunity to magnetic fields. In the standard, various test levels and test methods are described.

### 3.4 Voltage dips

Voltage dips, brownouts and blackouts have been forming a serious power quality problem for many years [4, 10]. According to the IEEE 1159, a voltage event is considered a sag or dip when the rms voltage decreases between 0.1 and 0.9 p.u of the nominal voltage for duration between half cycle and one minute. The main causes of voltage dips are faults, induction motor starting, transformer energizing, load switching and frequently tripping of motors, are some common consequences of voltage dip.

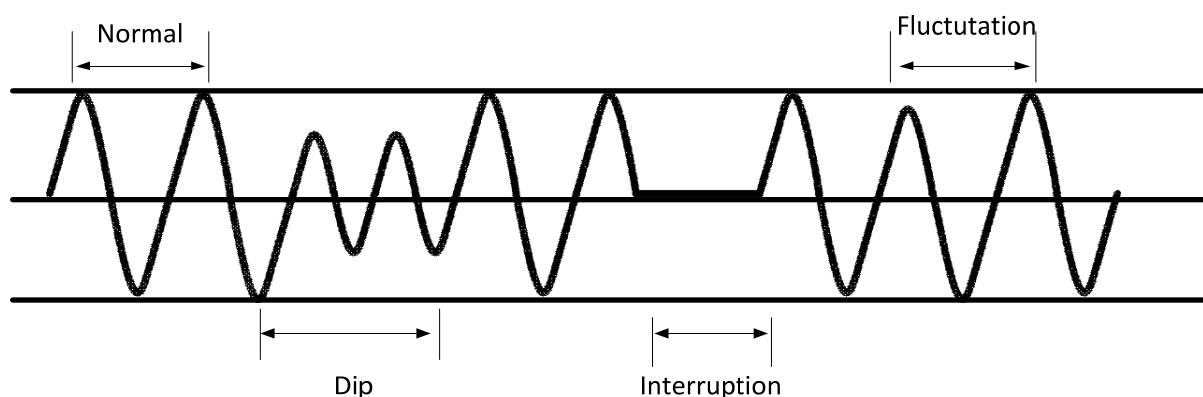


Figure 3.1 Voltage dip, brownout and blackout

Figure 3.1 shows how voltage dips, brownouts and blackouts can be seen with reference to normal line voltage.

The **IEC/EN61000-4-11** is the international standard that describes methods for testing for immunity to voltage dips, brownouts and blackouts. In the standard, various test levels and test methods are described.

### 3.5 Electrostatic discharge (ESD)

ESD is the release of static electricity when two objects are in contact. This occurs when two different materials rub together. One of the materials becomes positively charged; the other becomes negatively charged. The positively-charged material now has an ESD. When that charge comes into contact with the right material, it is transferred and has an ESD event.

The most common causes of ESD are moving people, low humidity, improper grounding, unshielded cables and poor connections. For example the human body can build up static charges that range up to 15 kV. These build-ups can discharge very rapidly into an electrically grounded body or device.

ESD can also destroy most static sensitive electronic devices, MOSFET; CMOS and MOS based circuits. The high voltage pulse from the ESD can burn out the inputs of these devices and circuits. This damage may be full or partial which will eventually cause the device to fail. Further the circulating currents caused by ESD can generate electromagnetic emissions that can interfere with associated circuits. Figure 3.2, shows a representative circuit explaining this phenomenon.

ESD is most likely to occur during the periods of low humidity as low humidity facilitates build-up of charge. If the relative humidity is below 50 %, static charges can accumulate easily. ESD generally does not occur when the humidity is above 50 % [11]. Figure 3.3, shows how humidity influences charge build-up for different materials.

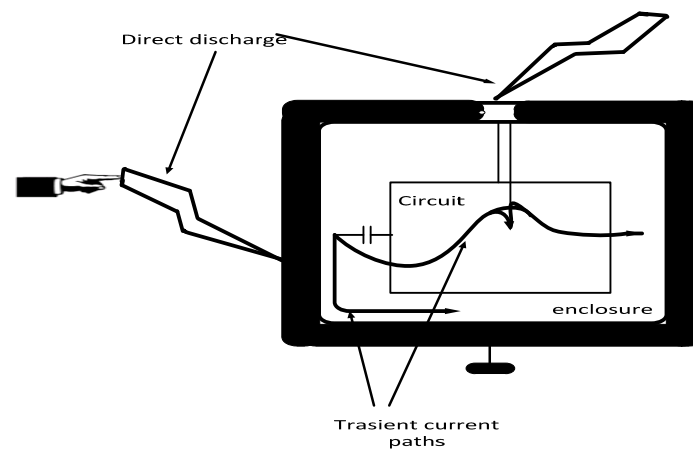


Figure 3.2 Circulating current caused by ESD

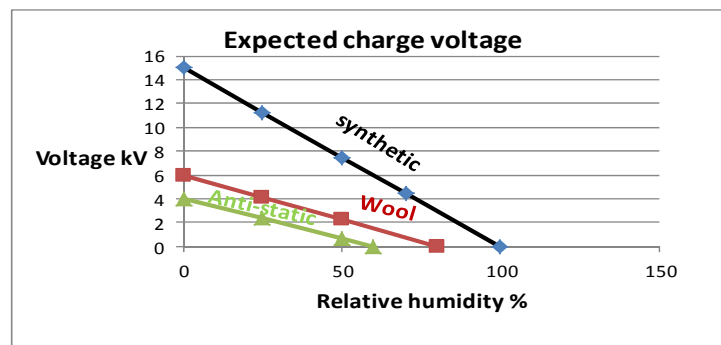


Figure 3.3 Charge built up for different material

The IEC/EN 61000-4-2 is the international standard that describes methods for testing for immunity to ESD. In the standard, various test levels and test methods are described.

### 3.6 Surges and fast transients

Surges and fast transients are forms of electrical disturbance that cause by sudden and brief rise or spike in voltage [12], current and/or magnetic field. They can vary in duration and magnitude, varying from a few hundred volts to several thousand volts.



Lightening causes surge overvoltages. Fast transients are caused by rapid switching of reactive loads and systems faults or power grid switching. A surge or transient is conducted through both power and data lines and can damage or destroy downstream equipment or shorten the lifetime of the equipment. For example, telephone, cable TV and satellite services that enter commercial or residential premises are subject to surge and transient events. The surge can find their way onto these services and subsequently into the building, damaging or destroying connected equipment unless proper protection is used. Surge and fast transient events occur randomly [13-14].

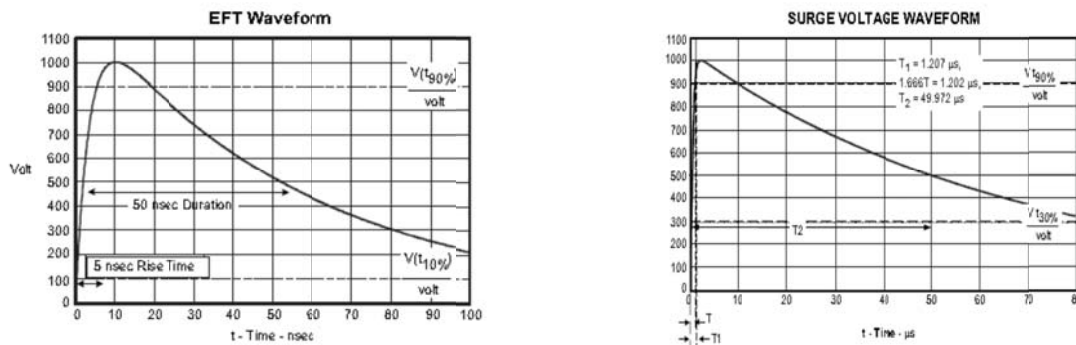


Figure 3.4 Typical wave profile of fast transients and surges [14]

Figure 3.4 [14], shows how fast transients and surges can superimpose on the input AC lines, can be seen with reference to normal line voltage.

The **IEC/EN 61000-4-4** is the international standard that describes methods for testing for immunity to fast transients while the **IEC/EN 61000-4-5** is the international standard that describes methods for testing immunity to surges. In the standard, various test levels and test methods are described.

### 3.7 Interferences caused by inverters that drive electric machines

Inverters generate high frequency PWM voltages to control the motor. While this provides excellent motor control, the high frequency PWM voltages may cause interference in the system. This interference can be radiated emission or high frequency circulating currents in the motor that can damage the motor bearings rapidly and this is often termed as bearing current EMI.

This power inverter use the fast switching power semiconductor switches, such as MOSFET and IGBT as the preferred switching devices as they have many properties, such as higher efficiency, smaller size, lower overall cost and low losses associated with switching device [15]. However, fast switching speeds of new converter/inverter technologies have the potential to cause EMI and high  $dv/dt$ . These phenomena are detailed below.

#### 3.7.1 Bearing currents

Bearing currents are created due to asymmetric phase voltage in the motor. The bearing currents can be either low frequency or high frequency in nature. Low frequency bearing

currents are generated by either by the inherent asymmetry of the machine or asymmetry during transient state. Modern motor design and manufacturing practices have nearly eliminated the low frequency bearing currents induced by the asymmetry of the motor [16].

High frequency bearing current is generated when the motor is connected to an inverter. The source of this bearing current is the voltage that is induced over the bearing due to the high frequency PWM high voltage waveform at the inverter output. This current can be generated in three different ways [16].

1. Circulating current
2. Shaft grounding current
3. Capacitive discharge current

The most important factors that define which mechanism is prominent are the size of the motor and how the motor frame and shaft are grounded.

### 1. Circulating current

In large motors, high frequency voltage is induced between the ends of the motor shaft by the high frequency flux circulating around the stator. This flux is caused by a net asymmetry of capacitive current leaking from the winding into the stator frame along the stator circumference. When this induced voltage between the shaft ends is high enough to overcome the impedance of the bearings' oil film, a current that tries to compensate the net flux in the stator starts to flow in the loop formed by the shaft, the bearings and the stator frame. This current is a circulating type of high frequency bearing current. Figure 3.5 shows a representative circuit explaining this phenomenon [16].

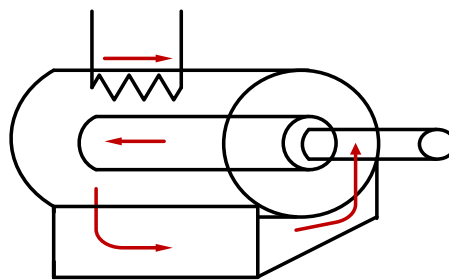


Figure 3.5 Showing flow of circulating current

### 2. Shaft grounding current

The current leaking into the stator frame needs to flow back to the inverter, which is the source of this current. The voltage develops in impedance due to current returning back to the inverter, results in the voltage at the motor frame increasing with respect to the source ground. If the motor shaft is earthed via the driven machinery, the motor frame voltage drives a current to ground over the bearings' oil film. Alternately the motor frame voltage could also drive a current back to the inverter ground over the bearings through the ground connection between the two. Either way this flow of current to the ground over the bearings does damage

the bearings and is called shaft grounding current. Figure 3.6 shows a representative circuit explaining this phenomenon.

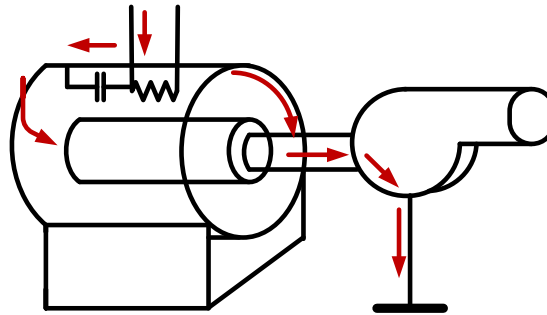


Figure 3.6 Shaft grounding current

### 3. Capacitive discharge current

In small motors, the internal voltage division of the common mode voltage over the internal stray capacitances of the motor may cause shaft voltages high enough to create high frequency bearing current pulses. This can happen if the shaft is not earthed via the driven machinery while the motor frame is earthed. Figure 3.7 shows a representative circuit explaining this phenomenon.

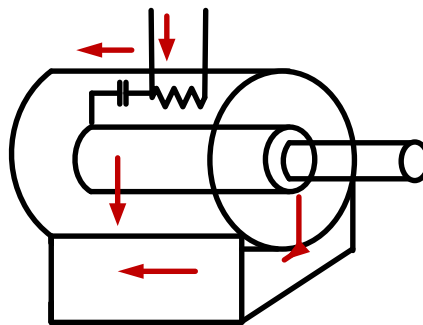


Figure 3.7 Capacitive discharge current

#### 3.7.2 Noise due to $dv/dt$

Power electronic inverters are widely used in many applications including renewable energy generation, industrial equipment/motor drives, aircraft, household appliances and computer power supplies.

While the high switching speeds and advanced PWM schemes significantly improve the performance of the PWM-inverter-fed-motors, the high rate of voltage rise ( $dv/dt$ ) has adverse effects on the motor insulation. The high  $dv/dt$  is caused by the fast switching semiconductor devices in today's inverters. It is possible to lower this  $dv/dt$ , but this will increase the inverter switching losses since the switching losses are proportional with the fall/rise time of the voltage. Further explanation is given in chapter four.

## 4 Types of filters

### 4.1 Introduction to filters

Power electronic converters are widely used in many applications including renewable energy generation, motor drives, aircraft, household appliances and power supplies.

The high-switching frequency characteristics of inverter schemes significantly improve the performance of the PWM-inverter-fed motors but this characteristic has adverse effect on the motor insulation.

If a long cable is employed between the inverter and the motor, damped high frequency ringing at the motor terminals resulting in overvoltage at the motor terminal, which adds more stresses the motor insulation.

Filter is the most common solution to have supply reliability, withstand sudden disturbances, to have voltage quality, to filter harmonics and to mitigate overvoltage from high frequency switching power electronics devices. Filters offer a simpler inexpensive alternative with high benefits. There are different filter types, generally described by their operational characteristics, cost and implementation.

This chapter describes, why and when to use output filters within the systems.

### 4.2 The use of filters

Depending on the filter, some usage of filter can be categorized as follows [17]:

- To reduce harmonics
- To reduce reflected voltages in systems due to long cables and also from fast switching device
- To reduce conducted EMI in the frequency range of 150 kHz - 30 MHz
- Protection of motor insulation
- Reduction of motor acoustic noise

#### 4.2.1 Protection of motor insulation

##### The output voltage

The output voltage of the frequency converter is a series of trapezoidal pulses with a variable width (pulse width modulation) characterized by a pulse rise-time  $t_r$ .

When a transistor in the inverter switches, the voltage across the motor terminal increases by a  $dv/dt$  ratio that depends on [17]:

- The motor cable associated characteristics of its inductance and capacitance, type of cross-section, length, screened or unscreened
- High frequency surge impedance of the motor

Figure 4.1[17] illustrates, the impedance mismatch between the cable characteristic impedance and the motor surge impedance a wave reflection occur, causing a ringing voltage overshoot at the motor output.

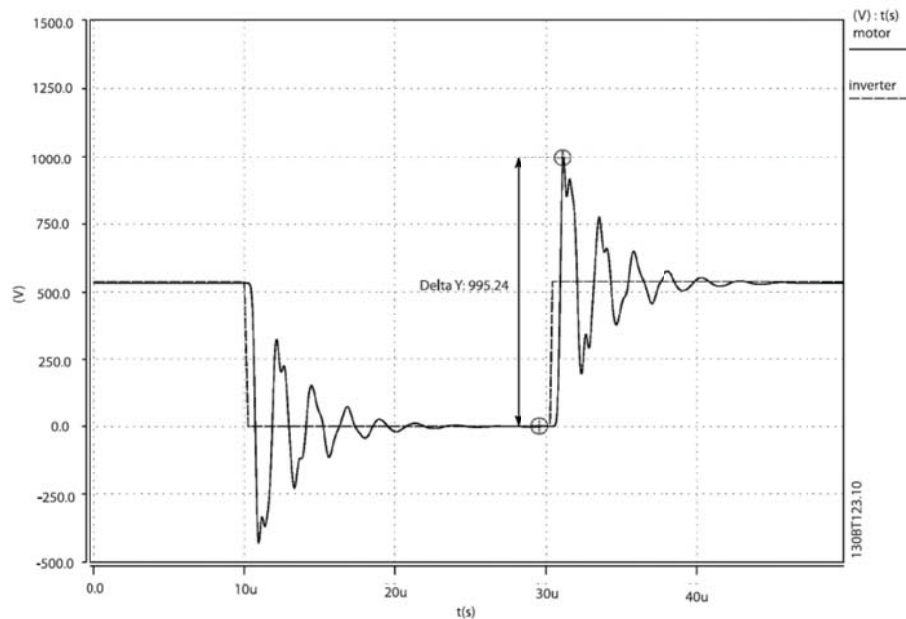


Figure 4.1 Converter output voltage (dotted line) and motor terminal voltage (solid line)

### Cable between the frequency converter and the motor

The following section gives background description about the relation between cable characteristic impedance and motor surge impedance.

A motor connection cable impedance can be represented as a set of RLC circuits with component characteristic inductance  $L_c$ , characteristic capacitance  $C_c$ , characteristic resistance of the conductor  $R_c$  and characteristic conductance of the insulation  $G_c$ . (where  $i$  changes from 1 to  $n$ ), the following figure present such circuit representation of a transmission line of cable impedance [18,19].

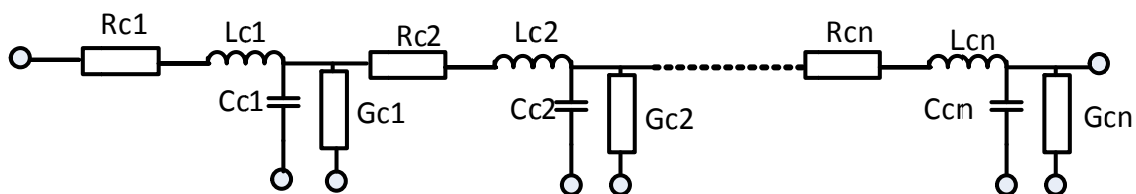


Figure 4.2 Cable impedance as a set of RLC circuits

The relation between cable characteristics ( $Z_c$ ) impedance and motor surge impedance ( $Z_m$ ) given as follows [20].

The pulses travel along the motor cable with a propagation velocity given by:

$$V = \frac{1}{\sqrt{L_c C_c}} \quad 4.1$$

Where

$V$  is the velocity where the pulses travel along the cable

$C_c$  is the cable capacitance

$L_c$  is the cable inductance

A critical cable length  $L_{cr}$  can be defined, representing the cable length where a pulse travels along the motor cable, reflects at the motor terminals and returns to the power converter output after a time interval which equals the rise time  $t_r$ :

$$L_{cr} = \frac{V \cdot t_r}{2} \quad 4.2$$

Because of the impedance mismatch between the cable characteristic impedance ( $Z_c$ ) and the motor surge impedance ( $Z_m$ ) a wave reflection occurs causing a ringing voltage overshoot at the motor terminals [20]:

At cable length above the critical length  $L_{cr}$  the peak voltage at the motor terminals will be:

$$V_{mot} = (1 + \Gamma) V_{inv} \quad 4.3$$

At cable length below the critical length  $L_{cr}$  the maximum peak voltage can be approximated by:

$$V_{mot} = \left( \frac{l_c \cdot \Gamma}{L_{cr}} + 1 \right) \cdot V_{inv} \quad 4.4$$

Where

$V_{mot}$  is the peak voltage at the motor terminal

$V_{inv}$  is the inverter output voltage

$l_c$  is the cable length

$\Gamma$  (gamma) reflection coefficient

Then, depending on the impedance mismatch between the motor cable and motor:

$\Gamma$  can be written:

$$\Gamma = \frac{Z_m - Z_c}{Z_m + Z_c} \quad 4.5$$

$Z_c$  becomes:

$$Z_c = \sqrt{\frac{R_o + j\omega L_c}{G_o + j\omega C_c}} = \sqrt{\frac{L_c}{C_c}} \quad 4.6$$

The motor surge impedance is not well documented and not easy to measure. Some typical values and the resulting reflection coefficients are given in the table below [20].

Table 4.1 resulting reflection coefficients for different motor frame sizes.

Table 4.1 Reflection coefficients for different motor size [20]

Motor Power [kW]	Zm [ $\Omega$ ]	$\Gamma$
< 3.7	2000-5000	0.95
90	800	0.82
355	400	0.6

### dv/dt definition

The following formula illustrates dv/dt definition based on international IEC 61800-8 standards and US National Electrical Manufacturers Association (NEMA).

IEC 61800-8 defines dv/dt,

- The rise-time as the time between 10 % to 90 % of the peak voltage  $V_{peak}$
- $\frac{dV}{dt} = \frac{0.8 \times V_{peak}}{t_r}$

Figure 4.3 shows this phenomenon.

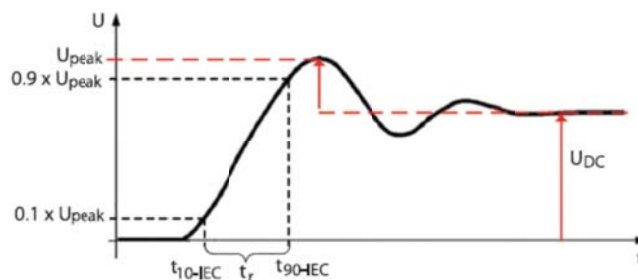


Figure 4.3 Definition of dv/dt IEC standard

NEMA defines dv/dt,

- Rise-time as the time between 10 % and 90 % of the final, settled voltage, that is equal to the dc link voltage  $V_{DC}$
- $\frac{dV}{dt} = \frac{0.8 \times V_{DC}}{t_r}$

Figure 4.4 shows this phenomenon.

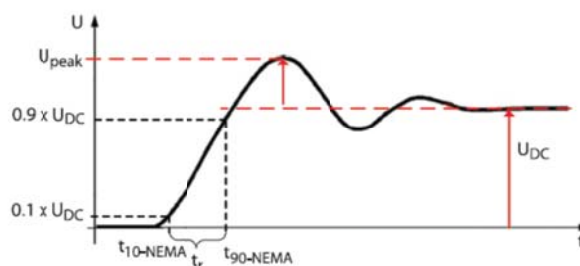


Figure 4.4 Definition of dv/dt NEMA standard

Bearing this in mind, if there is high overshoot and rise time occur at the motor terminal, both IEC and NEMA give their respective standards for withstand characteristics for motor insulation up to 690 V<sub>AC</sub> as illustrated in the following graph, however, if it exceeds above IEC and NEMA standard limit, different filter topology is needed to protect the motor insulation.

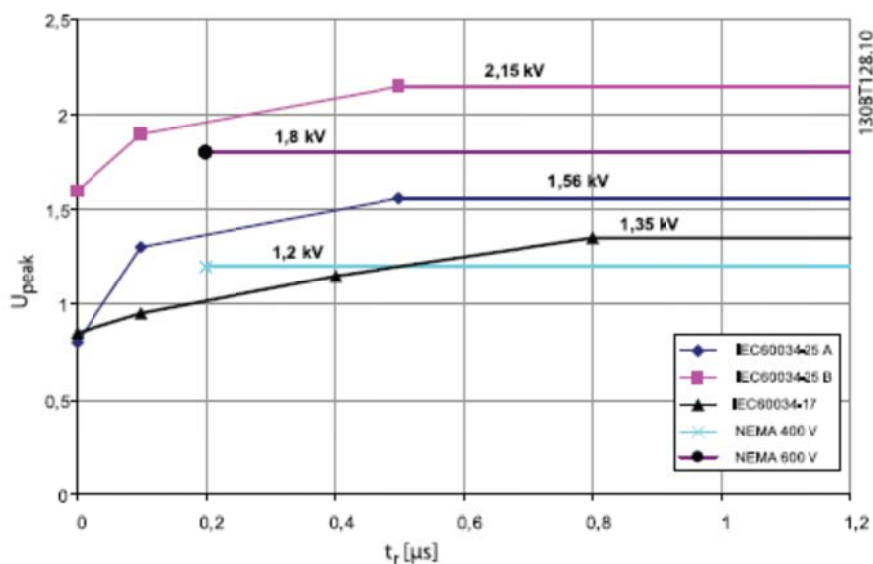


Figure 4.5 Limit lines for  $V_{Peak}$  and rise time  $t_r$  [14]

#### 4.2.2 Reduction of motor acoustic noise

The acoustic noise generated by motors has three main sources [17]:

1. The magnetic noise produced by the motor core
2. The noise produced by the motor bearings
3. The noise produced by the motor ventilation

When a motor is fed by a frequency converter, the high switching frequency character of the converter not only create high  $dv/dt$  at the motor terminal but also high acoustic noise to the motor, this can also eliminated by different filter topologies and/or appropriate design of motor.

#### 4.2.3 Reduction of high frequency EM noise in the motor cable

Even if high frequency switching operations in power electronic devices has improved the dynamic performance of AC motor drives, but most often it creates high levels of conducted EMI. As it is described in chapter two, this high level of conducted EMI generates two types of noise: common mode (CM) and differential mode (DM) noise. The CM noise is the one that flows from the power line to the ground and the DM noise flows between two power lines. Each of these current sources can cause series application problems such as overvoltage in the motor winding and bearing current. However the effect can be reduced by different EMI filter topologies.



### 4.3 Filter types

Several solutions in the literature have been found to mitigate overvoltage and EMI at the motor terminals. Some of them are  $R_fL_fC_f$  filter at the inverter terminal,  $L_fC_f$  at the inverter terminal, output reactor ( $L_f$ ) at the inverter terminal,  $R_fC_f$  at the motor terminal and EMI filter LC. The following section discusses these filter types based on their performance, cost and limitation.

### 4.4 Harmonic and overvoltage filter types

#### 4.4.1 Reactor ( $L_f$ ) filter at the inverter terminal

Inserting an  $L_f$  in series between the inverter and the motor is the simplest filtering techniques method used to reduce harmonics. Harmonics filters are often tuned, and they are designed for operating at harmonics for the fundamental, which make them to be designed similar as the 50/60 Hz technology.

$L_f$  solves problem on either the input or the output of the drive if the reactor is compensated to handle the effects of harmonics. The  $L_f$  acts as a current-limiting device and filters the waveform and attenuates electrical noise and harmonics associated with the inverter/drive output [21,22].

The following figure shows line reactor placed on the output of drive.

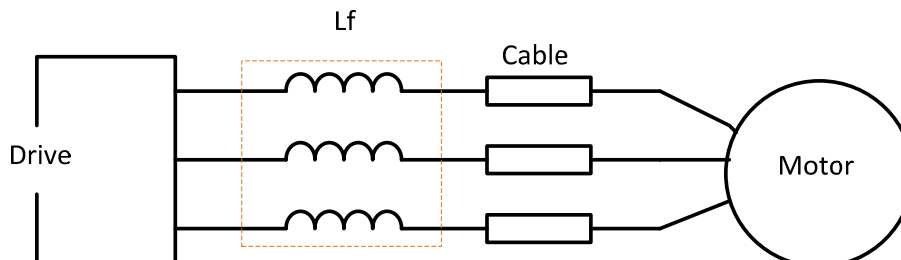


Figure 4.6 Typical output reactor configuration

Among the harmonic compensated line reactors benefits are [21, 22]:

- Compare to other types of filter they are cheaper
- Attenuation of line harmonics
- Extended switching component life (transistors)
- Filtered electrical noise (pulsed distortion and line notching)
- Decrease motor cost by 15 %, increased losses of 0.5-1.0 % (500 kW) [23]

#### Mathematical selection of reactor [21, 22, 24]

##### Procedure

1. Determine the power in kW or MW rating or the current rating of the drive
2. Select the supply voltage

### 3. Determine the percent impedance required for the application

The derived formula for the inductance that provides impedance in % ( $Z$  %) for the application under full load is:

$$L = \frac{Z \cdot V}{I \cdot 2 \cdot \pi \cdot f \cdot \sqrt{3}} \quad 4.7$$

Where

$L$  is the inductance in Henry

$Z$  is the percent impedance desired

$V$  is the supply voltage (line to line)

$I$  is the fundamental load current demanded from AC line (Amperes)

$f$  is the supply frequency (Hz)

$Z$  can be found for three-phase reactor with all three phases energized at rated current, first measure the voltage across any one phase and divide it by the system voltage. Multiply this value by 1.73 ( $\sqrt{3}$ ) and again by 100 for percent impedance.

For example:

If the reactor drop is 10 V with a 600 V line, the percent impedance is  $(10/600) \times 1.73 \times 100$ , or 3 %. Then this called 3 % reactor.

Most line reactor applications typically require an impedance of 2 to 5 %.

#### 4.4.2 $R_f C_f$ filter at the motor terminal

One method to suppress over voltage is, to use the  $R_f C_f$  filter at the motor terminal.  $R_f C_f$  is a  $dv/dt$  filter that consists of resistor and capacitor.  $R_f C_f$  filter helps to reduce high frequency ringing due to the distributed nature of the cable leakage inductance and coupling capacitance ( $L_c$ - $C_c$ ) at the motor terminal [25].

When using this filter, the distributed nature of the cable is minimized because of the filter value is matched with the surge impedance of the motor, and this provide proper level of damping and control the voltage overshoot at the motor terminal.

Figure 4.7 shows the  $R_f C_f$  filter type at the motor terminal.

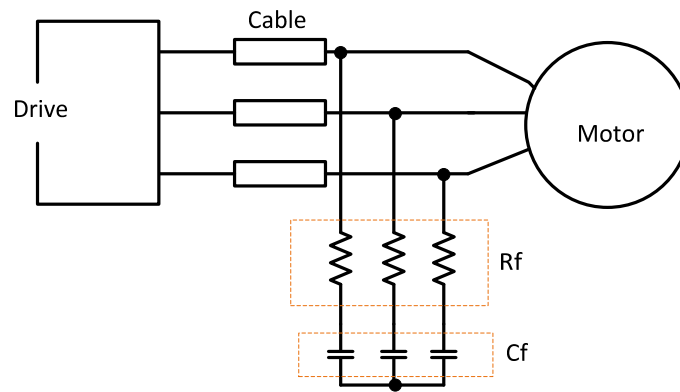


Figure 4.7  $R_f C_f$  filter at the motor terminal

Advantages of  $R_f C_f$  filters are as follows

- Uses simple method to configure
- Limits the overvoltages at the motor terminal
- Decrease motor cost by 1 %, increased losses of 0.5-1.0 % (500 kW) [23]

Disadvantages of  $R_f C_f$  filter is

- High charging currents, may trip the drive

#### Mathematical design of $R_f C_f$ filter at the motor terminal [26]

#### Design procedure to find the value of $R_f C_f$ filter in terms of the cable length

1. To design  $R_f C_f$  filter at the motor terminal, first the equivalent circuit of the cable must be approximated with small but finite lumps of inductances and capacitances and the output of this connected in series with  $R_f C_f$  motor terminal filter, and the following equivalent circuit demonstrates this expression:

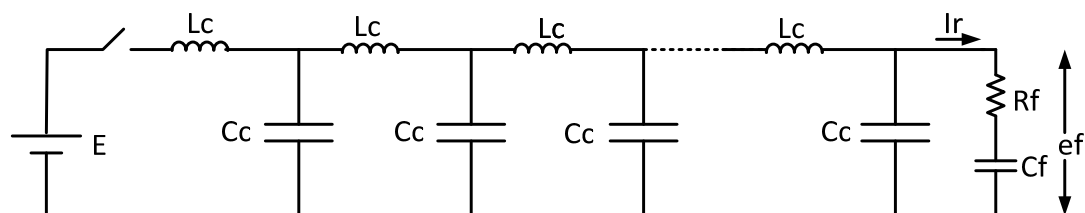


Figure 4.8 Equivalent circuit of the cable with  $R_f C_f$  filter

Where

$E$  is the supply voltage

$C_c$  is the capacitance of cable

$L_c$  is the inductance of cable

$R_f$  is the resistance filter

$C_f$  is the capacitance filter

2. The next step is to formulate how the incident current and voltage will charge the cable parameters (the inductances and the capacitances) one by one, starting from the nearest to the source all the way to the load, resulting in traveling wave phenomenon.

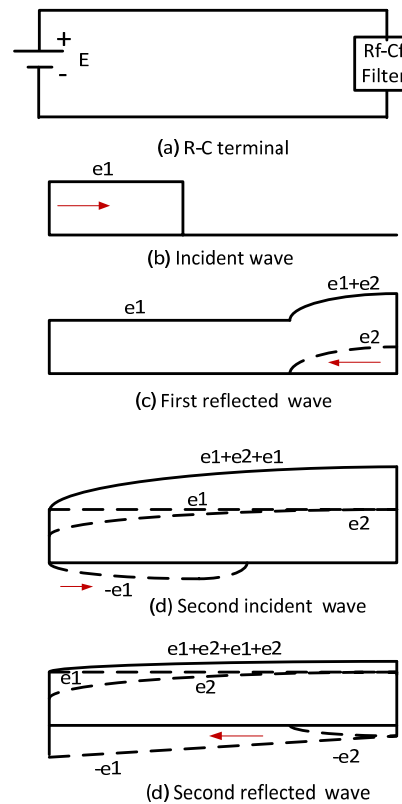


Figure 4.9 Repeated wave reflection with  $R_f C_f$  motor terminal filter where  $R_f = Z_c$

3. The third step is to know the incident wave current and voltage relationship, this is given by:

$$e_1 = Z_c \cdot i_1 \quad 4.8$$

Next the reflected wave given by:

$$e_2 = -Z_c \cdot i_2 \quad 4.9$$

Where

$e_1$  is the first incident voltage across the cable

$i_1$  is the first incident current through the cable

$e_2$  is the first reflected voltage across the cable

$i_2$  is the first reflected current through the cable

4. Once  $e_1$  and  $e_2$  is known, the total voltage and current across the  $R_f C_f$  filter will be:

$$e_f = e_1 + e_2 \quad 4.10$$

And

$$i_f = i_1 + i_2 \quad 4.11$$

Where

$e_f$  is the total voltage across  $R_f C_f$

$i_f$  is the total current through  $R_f C_f$

5. By applying the boundary condition,  $e_f$  can be expressed by :

$$e_f = R_f i_f + \frac{1}{c} \int i_f dt \quad 4.12$$

6. Then substituting equations (4.8 – 4.11) into Equation (4.12) and gives the following expression, which applies at the receiving end of the line:

$$e_1 + e_2 = R_f \left( \frac{e_1}{Z_c} - \frac{e_2}{Z_c} \right) + \frac{1}{c} \int \left( \frac{e_1}{Z_c} - \frac{e_2}{Z_c} \right) dt \quad 4.13$$

7. Solution  $e_2$  in terms of  $e_1$  can be expressed by:

$$(Z_c + R_f)e_2 + \frac{1}{c} \int e_2 dt = (R_f - Z_c)e_1 + \frac{1}{c} \int e_1 dt \quad 4.14$$

Differentiating both sides once, one can get:

$$(Z_c + R_f) \frac{de_2}{dt} + \frac{e_2}{c} = (R_f - Z_c) \frac{de_1}{dt} + \frac{e_1}{C_f} \quad 4.15$$

8. Then assume the shape of the first incident voltage of  $e_1$  is known and it is assumed to be  $e_1 = E$ , in this case, the solution is straightforward and is given by:

$$e_2 = E - K e^{\frac{t}{(Z_c + R_f)C_f}} \quad 4.16$$

9. The next step is to find the value of K, by using the boundary condition at the receiving end, at first the voltage across the capacitor of the cable at time  $t=0$ , during this time the capacitor is short circuited, then the incident voltage only sees the resistive value. Then the reflected voltage  $e_2$  at  $t = 0$  is given by:

$$e_2 = e_1 \frac{R - Z_c}{R + Z_c} \quad 4.17$$

Then substituting equation (4.16) into equation (4.17) with  $t = 0$ , K will be:

$$K = E \frac{2Z_c}{R + Z_c} \quad 4.18$$

The equation for the reflected voltage  $e_2$  will be:

$$e_2 = E - E \frac{2Z_c}{R + Z_c} e^{-\frac{t}{(Z_c + R_f)C_f}} \quad 4.19$$

The solution for the total voltage across the  $R_f C_f$  will be:

$$e_f = e_1 + e_2 = 2E - E \frac{2Z_c}{R + Z_c} e^{-\frac{t}{(Z_c + R_f)C_f}} \quad 4.20$$

10. Then, the next task is to find the value of  $C_f$ , considering the second incident wave arrives at the terminating end (reflected from the inverter), the magnitude of  $e_2$  is less than  $0.2E$ . The design criteria is to limit  $e_2$  such that  $e_2 \leq 0.2E$  when the wave  $e_2$  has traveled twice the length of the cable. This ensures that the motor terminal's voltage is limited to 20 % above the inverter DC-link voltage. Hence, using Equation (4.19),  $e_2$  will be

$$e_2 = E - E \frac{2Z_c}{Z_c + Z_c} e^{-\frac{2t}{(Z_c + Z_c)C_f}} = 0.2E \quad 4.21$$

Collecting common terms, the value will be:

$$E e^{-\frac{2t}{(Z_c + Z_c)C_f}} = 0.8E \quad 4.22$$

Solving for  $C_f$ :

$$C_f = -\frac{2(l_c \sqrt{L_c C_c})}{2Z_o \ln(0.8)} \quad 4.23$$

Using equation 4.6  $C_f$  will be

$$C_f = \frac{l_c C_c}{0.22314} \quad 4.24$$

Where

$l_c$  is the length of the cable

From equation 4.6  $R_f$  is:

$$R_f = Z_c = \sqrt{\frac{L_c}{C_c}}$$

Finally, the value of  $R_f C_f$  filter at the motor terminal is:

**Table 4.2** Filter parameter of  $R_f C_f$

$R_f = Z_c = \sqrt{\frac{L_c}{C_c}}$	$C_f = \frac{l_c C_c}{0.22314}$
--------------------------------------	---------------------------------

#### 4.4.3 $R_f L_f C_f$ filter at the inverter terminal

Another method to suppress overvoltage at the motor terminal is to use  $R_f L_f C_f$  filter at the inverter output.  $R_f L_f C_f$  is a  $dv/dt$  filter that consists of inductor and capacitor in a low pass filter arrangement and their cut off frequency is above the nominal switching frequency of the

drive. This filter also helps to reduce the high frequency ringing of the cable due to distributed nature of the cable leakage inductance and coupling capacitance ( $L_c$ - $C_c$ ) at the motor terminal [27].

The following figure shows when  $R_fL_fC_f$  filter is at the inverter terminal.

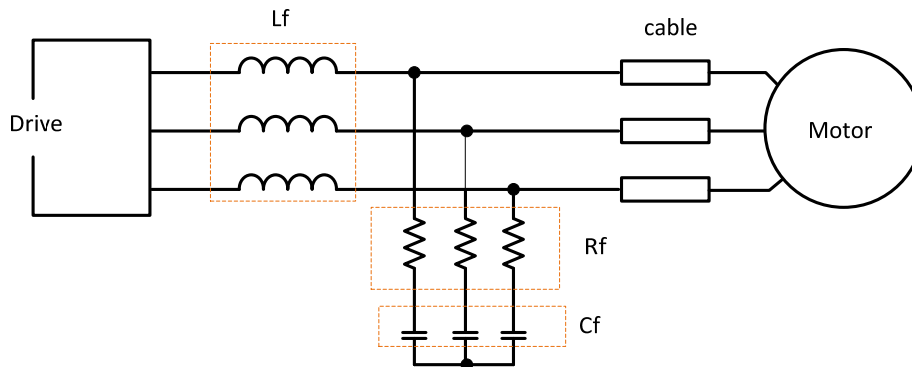


Figure 4.10  $R_fL_fC_f$  filter at the inverter terminal

Advantages of  $R_fC_f$  filters are as follows

- Extended motor life
- Minimized power disturbances
- Limits the overvoltages, reduces the cable charging current
- Decrease motor cost by 35 %, increased losses of 0.5-1.0 % (500 kW)[23]
- Compared to  $L_fC_f$  filters (described in section 4.4.5 ) they are cheaper and smaller

#### 4.4.4 $R_fL_fC_f$ split RC to +/- DC link filter at the inverter terminal

In most cases the ASD DC-link is typically configured by connecting two capacitors in series figure 4.11, and then a midpoint can be accessible between the two capacitors. For example, if the capacitor is built of three or one capacitors in series, there is no midpoint available, and this midpoint is not always available in the commercial ASD's. In such cases, other filter configurations may be considered, for example, a solution proposed by [19,28], helps to avoid direct connection the midpoint then to the DC link as shown in Figure 4.12.

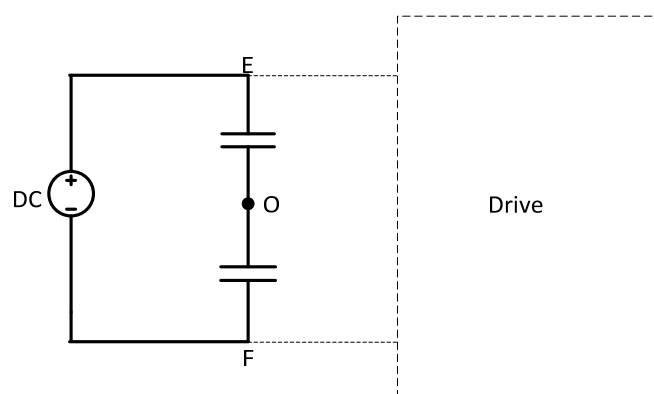


Figure 4.11  $R_fL_fC_f$  split RC to +/- DC link configuration filter

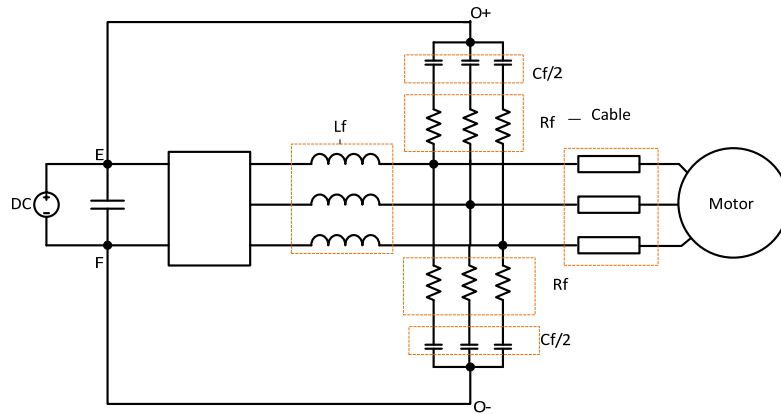


Figure 4.12  $R_f L_f C_f$  split RC to +/- DC link filter at the inverter terminal filter

Advantages of  $R_f L_f C_f$  split filters are as follows

- Reduces both differential and common mode noise at the motor terminals [28]
- Permits the use of long cable between the inverter and motor [28]
- The filter size, losses and cost are low since it addresses both common and differential mode problems [28]

#### Mathematical design for $R_f L_f C_f$ & $R_f L_f C_f$ filter split RC to +/- DC link motor terminal filter [29]

1. The pulses travel along the motor cable with a propagation velocity is given in equation 4.1; that is  $v = \frac{1}{\sqrt{C_c \cdot L_c}}$ :
2. If the length of the cable is  $l_c$ , then the time to travel from one end to the other end of the cable is:

$$t_t = \frac{l_c}{v} = l_c \sqrt{C_c \cdot L_c} \quad 4.25$$

Where

$t_t$  the time to travel one end to another end of the cable

3. Then the travelling time is selected to be at least more than 3 times the travelling time  $t_t$ . To limit the overvoltage at the cable terminals to 20 % the rise time at inverter should be at least equal the critical rise time:

$$t_{cr} = \frac{3 \cdot l_c \cdot r_L}{v \cdot 0.2} = 13.5 \frac{l_c}{v} \quad 4.26$$

Where

$t_{cr}$  is the critical rise time

$r_L$  is the reflection coefficient of the load

$r_L = 0.9$  is selected for small motor, then the cutoff frequency  $f_{co}$  will be:



$$f_{co} = \frac{1}{2 \cdot t_{cr}} = \frac{1}{27 \cdot l_c \cdot \sqrt{L_c \cdot C_c}} \quad 4.27$$

4.  $R_f L_f C_f$  filter is the second order filter and the transfer function can be expressed as:

$$h_f(s) = \frac{1 + R_f \cdot C_f \cdot s}{1 + R_f \cdot C_f \cdot s + L_f \cdot C_f \cdot s^2} \quad 4.28$$

Then the transfer function can be rewritten with the frequency expressed in radians form will be:

$$h_f(s) = \frac{1 + 2 \cdot \xi \cdot \frac{s}{\omega_o}}{1 + 2 \cdot \xi \cdot \frac{s}{\omega_o} + \left(\frac{s}{\omega_o}\right)^2} \quad 4.29$$

$$\xi = \frac{R_f}{2} \sqrt{\frac{C_f}{L_f}}, \text{ damping coefficient} \quad 4.30$$

$$\omega_o = \frac{1}{\sqrt{L_f C_f}}, \text{ undamped natural frequency}$$

5. Then the cut off angular frequency  $\omega_{co}$  is the frequency at which the magnitude of the transfer function becomes  $\frac{1}{\sqrt{2}}$ . From equation 4.29 the cut off frequency will be:

$$\frac{1}{2} = \frac{1 + \left(2 \cdot \xi \cdot \frac{\omega_{co}}{\omega_o}\right)^2}{\left(1 - \left(\frac{\omega_{co}}{\omega_o}\right)^2\right)^2 + \left(2 \cdot \xi \cdot \frac{\omega_{co}}{\omega_o}\right)^2} \quad 4.31$$

6. Finally rearranging the above equation, the cut off frequency can expressed as:

$$\omega_{co} = \frac{1}{\sqrt{C_f \cdot L_f}} \cdot \sqrt{1 + 2 \cdot \xi^2 + \sqrt{(1 + 2 \cdot \xi^2)^2 + 1}} \quad 4.32$$

$$f_{co} = \frac{1}{2 \cdot \pi \sqrt{C_f \cdot L_f}} \cdot \sqrt{1 + 2 \cdot \xi^2 + \sqrt{(1 + 2 \cdot \xi^2)^2 + 1}}$$

For this derivation the dv/dt filter is designed based on the conditions of:

- The cut off frequency( $f_{co}$ ) far below the resonance frequency( $f_c$ )
- $R_f = Z_c/2$
- Selecting over damped filter response  $\xi = 2$

*Note that, in the latter case (chapter six), to make the equation more flexible, the GUI Matlab user interface used to help the user to select damping coefficient as he/she wants.*

From equation 4.6, the filter resistance is taken half of the cable impedance that is:

$$R_f = \frac{Z_c}{2} = \frac{1}{2} \sqrt{\frac{L_c}{C_c}} \quad 4.33$$

The cut off frequency when  $\xi = 2$ :

$$\omega_{co} = \frac{\sqrt{18}}{\sqrt{C_f \cdot L_f}} \quad 4.34$$

Selecting over damped filter response  $\xi = 2$ , the filter capacitance and inductance will be:

$$\xi = \frac{R_f}{2} \sqrt{\frac{C_f}{L_f}} = 2, \text{ or} \quad 4.35$$

$$L_f = C_f \left(\frac{R_f}{4}\right)^2$$

Then, the capacitance filter can be calculated by combining equations 4.34 and 4.35:

$$C_f = \frac{2\sqrt{18}}{\pi \cdot R_f \cdot f_{co}} \quad 4.36$$

Where,

$R_f$  is the resistance filter

$L_f$  is the inductance filter

$C_f$  is the capacitance filter

The summarized final filter values are shown in the following table:

Table 4.3 Filter parameter of  $R_f, L_f, C_f$

$R_f = \frac{Z_c}{2} = \frac{1}{2} \sqrt{\frac{L_c}{C_c}} [\Omega]$	$f_{co} = \frac{1}{27 \cdot L_c \cdot \sqrt{L_c \cdot C_c}} [\text{KHz}]$	$C_f = \frac{2\sqrt{18}}{\pi \cdot R_f \cdot f_{co}} [\mu\text{F}]$	$L_f = C_f \left(\frac{R_f}{4}\right)^2 [\text{mH}]$
---	---	---	--

*For  $R_f, L_f, C_f$  split RC to +/- dc link filter type, the capacitor filter will be half of the original value.*

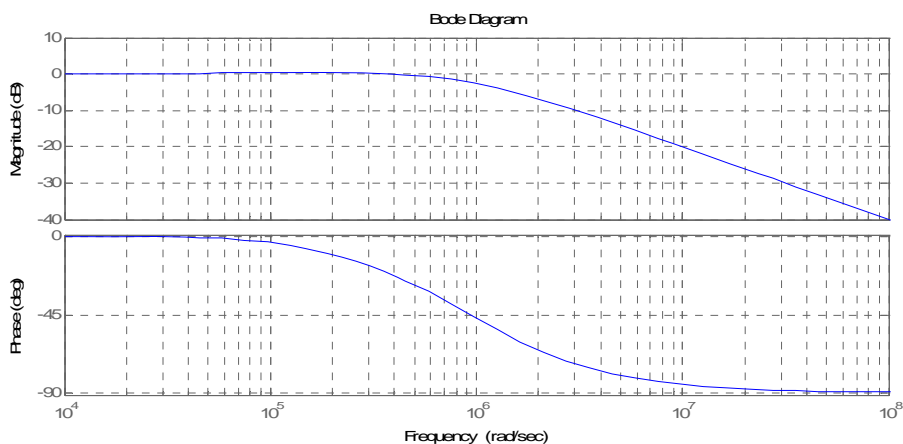


Figure 4.13 Frequency response curve

#### 4.4.5 $L_f C_f$ filter at the inverter terminal

$L_f C_f$  filter is used to mitigate overvoltage at the motor terminal, and the corresponding topology is shown in Figure 4.14. Using this filter,  $V_{out}$  shows a nearly sinusoidal waveform and contains mainly the fundamental frequency of  $V_{in}$ .

This filter is often designed with a cutoff frequency significantly below the switching frequency, and above the output fundamental frequency to avoid resonance with the load. The resonance frequency of the  $L_f C_f$  filter will be chosen between the fundamental frequency and the pulse frequency [20].

$$f_1 < f_{co} < f_{sw} \quad 4.37$$

Where

$f_1$  is the fundamental frequency

$f_{co}$  is the cutoff frequency

$f_{sw}$  is the switching frequency

With the  $L_f C_f$  filter, all negative aspects described earlier (in section 4.2) can be improved significantly; especially the motor losses and the acoustic motor noise can only be improved by  $L_f C_f$  filter.

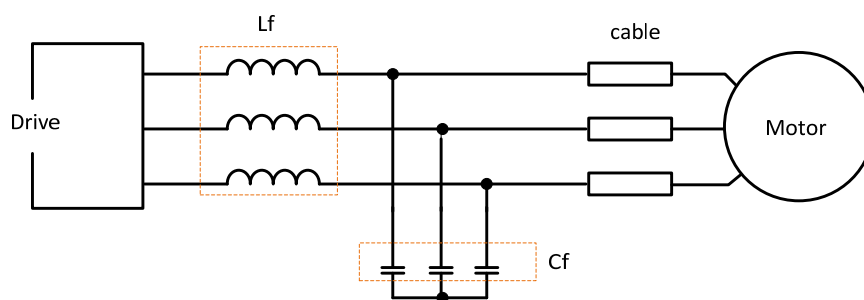


Figure 4.14  $L_f C_f$  filter at the inverter terminal

Advantages of  $L_f C_f$  filters are as follows

- Limits overvoltage at the motor terminal, reduces the cable charging current, reduces motor noise and motor losses
- Decreased motor cost by >50 %, increased losses of 1-3 % (500 kW) [23]
- Minimized power disturbances
- Extended motor life

Disadvantages of  $L_f C_f$  filters

- They are expensive and bigger

## 4.5 Filters for EMI

### 4.5.1 High frequency EM noise filter

For reduction of conducted EMI in the frequency range from 150 kHz - 30 MHz. EMI filter is needed. EMI filter comprise of only basic L and C components and are connected in various combinations for providing best noise attenuation. The major filter configurations are Pi, LC, CL, T, Delta and Wye. EMI filter divided into two parts. EMI filters that attenuate DM noise are called DM filter and those that attenuate CM noise are called CM filter.

#### A typical mains filter

A typical main filter (Figure 4.15) includes components to block both CM and DM noise.

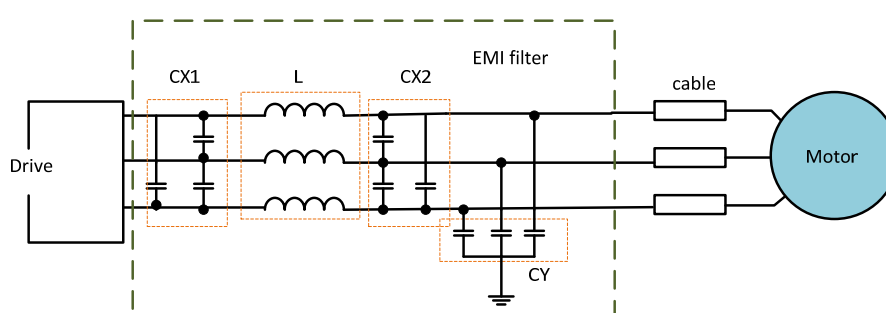


Figure 4.15 EMI filter

To suppress EMI, a typical filter will include CM inductors, DM inductors and X and Y capacitors. The Y capacitors and the CM inductors contribute to attenuate the CM noise. The inductors become high impedances to the high frequency noise and either reflects or absorbs the noise while the capacitors become low impedance paths to ground and redirect the noise away from the main line. CM inductors are wound with two windings of equal numbers of turns. The windings are placed on the core so that the line currents in each winding create fluxes that are equal in magnitude but opposite in phase. These two fluxes "cancel" each other, thus leaving the core in an unbiased state. The DM inductor has only one winding, requiring the core to support the entire line current without saturating. Herein lays the great difference between CM and DM inductors. To prevent saturation, the DM inductor must be made with a core that has a low effective permeability (gapped ferrites or powder cores). And To reduce the stray C, sometimes only one layer can be used. The CM inductor, however, can use a high permeability material and obtain a very high inductance on a relatively small core [4, 30].

#### Common mode filter

CM noise can be suppressed using a standard LC filter which act as high frequency shunts for the CM noise to ground by Y-capacitors. The CM filter is often connected between the power lines (line and neutral) carrying the converter's input current. Care needs to be taken during the design of the CM inductor such that it does not get saturated due to this current flow. This is achieved by having both the inductor windings wound on the same magnetic core and

connecting them in the circuit in such a way that magnetization provided by one coil is balanced by the magnetization provided by the other coil, requiring that both inductors have same number of turns and wound on the same direction on the core. Thus the net flux excursion in the core is almost zero [30, 31].

Since the CM noise is filtered only by  $L$  and  $CY$ , the transformation of figure 4.15 becomes as shown in the following figure.

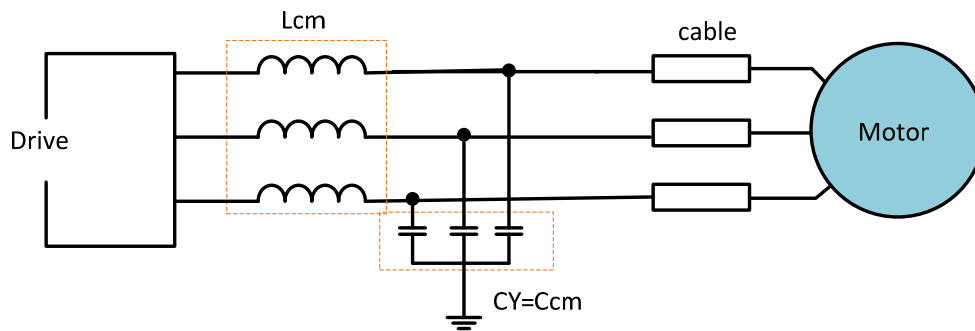


Figure 4.16 Common mode filter

Capacitors  $CY$  attenuate CM noise. Since these capacitors introduce a leakage current on the earth line, the maximum capacitance that can be used is often limited due to safety considerations. In fact these capacitances are usually never more than 10 nF and must meet special safety requirements.

### Differential mode filter

DM noise can be suppressed using a standard LC filter. Which act as a high frequency shunt for the DM noise. As the DM filter is often connected between the power lines (line and neutral) carrying the converter's input current, again care needs to be taken during the selection/design of the inductor such that it does not get saturated due to this current flow. Thus often the core of a DM filter's inductor is either gapped or it has distributed air gap.

Since the DM noise is filtered only by  $L$  and  $CX$ , the transformation of figure 4.15 becomes as shown in the following figure.

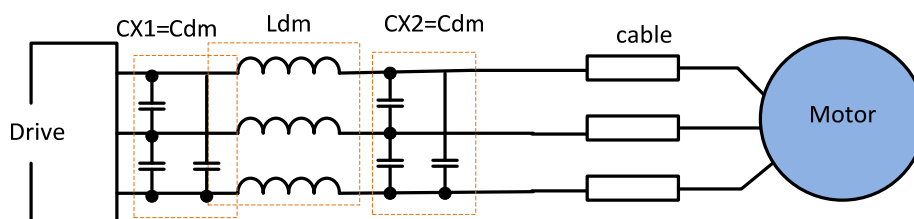


Figure 4.17 Differential mode filter

Capacitors  $CX1$  and  $CX2$  attenuate differential mode noise and can have fairly high values. While values between 0.1 to 1 $\mu$ F are typical, using much higher values are not uncommon [4].

## 5 Downhole system and EMI consideration

SmartMotor AS was proposed two options for the downhole system configuration. These options were [32]:

1. Distributed converters
2. Concentrated converters

These options are shown in Figure 5.1. Each of the configurations has its pros and cons. In the distributed converter oscillations in the DC-link have to be investigated. In the concentrated converter, however long motor cables with possible voltage oscillations at the motor terminals may occur. The latter case this can destroy motor insulation and bearings [32].

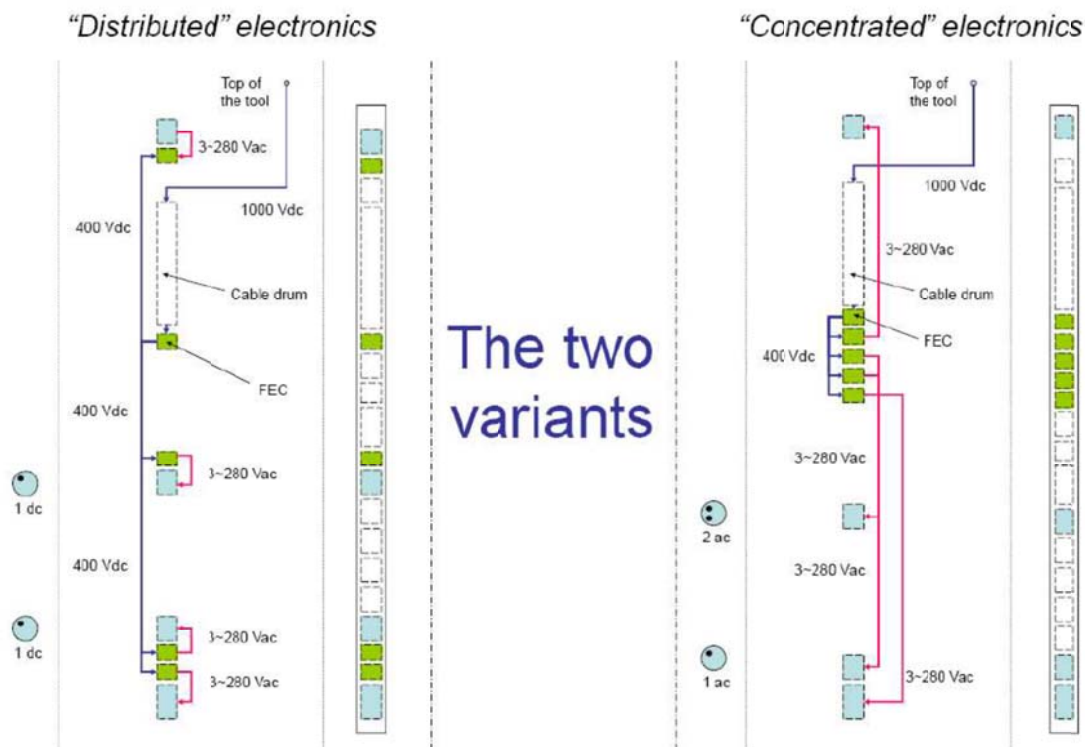


Figure 5.1 Two possible configurations of the converters

Then the distributed DC-link is to be preferred from noise (EMI,  $dv/dt$  and bearing current) point of view [32]. The topology of the drives is shown in Figure 5.2.

## 5.1 Downhole systems

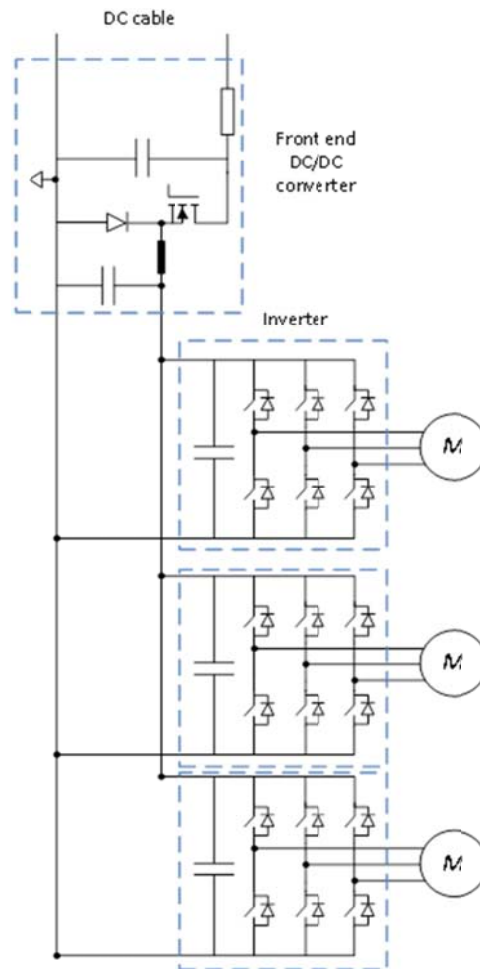


Figure 5.2 Downhole system topology

The proposed downhole system topology includes converter, distributed three inverters linked to the DC-link capacitor and each inverter fed the motors by the cable.

PDS are increasingly used in offshore power system for oil and gas exploration. As shown in the above figure, offshore electrical systems are often characterized by local generation, motor drives, and long cable runs [33]. In downhole system EMI is one of the undesirable effects caused by high rate switching characteristics of frequency converter and the long cable that is employed between the inverter and motor.

For downhole applications includes, the switching device SiC proposed for the converters due to promising features of SiC that is, wider band gap allows higher junction temperature thereby reducing heat-sink size, cooling efforts, weight and cost of the converter; in addition also SiC improve EMI effect, improve system efficiency and simplify design circuitry [34, 35]. SiC power devices manufactured today have the maximum voltage rating 1700 V, switching frequency 35 MHz, temperature 250 °C and current 30 A [36,37].

## 5.2 EMI consideration

From chapter three, high switching characteristics of converters, create conducted emission, in low and high frequency range that worsen the quality of power, increase power losses, damaging insulation of motor and in general they adversely affects the reliability of connected appliances. The indicated problems should be addressed in the downhole design phase stage.

In downhole system the high switching characteristics of inverter is not the only device that create EMI, the cable between the inverter and motor terminal has also an influence on EMI, this is due to the motor and cable impedance mismatch characteristics, then this creates voltage spikes and bearing at motors and steep  $dv/dt$  due to power semiconductor switching and also to breakers. If this EMI issues aren't minimized at design stage then the designer should has to concern another replacement of bearings in at the motor often difficult.

Table 5.1 EMI effects to consider for downhole

#	EMI effect	Comment
1	e.g voltage dip	Grid side
2	e.g. harmonics	Grid side
3	e.g overvoltage	Motor side
4	e.g. bearing currents	Motor side
5	e.g. radiations	Environment

The **IEC61800-3** standard specifies essential EMC requirements and specific test methods for adjustable speed electrical power drive systems, this standard help to test EMC requirements for downhole system.

Table 5.2 Applicable EMC standards for downhole

#	Standard code	Standard name	Comment
1	<b>IEC61800-3</b>	International standard	The objective of this standard is to define the limits and test methods for a PDS according to its intended use. This standard includes immunity requirements and requirements for electromagnetic emissions.
2	<b>IEC61800-3</b>	International standard	Power port: conducted emission from 150 kHz to 30 MHz
3	<b>IEC61800-3</b>	International standard	Power port: radiated emission from 30 MHz to 1000 MHz

Before testing the downhole system for EMC requirement it is important to know the downhole drive system in which environment and category are lie.



## Installation environments

**IEC61800-3** defines **two environments** for PDS installed in the network. These are **first environment** and **second environment**. In each environment there are two categories depending on the way the PDS is connected to power supply.

**First environment** includes domestic premises it also includes establishments directly connected without intermediate transformers to a low-voltage power supply network which supplies buildings used for domestic purposes [8].

**Second environment** includes all establishments other than those directly connected to a low voltage power supply network which supplies buildings used for domestic purposes. Industrial areas, technical areas of any building fed from a dedicated transformer are examples of second environment locations [8].

Based on this, downhole system must has to fulfill the EMC requirements for the second environment, then the next task should be to find the categories, for the **first environment category one and two** are intended to use. For the **second environment category three and four** are intended to use [8].

PDS with rated voltage less than 1,000 V can be fall in category three PDS with rated voltage greater than or equal to 1,000V can be fall in category four.

Based on the above information the downhole system has to fulfill EMC requirement in **second environment and category three**.

The following three consecutives graph shows EMC emission limit that is found in **IEC61800-3** second environment category three.

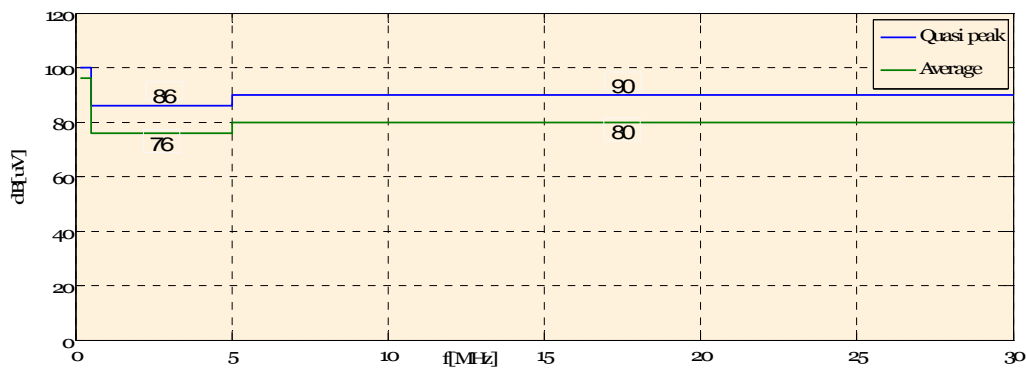


Figure 5.3 Conducted emission from 150 kHz-30 MHz I>1000A

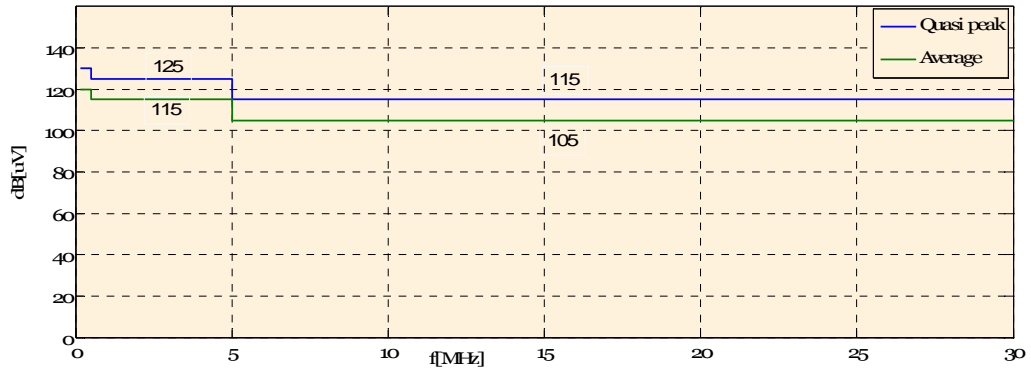


Figure 5.4 Conducted emission from 150 kHz-30 MHz I <1000A

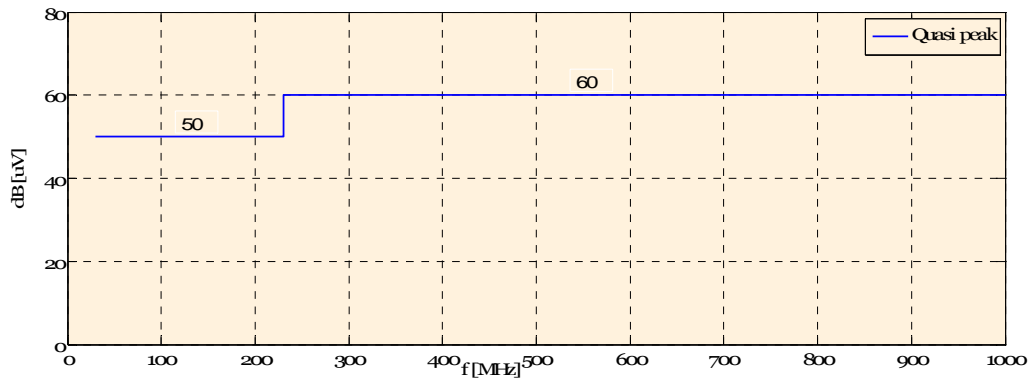


Figure 5.5 Radiated emission from 30 MHz-1 GHz

## 6 Simulation results

Chapter four discussed theoretical background of different filter types and compared them to each other based on their cost, limitation and efficiency. In this chapter simulation models were made, for those filter types, and used to reduce  $dv/dt$ , harmonics and overvoltage at the motor terminals.

### The chosen cable type

A cable 14 AWG  $m^2$  3 phase (ca  $2.0mm^2$ ) power cable was chosen. The following table shows the electrical parameters of the cable:

Table 6.1 Cable parameters

The electrical parameters of the cable per feet are:	The electrical parameters of the cable per km are:
Resistivity $R=2.52$ [m $\Omega$ /ft]	Resistivity $R=8.267$ [ $\Omega$ /km]
Inductivity $L=0.213$ [ $\mu$ H/ft]	Inductivity $L=0.698$ [mH/km]
Capacitance $C=42$ [pF/ft]	Capacitance $C=137.79$ [nF/km]

As input to the model in Matlab Simpow, the parameters in the +system and zero system had to be calculated. It was assumed that each phase has its own screen and that these screens were connected together at input and output of the cable. The cable was connected to earth/ground and the input, one could also connect it to art at both ends, but then it needs more information on the ground conditions.

The resistivity in the screen was assumed to be 2.5 the value in one phase, due to the ratio area conductor screen/area screen equal 60/145 cross area. The inductance value was assumed equal the phase values. The mutual capacitance was assumed zero, one then gets as shown in table 6.2.

Table 6.2 Cable parameters values in the positive and zero system

The electrical parameter in the positive system	The electrical parameters in the zero system
$R+=R_{c,phase}=0.154$ [ $\Omega$ /km]	$R_o=R_{c,phase}+3(2.5.R_{c,phase})=70.25$ [ $\Omega$ /km]
$L+=L_{c,phase}=0.36$ [mH/km]	$L_o=L_{c,phase}+3.L_{c,phase}=2.79$ [mH/km]
$C+=C_{c,phase}=410$ [nF/km]	$C_o=0.75*C_{c,phase}=103.3$ [nF/km]

## 6.1 System simulation for reactor ( $L_f$ ) filter

The following figure shows the two level inverter fed a motor by distributed cable of model. And an output reactor ( $L_f$ ) is used at the inverter terminal.

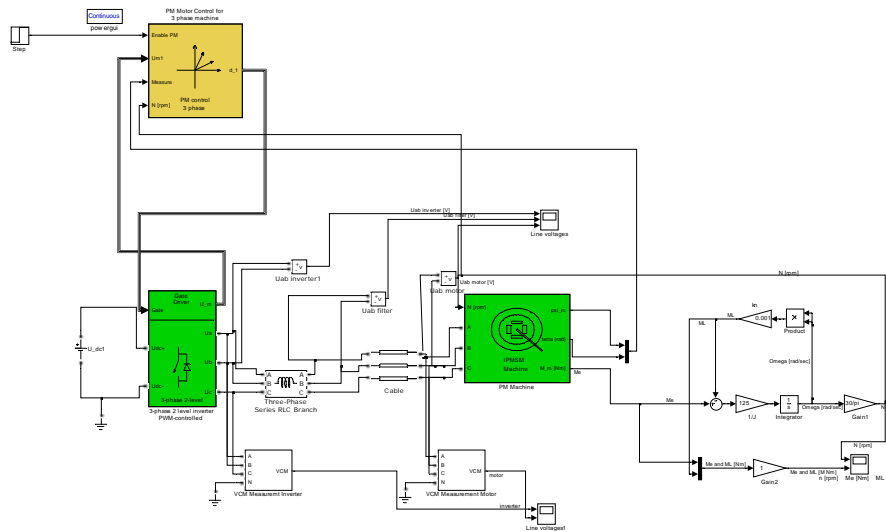


Figure 6.1 System model for reactor ( $L_f$ ) filter using two level inverter

Based on the derived filter from chapter four, simulation made for 100 m, 300 m and 600 m cable of length. Table 6.3 shows the calculated filter parameters for the chosen cable length.

Simulation results for different cable length with their respective filters are shown from figure 6.3 through 6.11.

Table 6.3 Calculated filter parameters for 100 m, 300 m and 600 m cable length

$L$ [m]	$L_f = \frac{Z \cdot V}{I \cdot 2 \cdot \pi \cdot f \cdot \sqrt{3}}$ [H]
100m	7.6573e-5
300m	7.6573e-5
600m	7.6573e-5

Figure 6-2, shows motor output voltage without a filter.

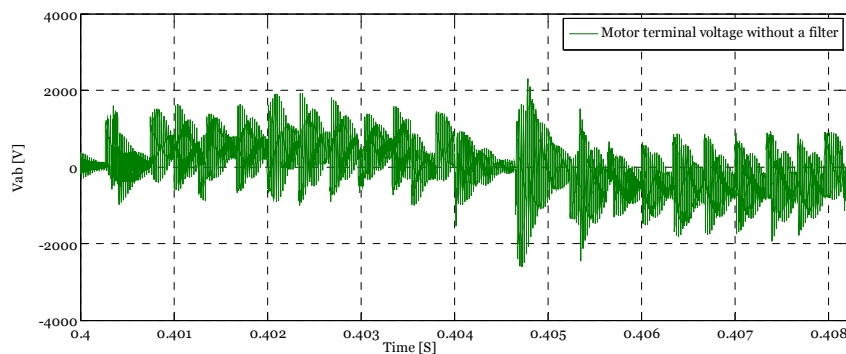


Figure 6.2 Motor terminal voltage without a filter

Figure 6.3 through 6.11, depicts the results of inverter, filter and motor terminals voltage, using an output reactor ( $L_f$ ) at the inverter terminal.

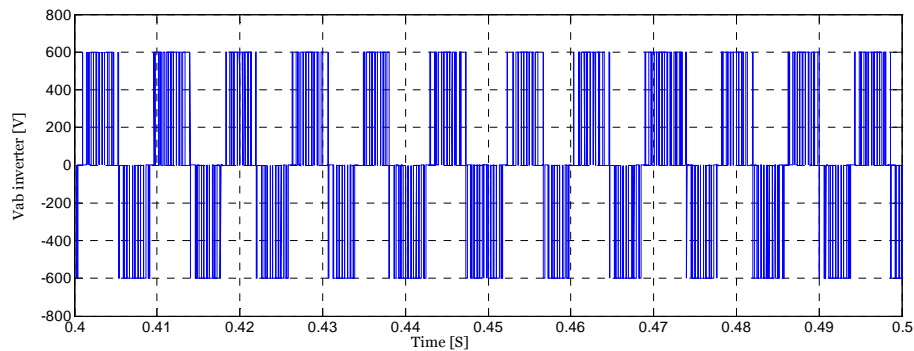


Figure 6.3 Zoomed out view for 100 m  $V_{ab}$  inverter vs time with the calculated  $L_f$  filter

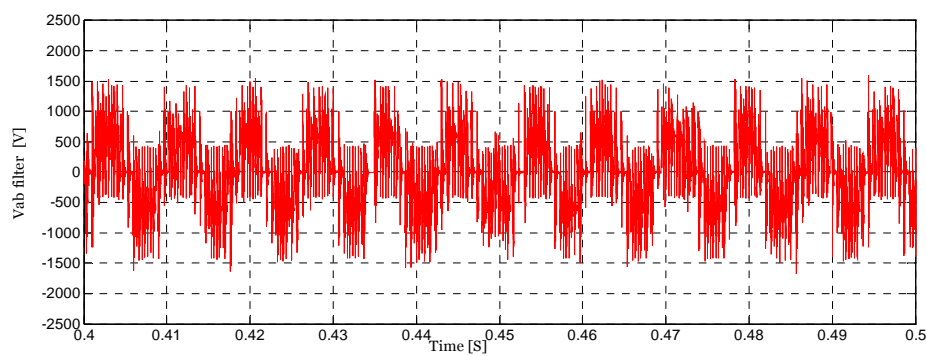


Figure 6.4 Zoomed out view for 100 m  $V_{ab}$  filter vs time with the calculated  $L_f$  filter

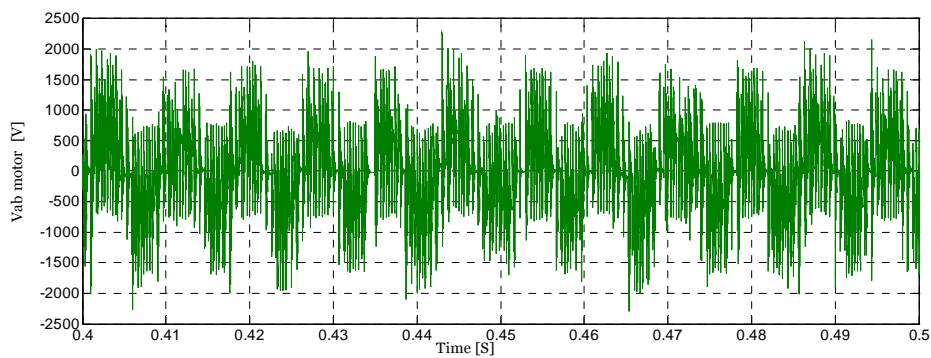


Figure 6.5 Zoomed out view for 100 m  $V_{ab}$  motor vs time with the calculated  $L_f$  filter

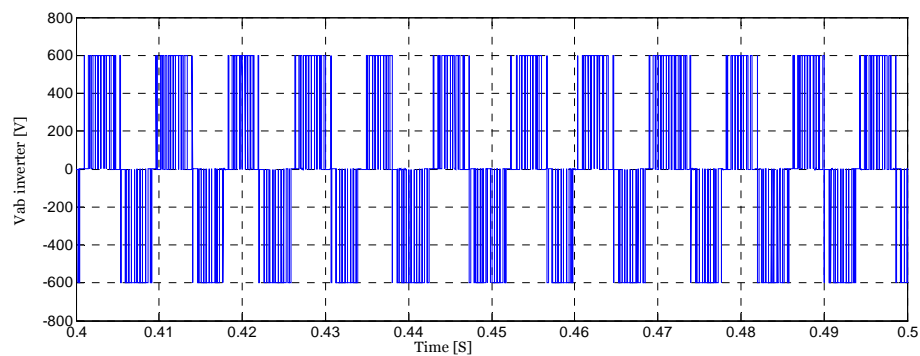


Figure 6.6 Zoomed out view for 300 m  $V_{ab}$  inverter vs time with the calculated  $L_f$  filter

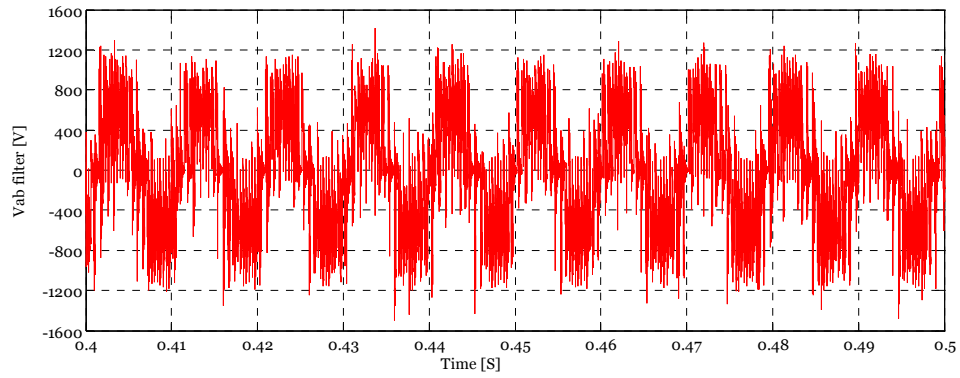


Figure 6.7 Zoomed out view for 300 m  $V_{ab}$  filter vs time with the calculated  $L_f$  filter

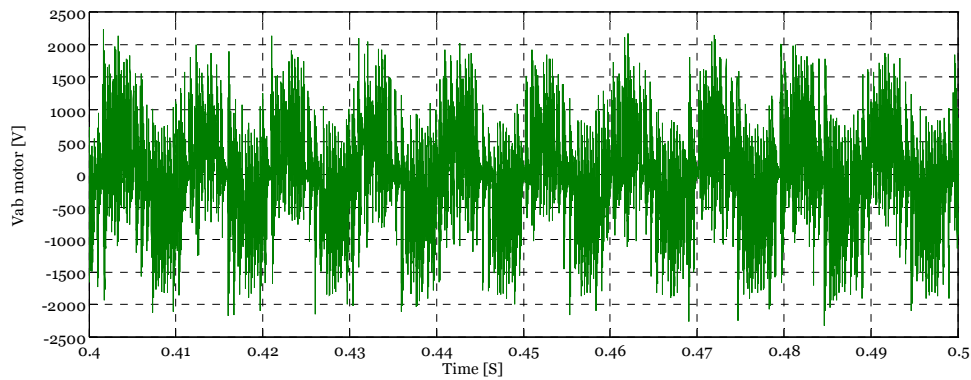


Figure 6.8 Zoomed out view for 300 m  $V_{ab}$  motor vs time with the calculated  $L_f$  filter

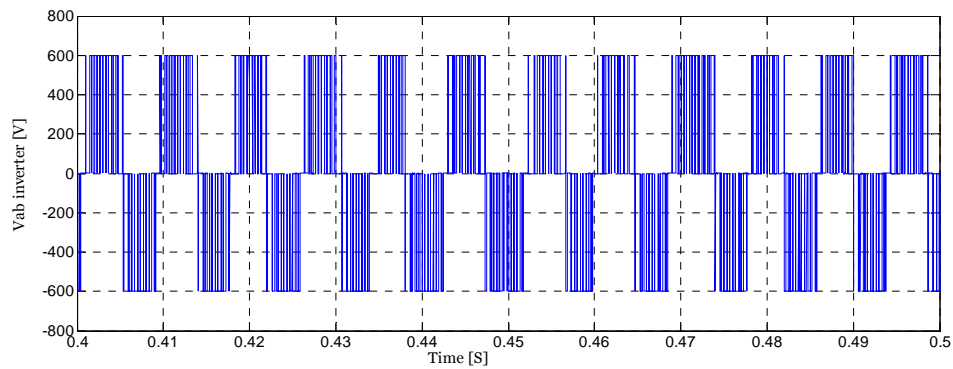


Figure 6.9 Zoomed out view for 600 m  $V_{ab}$  inverter vs time with the calculated  $L_f$  filter

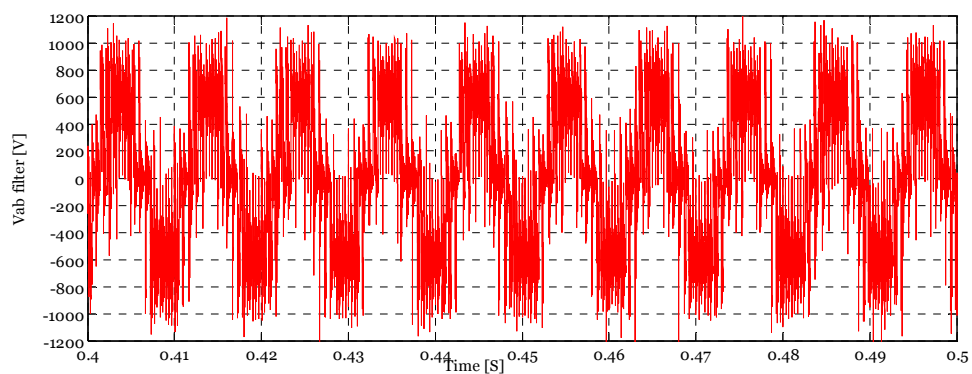


Figure 6.10 Zoomed out view for 600 m  $V_{ab}$  filter vs time with the calculated  $L_f$  filter

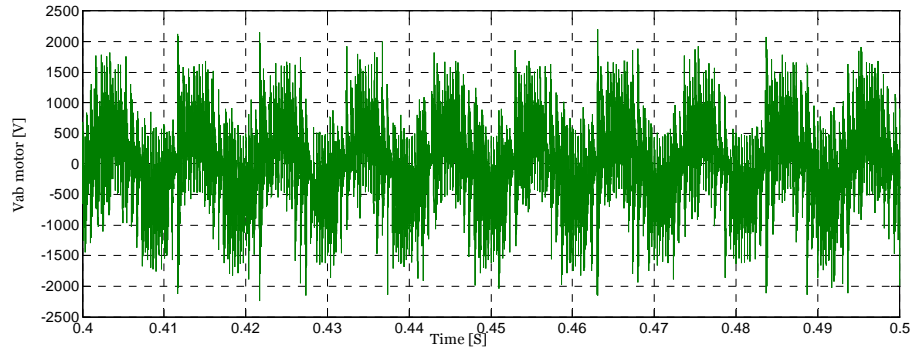


Figure 6.11 Zoomed out view for 600 m  $V_{ab}$  motor vs time with the calculated  $L_f$  filter

Figure 6.12 through 6.14, depicts the total harmonic distortion (THD) results, using reactor ( $L_f$ ) at the inverter terminal.

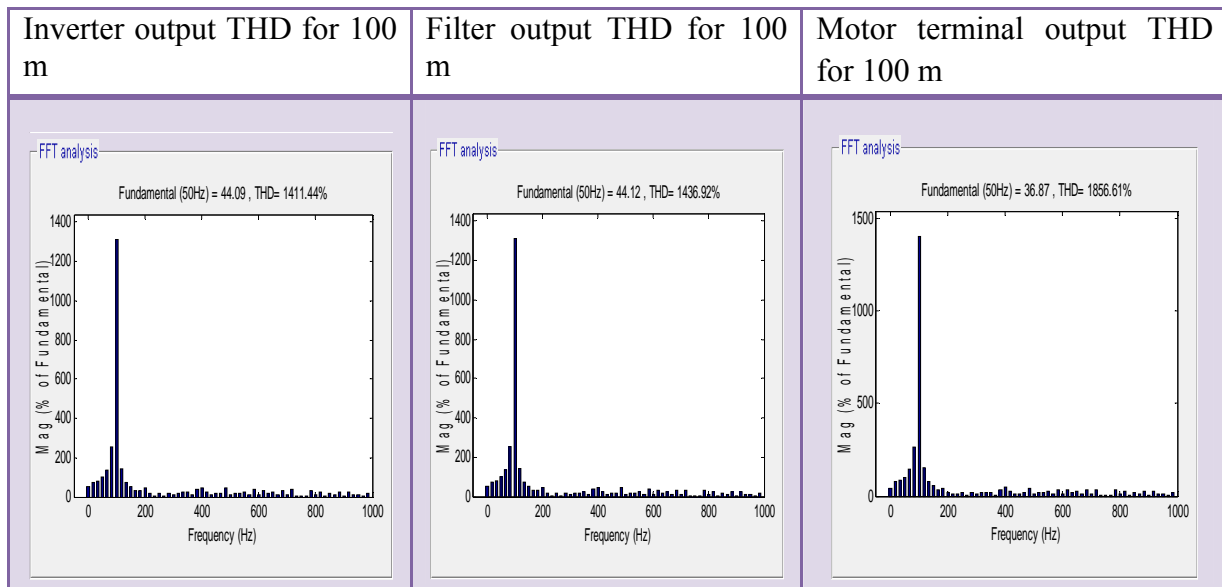


Figure 6.12 THD for inverter, filter and motor when the cable length is 100 m

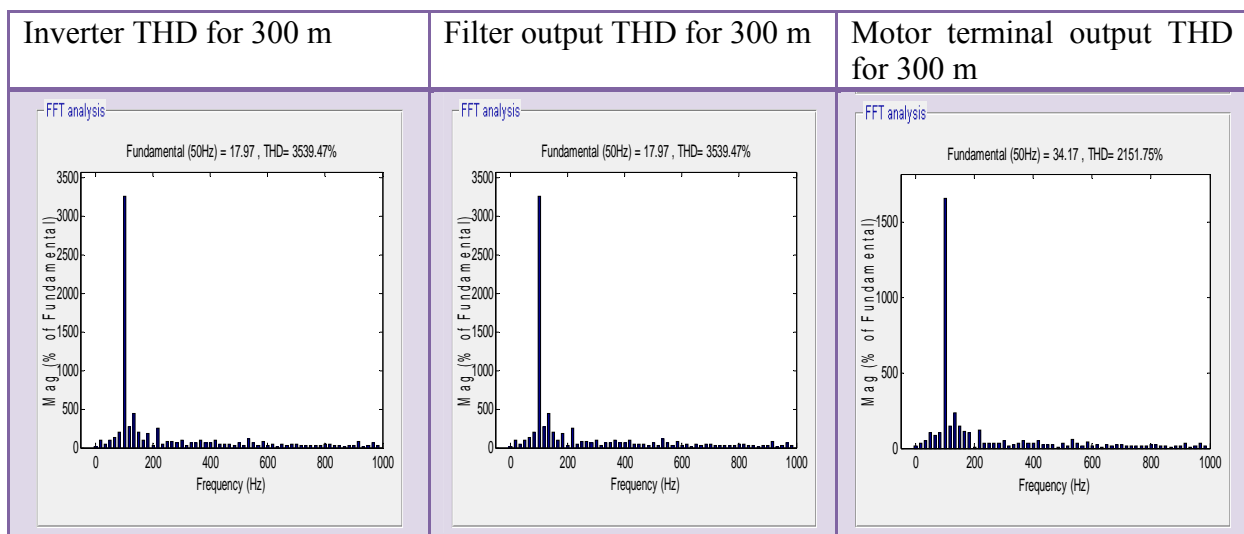


Figure 6.13 THD for inverter, filter and motor when the cable length is 300 m

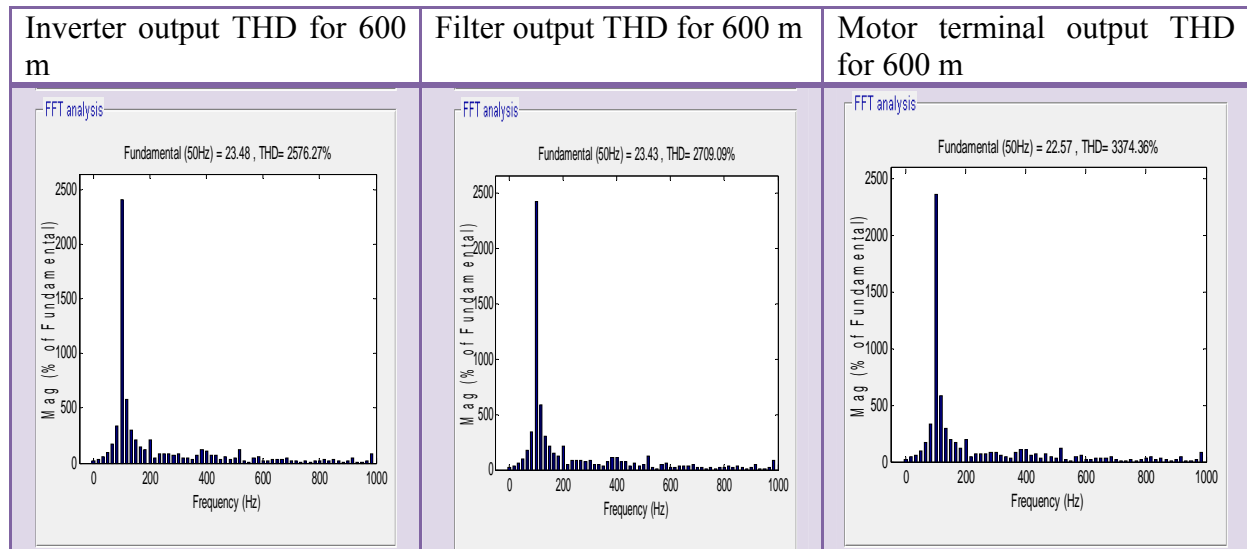
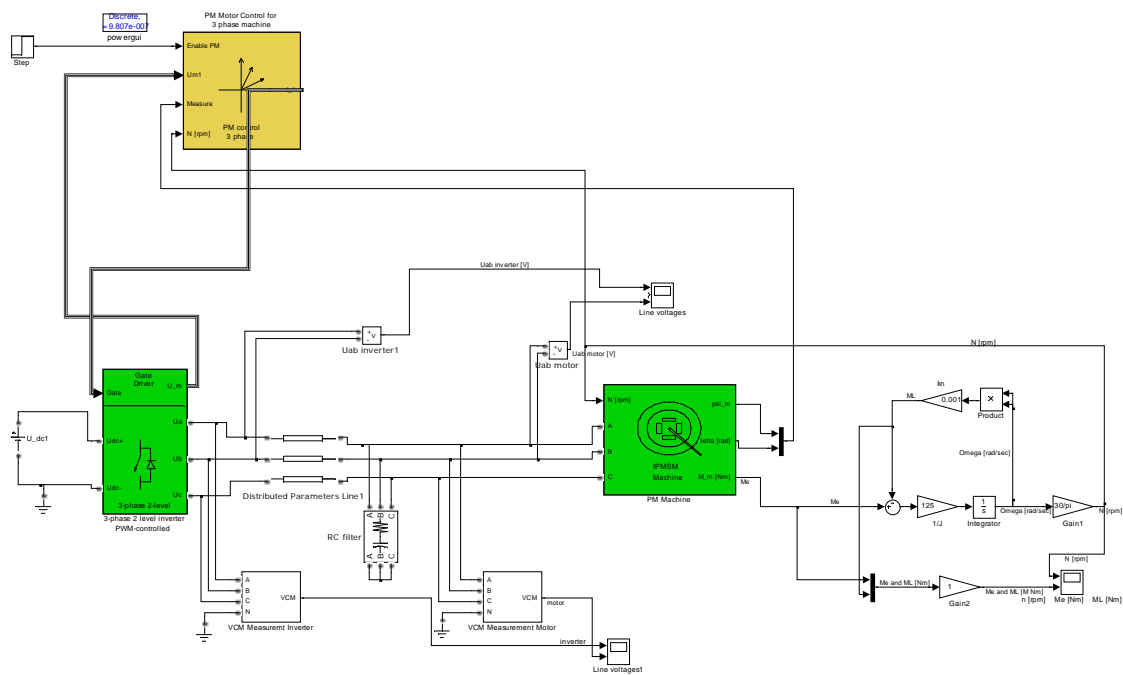


Figure 6.14 THD for inverter, filter and motor when the cable length is 600 m

## 6.2 System simulation for $R_fC_f$ filter

The following figure shows two level inverter fed a motor by distributed cable of model. And an  $R_fC_f$  filter is used at the motor terminal.

Figure 6.15 System model for  $R_fC_f$  filter using two level inverter

Based on the derived filter from chapter four, simulation made for 100 m, 300 m and 600 m cable length. Table 6.4 shows the calculated filter parameters for the chosen cable length.

Simulation results for different cable length with their respective filters are shown from figure 6.17 through 6.19.



Table 6.4 Calculated filter parameter for 100 m, 300 m and 600 m cable length

L[m]	$R_f = Z_o[\text{ohm}]$	$C_f = \frac{l_c C_c}{0.22314}[\text{nF}]$
100m	72	61.75
300m	72	185.2
600m	72	370.51

## Result representation

The following figure represents for each simulation that is made for different cable length, the result of inverter and motor terminal voltage were zoomed in and put in the same axis.

To compare the results, the zoomed in view results were used for comparison in this section, the zoomed out view results are found in appendix A1.

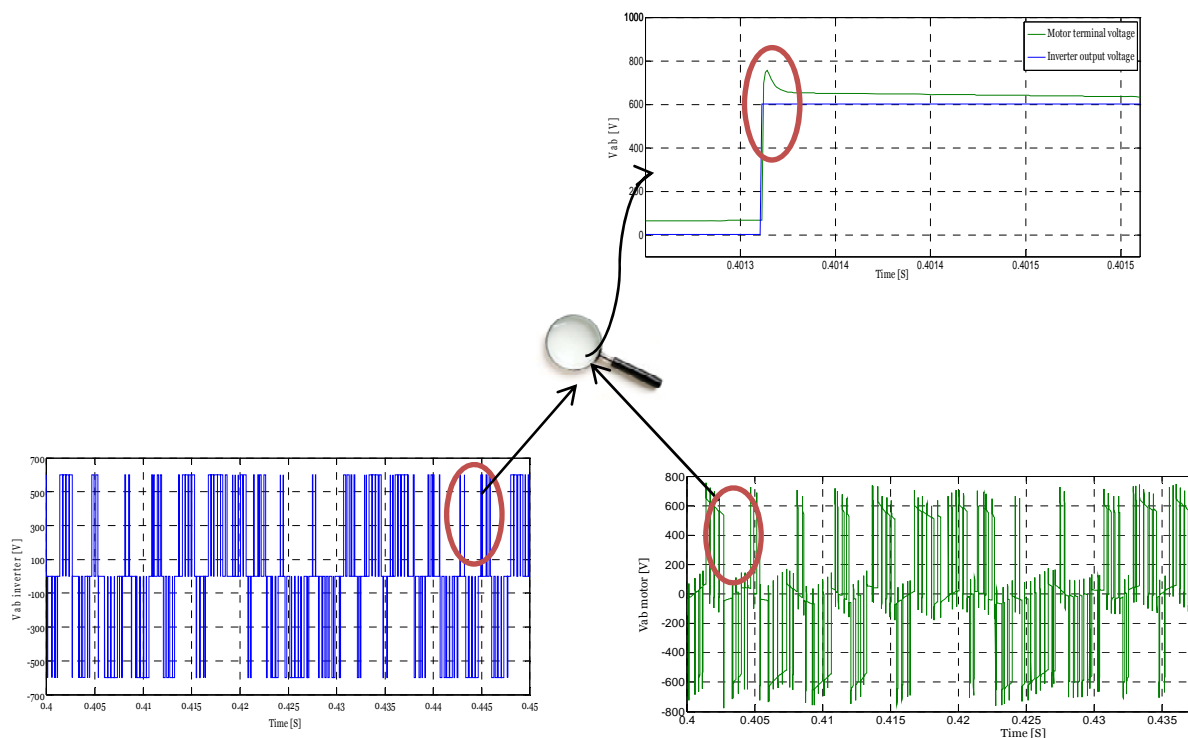


Figure 6.16 Result representation for  $R_f C_f$  filter

Figure 6.17 through 6.19, depicts the results of inverter, filter and motor terminal voltage when an  $R_f C_f$  filter is at the motor terminal.

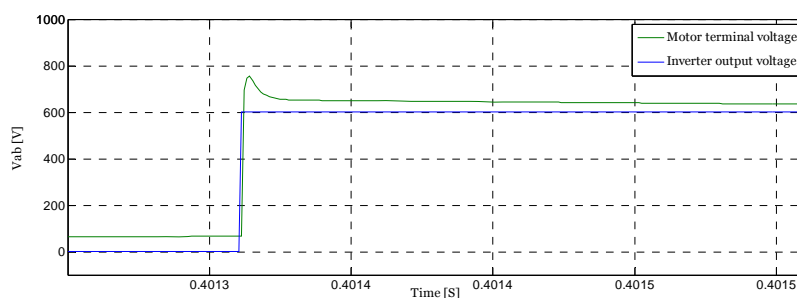


Figure 6.17 Zoomed in view for 100 m  $V_{ab}$  inverter & motor vs time with calculated  $R_f C_f$  filter

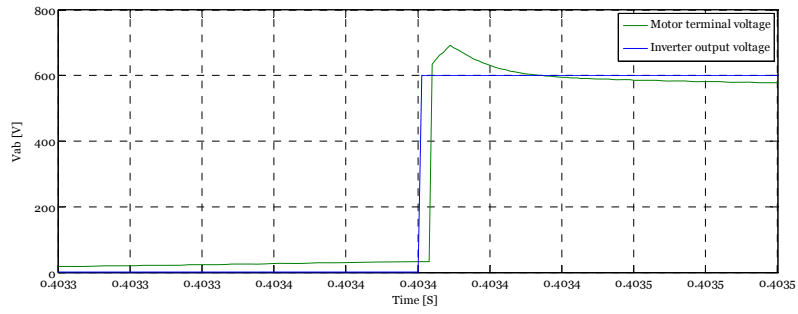


Figure 6.18 Zoomed in view for 300 m  $V_{ab}$  inverter & motor vs time with calculated  $R_f C_f$  filter

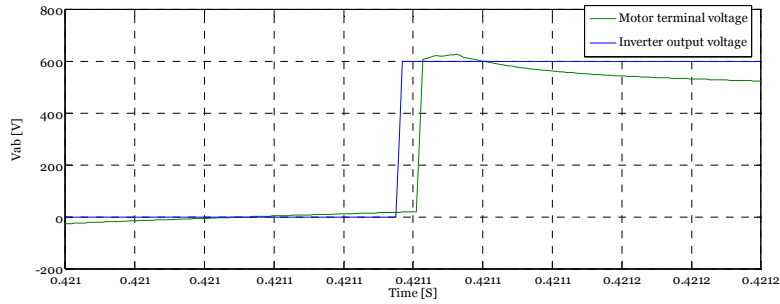


Figure 6.19 Zoomed in view for 600 m  $V_{ab}$  inverter & motor vs time with calculated  $R_f C_f$  filter

Figure 6.20 through 6.22, depicts the THD of inverter and motor output results using an  $R_f C_f$  filter at the motor terminal.

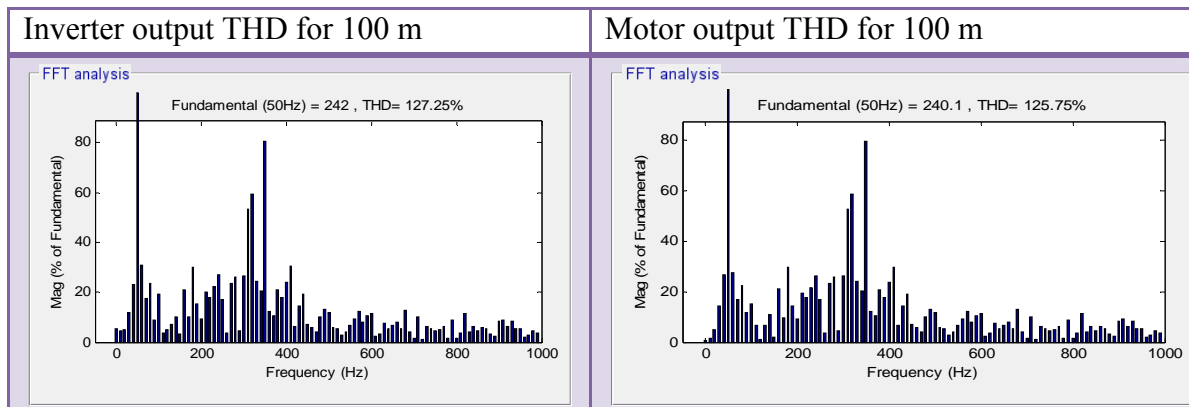


Figure 6.20 THD for inverter, filter and motor when the cable length is 100 m

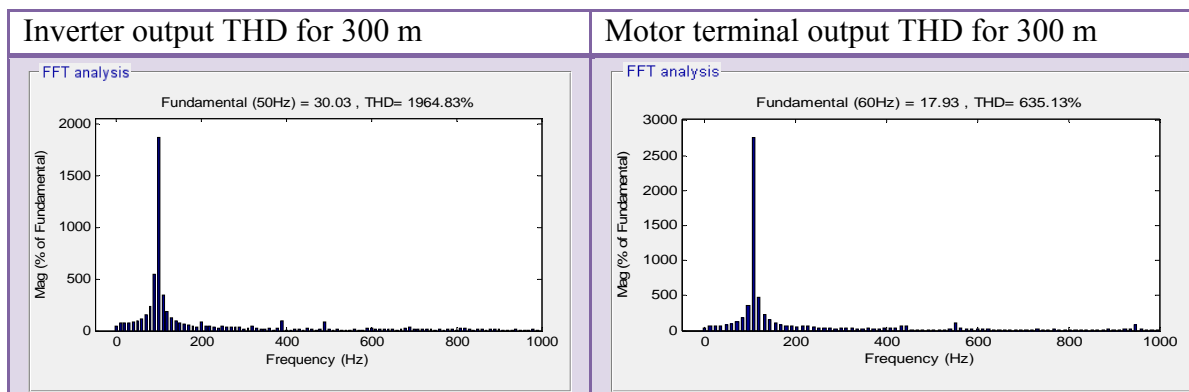


Figure 6.21 THD for inverter, filter and motor when the cable length is 300 m

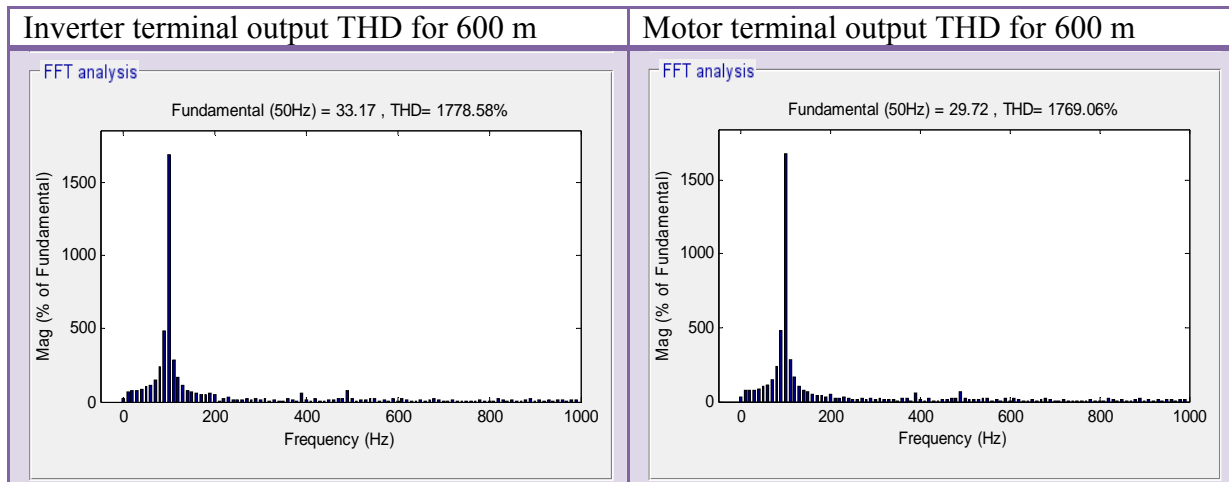


Figure 6.22 THD for inverter, filter and motor when the cable length is 600 m

### 6.3 System simulation for $R_fL_fC_f$ filter

The following figure shows two level inverter fed a motor by distributed cable of model. And  $R_fL_fC_f$  filter is used at the inverter terminal.

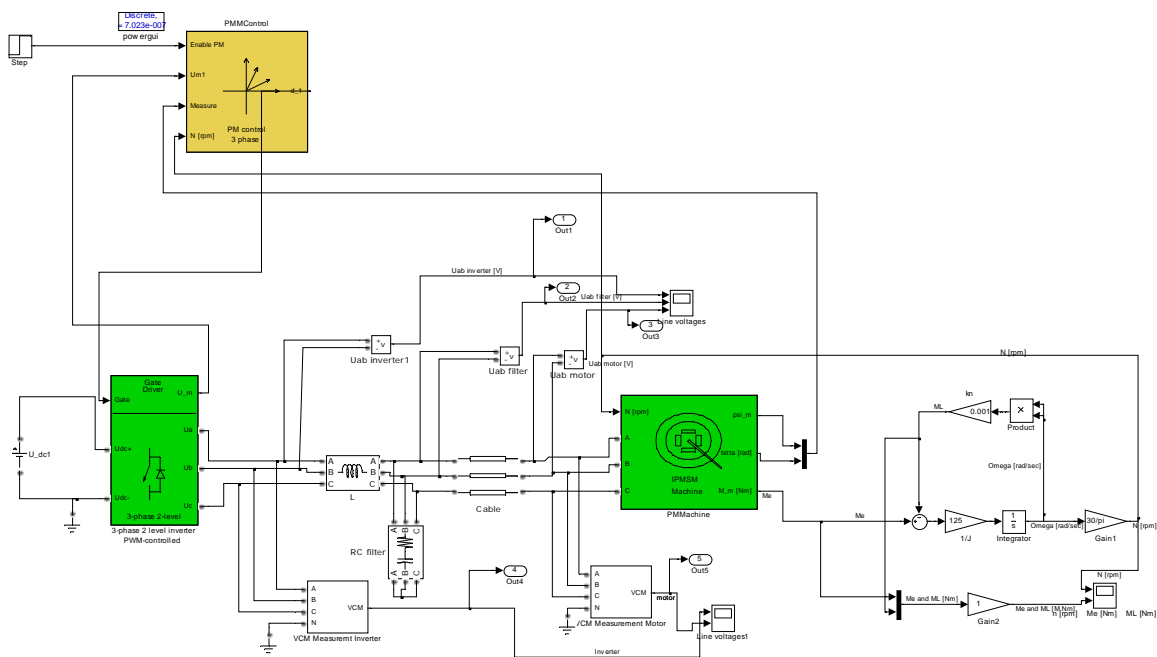


Figure 6.23 System model for  $R_fL_fC_f$  filter using two level inverter

Based on the derived filter from chapter four, simulation made for 100 m, 300 m and 600 m cable length, table 6.5 shows the calculated filter parameters for the chosen cable length.

Simulation results for different cable length with their respective filters are shown from figure 6.25 through 6.27.

Table 6.5 Calculated filter parameter for 100 m, 300 m and 600 m cable length

L[m]	$R_f = \frac{Z_c}{2} = \frac{1}{2} \sqrt{\frac{L_c}{C_c}} [\Omega]$	$f_{co} = \frac{1}{27 \cdot L_c \cdot \sqrt{L_c \cdot C_c}} [\text{kHz}]$	$C_f = \frac{2\sqrt{18}}{\pi \cdot R_f \cdot f_{co}} [\mu\text{F}]$	$L_f = C_f \left(\frac{R_f}{4}\right)^2 [\text{mH}]$
100	35	37.743	2.09	0.163
300	35	12.58	6.027	0.477
600	35	6.29	12.54	0.95

The following figure represent for each simulation that is made for different cable length the result of inverter, filter and motor output voltage are zoomed in and put in the same axis.

To compare the results, the zoomed in view results are used for comparison in this section, the zoomed out view results are found in appendix A2 and A3.

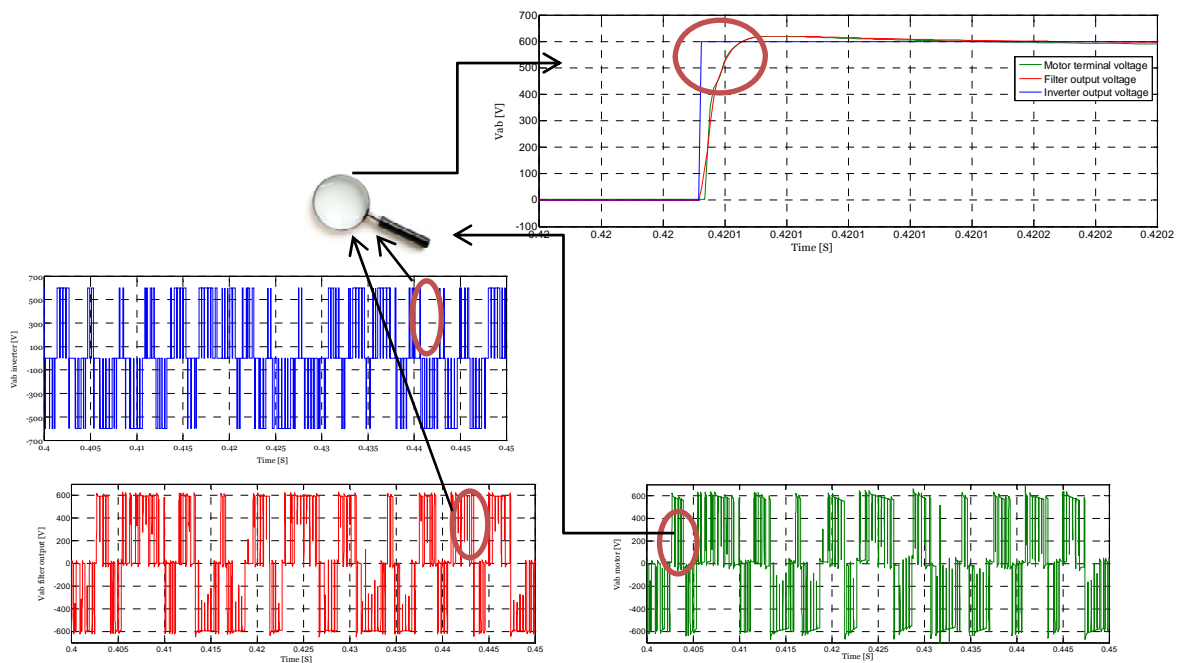
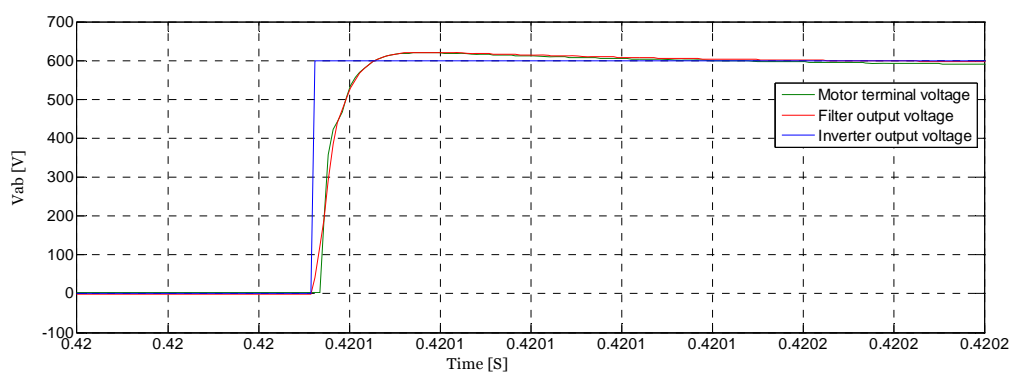
Figure 6.24 Result representation for  $R_f L_f C_f$  filter

Figure 6.25 through 6.27 depicts the results of inverter, filter and motor terminals voltage when  $R_f L_f C_f$  at the inverter terminal.

Figure 6.25 Zoomed in view for 100 m  $V_{ab}$  inverter, filter & motor vs time with calculated  $R_f L_f C_f$  filter

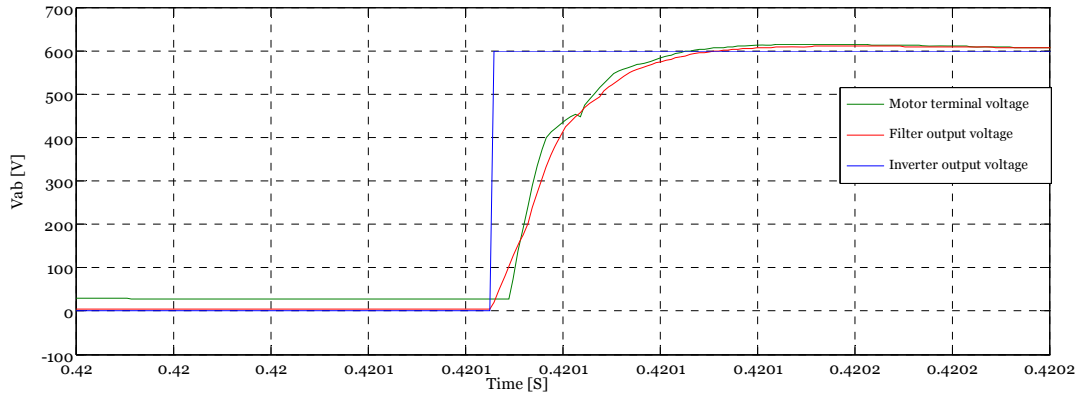


Figure 6.26 Zoomed in view for 300 m  $V_{ab}$  inverter, filter & motor vs time with calculated  $R_f L_f C_f$  filter

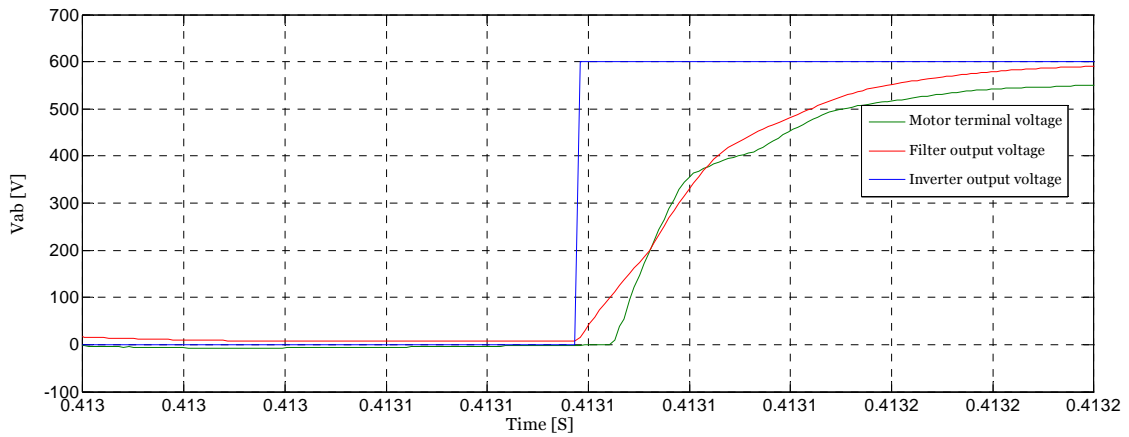


Figure 6.27 Zoomed in view for 600 m  $V_{ab}$  inverter, filter & motor vs time with calculated  $R_f L_f C_f$  filter

Figure 6.28 through 6.30, depicts the THD of inverter, filter and motor output results using  $R_f L_f C_f$  filter at the inverter terminal.

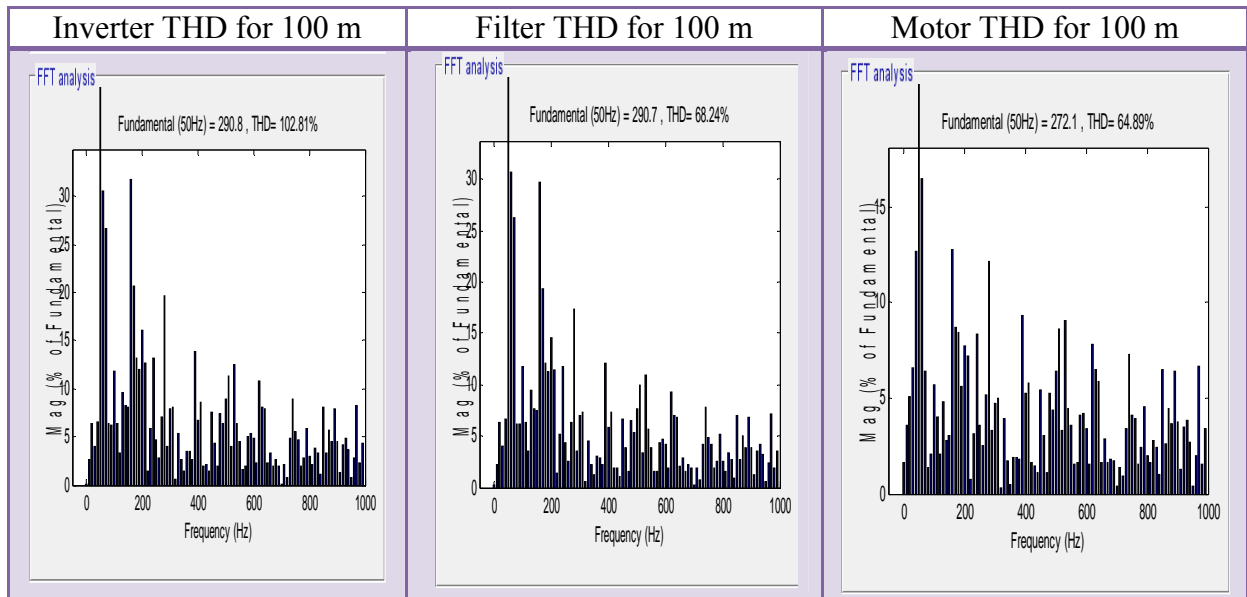


Figure 6.28 THD for inverter, filter and motor when the cable length is 100 m

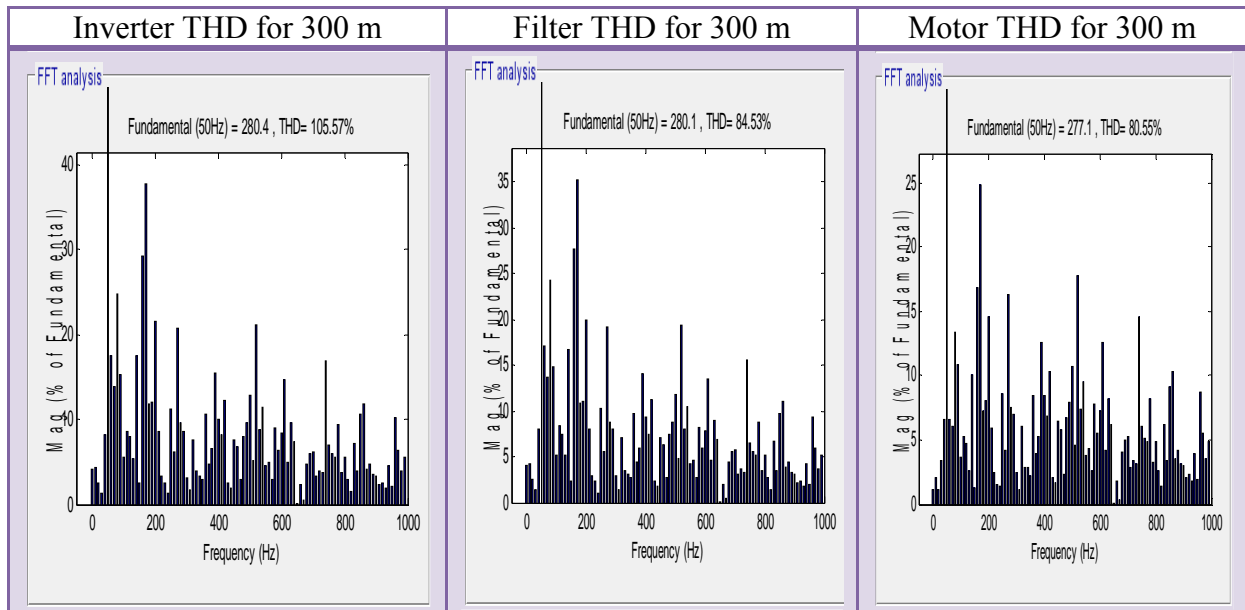


Figure 6.29 THD for inverter, filter and motor when the cable length is 300 m

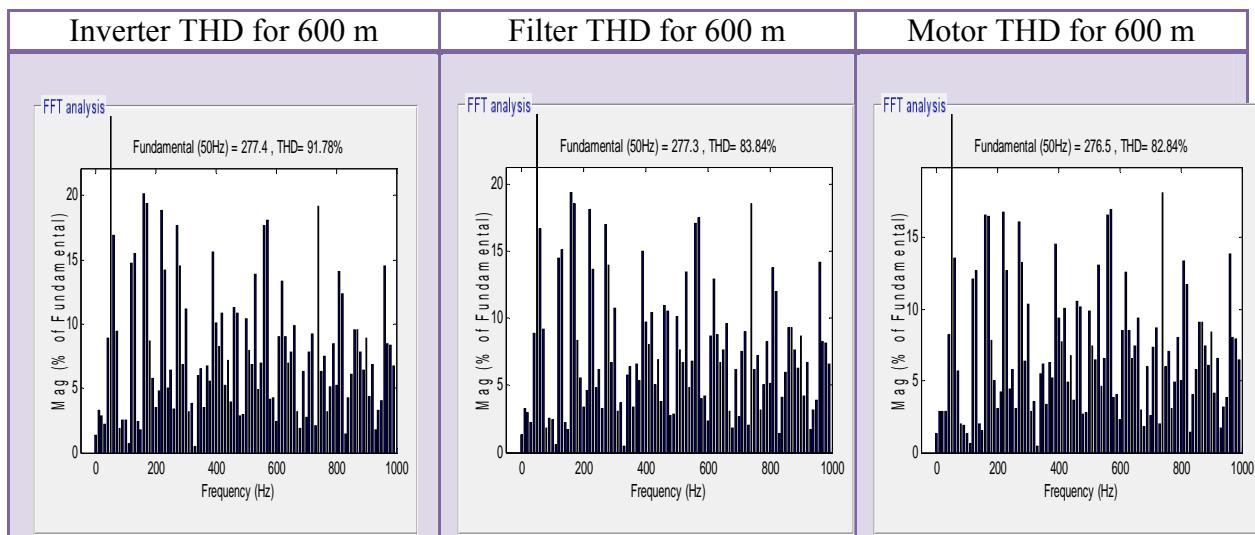


Figure 6.30 THD for inverter, filter and motor when the cable length is 600 m

#### 6.4 System simulation for $R_fL_fC_f$ split RC to +/- DC link filter

The following figure shows two level inverter fed motor by distributed cable of model. And an  $R_fL_fC_f$  split filter placed at the inverter terminal.



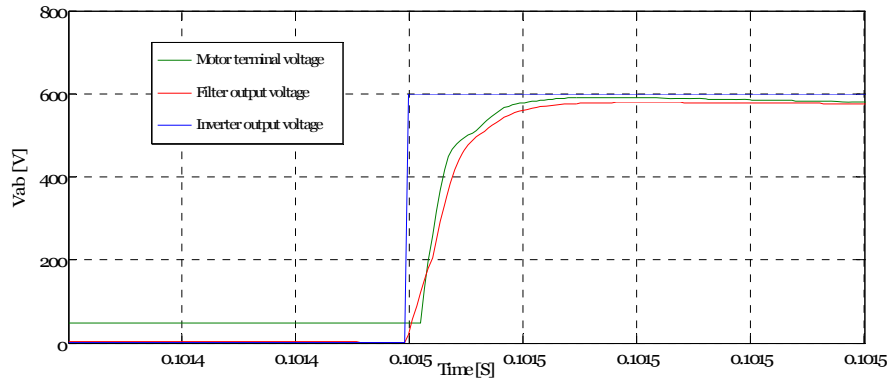


Figure 6.32 Zoomed in view for 100 m  $V_{ab}$  inverter, filer & motor vs time with calculated  $R_fL_fC_f$  split filter

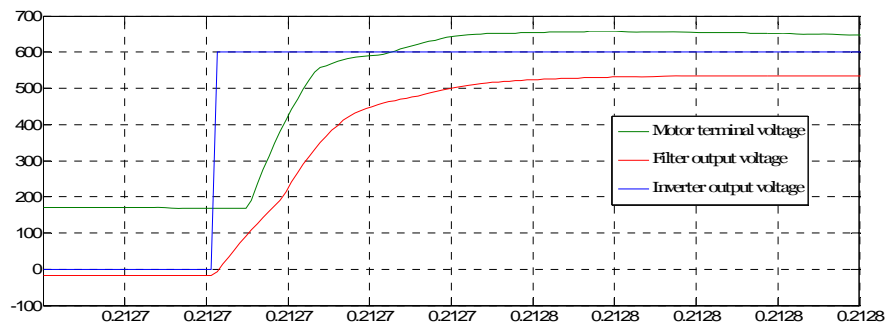


Figure 6.33 Zoomed in view for 300 m  $V_{ab}$  inverter, filer & motor vs time with calculated  $R_fL_fC_f$  split filter

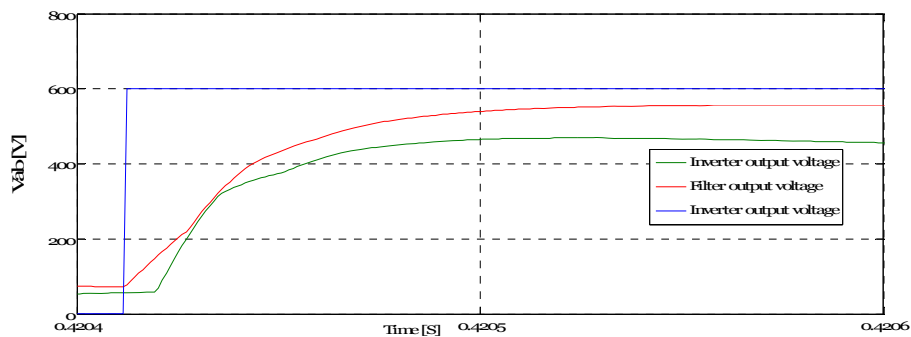


Figure 6.34 Zoomed in view for a 600 m  $V_{ab}$  inverter, filer & motor vs time with calculated  $R_fL_fC_f$  split

Figure 6.35 through 6.37, depicts THD results of inverter, filter and motor using  $R_fL_fC_f$  split RC to +/- DC link at the inverter terminal.



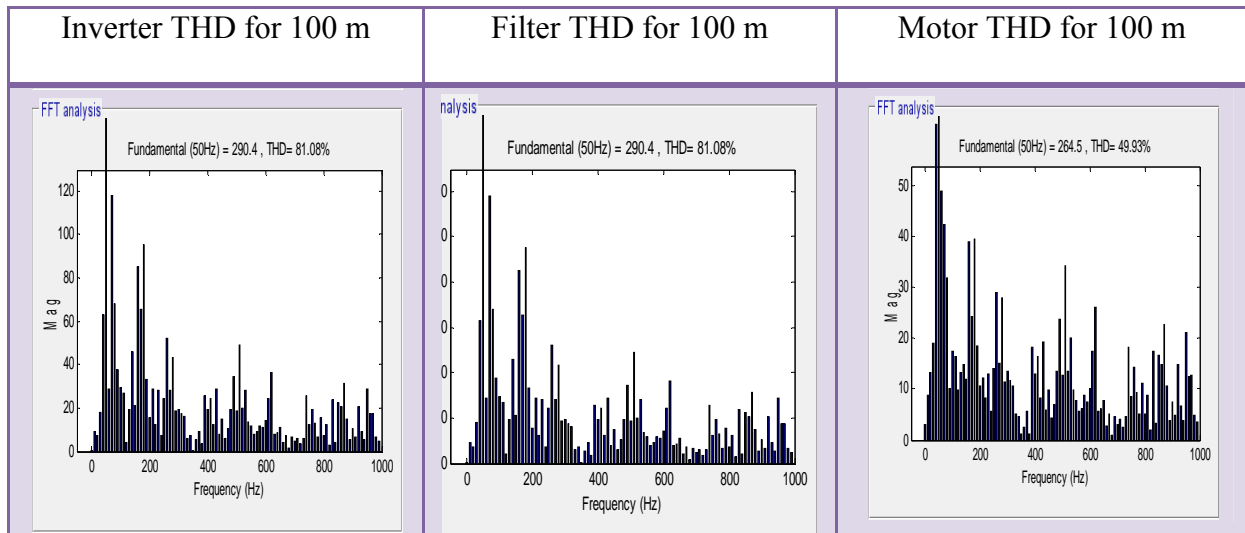


Figure 6.35 THD for inverter, filter and motor when the cable length is 100 m

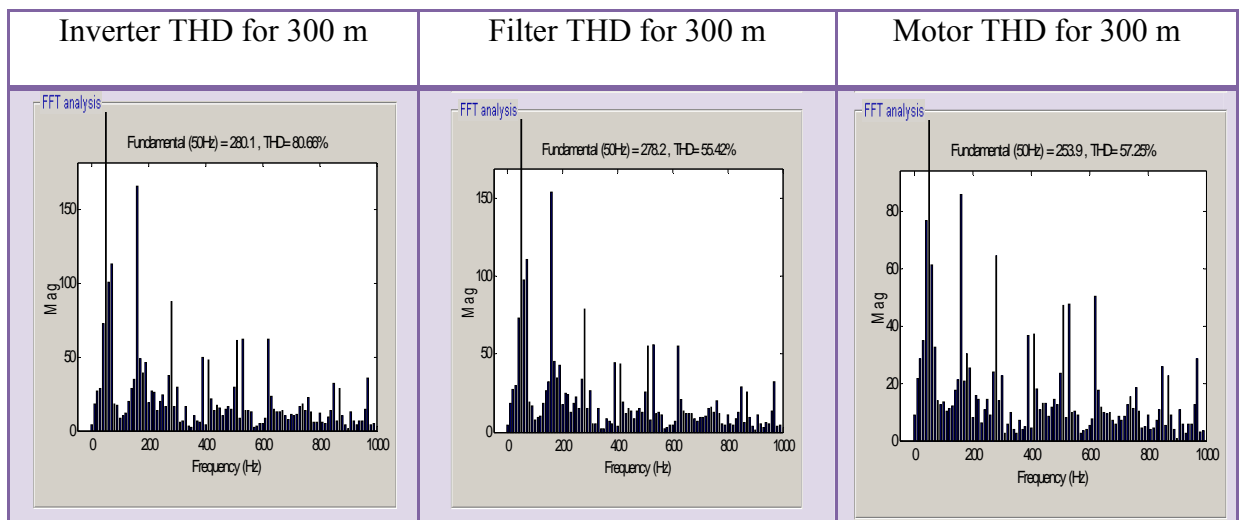


Figure 6.36 THD for inverter, filter and motor when the cable length is 300 m

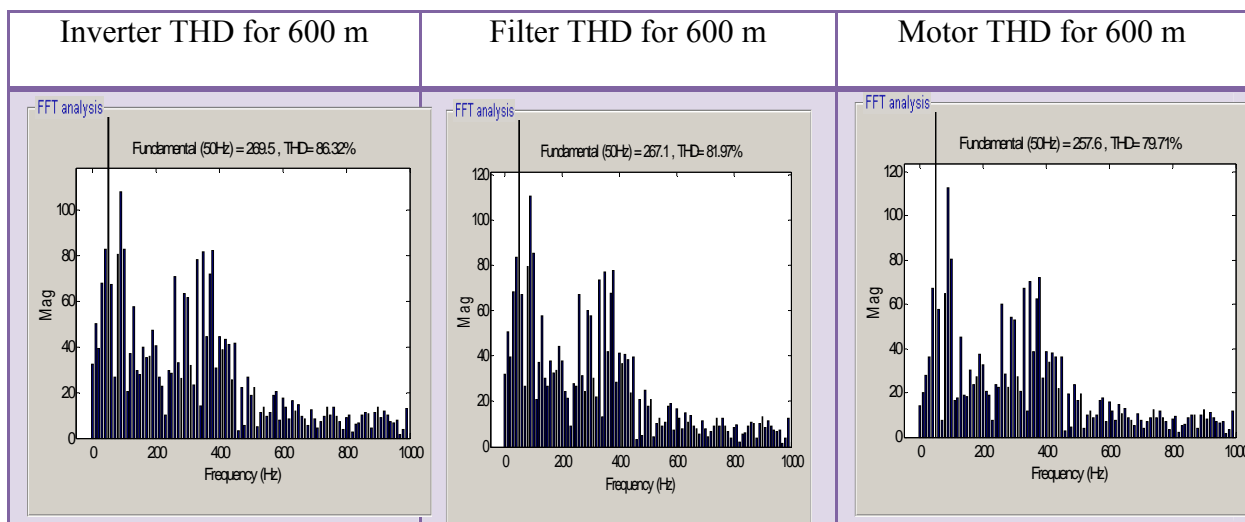


Figure 6.37 THD for inverter, filter and motor when the cable length is 600 m

### 6.5 System simulation for $L_f C_f$ filter

The following figure shows two level inverter fed motor by distributed cable of model. And the  $L_f C_f$  filter placed at the inverter terminal.

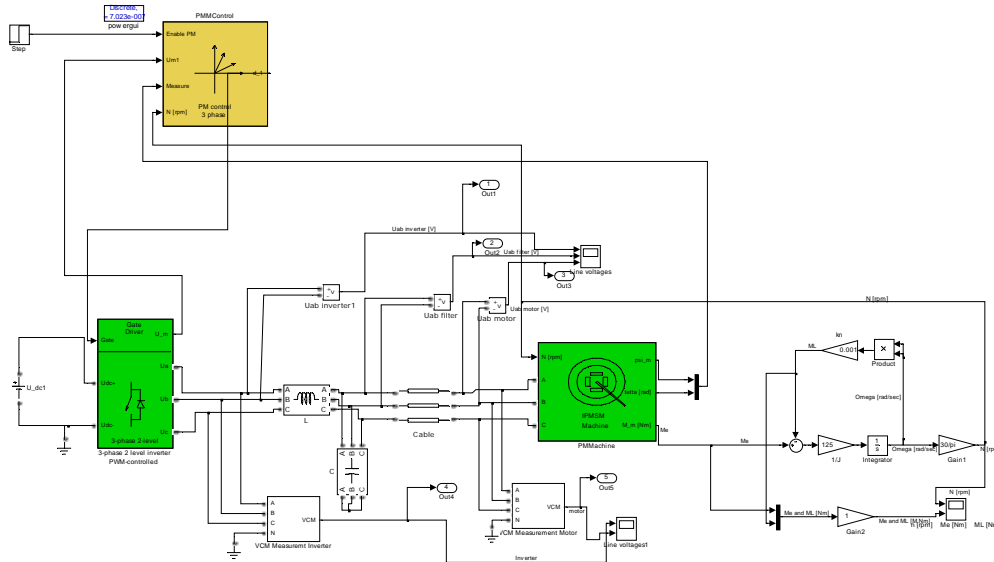


Figure 6.38 System model for  $L_f C_f$  filter using two level inverter

Based on the derived filter from chapter four, simulation made for 600 m cable length. Table 6.7 shows the calculated filter parameters for the chosen cable length.

A simulation result for 600 m cable length with its respective filter is shown from figure 6.39 through 6.41.

Table 6.7 Calculated filter parameter for 100 m, 300 m and 600 m cable length

$L[m]$	$f_{co} = \frac{1}{27.l_c.\sqrt{L_c.C_c}} [kHz]$	$C_f = \frac{\sqrt{18}}{\pi.\sqrt{C_c}.f_{co}} [\mu F]$	$L_f = C_f \left( \frac{\sqrt{L_c}}{4} \right)^2 [mH]$
600	6.29	12.54	0.95*2

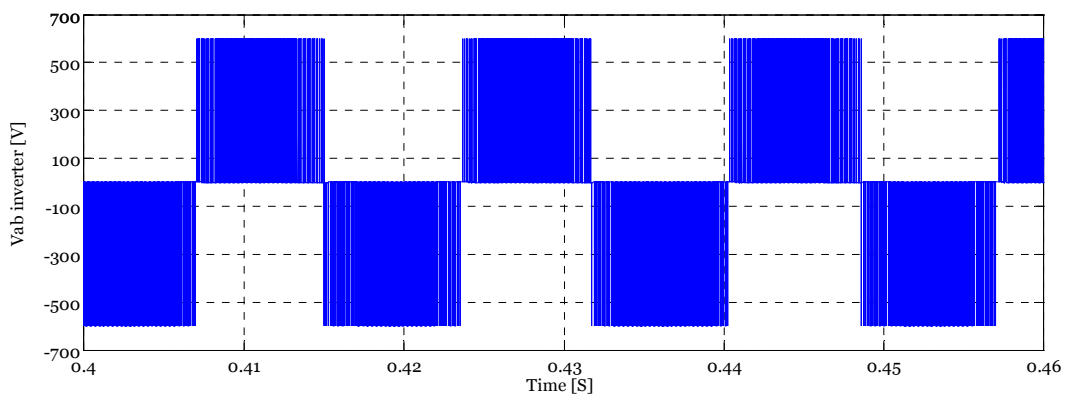


Figure 6.39 Zoomed out view for 600m  $V_{ab}$  inverter vs time with calculated  $L_f C_f$  filter

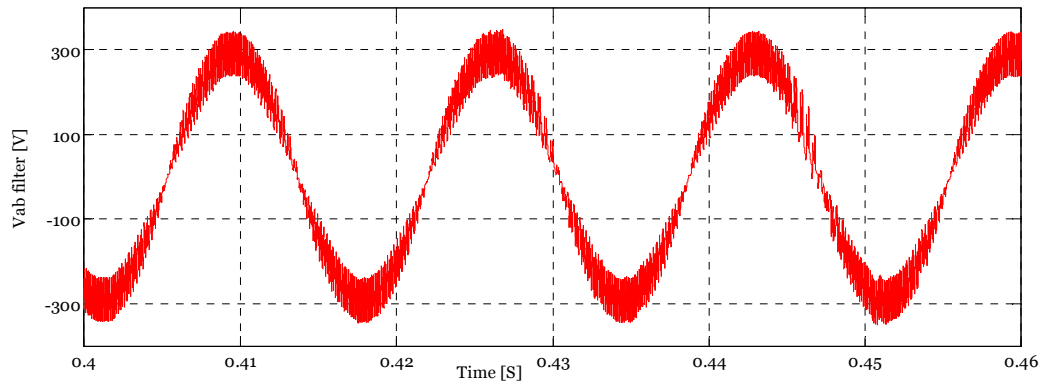


Figure 6.40 Zoomed out view for 600 m  $V_{ab}$  filter vs time with calculated  $L_f C_f$  filter

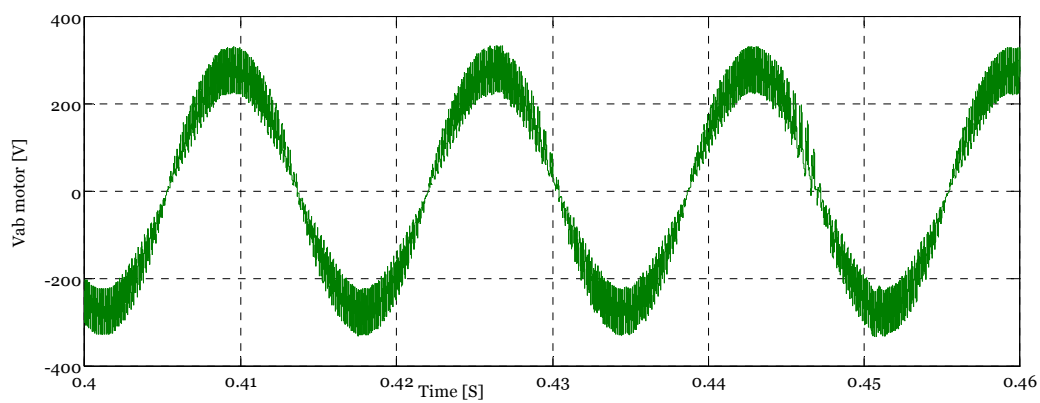


Figure 6.41 Zoomed out view for 600 m  $V_{ab}$  motor vs time with calculated  $L_f C_f$  filter

Figure 6.42, depicts the THD of inverter, filter and motor results using an  $L_f C_f$  filter at the inverter terminal.

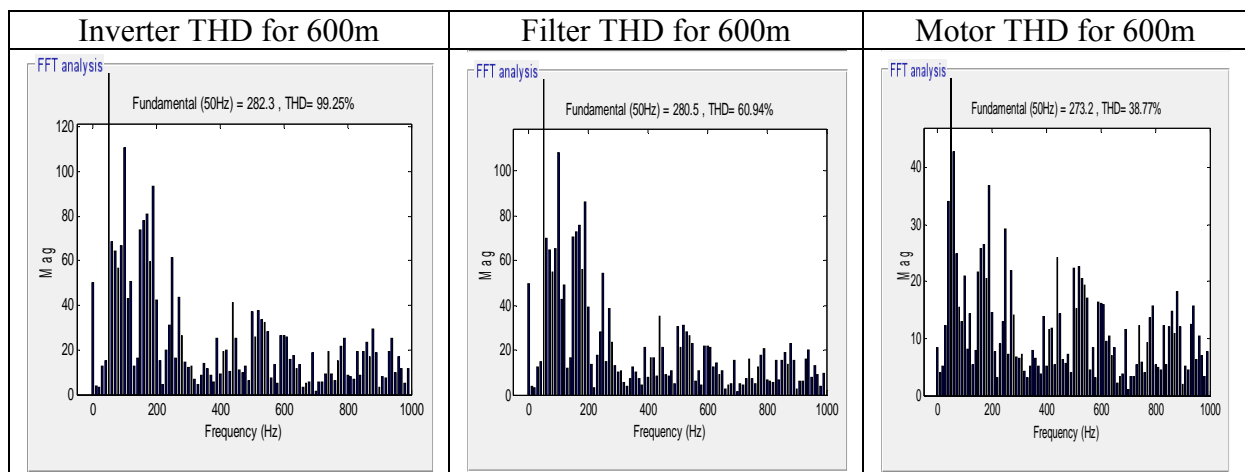


Figure 6.42 THD for inverter, filter and motor when the cable length is 600 m

## 6.6 The tool (GUI environment)

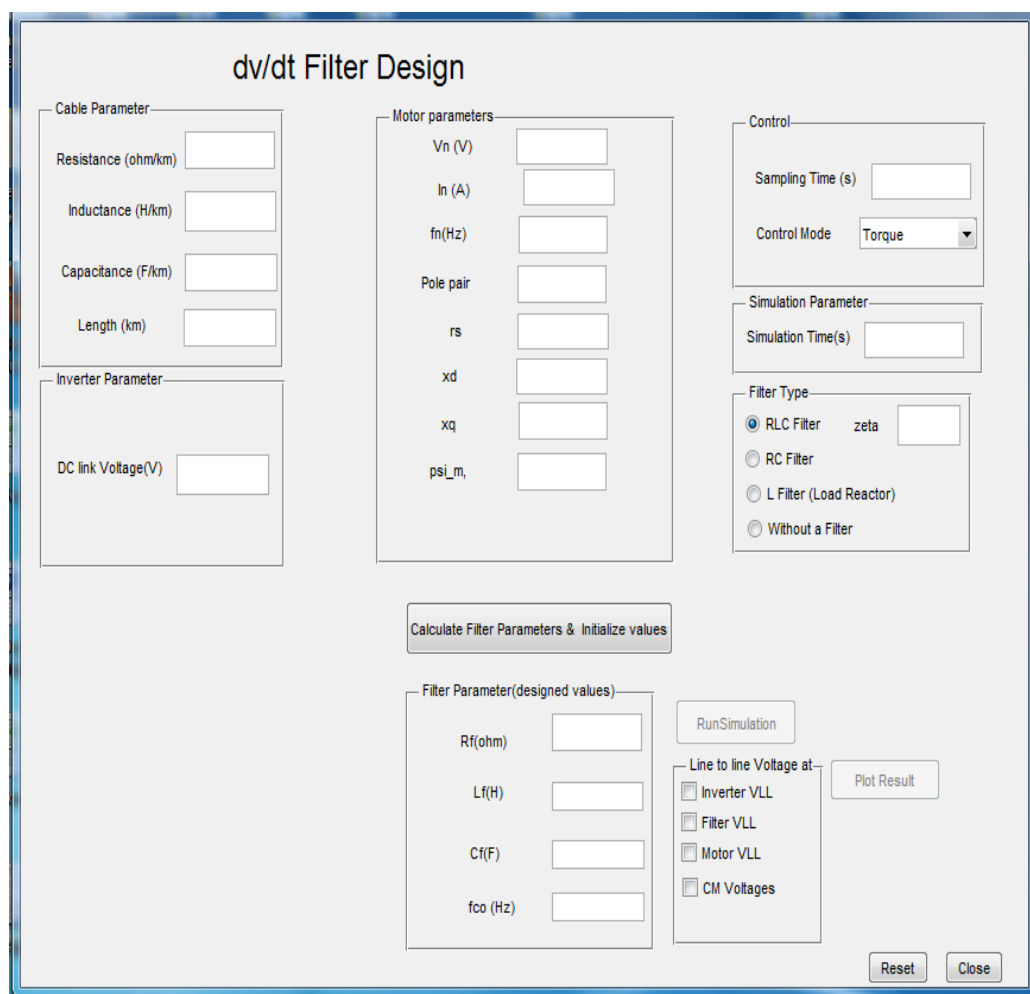


Figure 6.43 GUI user interface tool

The use of this GUI tool was to make the design of dv/dt filter and system simulation easy for the user, the following section guide how it can be used. Matlab code is found in appendix B.

### 1. Cable parameter group

The user can inputs the cable resistance  $R_c$  (ohm/km), cable inductance  $L_c$  (H/km), cable capacitance  $C_c$  (F/km) and cable length (km) in this group.

### 2. Inverter parameter group

The user can input the DC link voltage through **DC link voltage (V)** in this group.

### 3. Motor parameters group

The user can inputs the  $V_n$  (V),  $I_n$  (A),  $f_n$  (Hz), pole pair,  $r_s$  (pu),  $x_d$  (pu),  $x_q$  (pu) and  $\psi_{il\_m}$  in this group.

### 4. Control group

The user can input the sampling time (s) and control mode i.e torque or speed in this group.

5. Simulation parameter

The user can limit the duration of the simulation time using the input **simulation time (s)**.

6. Filter type group

The user can select  $R_fL_fC_f$ ,  $R_fC_f$  or  $L_f$  filter types from this group. Zeta ( $\xi$ ) only can be selected if  $R_fL_fC_f$  filter type is chosen.

7. A click on push button '**Calculate Filter Parameter & Initialize values**'

First, the filter parameters are calculated based on the design assumptions and method presented in chapter four. The calculated filter parameters will be displayed to the user. Then GUI automatically passes all the necessary variables to the Matlab Simpow model under use (system model using two level inverter). Finally, it enables on the push button '**Run Simulation**'.

8. A click on push button '**Run Simulation**'

It lets the user to run the Matlab Simpow model. When the simulation is completed, the push button '**Plot Result**' is enabled thereby the simulation results are ready for use.

9. Output line to line voltage selectors:

The GUI also allows the user to choose one and/or a combination of the three simulation outputs (Inverter output voltage, Filter output voltage Motor voltage, CM voltage) using the check boxes.

10. A click on push button '**Plot Result**'.

It plots the selected output voltage (s) in separate figure (s) based on the selection in guide 6.

11. A click on push button '**Reset**'.

It clears all the inputs and outputs and prepares the GUI for another use.

12. A click on push button '**Close**'. And it exits the **GUI tool**.

## 6.7 Summary of comparison filter types

A simulation models were developed in Matlab to simulate the effect of  $dv/dt$  and overvoltage when the motor terminals fed by long cable. Simulations were made for the cable lengths of 100 m, 300 m and 600 m fed the motor. The parameters of the cable are shown in table 6.2.

Figure 6.1 through figure 6.42, show the simulation models, results of THD and the normalized line to line voltage at the inverter, filter and motor terminals with the filters discussed in chapter four.

For 100 m cable length, figure 6.17 shows that the voltage at the motor terminal was suppressed with a maximum overshoot of 20 % which was achieved by placing an  $R_fC_f$  at the motor terminal. Figure 6.25 and 6.32 show the effect of overvoltage elimination after using an  $R_fL_fC_f$  filter and  $R_fL_fC_f$  split RC to +/- DC link filters at the inverter terminals for which case the voltage overshoots are 7 % and 2 %, which are somewhat lower than of an  $R_fC_f$  filter. Figure 6.5 shows the simulation results of line reactor ( $L_f$ ) filter installed at the inverter terminal. For this filter, the overshoot is 150 %. This is shown that the filter is not compatible for the chosen parameter of cable.

For 300 m and 600 m cable length, figure 6.18 and 6.19 show the simulation results of  $R_fC_f$  filter installed at the motor terminal was suppressed with a maximum overshoot of 24 % and 10 % consecutively, figure 6.26 and 6.27 show the effect of overvoltage elimination after using an  $R_fL_fC_f$  filter at the inverter terminal, for which case the voltage overshoots are 6 % and 3 %. Figure 6.33 and 6.34 also show the overvoltage filtered by  $R_fL_fC_f$  split RC to +/- DC link filter with a maximum overshoot of 8 % and 0 % at the motor terminal.

For 600 m cable length, figure 6.41 shows, using  $L_fC_f$  filter at the motor terminal was effectively suppressed with an overshoot of 0 %.

Figure 6.17 shows using the  $R_fC_f$  filter at the motor terminal has shown a good switched voltage waveform, faster response and smaller settling time. Figure 6.25 and 6.32 shows using  $R_fL_fC_f$  and  $R_fL_fC_f$  split RC to +/- DC link filter topologies give a good switched voltage waveform at the motor terminal and they did fulfill chapter 4 i.e  $dv/dt$  definition of IEC and NEMA standard.

Figure A.31-A.34 in appendix A6 and A7 show,  $R_fL_fC_f$  split RC to +/- DC link filter and  $L_fC_f$  filter topologies are the best, in terms of eliminating the common mode noise voltage at the motor terminals.

Moreover, for comparison, it is best to consider the results until 100 m cable length (for  $R_fC_f$ ,  $R_fL_fC_f$  and  $R_fL_fC_f$  split RC to +/- DC link filter types) because greater than 100 m cable length the system was shows instability. And figure 6.19, 6.27 and 6.34 show the normalized line-to-line voltage have under voltage at the motor terminals.

Table 6.8 Summary results of filters when motor fed by 100 m cable length

Comparative factors	Various types of filters for 3-phase 600-V motor fed by 100 m cable				
	Reactor @inverter	R <sub>f</sub> C <sub>f</sub> filter @motor	R <sub>f</sub> L <sub>f</sub> C <sub>f</sub> filter @inverter	R <sub>f</sub> L <sub>f</sub> C <sub>f</sub> filter split RC to +/- dc link @inverter	L <sub>f</sub> C <sub>f</sub> filter @inverter
Resistors(R <sub>f</sub> )	-	72 Ω	35 Ω	35 Ω	-
Inductors(L <sub>f</sub> )	7.65e-5 mH	-	0.16e-3 mH	0.16e-3 mH*2	-
Capacitors(C <sub>f</sub> )	-	61.75 nF	2.01e-6 μF	1.04e-6 μF	-
Voltage overshoot	150 %	20 %	7 %	2 %	-
THD @motor terminal	1856.61 %	125.75 %	64.89 %	49.93 %	-
Power losses	Low	High	High	High	-

Table 6.9 Summary results of filters when motor fed by 300 m cable length

Comparative factors	Various types of filters for 3-phase 600-V motor fed by 300 m cable				
	Reactor @inverter	R <sub>f</sub> C <sub>f</sub> filter @motor	R <sub>f</sub> L <sub>f</sub> C <sub>f</sub> filter @inverter	R <sub>f</sub> L <sub>f</sub> C <sub>f</sub> filter split RC to +/- dc link @inverter	L <sub>f</sub> C <sub>f</sub> filter @inverter
Resistors(R <sub>f</sub> )	-	72 Ω	35 Ω	35 Ω	-
Inductors(L <sub>f</sub> )	7.65e-5 mH	-	0.47e-3 mH	0.47e-3 mH*2	-
Capacitors(C <sub>f</sub> )	-	185.2 nF	6.02e-6 μF	3.01e-6 μF	-
Voltage overshoot	150 %	24 %	3 %	8 %	-
THD @motor terminal	2151.75 %	635.13 %	80.55 %	57.25 %	-
Power losses	Low	High	High	High	-

Table 6.10 Summary results of filters when motor fed by 600 m cable length

Comparative factors	Various types of filters for 3-phase 600-V motor fed by 600 m cable				
	Reactor @inverter	R <sub>f</sub> C <sub>f</sub> filter @motor	R <sub>f</sub> L <sub>f</sub> C <sub>f</sub> filter @inverter	R <sub>f</sub> L <sub>f</sub> C <sub>f</sub> filter split RC to +/- dc link @inverter	L <sub>f</sub> C <sub>f</sub> filter @inverter
Resistors(R <sub>f</sub> )	-	72 Ω	35 Ω	35 Ω	-
Inductors(L <sub>f</sub> )	7.65e-5 mH	-	0.95e-3 mH	0.95e-3 mH*2	0.95 mH*2
Capacitors(C <sub>f</sub> )	-	370.51 nF	12.54e-6 μF	6.27e-6 μF	12.54 μF
Voltage overshoot	150 %	10%	0 %	0 %	0 %
THD @motor terminal	3374.38 %	1789 %	82.84 %	79.71 %	38.77 %
Power losses	Low	High	High	High	Low

Simulation results and the comparative factors shows that each filter has its pros and cons, an  $R_f C_f$  at motor terminal is the best; in terms of faster response and smaller settling time, the  $R_f L_f C_f$  filter at the inverter terminal may be the most convenient in terms of eliminating the overvoltage. An  $L_f$  filter at the inverter terminal is the best; in terms of power losses.

How to select and solve the problem of overvoltage and  $dv/dt$  should be decided by the designers based on their specification and requirement.



## 7 Introduction to conducted EMI measurement

Any electrical device has to operate in its electromagnetic environment without disturbing or being disturbed by other devices. Every product designer has to know that EMI compliance testing is important in their product development process. To ensure successful EMI compliance testing, it is useful to add pre-compliance testing in the development cycle. During pre-compliance testing, the EMC performance is evaluated from design through production units [38].

Many product designers use EMI pre-compliance measurement systems to perform conducted and radiated EMI emissions evaluation prior to sending their product to a test facility for full compliance testing.

This chapter provides background information the method that is used for conducted EMI pre-compliance testing. In addition also it is discussed measuring instrument that is used for EMI measurement system and gives description how the laboratory setup and the EMI measurement results looks like.

### Radio frequency (RF) emission

EMI measurements require a different approach than other types of general RF tests. RF emissions tests are one of the basic requirements for electromagnetic compatibility compliance of most electronic and electrical products [4]. The purpose of this test is to ensure that other users are protected from the emissions generated when the product is used in their neighborhoods. Everything from phone, computer, converter, motor, wind turbine and downhole systems go through this process.

Conducted and radiated emission test is differentiated based on their radio frequency range. Conducted emissions (CE) testing focuses on unwanted signals is generated by the device under test (DUT) and traverses on the AC mains input cables or any interconnecting cables including the output. The frequency range for this commercial measurement is from 150 kHz to 30 MHz. Radiated emissions (RE) testing looks for signals broadcasted by the DUT through space. The frequency range for this measurement is between 30 MHz and 1 GHz.

But in conducted EMI compliance tests measurement, the CM and DM noise components are irrelevant. However, they are of the utmost importance in the design stage during pre-compliance testing.

### RF emission limit

Measurements of the RF emissions generated by electronic devices are nearly always prompted by the need to conform to harmonized standards limiting these emissions. These standards are in turn designed to preserve the usability of the radio spectrum for its legitimate users—broadcasting, communications, navigation and so forth [4, 39].

Lists of the most common standards that apply to users are given in chapter three. Most of these standards within the EN 660XX series have harmonized limit levels for conducted and radiated emissions. [39].

According FCC (Federal Communications Commission), those standards within the EN 660XX series divided in general in to two parts non-consumer products and consumer products. The following figure shows the limits in graphical form for the emissions standards discussed above [39].



Figure 7.1 Conducted limits [39]

From FCC the two categories that products can fall are class A (non-consumer products) and class B (consumer products). Class A referees to a product that is intended to use for commercial, industrial, light-industry environments and may be used in residential, where class B device is a product that is intended to use for residential or home, as it can see in the above figure class B requirements stricter than class A requirements.

The following topic discussed measurement instruments that are needed for conducted emission test.

## 7.1 Measurement instrumentation

### Spectrum analyzer

EMI conformance test measurements are normally taken with a spectrum analyzer. Spectrum analyzer measures power, frequency and noise. This instrument measures the amplitude of signals in the frequency range domain. The main feature of this device is, it helps to see EMI noise from the frequency range 9 kHz-3 GHz.

For this thesis EMI measurement were made by using Agilent N9000A series CXA signal analyzer, figure 7.2 [40].



Figure 7.2 Agilent spectrum analyzer N9000A series CXA signal analyzer

### Transducers for CE measurements

Most of the time transducers for CE measurements are voltage probe and current probe. The following topic discussed these transducers that are used for the laboratory measurement.

### Transducers

For any RF emissions measurement a device is needed to couple the measured variable into the input of the measuring instrumentation. Measured variable take one of three forms [4].

- Radiated electromagnetic field
- Conducted cable voltage
- Conducted cable current

And their measuring units are as follows:

- EMI noise voltage level measurement unit is  $\text{dB}\mu\text{V}$
- EMI noise current level measurement unit is  $\text{dB}\mu\text{A}$
- EMI H Field level measurement unit is  $\text{dB}\mu\text{A}/\text{m}$
- EMI E Field level measurement unit is  $\text{dB}\mu\text{V}/\text{m}$

### Voltage probe

A voltage probe is a valuable tool for EMI measurement. For the lab setup, the Agilent 41800A series active Probe is used, the main feature of this probe is, it has high input impedance from 5 Hz - 500 MHz [40].



Figure 7.3 Agilent 41800A series active Probe

## Current probe

The use of current probe is to measure the common mode and the differential mode noise that comes from the DUT, this probe can be directly connected to the voltage probe then the voltage probe goes to the spectrum analyzer and sees the noise form this. The selected current probe for the lab setup is PEARSON current monitor model 110 series. Key feature of this model is; it can measure in the frequency range from 1 Hz -20 MHz [41].



Figure 7.4 Pearson current Probe

## Line impedance stabilization network (LISN)

When testing a device for compliance to the EN 55022 or other standards, a LISN must be inserted between the AC or DC input or output power cord of the DUT. For input power, depending on the product the source could be the commercial power outlet or even a battery. The purpose of LISN is to provide stabilized impedance to conducted emissions and isolate noise from source (mains or DC) to DUT, without interfering with the normal power flow required by the DUT. The LISN's internal circuit is defined in CISPR 16-1 and its internal circuit is shown in figure 7.5.

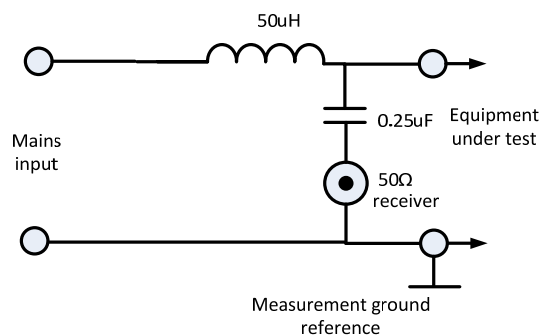


Figure 7.5 Internal circuit of LISN-50-50-4

The LISN contains inductors, capacitors and resistors. For 50/60 Hz line frequency, the inductors are basically shorted; the capacitors are open and the power and frequency passes through to supply the DUT. For EMI noise frequency, the inductors are essentially open, the capacitors are shorted and the noise sees a 50 Ω resistor at the measuring point due its 50 Ω termination, which is usually used [42]. The following section elaborates this phenomenon more.

## Frequency response of LISN

The following graph shows the frequency response of LISN from 9 kHz -30 MHz. Note that its impedance is not defined above 30 MHz; partly because commercial conducted measurements are not required above this frequency (aerospace and automotive standards do call for conducted tests above 30 MHz, but use different circuit values) [4].

Even if the LISN helps isolates noise from source to DUT, the pure noise separation starts to occur when the frequency range is approximately greater than 1 MHz and the impedance is 50  $\Omega$ . After this range the impedance is constant (50  $\Omega$ ), and the noise only see this impedance value.

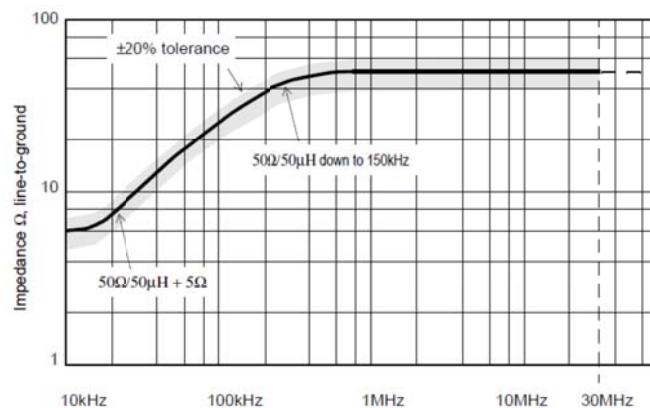


Figure 7.6 LISN impedance versus frequency

One approach to measure the noise of DUT is by connecting fiber cable directly from LISN to 50  $\Omega$  input impedance of a spectrum analyzer. Further explanation made under measurement of CM noise from LISN.

Another approach is to see the noise of the DUT from the spectrum analyzer by using current probe. Further explanation made under Measurement of CM and DM noise by using the current probe.

FCC-LISN-50-50-4 type is used for test measurement [43].



Figure 7.7 FCC-LISN-50-50-4

## Typical conducted emission measuring set-up

According to EN 55022, the typical requirement placement of layout for conducted emission test set up shown in the following diagram, this is one type of method that is used to test compliance with conducted emissions limits.

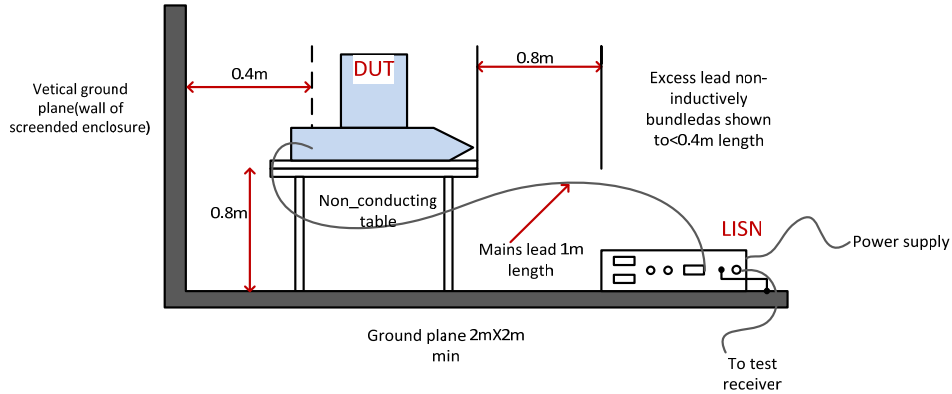


Figure 7.8 Typical conducted emission measuring lab set-up

As shown in the above diagram, the AC power cord of the DUT is plugged into the output of the LISN, and the input LISN is plugged into the commercial power system outlet, then the test receiver connected to the LISN and conducted interference can be determined by measuring the voltage developed across the LISN 50  $\Omega$  measuring resistor without the need for a current transducer.

## Conducted EMI measurement

### 7.2 Test circuit one

For the first part of the laboratory measurements, the chopper was used as test circuit for the investigations of conducted EMI pre-compliance test. The following figure represents EMI measurement lab setup.

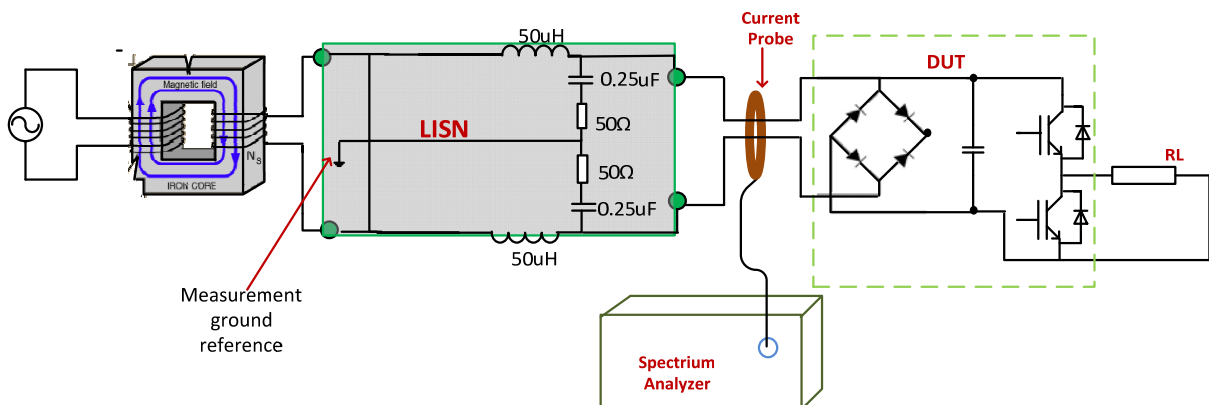


Figure 7.9 EMI measurement laboratory setup

The AC power supply was plugged in the input of transformer, and the output of the transformer was plugged in to the LISN, the ground terminal of the LISN is used as the

reference for the whole setup, and the output of the LISN goes to the DUT, then the LISN filtered the AC power supply noise. However from the power flow point of view, the DUT was the load but from the conducted EMI point of view, the DUT was the source because it produces the noise, which should not exceed the limits in the standards.

A spectrum analyzer measured the conducted emissions from the DUT by using the current probe or by directly connected to the LISN.

The following section discusses how one can use the current probe for measuring CM noise and DM noise in the test circuit.

### Measurement of CM noise by using the current probe

Figure 7.10, shows the current probe that is configured to measure the CM emission, the two power line that passes the hole of the current probe are; it may the input power line that goes to DUT or output power line that comes from DUT and plugged to the load etc. This kind of measurement needed when someone wants to measure CM emission from different point of test circuit. For example, EMI compliance test can be made by taking CM emission measurement between the connecting power line of LISN and DUT.

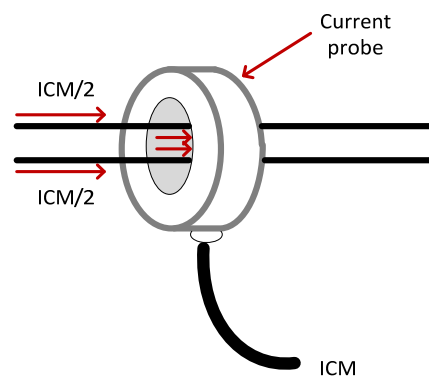


Figure 7.10 Line and neutral inserted into the probe for CM noise measurement

### Measurement of DM noise by using the current probe

Figure 7.11, shows the current probe that is configured to measure the DM emission, unlike CM emission measurement the first power line directly passes through the hole of the current probe, the second power line instead of going directly to the hole, it roll in upper side of the current probe and goes through the hole. This is helpful to make the DM current in anti-parallel mode. These two power line that passes through the hole of the current probe were, it may the input power line that goes to DUT or output power line that comes from DUT and plugged to the load etc. This kind of measurement needed when someone wants to measure DM emission from different point of test circuit. For example, the source of DM emission due to the current switched by IGBTs or diodes can be measured in this way.

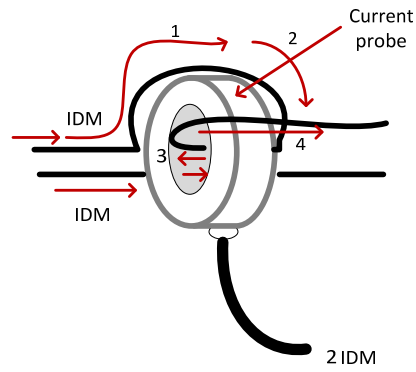


Figure 7.11 Line and neutral inserted into the probe for DM noise measurement

### Measurement of CM noise from LISN

From figure 7.8, conducted interference can also be determined by measuring the voltage developed across the LISN impedance ( $50\ \Omega$  measuring resistor) without the need for a current transducer. Most often this method is preferable compared to the current probe measurement, because EN 55022 standard recommends EMC compliance test according to this method.

### Comparison results for CM noise measurement from LISN and from current probe

The following figure presents the comparison that was made common mode noise measurement by using current probe and  $50\ \Omega$  receiver point of LISN.

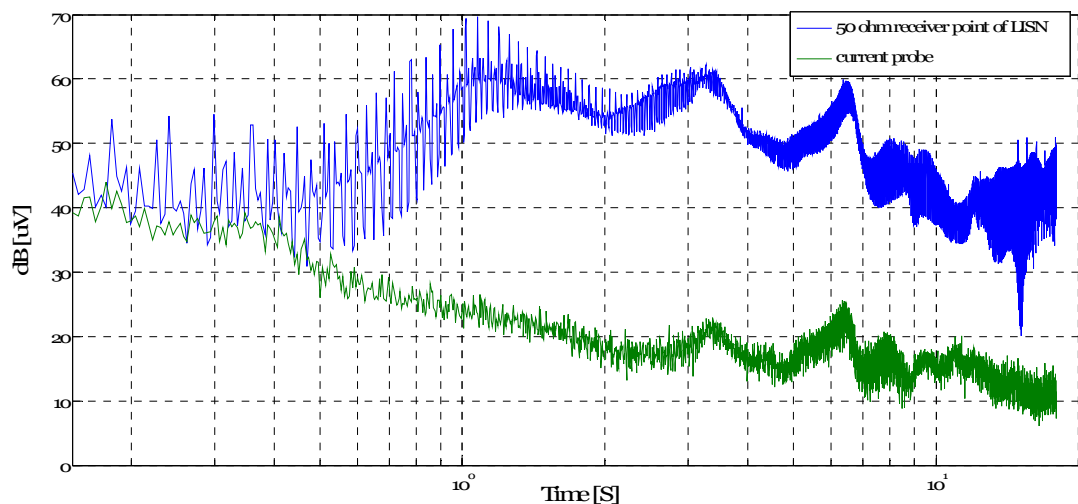


Figure 7.12 Measurement by using current probe and  $50\ \Omega$  receiver point of LISN

The influence of instrument on common mode noise measurement is tested, first from current probe then from  $50\ \Omega$  receiver point of LISN. In order able to compare the difference, their input voltage, switching frequency, duty cycle, gate resistance and RL load are kept constant.

Note that, current probe measurement has to be shifted 4 units up [1 unit= $10\ \text{dB}\mu\text{V}$ ] to get comparable result against measurement from LISN. In general  $20\ \text{dB}\mu\text{V}$  denoted  $20\ \text{dB}\mu\text{V} + [10\ \text{dB}\mu\text{V} + 10\ \text{dB}\mu\text{V} + 10\ \text{dB}\mu\text{V} + 10\ \text{dB}\mu\text{V}] = 60\ \text{dB}\mu\text{V}$ .



As shown in the graph after 1 MHz, the current probe and the LISN results appear almost similar in pattern. However before 1 MHz, the graph patterns are completely different. The reason behind this can be seen from impedance frequency response curve figure 7.6. The LISN can fully isolate noise from source to DUT, when the frequency range approximately greater than 1 MHz and the impedance is  $50 \Omega$ . This means that before 1 MHz range, the LISN sees the noise from AC power supply plus from the DUT. Unlike this the current probe measures only the CM noise from DUT i.e. from the two power lines. Thus a method of current probe measurement helps to see DUT common mode noise from 150 kHz to 30 MHz while LISN measurement see the noise of DUT from 1 MHz- 30 MHz.

## 7.3 Experimental results

### 7.3.1 The influence of reverse recovery on EMI

#### Switching characteristics

A power diode requires a finite time to switch from the blocking state (reverse bias) to the on state (forward bias) and vice versa. The user must be concerned not only with the time required for the transitions but also with how the diode current and voltage vary during the transitions. Both the transition time and the shapes of the waveforms are affected by the intrinsic properties of the diode and by the circuit in which the diode is embedded [6].

The switching properties of a diode are often given on specification sheets for diode current with a specified time rate of change,  $di/dt$  as shown figure 7.13. The reason for this selection is that power diodes are very often used in circuits containing inductance that control the rate of change of the current, or the diodes are used as freewheeling diodes where the turn off of a solid-state device controls  $di/dt$  [6].

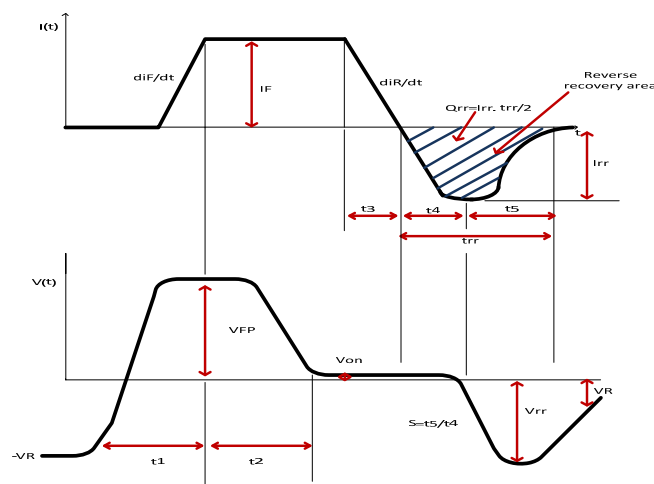


Figure 7.13 Switching properties of a diode voltage and current vs time

#### The influence of reverse recovery on EMI

The term reverse recovery time refers to the time associated during switching from the conducting to the blocking state of a diode as its stored charge that must first be discharged before the diode blocks reverse current. This discharge takes a finite amount of time known as

the reverse recovery time, or  $t_{rr}=t_4+t_5$  as shown in Figure 7.13. During this time, diode current may flow in the reverse direction [6,44].

As shown figure 7.13, the area that is shaded at the interval of  $t_{rr}$  and  $I_{rr}$  gives the charge  $Q_{rr}$  where,  $I_{rr}$  is the reverse recovery current. Most often diode specification sheets give detailed value of  $I_{rr}$  and  $Q_{rr}$  in addition with other diode parameter values.

When it comes to EMI, reverse recovery characteristic of diode is one type of phenomenon that influences EMI and will be tested in the test circuit. A lower or shorter recovery time creates high EMI than a longer or slower recovery time. However diodes with shorter recovery time have reduced recovery losses resulting in improved converter efficiency and are often preferred. Diodes whose recovery current decays smoothly approach are called soft recovery diodes and these generate the least EMI. Representative characteristics of these types are shown in figure 7.14 [45].

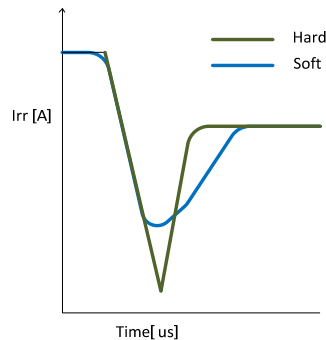


Figure 7.14 Reverse recovery current waveforms

## Result discussion

For the test circuit, measurements were made to compare two different IGBT modules having different recovery time of the internal freewheeling diode, by replacing them one at a time in the test circuit.

Conducted emission measurement made until 20 MHz since the current probe measured in the frequency range from 1 Hz -20 MHz.

The following table presents the freewheeling diode parameter values  $I_{rr}$  and  $Q_{rr}$  which is found in the IGBT specification data sheet.

Table 7.1 Data sheet

IGBT type	Values		
SKM400GB123D	$I_{rr}=140$ A	$Q_{rr}=13$ $\mu$ C	$t_{rr}=(2*Q_{rr})/I_{rr}=0.185$ $\mu$ s
SKM50GB063D	$I_{rr}=23$ A	$Q_{rr}=2.3$ $\mu$ C	$t_{rr}=(2*Q_{rr})/I_{rr}=0.2$ $\mu$ s

The influence of reverse recovery on EMI tested by replacing hard reverse recovery current IGBT by soft reverse recovery current IGBT was measured. In order to be able to compare the difference, their input voltage, switching frequency, duty cycle, gate resistance and RL load are kept the same.

Both the voltage and current output of the DUT are shown separately on the same axis, in figure 7.15 and 7.16. In addition also DM EMI noise level for hard, soft recovery current and background noise on the same axis shown in figure 7.17.

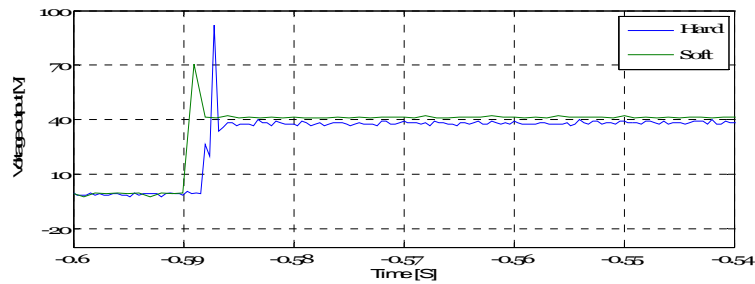


Figure 7.15 Voltage output vs time for hard and soft recovery current

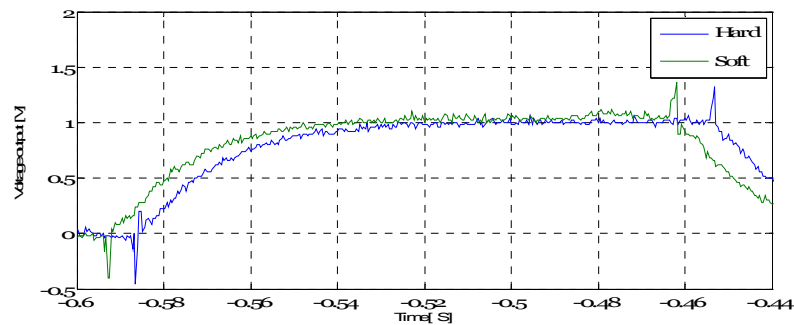


Figure 7.16 Current output vs time for hard and soft recovery current

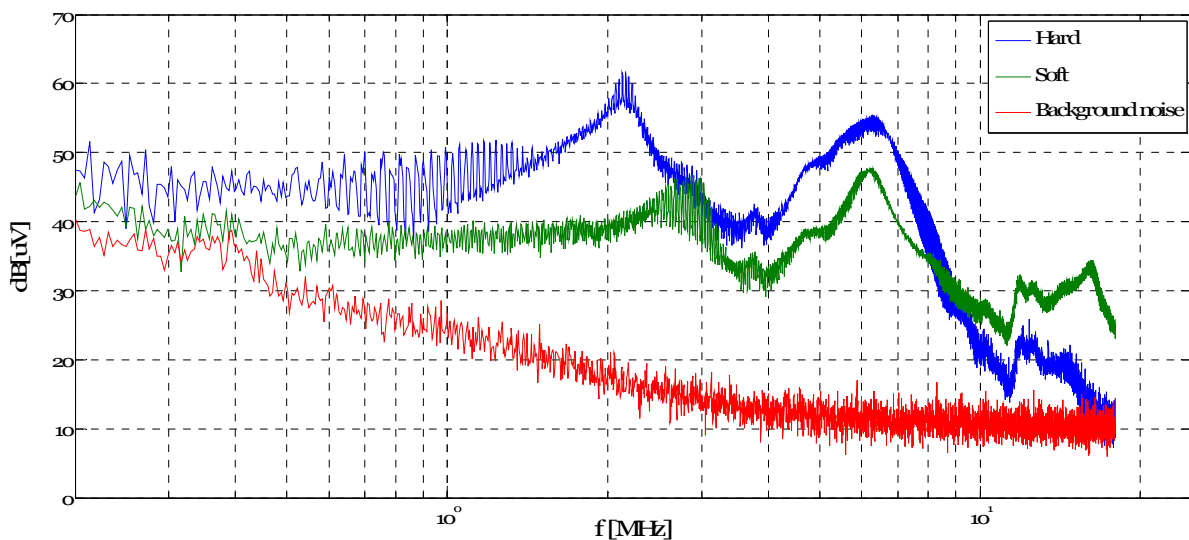


Figure 7.17 Differential mode noise level for hard and soft recovery current

From the result in figure 7.17, it can be concluded that the current with soft recovery compare to hard recovery freewheeling diode has less harmonics almost until 9 MHz where as hard recovery of the diode has high harmonics in this range. Keeping this in mind, one has to know for the IGBT modules the diode recovery characteristics is not the only characteristic that defines EMI phenomenon; their construction, other parameter value etc. may have also influence.

### 7.3.2 The influence of stray or leakage inductance on EMI

Stray inductance ( $L\sigma$ ) results in electromagnetic radiation that causes overvoltage in the circuit. Most of the practical causes are inappropriate design of the circuit, poor PCB layout and unshielded leads. The high  $di/dt$  is the one which has significant overvoltage in power converters due to stray inductance of current loops [46].

The DUT consists of the IGBT and the DC-link capacitor. At turn-off of the IGBT, large overvoltage may develop across it due to large values of  $dI_E/dt$  if the stray inductance is not minimized.

A positive gate current  $I_G$  that turns the IGBT on, which in turn causes the collector current  $I_c$  to increase rapidly. The stray inductance will induce voltage that will tend to reduce the gate current. If this then causes a reduction in the collector current, there will be a subsequent negative  $dI_c/dt$  and a voltage induced that will cause an increase in  $I_G$ . This then represents the start of unwanted oscillations [6].

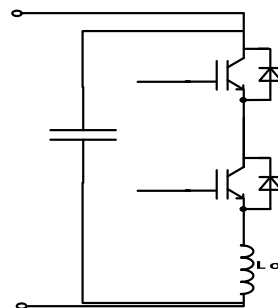


Figure 7.18 Stray inductance in the circuit

#### Reduction of stray inductance between dc bus bar

To overcome this problem, replacing DC bus bar cable line by copper plate strips line reduces magnetic flux and hence EMI as this helps to cancel magnetic flux in the copper plate [6].

Copper strips, with a thin insulator sandwiched between them as shown in figure 7.19, comprises a line and provide an excellent means of reducing the stray inductance. Figure 7.20, shows how the copper strip connected in power terminal [6].

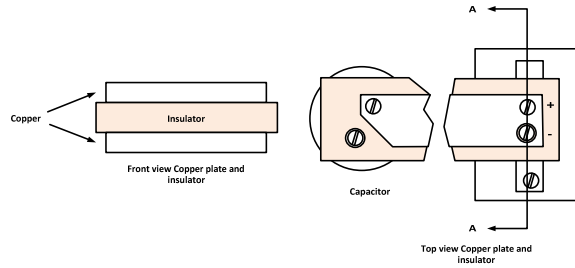


Figure 7.19 Front and top view of copper plate strip

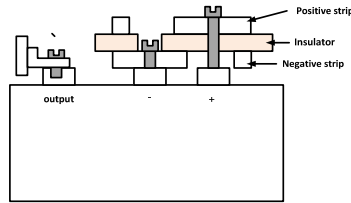


Figure 7.20 Example of copper plate strip

### Result discussion

The influence of stray or leakage inductance on EMI was tested by replacing the DC bus bar cable lines by copper plate strips lines. In order to be able to compare the difference, their input voltage, switching frequency, gate resistance, duty cycle and RL load are kept the same.

Both the voltage and current output of the DUT are shown separately on the same axis, with regular cable of wire and with copper strips in figure 7.21 and 7.22. In addition also DM EMI noise level with regular cable of wire and with copper strips and background noise on the same axis is shown in figure 7.23.

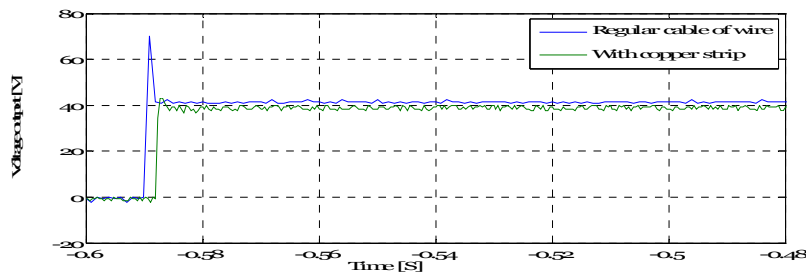


Figure 7.21 Voltage output vs time with regular cable of wire and with copper strip

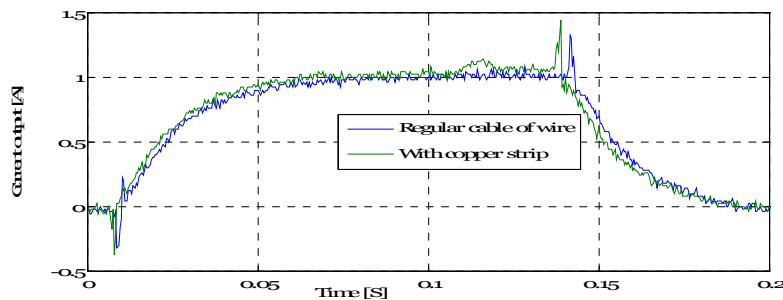


Figure 7.22 Current output vs time with regular cable of wire and with copper strip

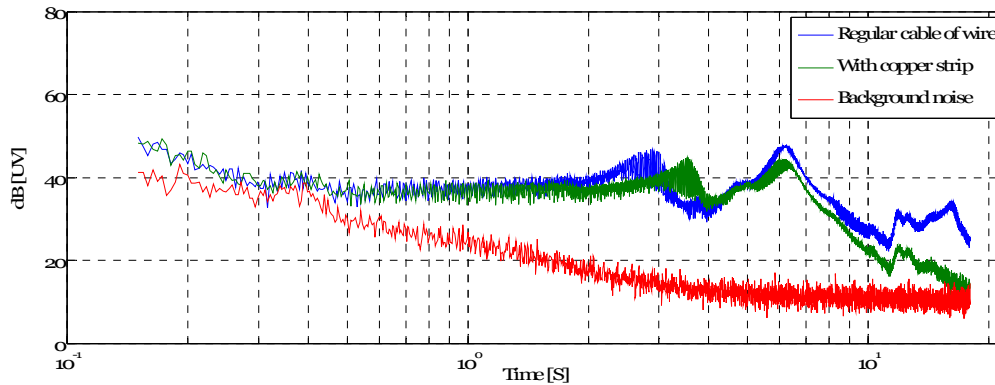


Figure 7.23 DM EMI noise level with regular cable of wire and with copper strip

From the result in figure 7.23, it can be concluded that replacing DC bus bar cable line by copper plate strips lines reduce the EMI noise after 5 MHz.

### 7.3.3 The influence of gate drive resistance ( $R_g$ ) on EMI

The switching behavior of IGBT is controlled by the gate capacitance recharge. This gate capacitance recharge may be controlled via a gate resistor.

As the gate capacitance of an IGBT is charged and discharged the gate resistor will dictate what time is needed to do this by limiting the magnitude of the gate current ( $I_g$ ) pulses during turn-on and turn-off. Due to the increase in the gate peak current, which is affected by reducing the turn-on and turn-off gate resistor values  $R_g$  (on) and  $R_g$  (off), the turn-on and turn-off time will be shorter and the switching losses will be reduced. But in contrary reducing the turn-on and turn-off gate resistor value  $R_g$  (on) and  $R_g$  (off) leads to increase EMI,  $dv/dt$  and  $di/dt$  in the circuit [47].

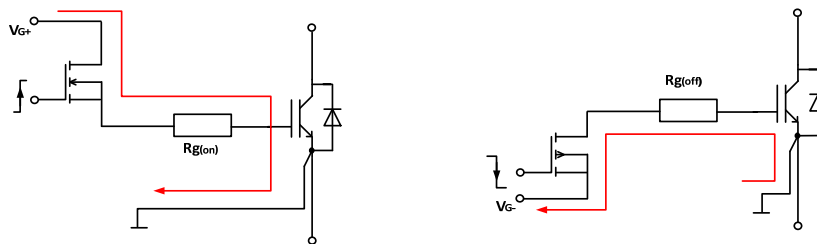
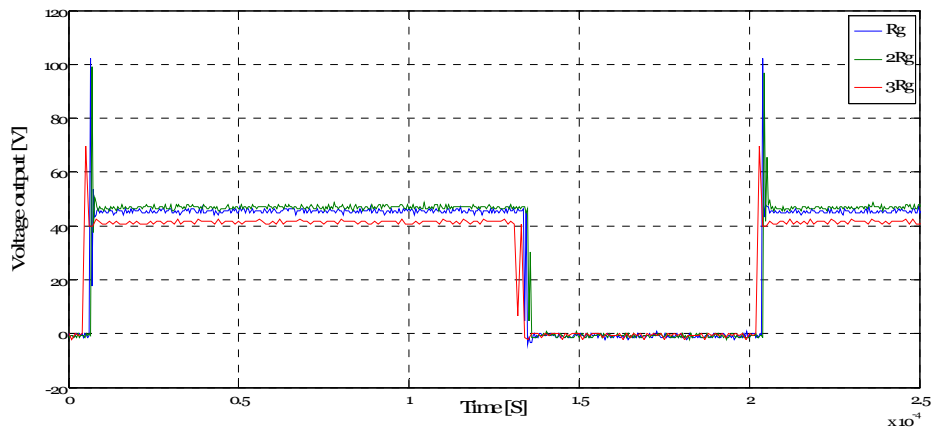
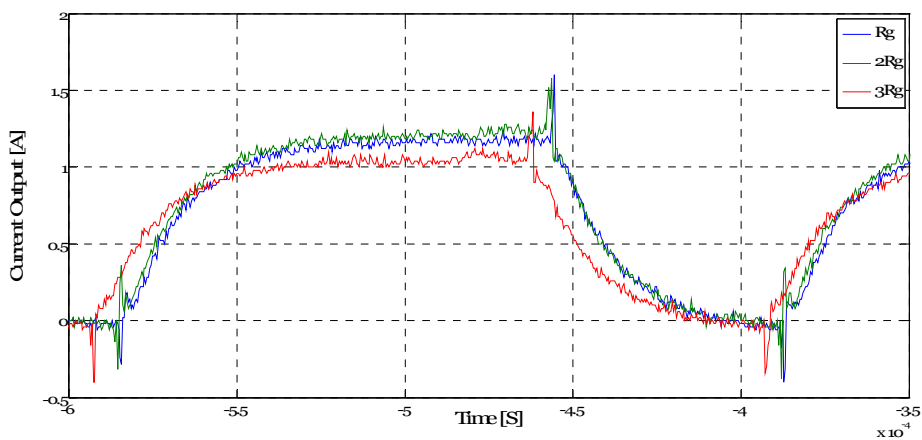
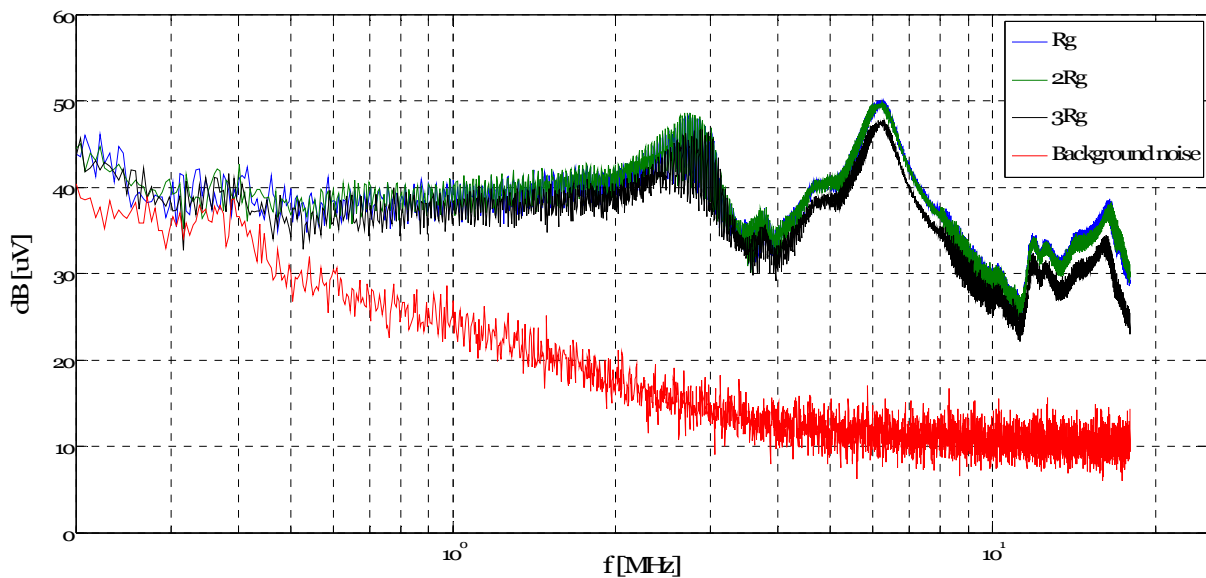


Figure 7.24 Turn on and turn off gate resistance

### Result discussion

The influence of  $R_g$  on EMI was tested by replacing different gate resistance values once at a time. In order to able to compare the difference, their input voltage, switching frequency, duty cycle and RL load are kept the same.

Both the voltage and current output of the DUT are shown separately on the same axis, with different gate resistance values in figure 7.25 and 7.26. In addition also DM EMI noise level with different gate resistance values and background noise on the same axis is shown in figure 7.27.

Figure 7.25 Voltage output vs time for different  $R_g$ Figure 7.26 Current output vs time for different  $R_g$ Figure 7.27 DM EMI noise level for different  $R_g$ 

From the result in figure 7.27, it can be concluded that when the  $R_g$  decreases EMI increase proportionally until 20 MHz.

### 7.3.4 The influence of heat sink grounding on EMI

In modern power electronics, fast operation of devices leads to further heat generation due to switching losses. This heat needs to be dissipated through a heat sink to keep the devices within safe operating condition [48].

As using a heat sink helps dissipate the heat generated, grounding heat sink increases conducted EMI due to capacitive coupling of switching noise from the device's drain or collector or cathode through the thermally conductive insulator between the device and the heat sink. In many power electronics applications heat sinks are often not grounded. The reason behind this the high  $dv/dt$  rates initiate CM current through the parasitic capacitance to the ground created by the insulation between IGBT collectors or MOSFET drain or diode cathodes to the heat sink [49].

In other words, if the heat sink is grounded, the CM currents from the device increase i.e. conducted EMI raises. On the other hand if the heat sink is not grounded, the CM currents from the device decrease, but the heat sink acts as a voltage driven antenna and can become a highly efficient antenna emission when EMI resonant phenomenon occur [48].

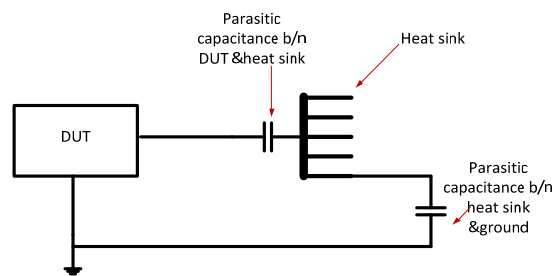


Figure 7.28 Parasitic capacitance between the DUT and the heat sink

### Result discussion

The influence of heat sink grounding on EMI was tested by connecting and disconnecting the heat sink to ground. In order to be able to compare the difference, their input voltage, switching frequency, gate resistance, duty cycle and RL load are kept the same.

Both the voltage and current output of the DUT are shown separately on the same axis, with the connecting and disconnecting of the heat sink to ground in figure 7.29 and 7.30. In addition also DM EMI noise level with the connecting and disconnecting of the heat sink to ground and background noise on the same axis is shown in figure 7.31.



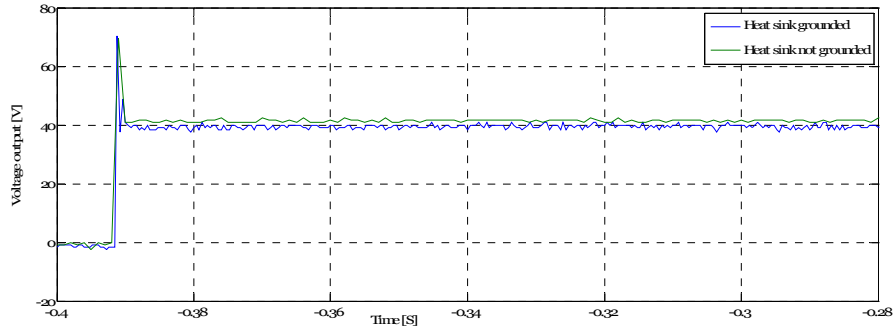


Figure 7.29 Voltage output vs time by connecting and disconnecting of the heat sink to ground

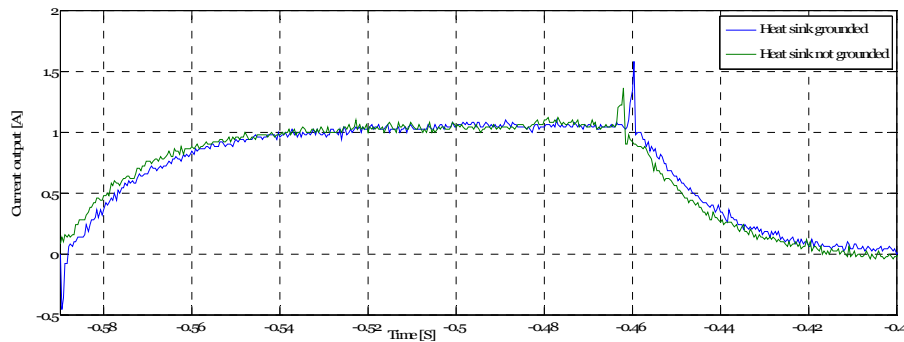


Figure 7.30 Current output vs time by connecting and disconnecting of the heat sink to ground

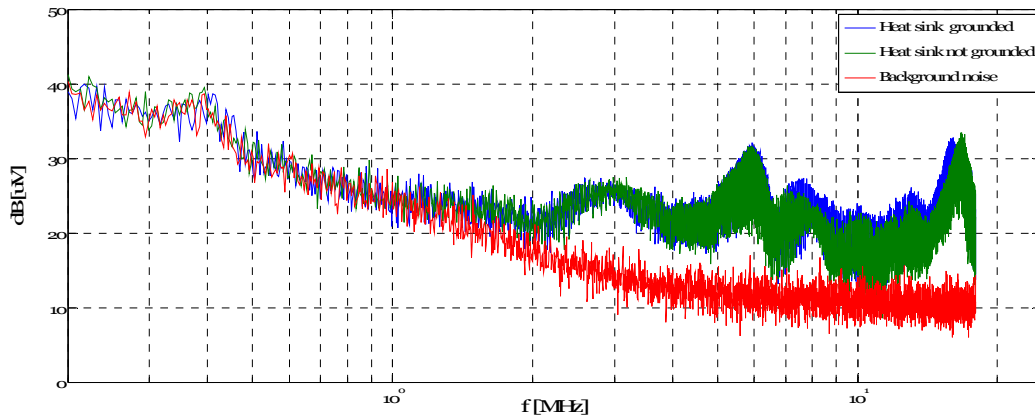


Figure 7.31 CM EMI noise level connecting and disconnecting of the heat sink to ground

From the result in figure 7.31, it can be concluded that making heat sink grounded increase CM EMI noise at higher frequency that means after 7 MHz.

### 7.3.5 The influence of duty cycle on EMI

#### Result discussion

The influence of duty cycle on EMI was tested by varying the duty cycle. In order to able to compare the difference, their input voltage, switching frequency, gate resistance and RL load are kept the same.

Both the voltage and current output of the DUT are shown separately on the same axis, for different duty cycle in figure 7.32 and 7.33. In addition also DM EMI noise level for different duty cycle and background noise on the same axis is shown in figure 7.34.

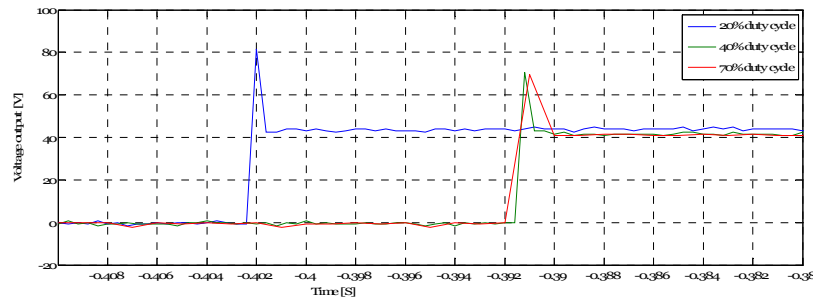


Figure 7.32 Voltage output vs time for different duty cycle

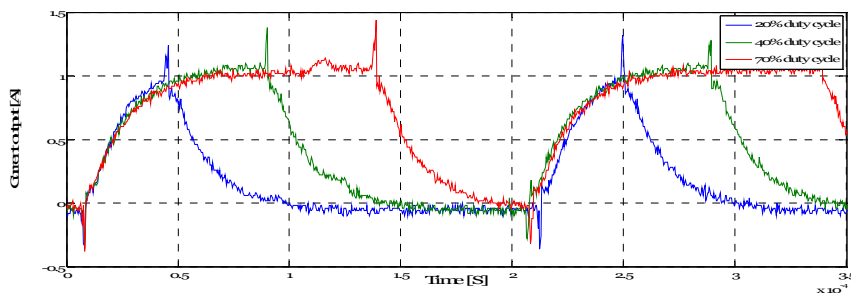


Figure 7.33 Current output vs time for different duty cycle

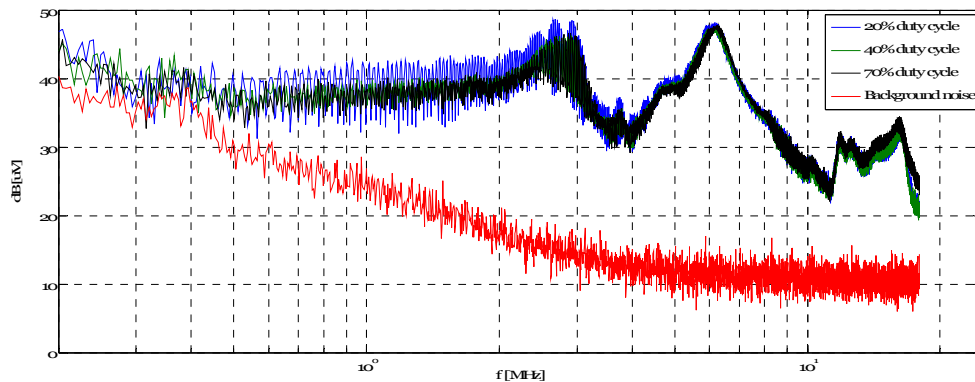


Figure 7.34 DM EMI noise level for different duty cycle

From the result in figure 7.34, it can be concluded that when the duty cycle decreases EMI increase and vice versa.

### 7.3.6 The influence of switching frequency on EMI

#### Result discussion

The influence of switching frequency on EMI was tested by varying the switching frequency. In order to be able to compare the difference, their input voltage, duty cycle,  $R_g$  and  $R_L$  load are kept the same.

Both the voltage and current output of the DUT are shown separately on the same axis, for different switching frequency in figure 7.35 and 7.36. In addition also DM EMI noise level for different switching frequency and background noise on the same axis is shown in figure 7.37.

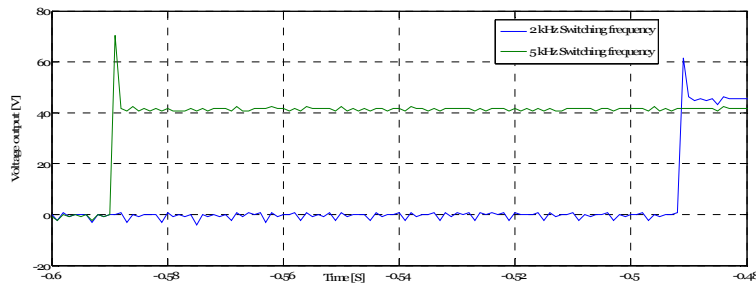


Figure 7.35 Voltage output vs time for different switching frequency

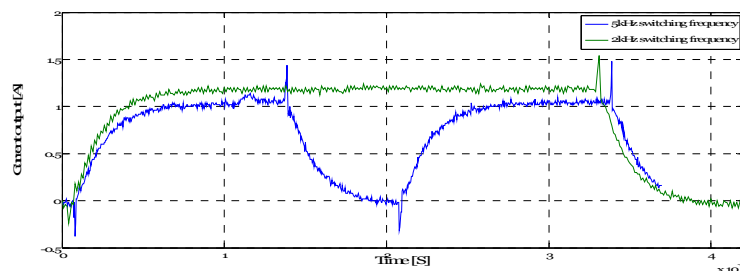


Figure 7.36 Current output vs time for different switching frequency

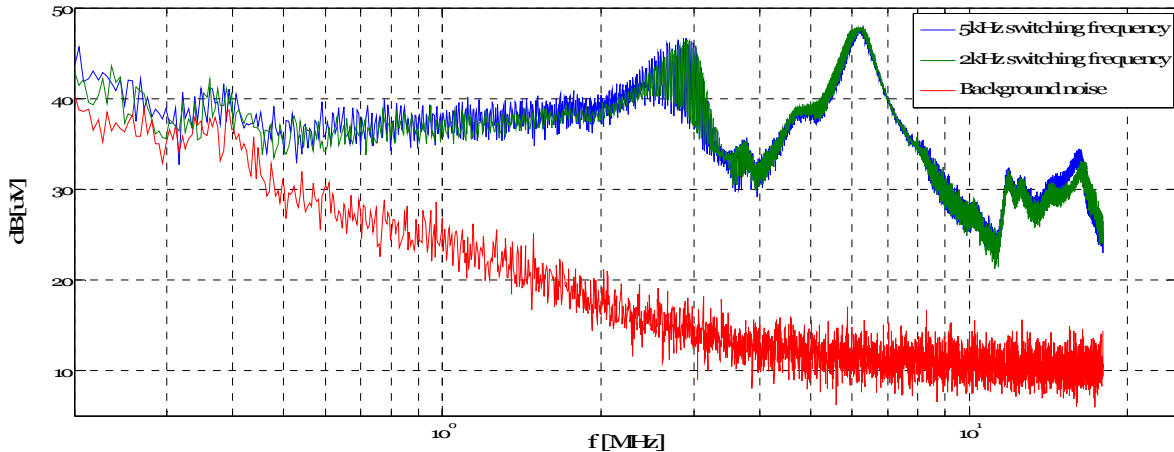


Figure 7.37 DM EMI noise level for different switching frequency

From the result in figure 7.37, it can be concluded that when the switching frequency increases EMI increases and vice versa.

## 7.4 Test circuit two

Recently, more than 60 % of the world's energy was used to drive electric motors. Due to this, the need of speed control in motor is growing and PWM inverters are used in adjustable speed drives, as using the PWM inverter to drive the motor the high switching speeds advanced PWM schemes significantly improves the performance of the PWM-inverter-fed

motors but the high rate of voltage rise has adverse effects on the motor insulation, high  $dv/dt$ , which causes leakage currents due to stray capacitances in an electric motor [50].

Most of the time the effect of stray capacitance may not be seen at low frequency but this has a major problem into the motor at higher frequency (EMI).

The figure on the left side of figure 7.38 showed (common mode transformer) when the stator and the rotor are magnetically coupled that the stray capacitance of motor holding most of the space (stator windings and the motor frame). This capacitance is distributed around the circumference and length of the stator, bearing this in mind when there is a current leak (high frequency content of current) into the stator through the coil then this current has higher value than leaving [51].

This high frequency current that will circulate in the stator laminations, inducing an axial voltage in the shaft ends, when the voltage increases this high frequency current starts to flow, internal to the motor, through the shaft and both bearings. This bearing current is considered to be the most damaging with typical peak values of 3 to 20 amps depending on the rated power of the motor,  $dv/dt$  of the AC drive power stage components and DC-link voltage level [51].

The figure on the right side of figure 7.38 showed (capacitive voltage divider) when the stator and the rotor capacitively coupled, the stray capacitance will be existing between the stator windings and the rotor or the motor's air gap between the stator iron and the rotor. The capacitively coupling between the stator windings and the rotor effectively couples the stator winding to the rotor iron, which is also connected to the shaft and the bearing's inner races. Fast changes in the common mode current from the inverter can not only result in currents in the capacitance around the circumference and length of the motor, but also between the stator windings and the rotor into the bearings [51].

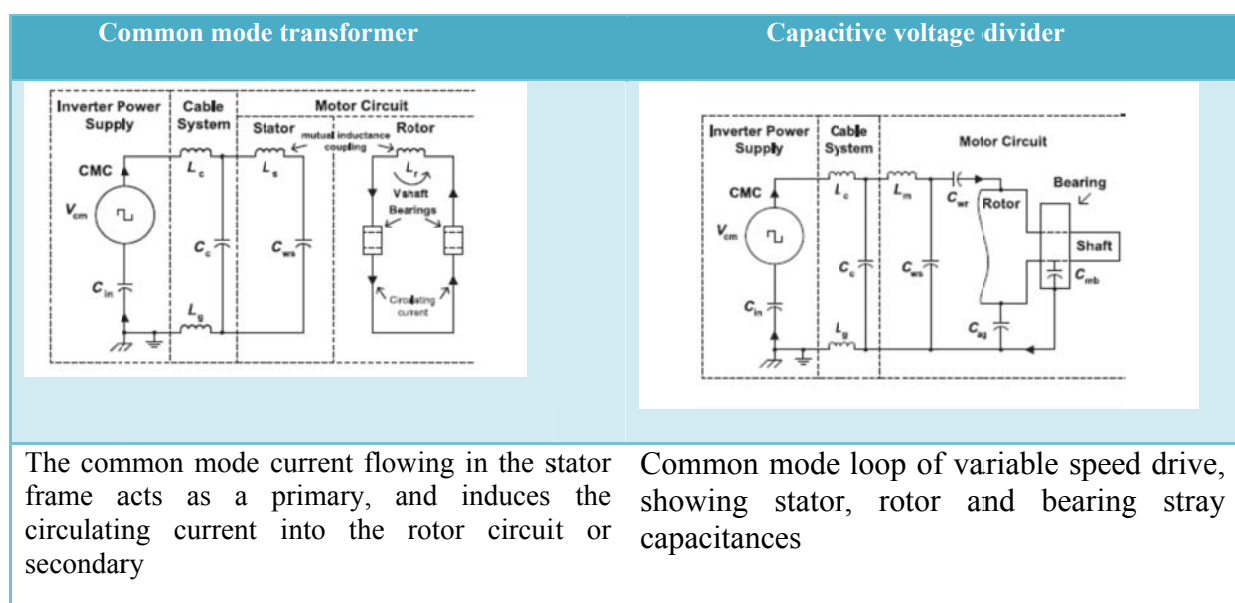


Figure 7.38 Motor equivalent circuit [51]

## 7.5 The influence of PWM-inverter-fed motors on EMI

The laboratory setup consisted of an induction motor and a DC motor that are mounted on the same shaft with a torque meter in between. To control these machines, two NTNU/SEfAS three-phase converters – permanently installed in the laboratory benches – as well as two DSP cards for measurements and control are used. The two measurement cards communicated with a PC through a standard serial connection (RS232). Both cards are also connected to a CAN bus so that they can communicate with each other [52].

In this laboratory bench figure 7.39 the LISN is equipped between the inverter and the AC induction motor, this way configuration helps to use the LISN as common mode filter.

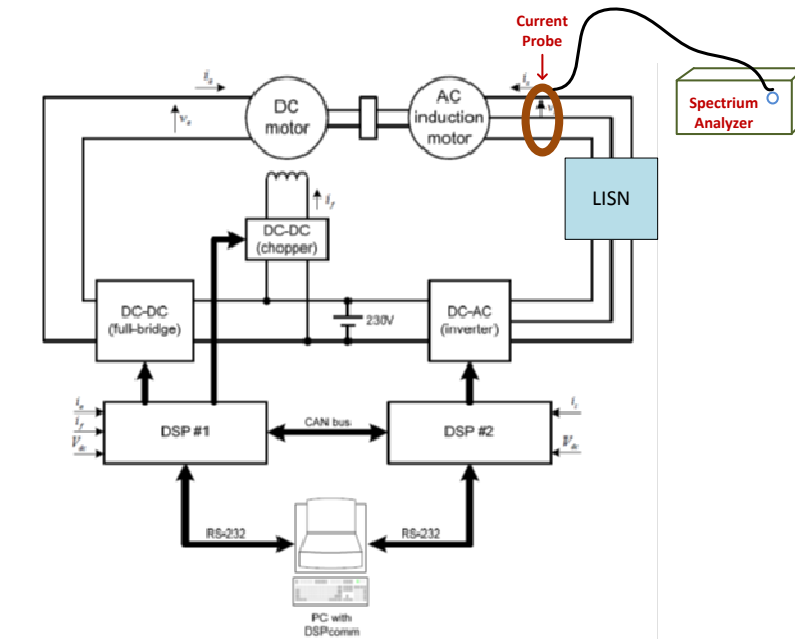


Figure 7.39 Laboratory setup

### 7.5.1 LISN filter between the inverter and motor terminal

#### Result discussion

As it is described earlier using the high switching speed drives improve the performance of the PWM-inverter-fed motors. This will cause the high rate of voltage rise at the motor terminal and has adverse effects on the motor insulation. This may not be seen at low frequency but this has a major problem into the motor at higher frequency (EMI).

Most often filter is the most common solution to have supply reliability, withstand sudden disturbances, to have voltage quality and to mitigate harmonics and EMI from high frequency switching power electronics devices.

To filter the common mode noise from the motor terminals, a LISN filter as shown in figure 7.39, has been used.

LISN consists of inductors and capacitors in a low pass filter arrangement, its equivalent circuit is shown below.

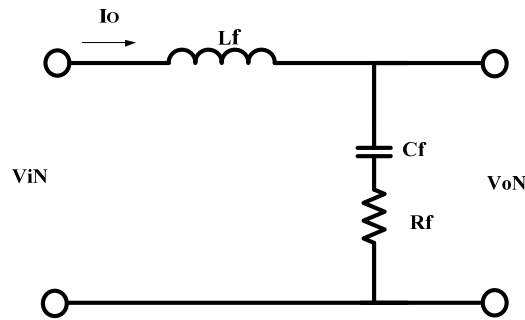


Figure 7.40 Low-pass filter

Where

$V_{iN}$  is the input noise voltage

$V_{oN}$  is the output noise voltage

Then the transfer function of the filter can be expressed as:

$$h_f(s) = \frac{1 + R_f \cdot C_f \cdot s}{1 + R_f \cdot C_f \cdot s + L_f \cdot C_f \cdot s^2} \quad 7.1$$

Since  $h_f$  is a second order system, it can be written in a general form:

$$h_f(s) = \frac{1 + 2 \cdot \xi \cdot \frac{s}{\omega_o}}{1 + 2 \cdot \xi \cdot \frac{s}{\omega_o} + \left(\frac{s}{\omega_o}\right)^2} \quad 7.2$$

$$\xi = \frac{R_f}{2} \sqrt{\frac{C_f}{L_f}}, \text{ damping coefficient}$$

$$\omega_o = \frac{1}{\sqrt{L_f \cdot C_f}}, \text{ undamped natural frequency} \quad 7.3$$

From the LISN internal circuit the inductor, capacitor and resistor values are 50  $\mu\text{H}$ , 0.25  $\mu\text{F}$  and 50  $\Omega$ . When these parameters are inserted in equation 7.3:

Then damping factor and the undamped natural frequency will be:

$$\xi = \frac{R_f}{2} \sqrt{\frac{C_f}{L_f}} = \frac{50}{2} \sqrt{\frac{0.25}{50}} = 1.76$$

$$\omega_o = \frac{1}{\sqrt{L_f \cdot C_f}} = \frac{1}{\sqrt{50\mu \cdot 0.25\mu}} = 0.282 \text{ Mrad/s}$$

After having  $\xi$  and  $\omega_o$  values, the normalized plots of the gain versus frequency when,  $L_f=50$   $\mu\text{H}$ ,  $C_f=0.25$   $\mu\text{F}$ ,  $R_f=50$   $\Omega$  and  $\xi=1.76$  will be:

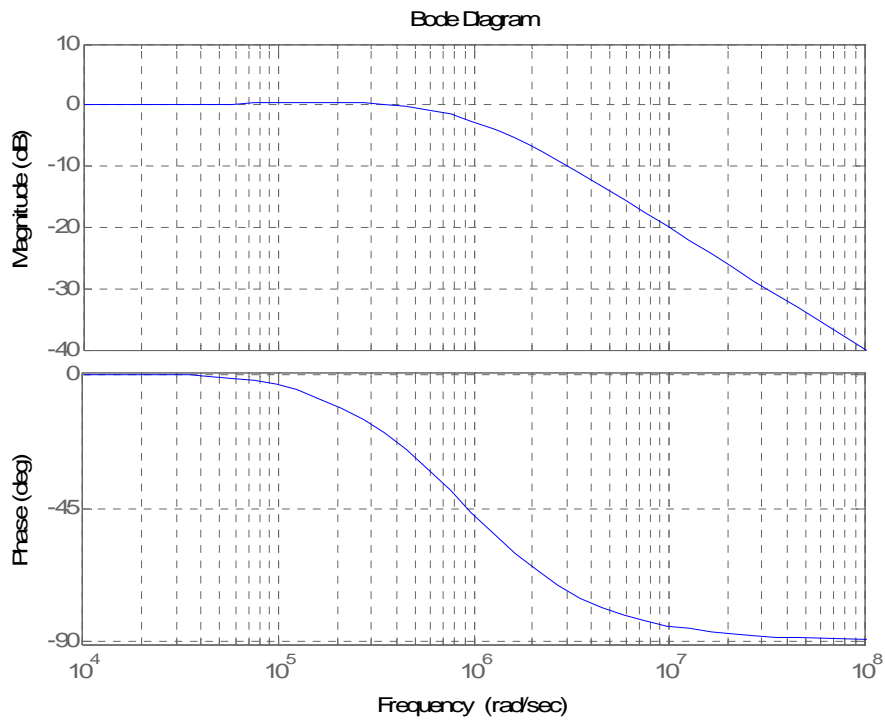


Figure 7.41 Second order frequency when  $\xi=1.76$

The influence of PWM-inverter-fed motor on EMI was tested with and without the LISN.

Both the voltage and current output of the inverter and motor terminals before inserting the LISN and after inserting the LISN are shown from figure 7.42 through figure 7.45. In addition also CM EMI noise level at the motor terminals before inserting the LISN and after inserting the LISN on the same axis is shown in figure 7.46.

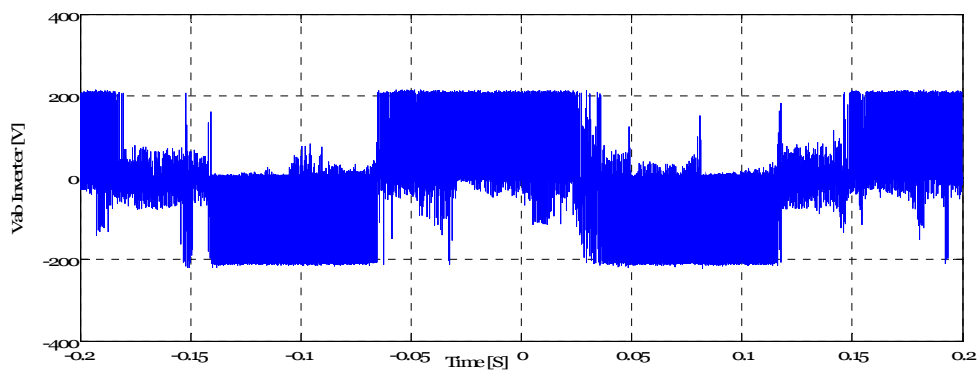


Figure 7.42 Inverter terminal output voltage

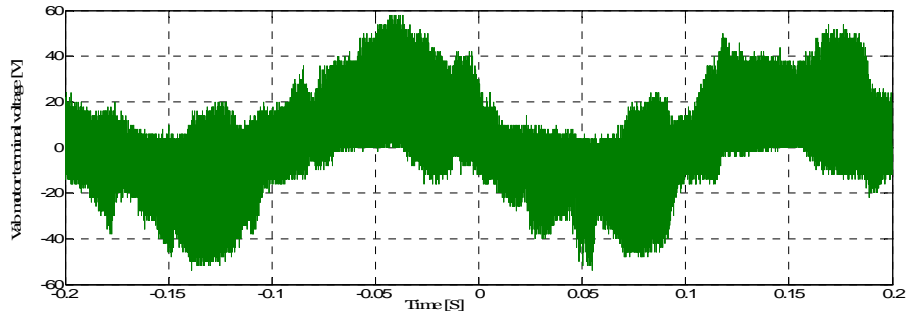


Figure 7.43 Motor terminal output voltage

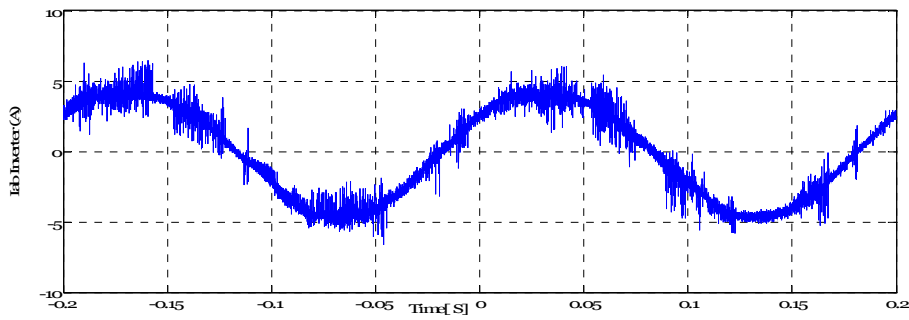


Figure 7.44 Inverter terminal output current

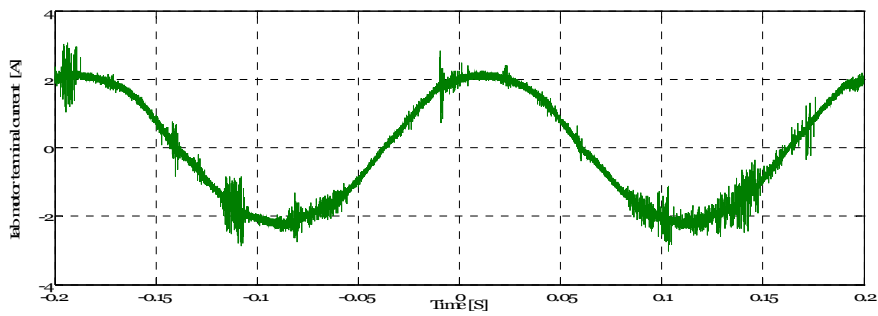


Figure 7.45 Motor terminal output current

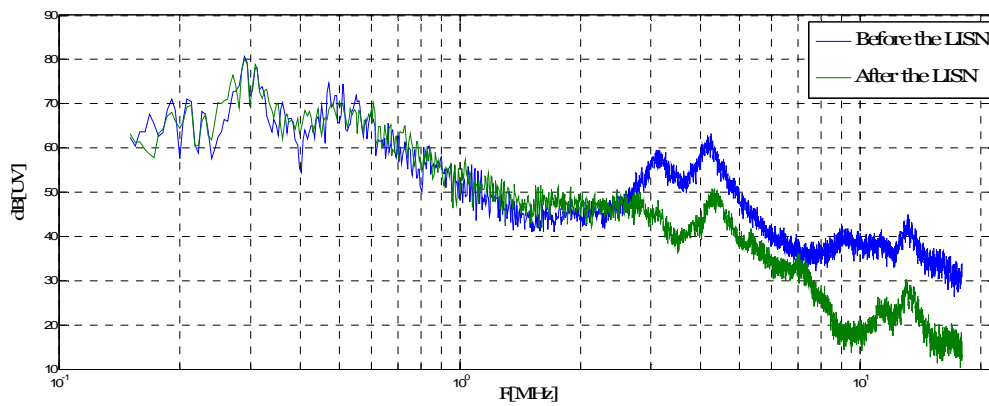


Figure 7.46 LISN as a filter



The above figure shows that the LISN used as an  $R_fL_fC_f$  filter when  $\xi$  is 1.76, the pattern of the two graphs are the same until 3 MHz, after this range the EMI measurement that is made when LISN is between the inverter and the motor terminal has decreased.

### 7.5.2 $L_fC_f$ filter between the inverter and motor terminal

Figure 7.39, changed to a new laboratory test up by placing  $L_fC_f$  harmonic filter between the inverter and motor terminal, the following figure shows this way of configuration.

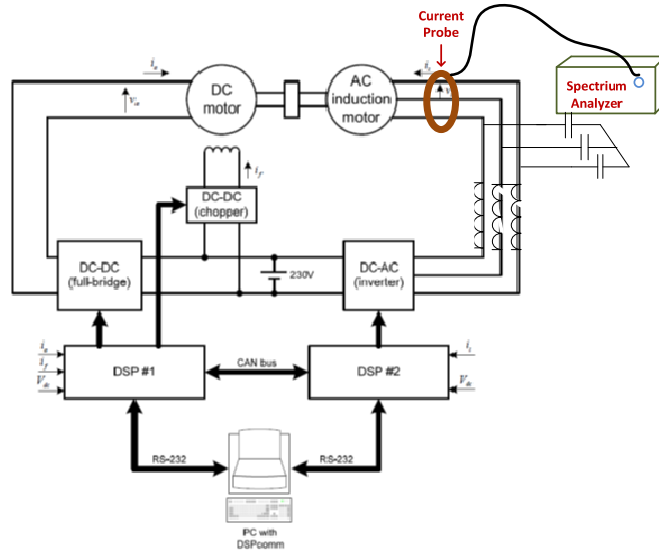


Figure 7.47  $L_fC_f$  filter between the inverter and the motor

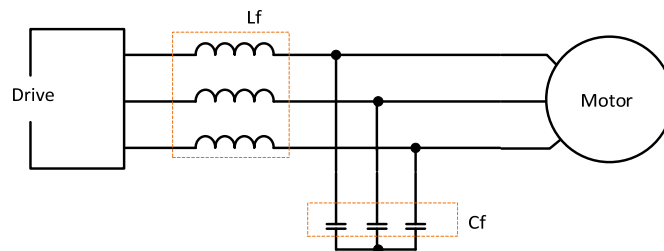
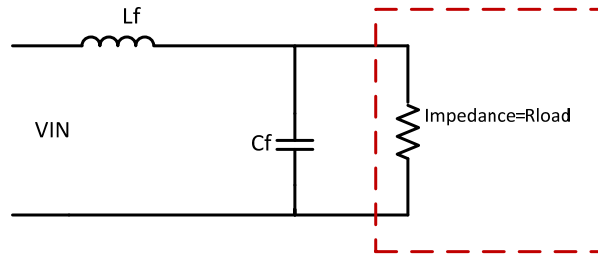


Figure 7.48  $L_fC_f$  filter arrangement

The  $L_fC_f$  harmonic filter that is placed between the inverter and the motor terminal used as to suppress differential mode noise at the motor terminal.

### Filter design guide

The following figure shows a simple  $L_fC_f$  harmonic passive filter arrangement.

Figure 7.49  $L_f C_f$  passive filter

The transfer function of filter can be expressed by:

$$h_f(s) = \frac{1}{1 + \frac{L_f}{R_{load}} \cdot s + L_f \cdot C_f \cdot s^2} \quad 7.4$$

Then transfer function can be rewritten with the frequency expressed in radians form will be:

$$h_f(s) = \frac{1}{1 + \frac{L_f}{R_{load}} \cdot j\omega + L_f \cdot C_f \cdot \omega^2} = \frac{1}{1 + j2 \cdot \xi \frac{\omega}{\omega_o} \cdot j\omega - \frac{\omega^2}{\omega_o^2}} \quad 7.5$$

Where  $s = j\omega$

An  $L_f C_f$  harmonic passive filter is a second order filter that provides 12 dB per octave of attenuation after the cutoff frequency  $f_{co}$ .

Then the cutoff frequency in radiant form:

$$\omega_o = \frac{1}{\sqrt{L_f \cdot C_f}} \quad 7.6$$

The damping factor ( $\xi$ ) is given by:

$$\xi = \frac{L_f}{2 \cdot R_{load} \sqrt{L_f \cdot C_f}} \quad 7.7$$

Where  $R_{load}$  is cable impedance value.

$$Z_C = R_{load} = \sqrt{\frac{L_C}{C_C}} \quad 7.8$$

The cable impedance equation also found in chapter four under equation 4.6.

Filter designed and used, for the above lab setup (figure 4.47) to eliminate the differential mode noise from the motor terminals. A H07RN-F LINEAX 4G6 mm<sup>2</sup> power cable was chosen. The following table shows the electrical parameters of the cable:

Table 7.2 Electrical cable parameter

Electrical parameters	Electrical parameters of the cable per km are
Resistivity	$R_c = 4,21 \Omega/\text{km}$
Inductivity	$L_c = 0.29 \text{ mH}/\text{km}$
Capacitance	$C_c = 0.17 \mu\text{F}/\text{km}$

### Filter type one

- The first filter parameters that were used in the circuit are  $L_f = 1 \text{ mH}$  and  $C_f = 0.15 \mu\text{F}$ .

Then  $R_{load}$  or cable impedance becomes,  $R_{load} = \sqrt{\frac{L_c}{C_c}} = \sqrt{\frac{0.29\text{m}}{0.17\mu}} = 41.3 \Omega$

Substituting the parameters of the cable and  $R_{load}$  in equation 7.7 & 7.8 one get  $\omega_o$  &  $\xi$ :

$$\omega_o = \frac{1}{\sqrt{1\text{m} \cdot 0.15 \mu}} = 0.0766 \text{ Mrad/s}$$

$$\xi = \frac{1\text{m}}{2.413 \sqrt{1\text{m} \cdot 0.15 \mu}} = 1$$

After finding zeta &  $\omega_o$ , the normalized plots of the gain versus frequency when  $L_f = 1 \text{ mH}$ ,  $C_f = 0.15 \mu\text{F}$ ,  $R_{load} = 41.3$  and  $\xi = 1$  will be:

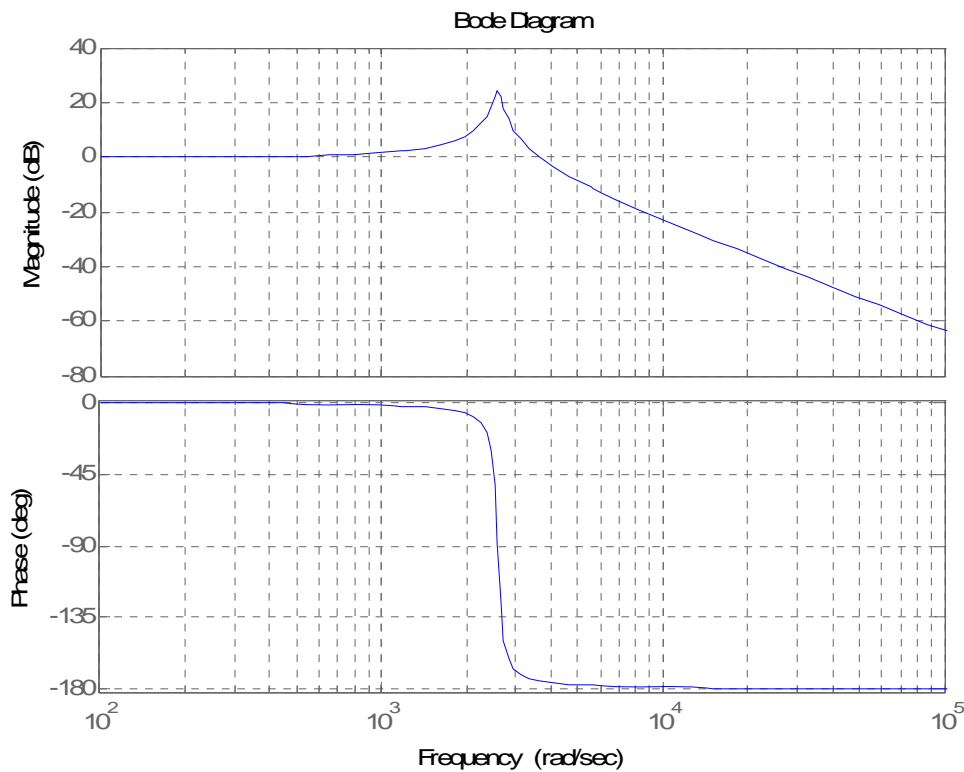


Figure 7.50 Second order frequency response when  $\xi = 1$

## Filter type two

- The second filter parameters that were used in the circuit are  $L_f=1$  mH &  $C_f=0.68$   $\mu$ F.

$R_{load}$  is the same as the previous one,  $R_{load}=41.3$   $\Omega$

Substituting the parameters of the cable and  $R_{load}$  in equation 7.7 and 7.8 one get  $\omega_o$  &  $\xi$ :

$$\omega_o = \frac{1}{\sqrt{1m \cdot 0.68 \mu}} = 0.0383 \text{ Mrad/s}$$

$$\xi = \frac{1m}{2.413 \cdot \sqrt{1m \cdot 0.68 \mu}} = 0.5$$

After finding zeta and  $\omega_o$ , the normalized plots of the gain versus frequency when  $L_f=1$  mH,  $C_f=0.68$   $\mu$ F,  $R_{load}=41.3$   $\Omega$  and  $\xi=0.5$  will be:

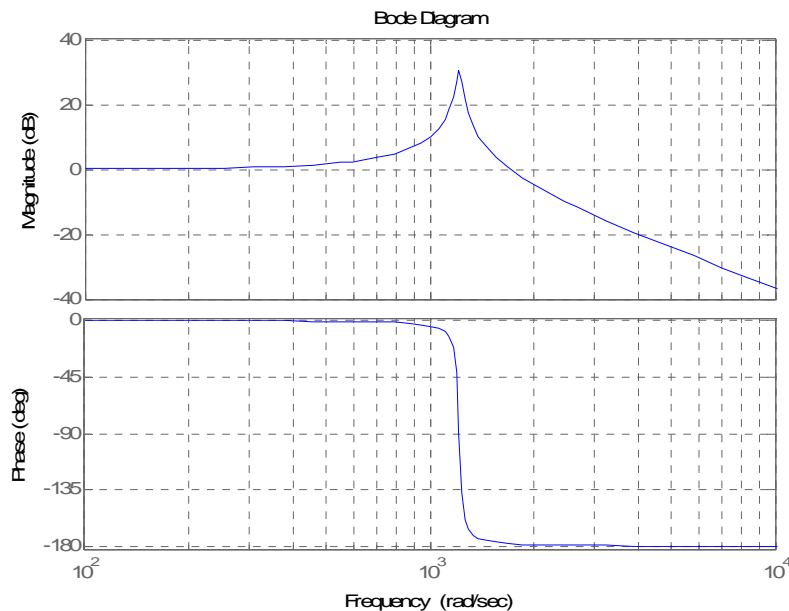


Figure 7.51 Second order frequency response when  $\xi=0.5$

## Filter type one results

The next task was to measure output voltage, current and DM EMI noise by placing harmonic filter components between the inverter and the motor terminals, then to see how they can successfully filter DM noise at the motor terminals. Measurements made by making the motor loaded and without load each at the time.

## Motor without loaded

The influence of PWM-inverter-fed motor on EMI was tested with and without the filters.

Both the voltage and current output of the inverter and motor terminals before inserting an  $L_f C_f$  filter after inserting an  $L_f C_f$  filter are shown from figure 7.52 through figure 7.55. In

addition also DM EMI noise level at the motor terminals before inserting an  $L_f C_f$  after inserting an  $L_f C_f$  filter on the same axis is shown in figure 7.56.

Note that, the filter parameter that were used are  $L_f=1$  mH and  $C_f=0.15$   $\mu$ F.

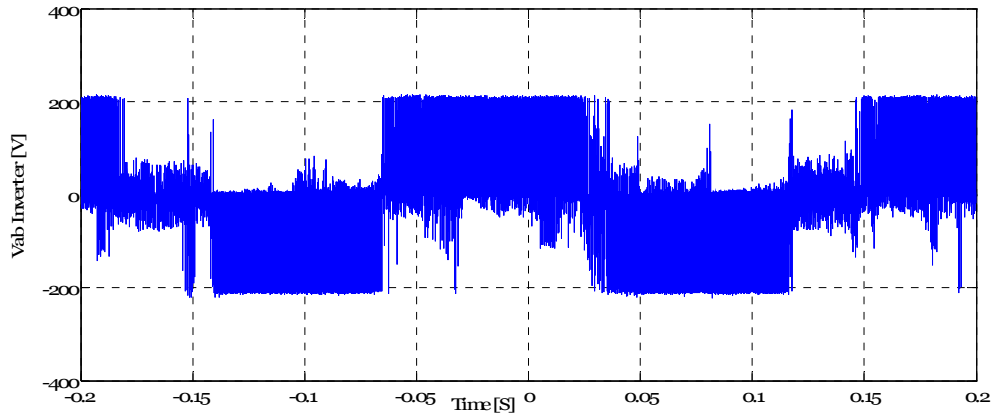


Figure 7.52 Inverter terminal output voltage without load

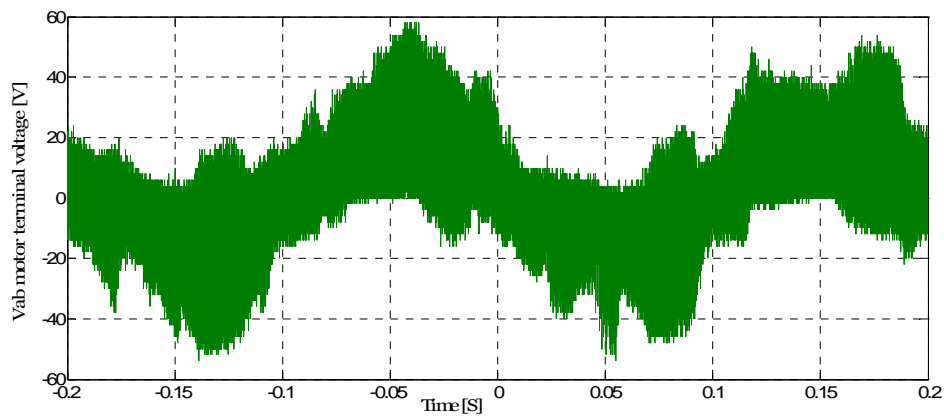


Figure 7.53 Motor terminal voltage without load

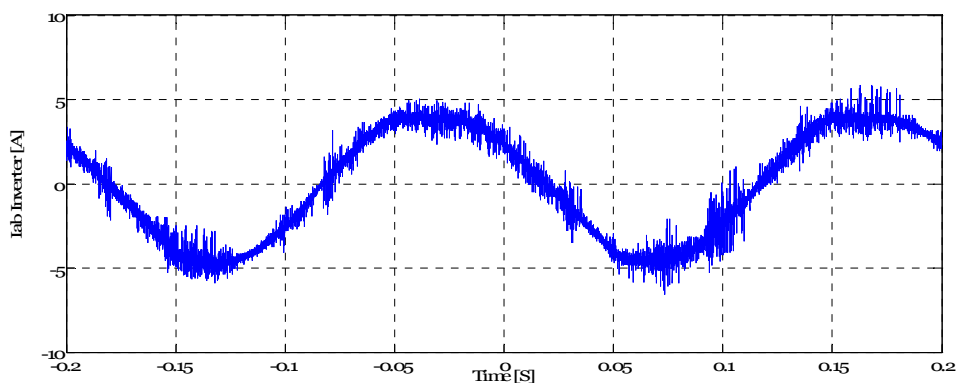


Figure 7.54 Inverter terminal output current without load

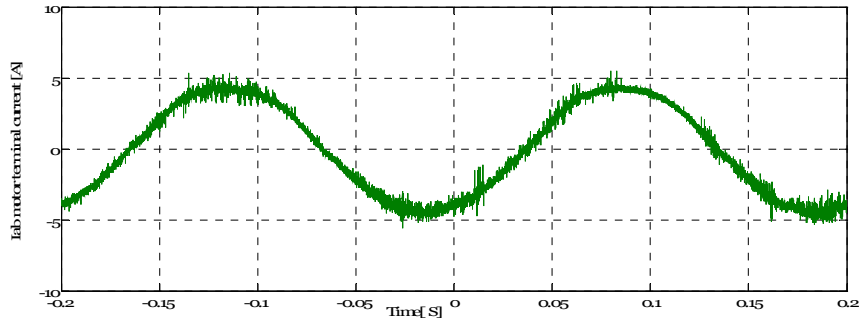


Figure 7.55 Motor terminal current without load

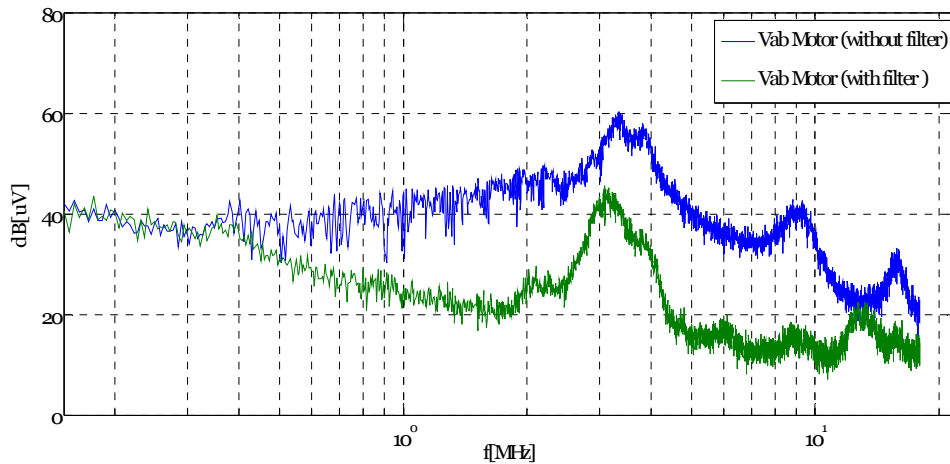


Figure 7.56 Reduction of DM noise after adding the filter

### Motor with loading

The influence of PWM-inverter-fed motor on EMI was tested with and without the filters.

Both the voltage and current output of the inverter and motor terminals before inserting an  $L_f C_f$  filter after inserting an  $L_f C_f$  filter are shown from figure 7.57 through figure 7.60. In addition also DM EMI noise level at the motor terminals before inserting the  $L_f C_f$  after inserting the  $L_f C_f$  on the same axis is shown in figure 7.61.

Note that, the filter parameter that were used are  $L_f=1$  mH and  $C_f=0.15$   $\mu$ F.

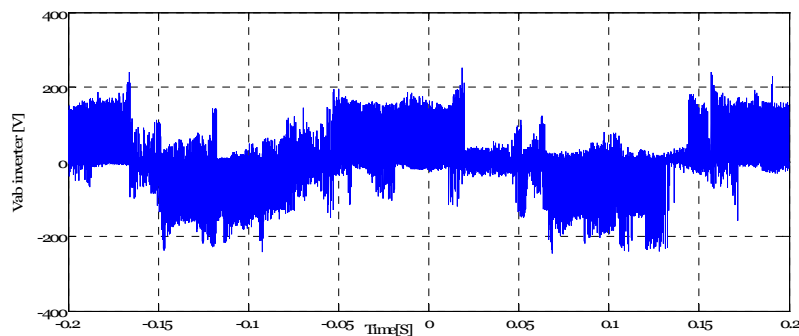


Figure 7.57 Inverter terminal output voltage with load

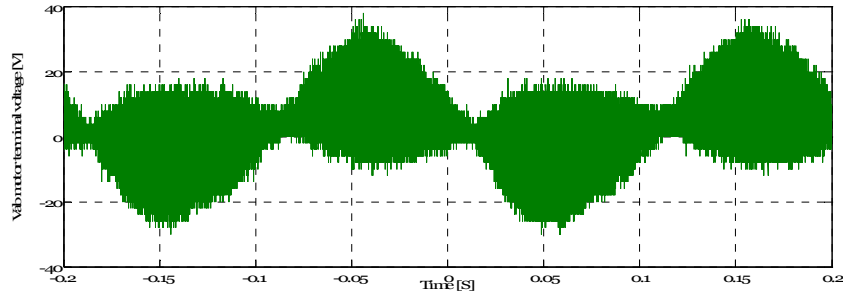


Figure 7.58 Motor terminal voltage with load

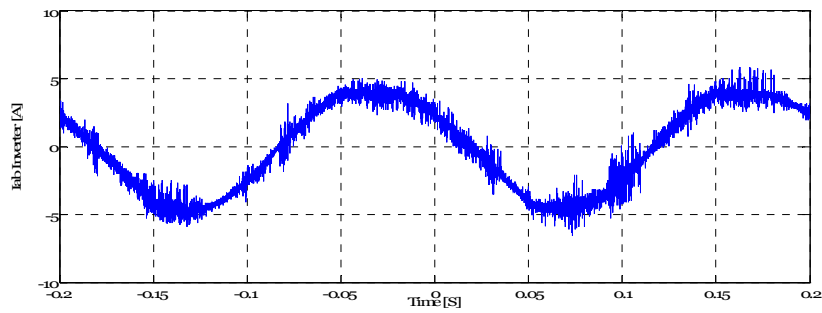


Figure 7.59 Inverter terminal output current with load

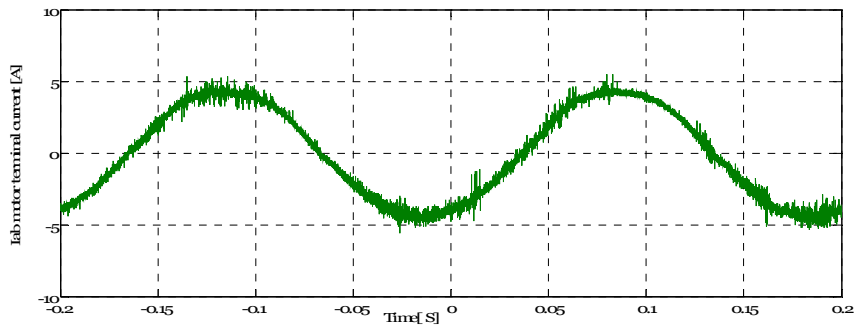


Figure 7.60 Motor terminal current with load

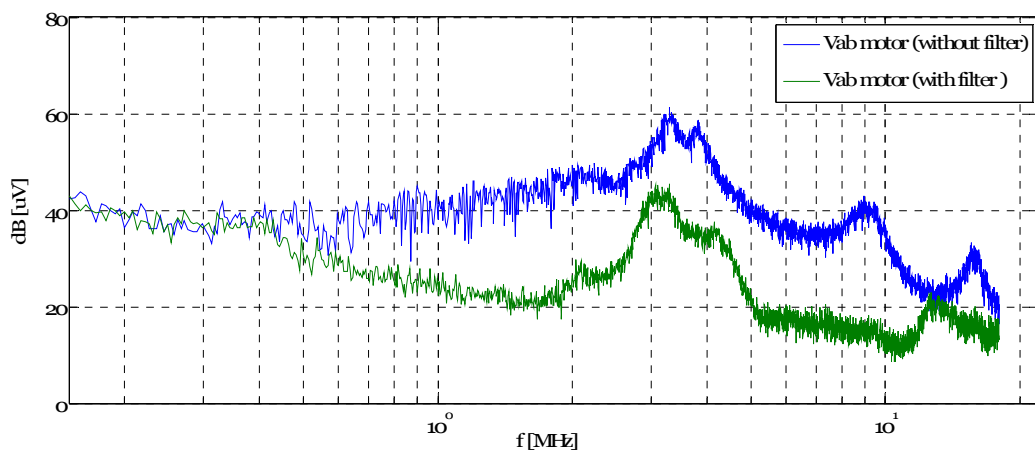


Figure 7.61 Reduction of DM noise after adding the filter

## Filter type two results

The influence of PWM-inverter-fed motor on EMI was tested with and without the filters.

Both the voltage and current output of the inverter and motor terminals before inserting an  $L_f C_f$  filter after inserting an  $L_f C_f$  filter are shown from figure 7.62 through figure 7.65. In addition also DM EMI noise level at the motor terminals before inserting an  $L_f C_f$  after inserting an  $L_f C_f$  on the same axis is shown in figure 7.66.

Note that, the filter parameter that were used are  $L_f=1$  mH and  $C_f=0.68$   $\mu$ F.

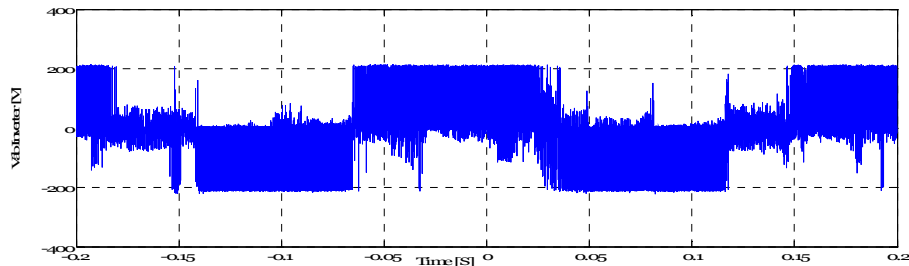


Figure 7.62 Inverter terminal output voltage without load

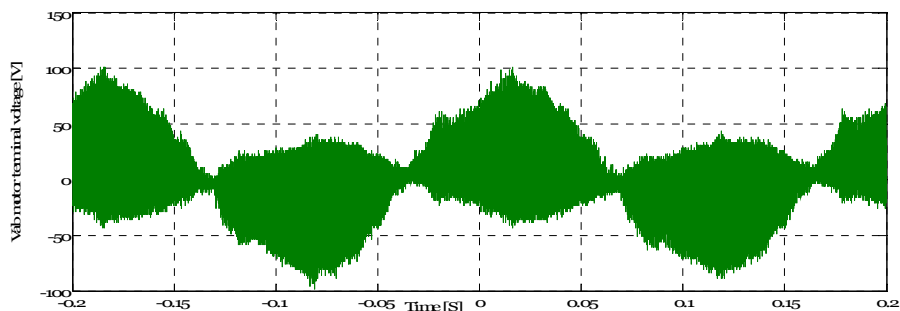


Figure 7.63 Motor terminal voltage without load

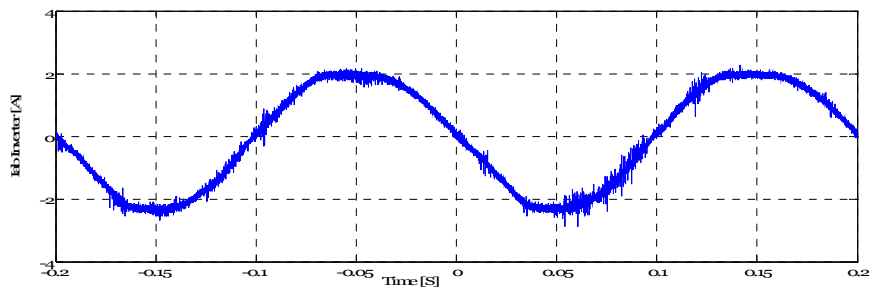


Figure 7.64 Inverter terminal output current without load

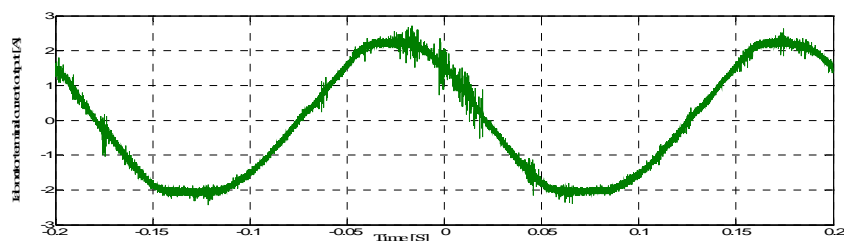


Figure 7.65 Motor terminal current without load



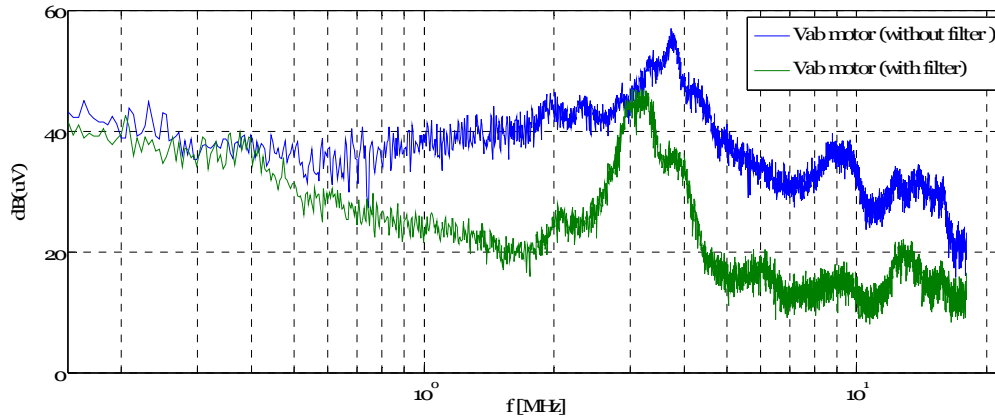


Figure 7.66 Reduction of DM noise after adding the filter

### Motor with loading

The influence of PWM-inverter-fed motor on EMI was tested with and without the filters.

Both the voltage and current output of the inverter and motor terminals before inserting an  $L_f C_f$  filter after inserting an  $L_f C_f$  filter are shown from figure 7.67 through figure 7.70. In addition also DM EMI noise level at the motor terminals before inserting an  $L_f C_f$  after inserting an  $L_f C_f$  on the same axis is shown in figure 7.71.

Note that, the filter parameter that were used are  $L_f=1$  mH and  $C_f=0.68$   $\mu$ F.

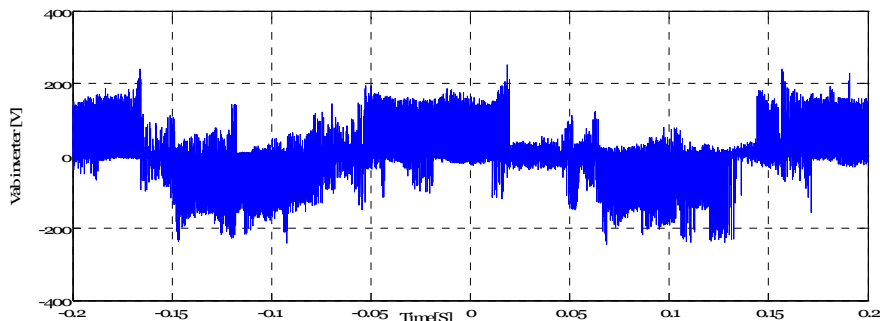


Figure 7.67 Inverter output voltage with load

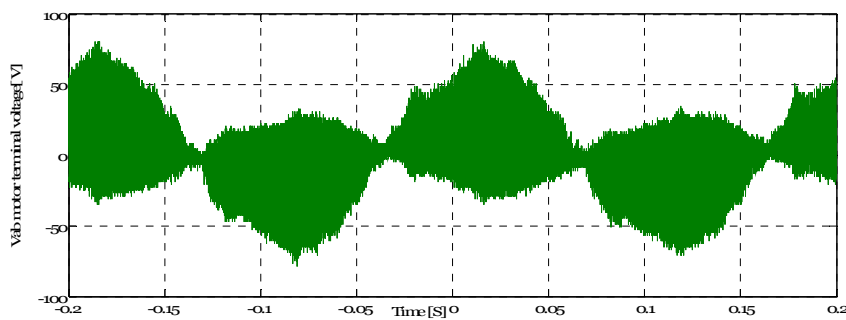


Figure 7.68 Motor terminal voltage with load

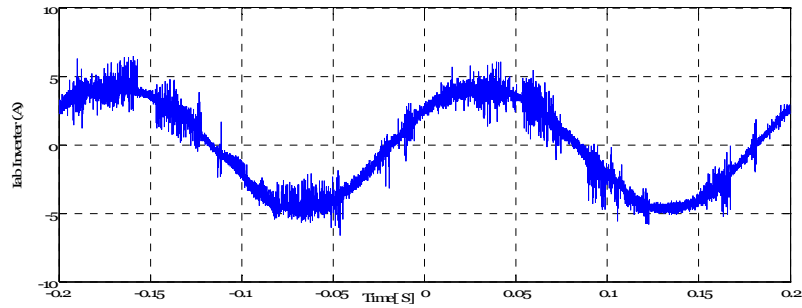


Figure 7.69 Inverter output current with load

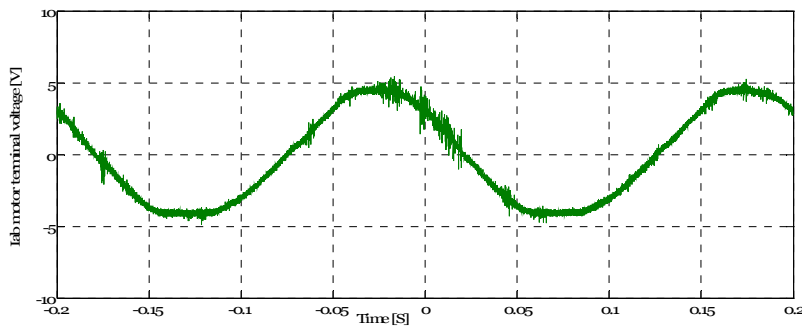


Figure 7.70 Motor terminal current with load

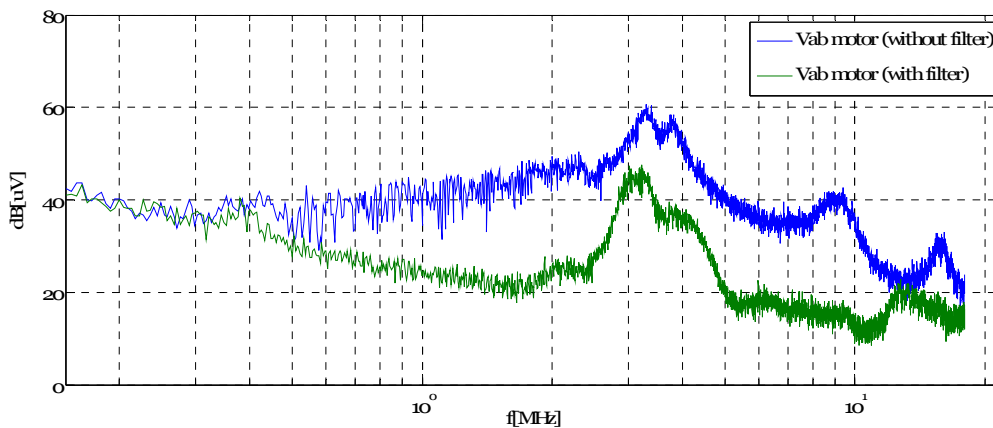


Figure 7.71 Reduction of DM noise after adding the filter

To filter DM noise at the motor terminals, An  $L_f C_f$  harmonic filter was used to mitigate the DM noise at the motor terminals and to see the practical applicability of the filter. Figure 7.56, 7.61, 7.66 and 7.71 show that, the filter that was made to filter harmonics, also able to reduce the effect of DM EMI noise significantly at the motor terminals.

Figure 7.71 shows that giving load to the motor has an effect on increasing EMI at the motor terminal.

## 7.6 Test circuit three

This section describes the silicon carbide power devices (SiC) transistor that was selected and the method that was used to drive this SiC transistor.

The objective of the third experiment was to test EMI on silicon carbide power devices for downhole applications. Due to the limited time and the lack of an appropriate device, the measurements for EMI were not successfully obtained for this laboratory setup.

### Topologies

For test circuit three, An CMF10120D-Silicon Carbide Power MOSFET was selected. The prominent features of this SiC are high speed switching, low capacitance and easy to parallel. The primary benefits are higher system efficiency, avalanche ruggedness and increased system switching frequency. They are mostly used in solar inverter, high voltage DC/DC converters and motor drives [53].

### Driver circuit background

The primary function of a driver circuit is to turn-on/off a power semiconductor device. The turn-on/off times should be kept as short as possible in order to minimize the time of device that spends in the active region where the instantaneous power dissipation is large [6]. SiC MOSFET isolated gate driver was selected to drive CMF10120D-Silicon Carbide Power MOSFET. The schematic of the driver is shown below in figure 7.72.

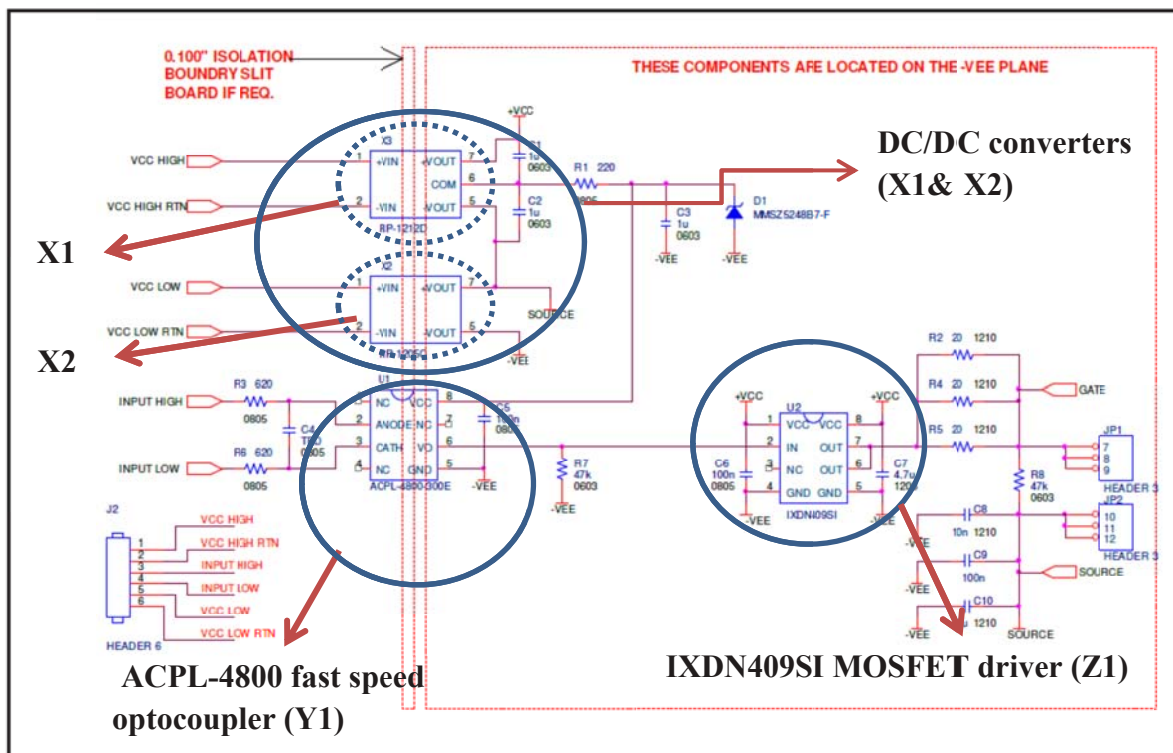


Figure 7.72 Isolated gate driver schematic [54]

*“The above circuit consists of two isolated DC-DC converters (X1 and X2), an optocoupler (Y1) and the gate driver integrated circuit (Z1). This integrated circuit, the IXDN409SI (Z1) can provide 35 V output swing and up to 9A of current with a typical output resistance of 0.8  $\Omega$ . Power is provided by isolated DC-DC converters; one for the positive bias and the other for negative bias. These converters are inexpensive with an isolation voltage rating of 5.2 kV resulting in very low isolation capacitance. X2 is a 12 V in 5 V out converter and X1 is a 12 V in, +/-12 V out converter. As shown in the schematic, the outputs of the converters are series connected and the common connection is referenced to the source terminal. Therefore, VCC determines the gate pulse positive voltage and -VEE determines the negative gate pulse voltage. The -VEE node is used as the ground reference for optocoupler and the gate driver, are designed to isolate electrical output from input for complete elimination of noise. The optocoupler are designed to isolate electrical output from input for complete elimination of noise. The optocoupler maximum operating voltage is 20 V therefore the power for this chip is taken from the common terminal of X1. Zener diode D1 is used to clamp the maximum voltage to 18 V. To minimize stray inductance, capacitors C8-C10 are located very close to the source output pin and the gate driver to provide very tight coupling between the source output terminal and the -VEE node [54].”*

### Challenge of the test setup

Since it was known that the order of ACPL-4800 (Y1) fast speed optocoupler and IXDN 409SI (Z1) MOSFET driver could not reach within the period of the project time. A modification was needed for the schematic of the driver that is shown in figure 7.72 with the device that is easily available in the market.

Therefore ACPL-4800 (Y1) fast speed optocoupler was replaced by SFH6701 - high speed optocoupler and also IXDN409SI (Z1) MOSFET driver was replaced by TC4422 MOSFET driver, and test circuit was made for the new test setup (figure D.3 in appendix D).

From the result it is seen that the new optocoupler and MOSFET driver could not be compatible each other to give an appropriate  $V_{GS}$  for SIC Power MOSFET.

## 8 Conclusion and further work

The rapid developments are taking place in electronic industry; most of these are the causes of EMI/EMC problems. This EMI can lead to devices generating and emitting unwanted electrical signals that can lead to performance degradation of other electronic devices. Most of these undesirable EMI effects are interference with wireless systems, electronic control systems in airplanes, the increase in power system losses associated with improper performance or failure of a range of industrial power equipment and motors.

In this thesis, EMI/EMC associated problems for PDS and means of mitigation techniques were investigated.

Simulation models for downhole drive train system, which consists of inverter, long cable, filters and motor was done. For different filter types ( $L_f$ ,  $R_fC_f$ ,  $R_fL_fC_f$ , and  $L_fC_f$ ),  $dv/dt$  and overvoltage at the motor terminal were investigated.

For 100 m cable length, the result shows that the voltage at the motor terminal was suppressed with a maximum overshoot of 20 % which was achieved by placing an  $R_fC_f$  at the motor end. The effect of overvoltage elimination seen at the motor terminal after using an  $R_fL_fC_f$  filter and an  $R_fL_fC_f$  split RC to +/- DC link filters at the inverter terminals, for which case the voltage overshoots are 7 % and 2 %, which are somewhat lower than of an  $R_fC_f$  filter. Using  $L_f$  filter at the inverter terminal shows an overshoot is 150 % at the motor end. This is shown that the filter was not compatible for the chosen parameter of cable.

From the simulation result, using the  $R_fC_f$  filter at the motor terminal had shown a good switched voltage waveform, faster response and smaller settling time at the motor end. Using the  $R_fL_fC_f$  filter topology gives good switched voltage waveform and was best to eliminate the common mode noise voltage at the motor terminal.  $L_fC_f$  filter was the best solution from all filter types by decreasing voltage overshoot, THD and power losses at the motor terminal.

In cost wise  $L_f$  filter is cheaper compared to the above filter types.  $L_fC_f$  filter is expensive and bigger.

Practical conducted EMI pre-compliance testing was made on chopper test circuit. The influence of EMI such as reverse recovery current of diode, stray or leakage inductance, gate drive resistance, heat sink grounding, duty cycle and switching frequency were investigated. It was observed that soft recovery current of diode, using copper strip for the DC bar, increasing the gate resistance of the drive, disconnecting heat sink from the ground, increasing the duty cycle and decreasing the switching frequency decrease EMI noise on the chopper test circuit.

EMI per-compliance testing was made on three phase inverter fed motor. An  $L_fC_f$  harmonic filter was placed between the inverter and motor terminals. The filter was able to reduced EMI noise significantly. The experiments show that giving load to the motor had an effect on increasing EMI.

The simulation results and the comparative factors show that each filter has its pros and cons, an  $R_f C_f$  at motor terminal is the best; in terms of faster response and smaller settling time, the  $R_f L_f C_f$  filter between the inverter and the motor may be the most convenient in terms of eliminating the overvoltage. An  $L_f$  filter at the inverter terminal is the best; in terms of power losses.

The common methods of EMI reduction on the chopper test circuit have its advantages and drawbacks. Increasing gate resistance ( $R_g$ ) of the drive it decreases EMI but it increases the switching losses. A shorter recovery time ( $t_{tr}$ ) creates high EMI than a longer recovery time. However diodes with shorter recovery time have reduced recovery losses resulting in improved converter efficiency.

Therefore how to solve the problem of overvoltage,  $dv/dt$  and EMI should be decided by the designers based on their specification layouts and requirements.

### **Further work**

In this thesis EMI/EMC problems for downhole applications had been studied. EMI phenomena clearly defined and a method of mitigation investigated.

For downhole applications simulation model developed to filter  $dv/dt$  and overvoltage at the motor terminals. Practical conducted EMI pre-compliance testing was made on chopper test circuit and also on three phase inverter fed motor. Due to the limited time and the lack of an appropriate device it was not possible to investigate EMI pre-compliance test on SiC transistor.

Having this as a foundation, the following points listed out for further work:

- EMI pre-compliance test on SiC transistor
- Practical EMI filter design
- Radiated EMI pre-compliance for different test circuits

## Bibliography

- [1] Oil and gas, <http://www.smartmotor.no/>.
- [2] Øyvind Holm Sneffjellå, “Silicon Carbide Technologies for High Temperature Motor Drives”, Master thesis, June 2011.
- [3] M Darnell, “Introduction & overview: Electromagnetic interference & electromagnetic compatibility”, June 1991.
- [4] T.Williams, “EMC for Product Designers”, Third Edition 2001.
- [5] Violette, J. L. Norman, White, Donald R. J, & Violette, Michael F, “Electromagnetic Compatibility Handbook”, New York: Van Nostrand Reinhold Company, 1987.
- [6] N.mohan, T.M.Undeland & W.P.Robbins, “Power Electronics”, J.Wiley & Sons, Third Edition, 2003.
- [7] Tim Williams, “EMC for systems and Installation”, First Edition 2000.
- [8] Technical guide No. 3, “EMC compliant installation and configuration for a power drive system”, ABB 2011.
- [9] “European Committee for Electrotechnical Standardization”, <http://www.cenelec.eu/aboutcenelec/whatwedo/whatisastandard/index>.
- [10] “Electrical Design”, CDA Publication 123, 1997.
- [11] “Electrostatic Discharge Precautions”, <http://www.informit.com>.
- [12] “AN9312 - Suppression of Transients in an Automotive Environment”, Littelfuse, 1999.
- [13] “Electrical fast transients and the EN 61000-4-4 test method”, Hand book on EN 61000-4-4.
- [14] “Electrical Transient Immunity for Power over Ethernet”, [www.ti.com/lit/an/slva233a/slva233a.pdf](http://www.ti.com/lit/an/slva233a/slva233a.pdf).
- [15] K. M. Muttaqi, M. E. Haque “Electromagnetic Interference Generated from Fast Switching Power Electronic Devices” IEEE International Journal of Innovations in Energy Systems and Power, Vol. 3, no. 1, April 2008 PP 19 of 45.
- [16] Technical guide No. 5, “Bearing currents in modern AC drive systems”, ABB 2011.
- [17] Output\_Filters\_Design\_Guide.pdf <http://www.danfoss.com/NR/rdonlyres/27F81E71-3779-4406-8EA0-849044873F59/0/>.
- [18] Installation\_guide\_3rd\_ed.pdf, “Variable speed drives and motors”.
- [19] Valentin Dzhanhotov, “Hybrid LC Filter for Power Electronic Drives: Theory and Implementation”, Doctoral thesis, 23th of October, 2009.
- [20] NEK IEC/TS 61800-8, “Adjustable speed electrical power drive systems”, part 8: Specification of voltage on the power interface.
- [21] <http://mtecorp.com/load.html>.
- [22] “Line reactors provide a low cost solution to inverter/Drive power quality”, Technical Guide - GE Industrial Solutions.pdf.
- [23] Richard Lund, “Motor winding problems caused by power electronic drives”, 02.02.2011, MEMO.
- [24] “AC line reactors and motor guarding transient filters”, [www.rexpowermagnetics.com/pdf/cat\\_line\\_reactors.pdf](http://www.rexpowermagnetics.com/pdf/cat_line_reactors.pdf).

- [25] H A. F. Moreira, T. A. Lipo, G. Venkataramanan, S. Bernet, "High Frequency Modeling for Cable and Induction Motor Over-voltage Studies in Long Cable Drives", IEEE Trnas. Ind.Applicat, Vol. 38, PP 1787-1794, Sept/Oct 2002.
- [26] A.von Jouanne, p. Enjeti and W.Gray, "Application issues for PWM Adjustable Speed AC motor Drives", IEEE Ind. Applicat Magazine, PP 10-18, Sept/Oot 1996.
- [27] Alessandro F. Moreira, Patrick M. Santos, Thomas A. Lipo, "Filter networks for long cable drives and their influence on motor voltage distribution and common-mode currents", IEEE Trnas. Ind. Applicat, Vol.52,No2,Apr, PP515-522,2005.
- [28] L. Palma, P. Enjeti, "An Inverter Output Filter to Mitigate dv/dt Effects in PWM Drive System", IEEE 0-7803-7404-5/02 PP 550-556 ,2002.
- [29] R.Nilsen, "Simulation of dV/dt filters", MEMO, 2011.
- [30] Robert West, "Common mode inductors for EMI filter require careful attention to core material selection", 1995 from PCIM magazine.
- [31] Fu-Yuan Shih, Dan Y. Chen, Yan-Pei Wu, and Yie-Tone Chen, "A procedure for designing EMI filters for AC line applications", IEEE Trnas. power electronics, Vol 11, NO.1 PP 170-182, Jan 1996.
- [32] R.Nilsen, "Distributed dc-link", MEMO, 2009.
- [33] K.S.Smith,L.Ran, "Earth leakage current in an isolated power system with power electronic converters", IPST'99-International conference on power systems transients, June 20-24,1999 Budapest-Hungary.
- [34] K.Shenai, "High-power robust semiconductor electronics technologies in the new millennium", Elsevier Science Ltd, 2001.
- [35] "CMF10120D-Silicon Carbide Power MOSFET", Datasheet.
- [36] <http://www.semisouth.com>.
- [37] <http://www.transic.com>.
- [38] <http://www.atmel.com>.
- [39] Tim Williams, "Emissions measurements on switch-mode power supplies", [www.elmac.co.uk](http://www.elmac.co.uk).
- [40] <http://www.home.agilent.com/>.
- [41] <http://www.pearsonelectronics.com/pdf/110.pdf>.
- [42] R.Dhanasekaran, M.Rajaram and S.N.Sivanandam, "Mixed Mode EMI Noise Level Measurement in SMPS", American Journal of Applied Sciences 3 (5): 1824-1830, 2006.
- [43] [http://www.emvgmbh.de/03\\_b\\_emv\\_messtech/PDF\\_FCC/LISN.pdf](http://www.emvgmbh.de/03_b_emv_messtech/PDF_FCC/LISN.pdf).
- [44] "Datasheet parameters for MOSFET, IGBT, MiniSKiiP- and SKiiPPACK modules".
- [45] Andreas Karvonen, "EMI from Switched Converters – Simulation Methods and Reduction Techniques", Doctoral thesis, Göteborg, Sweden 2011.
- [46] Firuz Zare, "EMI Issues in Modern Power Electronic Systems", [www.emcs.org/acstrial/newsletters/spring09/pp2.pdf](http://www.emcs.org/acstrial/newsletters/spring09/pp2.pdf).
- [47] Markus Hermwille, "Gate Resistor Principles and Applications", [www.Semikron.com/Application/GateResistor](http://www.Semikron.com/Application/GateResistor).
- [48] Andrea Dolente, "Analysis of the Heatsink Influence on Conducted and Radiated Electromagnetic Interference in Power Electronic Converters", Doctoral thesis, March 2007.



- [49] “Experimental and Simulative Investigations of Conducted EMI Performance of IGBTs for 5 - 10 kVA Converters”, Siemens.
- [50] Firuz Zare, “EMI in Modern AC Motor Drive Systems”, PP 53-58 IEEE 2009.
- [51] ABB drives, “Technical guide No. 1 Direct torque control -the world’s most advanced AC drive technology”.
- [52] Roy Nilsen, Giuseppe Guidi “AC motor control”, MEMO.
- [53] “CMF10120D - Cree - Cree, Inc”.pdf.
- [54] “Cree CPWR-AN08 Application Considerations for SiC MOSFETs”.pdf.

## Appendix

### A Zoomed out view filter results

#### A1 When $R_f C_f$ filter at the motor terminals

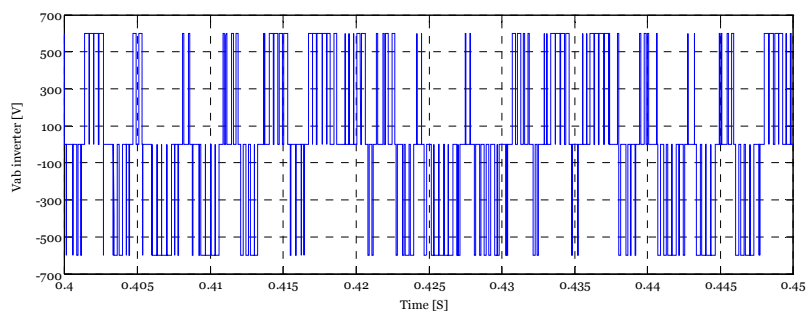


Figure A. 1 Zoomed out view 100 m  $V_{ab}$  inverter vs time with calculated  $R_f C_f$  filter

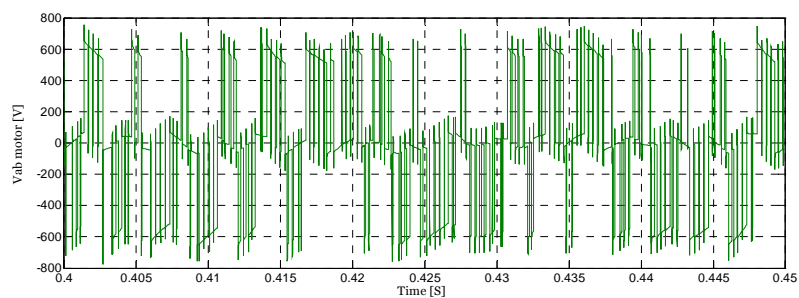


Figure A. 2 Zoomed out view 100 m  $V_{ab}$  motor vs time with calculated  $R_f C_f$  filter

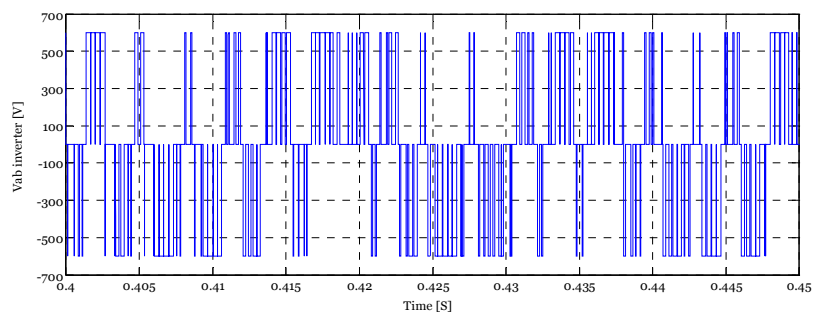


Figure A. 3 Zoomed out view 300 m  $V_{ab}$  inverter vs time with calculated  $R_f C_f$  filter

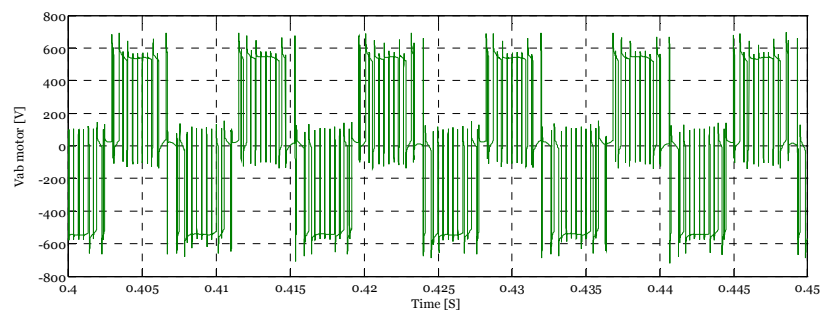
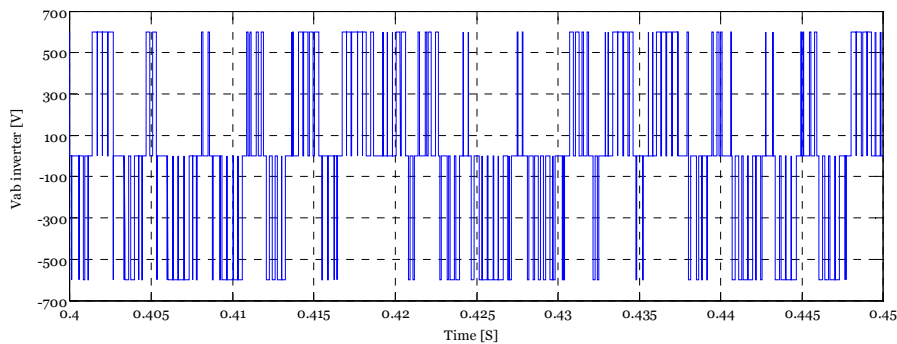
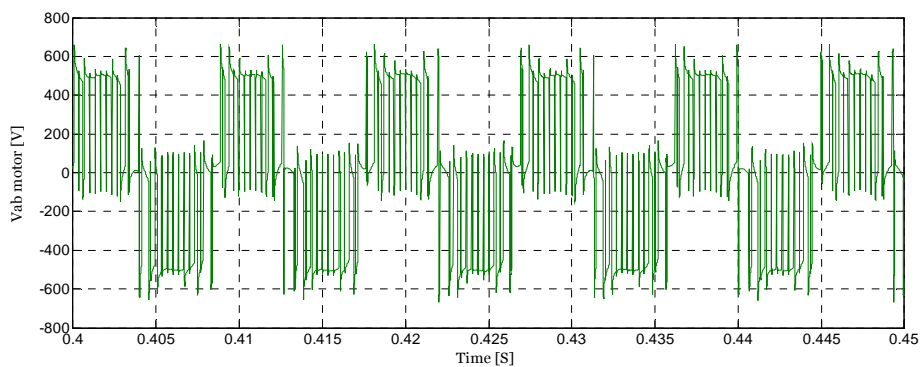
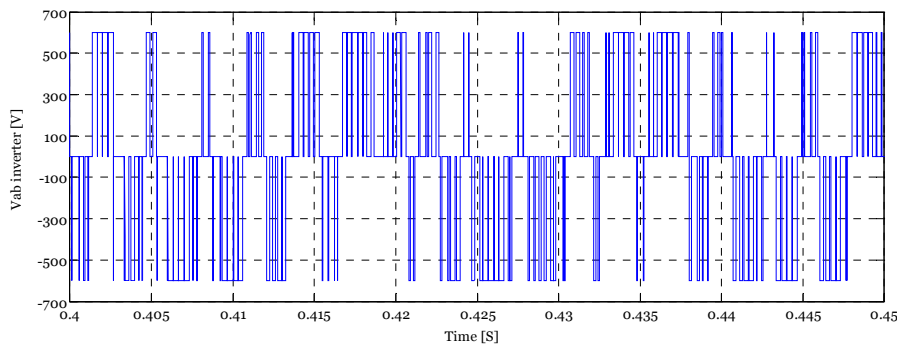
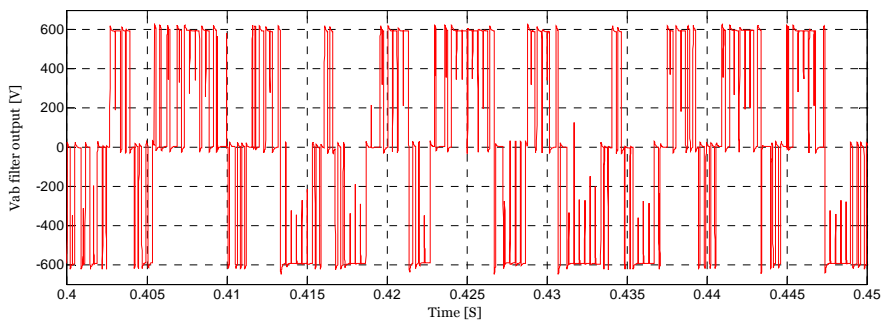
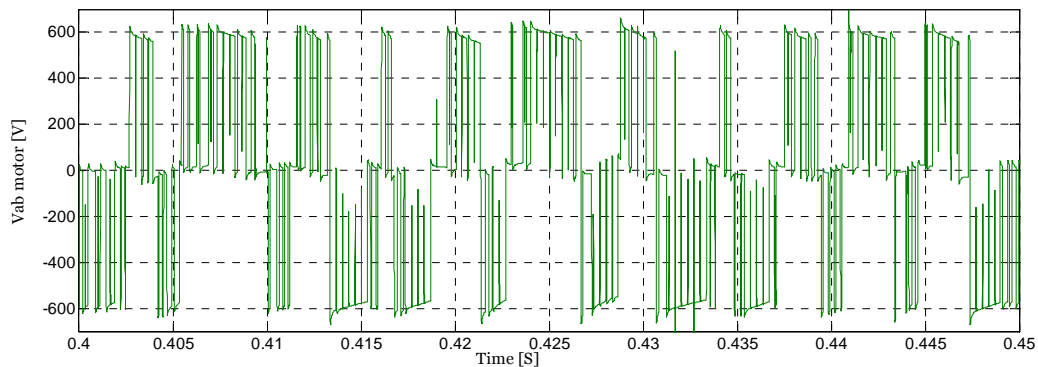
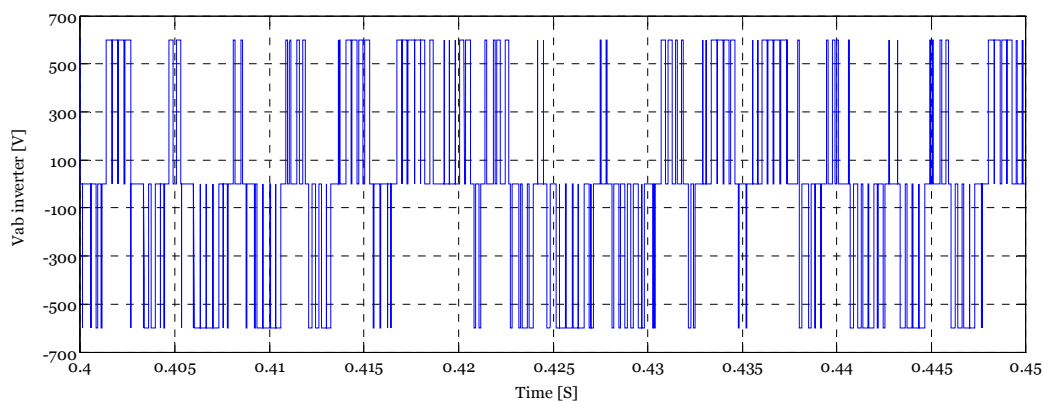
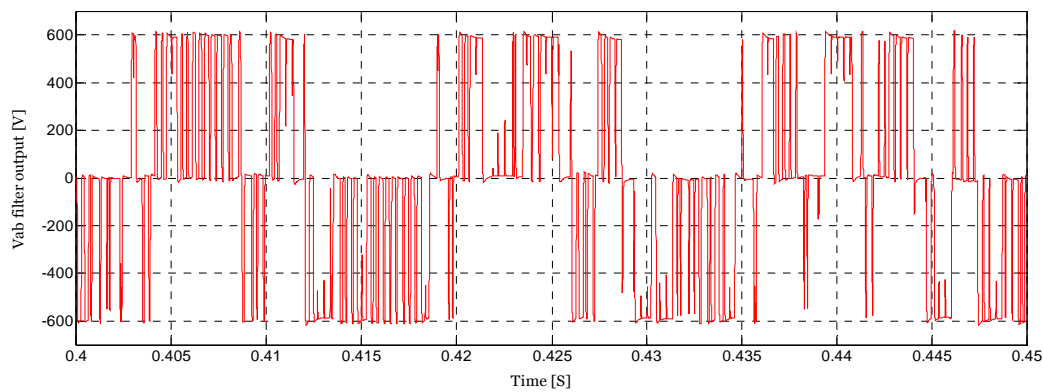
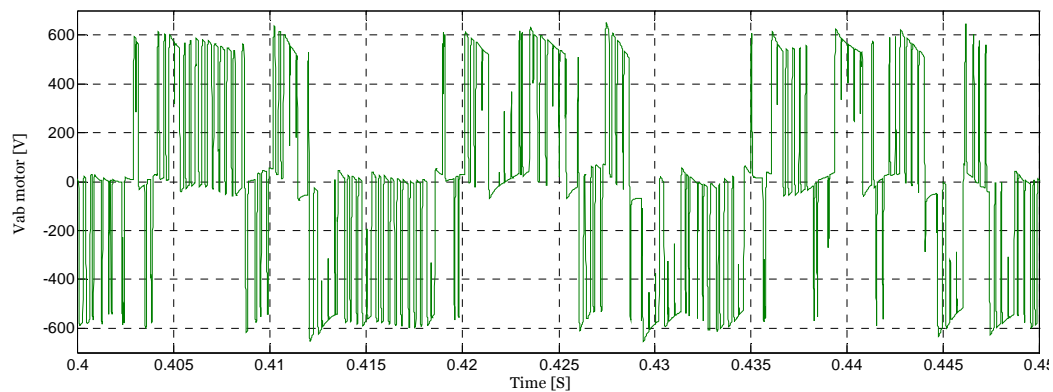


Figure A. 4 Zoomed out view 300 m  $V_{ab}$  motor vs time with calculated  $R_f C_f$  filter

Figure A. 5 Zoomed out view 600 m  $V_{ab}$  inverter vs time with calculated  $R_f C_f$  filterFigure A. 6 Zoomed out view 600 m  $V_{ab}$  motor vs time with calculated  $R_f C_f$  filter

## A2 When $R_f L_f C_f$ filter at the inverter terminals

Figure A. 7 Zoomed out view 100 m  $V_{ab}$  inverter vs time with calculated  $R_f L_f C_f$  filterFigure A. 8 Zoomed out view 100 m  $V_{ab}$  filter vs time with calculated  $R_f L_f C_f$  filter

Figure A. 9 Zoomed out view 100 m  $V_{ab}$  motor vs time with calculated  $R_fL_fC_f$  filterFigure A. 10 Zoomed out view 300 m  $V_{ab}$  inverter vs time with calculated  $R_fL_fC_f$  filterFigure A. 11 Zoomed out view 300 m  $V_{ab}$  filter vs time with calculated  $R_fL_fC_f$  filterFigure A. 12 Zoomed out view 300 m  $V_{ab}$  motor vs time with calculated  $R_fL_fC_f$  filter

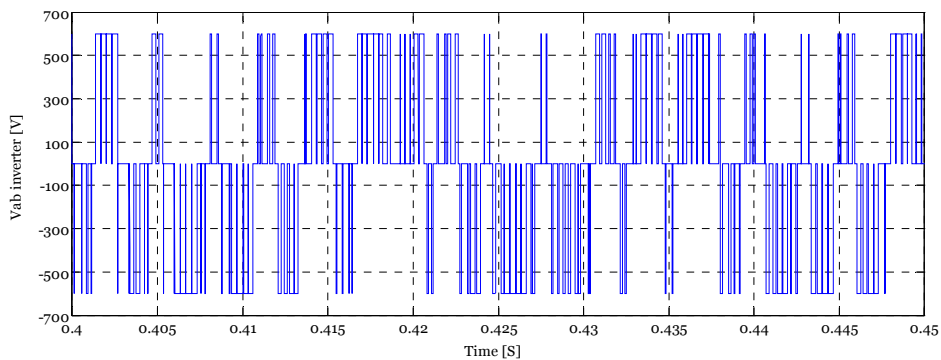


Figure A. 13 Zoomed out view 600 m  $V_{ab}$  inverter vs time with calculated  $R_f L_f C_f$  filter

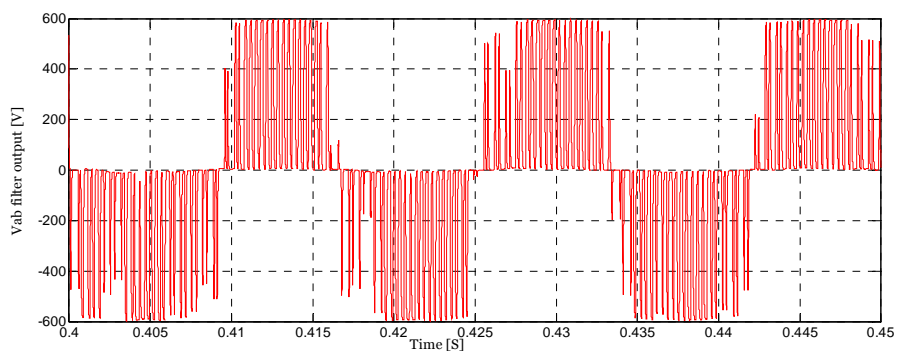


Figure A. 14 Zoomed out view 600 m  $V_{ab}$  filter vs time with calculated  $R_f L_f C_f$  filter

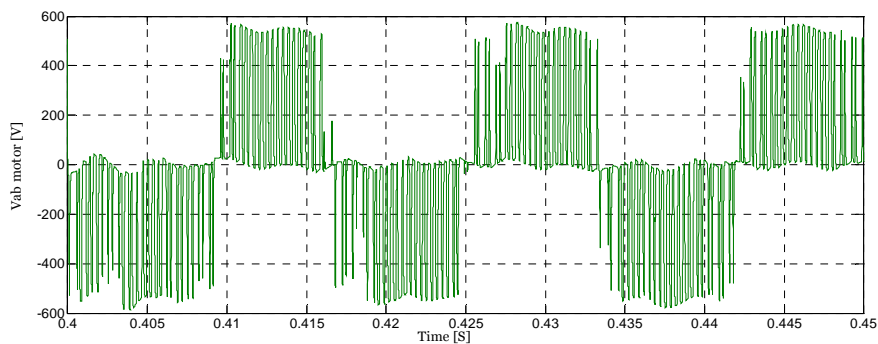


Figure A. 15 Zoomed out view 600 m  $V_{ab}$  motor vs time with calculated  $R_f L_f C_f$  filter

### A3 When $R_f L_f C_f$ split RC to +/- DC link filter at the inverter terminals

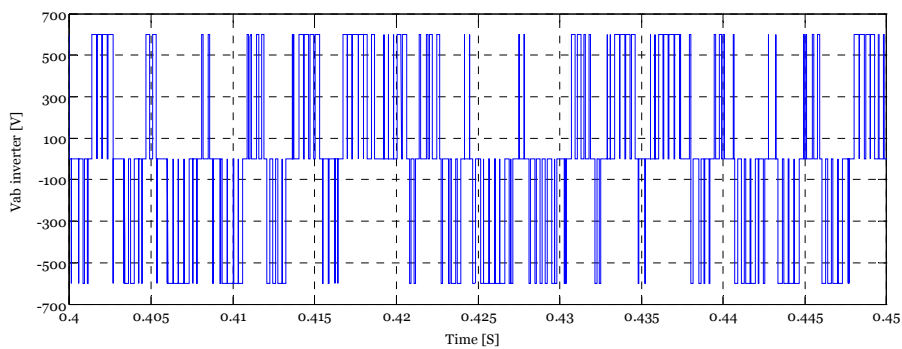


Figure A. 16 Zoomed out view 100 m  $V_{ab}$  inverter vs time with calculated  $R_f L_f C_f$  split filter

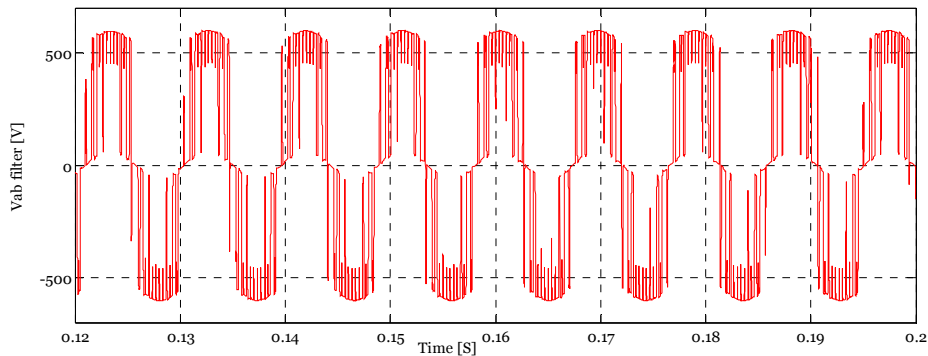


Figure A. 17 Zoomed in view 100m  $V_{ab}$  filter vs time with calculated  $R_fL_fC_f$  split filter

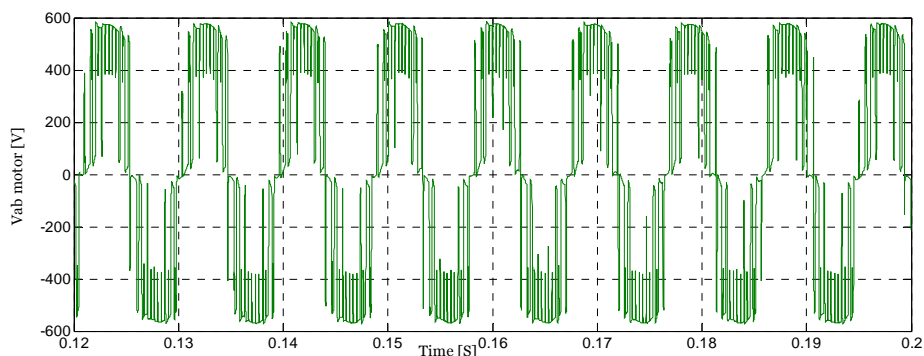


Figure A. 18 Zoomed out view 100 m  $V_{ab}$  motor vs time with calculated  $R_fL_fC_f$  split filter

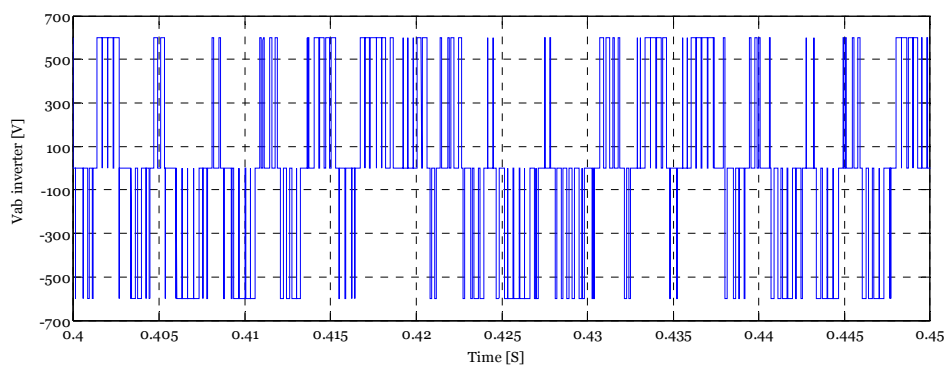


Figure A. 19 Zoomed out view 300 m  $V_{ab}$  inverter vs time with calculated  $R_fL_fC_f$  split filter

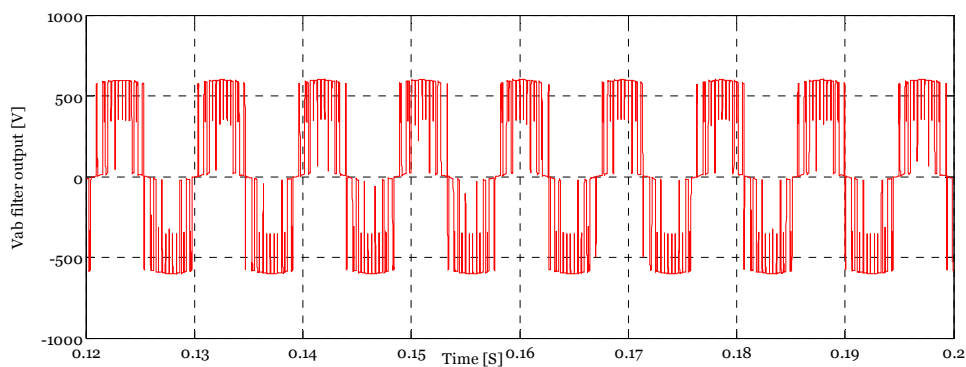


Figure A. 20 Zoomed out view 300 m  $V_{ab}$  filter vs time with calculated  $R_fL_fC_f$  split filter

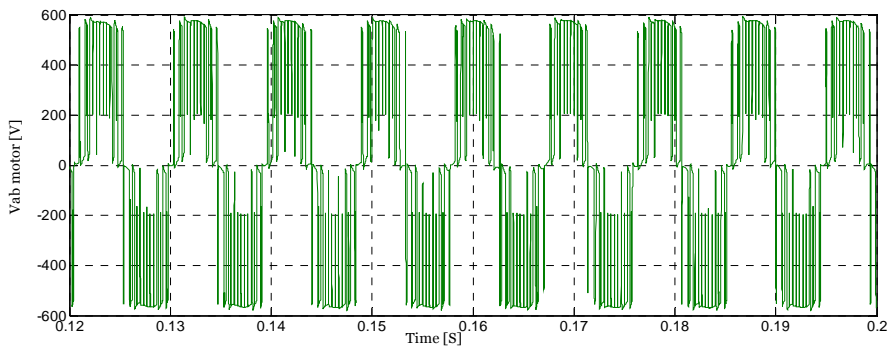


Figure A. 21 Zoomed out view 300 m  $V_{ab}$  motor vs time with calculated  $R_f L_f C_f$  split filter

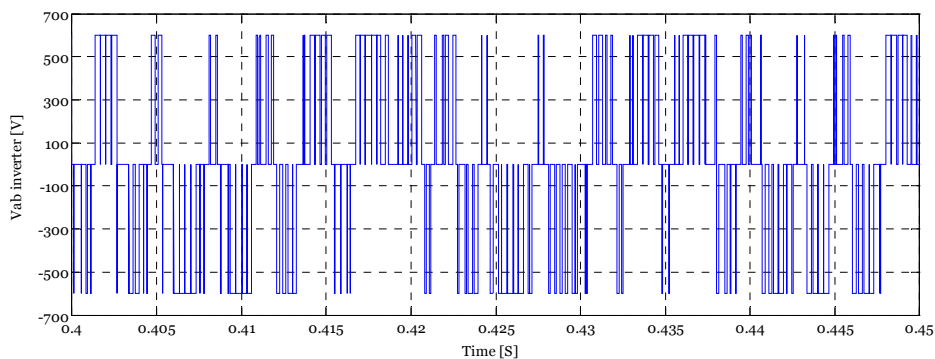


Figure A. 22 Zoomed out view 600 m  $V_{ab}$  inverter vs time with calculated  $R_f L_f C_f$  split filter

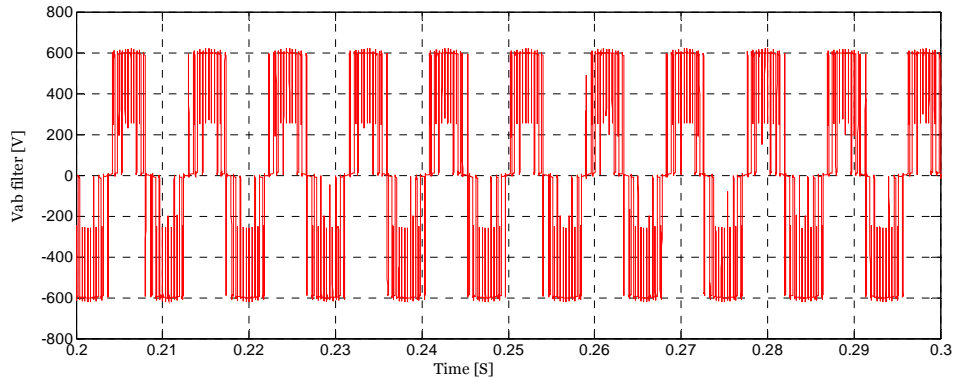


Figure A. 23 Zoomed out view 600 m  $V_{ab}$  filter vs time with calculated  $R_f L_f C_f$  split filter

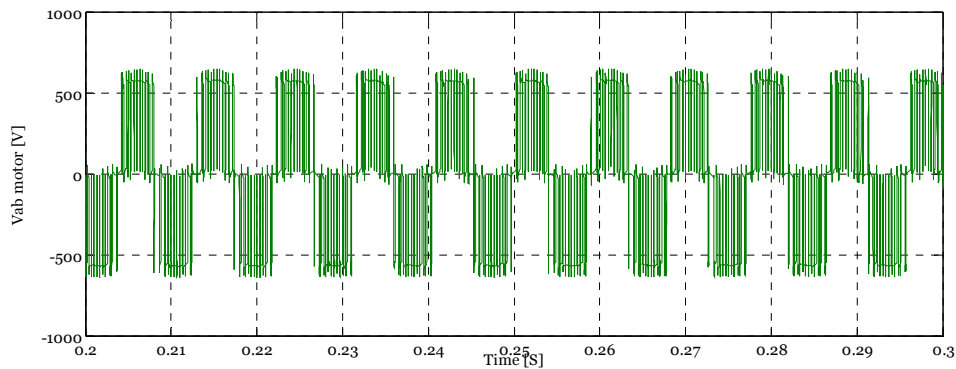


Figure A. 24 Zoomed out view 600 m  $V_{ab}$  motor vs time with calculated  $R_f L_f C_f$  split filter

## A4 CM noise voltage at inverter and motor terminals using $R_f C_f$ filter

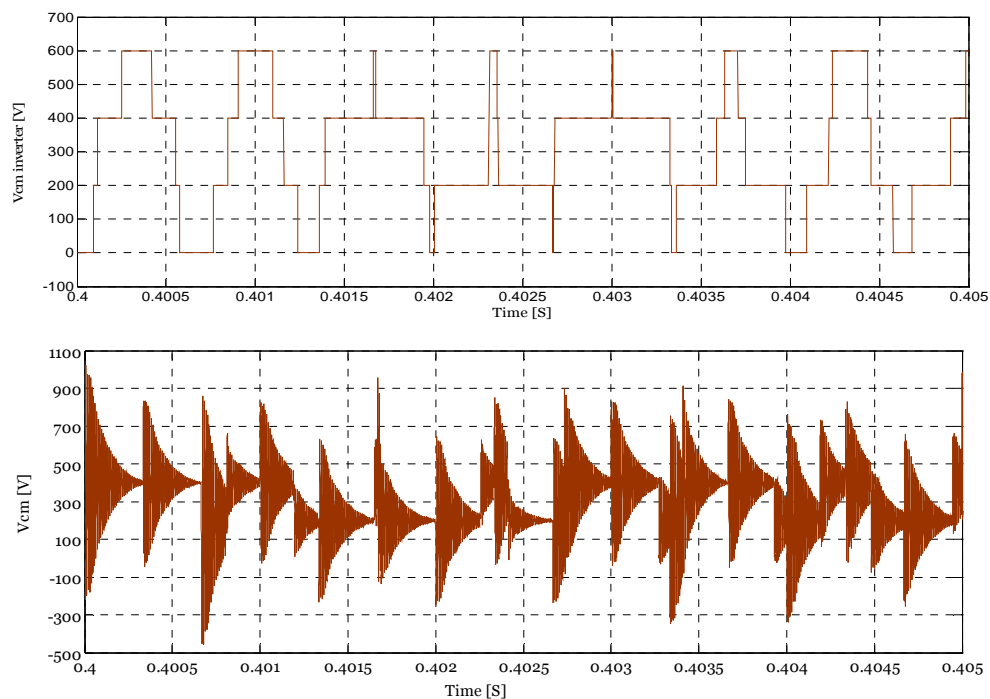


Figure A. 25 For 100 m  $V_{cm}$  inverter and motor terminal vs time with calculated  $R_f C_f$  filter

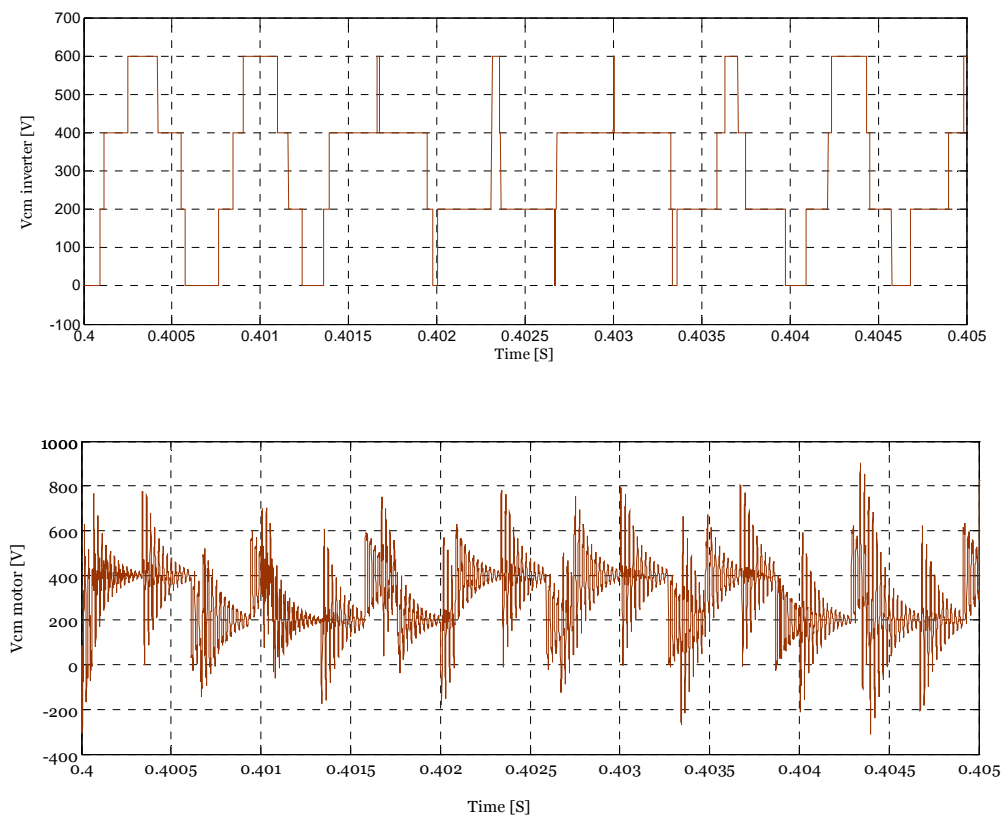


Figure A. 26 For 300 m  $V_{cm}$  inverter and motor terminal vs time with calculated  $R_f C_f$  filter



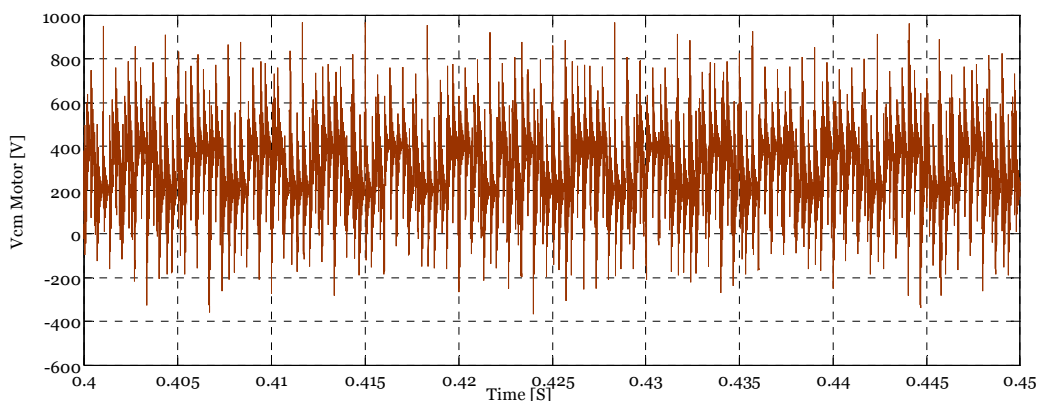
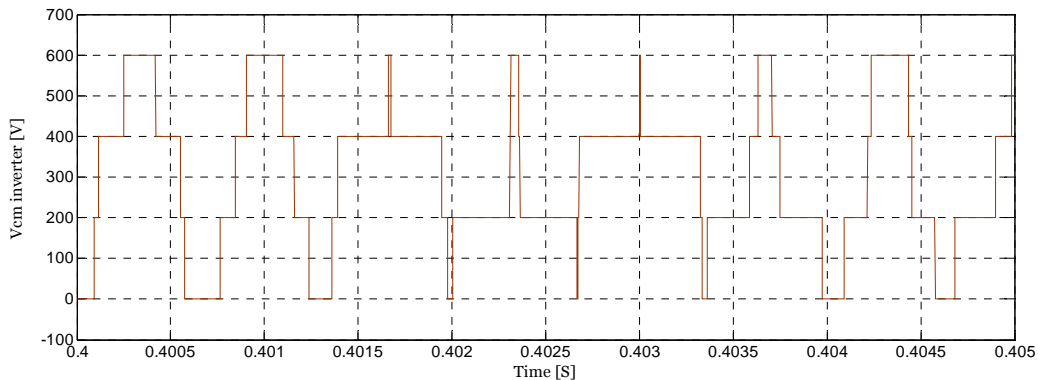


Figure A. 27 For 600 m  $V_{cm}$  inverter and motor terminal vs time with calculated  $R_f C_f$  filter

### A5 CM noise voltage at inverter and motor terminals using $R_f L_f C_f$ filter

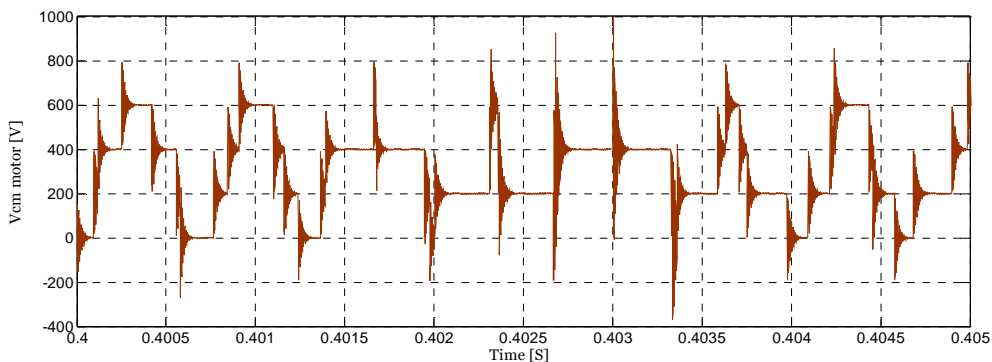
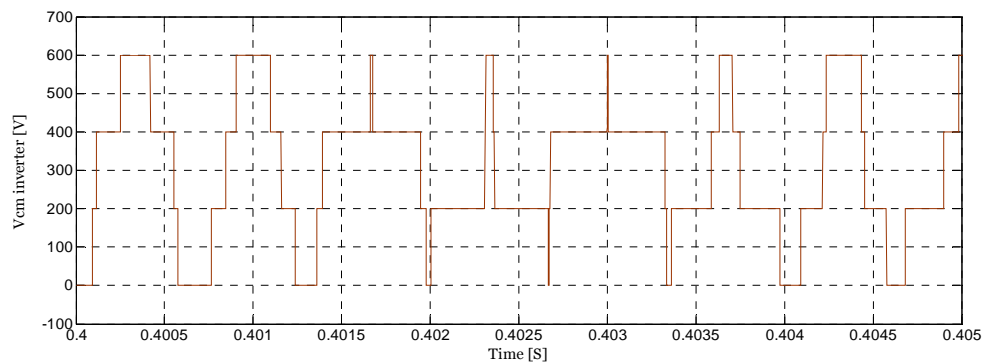


Figure A. 28 For 100 m  $V_{cm}$  inverter and motor terminal vs time with calculated  $R_f L_f C_f$  filter

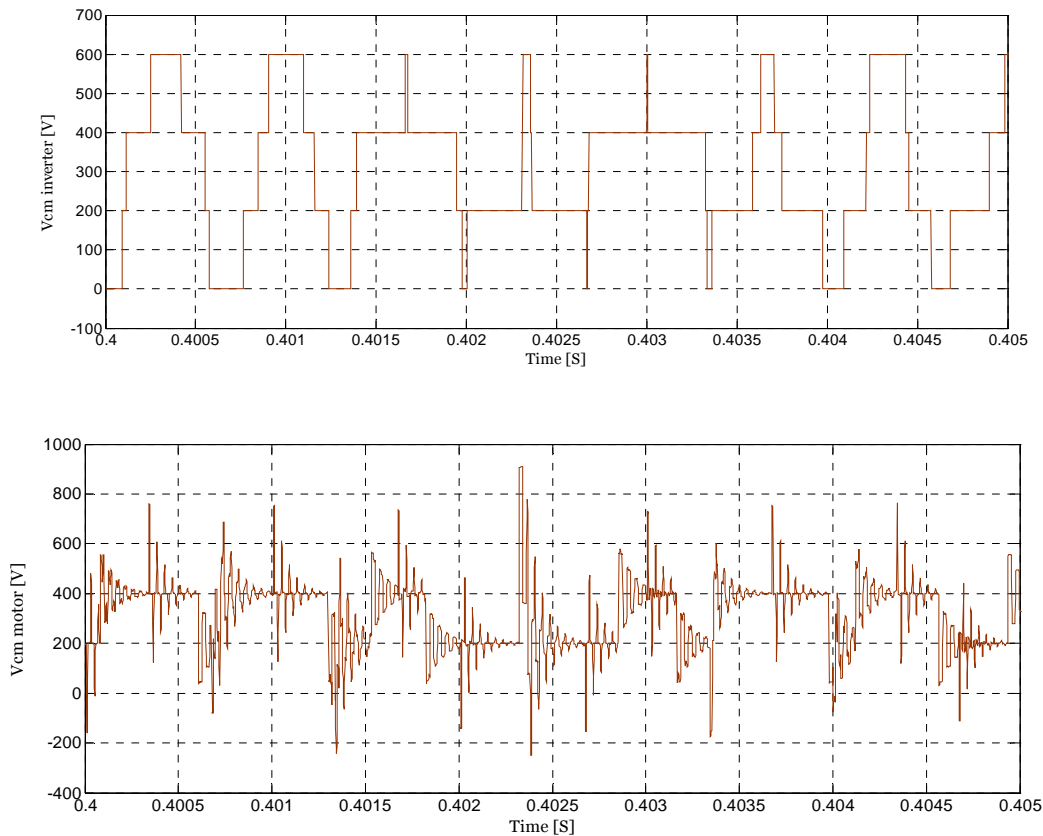


Figure A. 29 For 300 m  $V_{cm}$  inverter and motor terminal vs time with calculated  $R_fL_fC_f$  filter

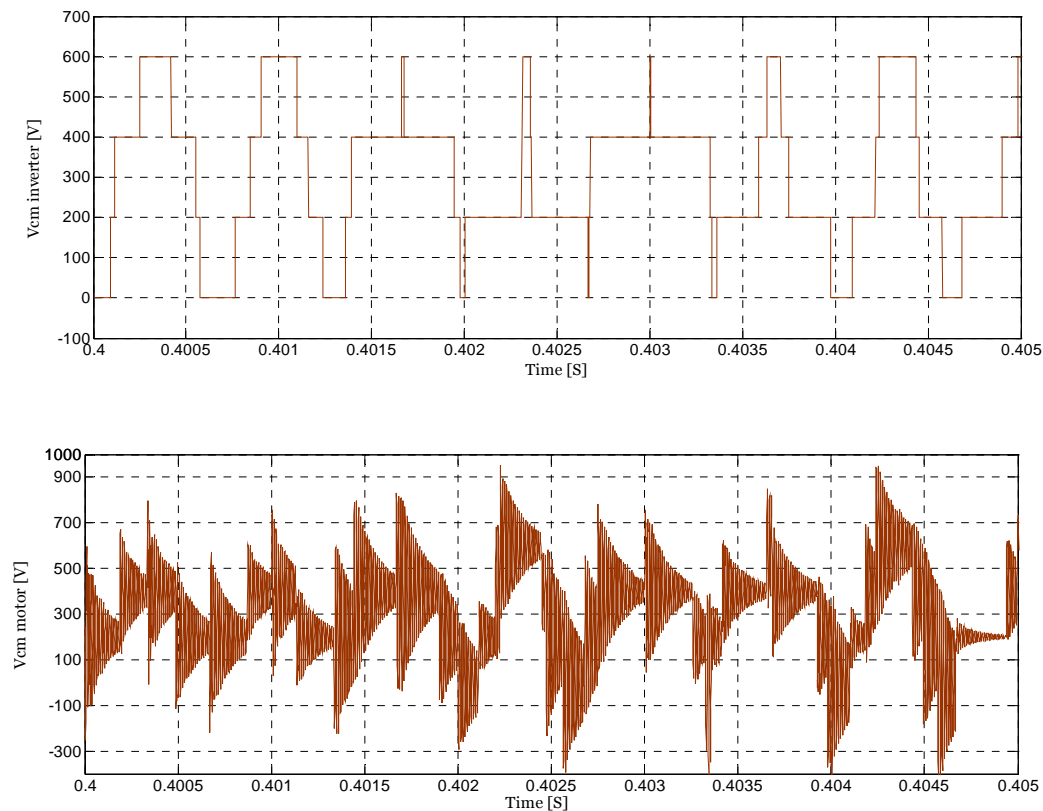


Figure A. 30 For 600 m  $V_{cm}$  inverter and motor terminal vs time with calculated  $R_fL_fC_f$  filter

## A6 CM noise voltage at inverter and motor terminals using $R_L L_f C_f$ split filter

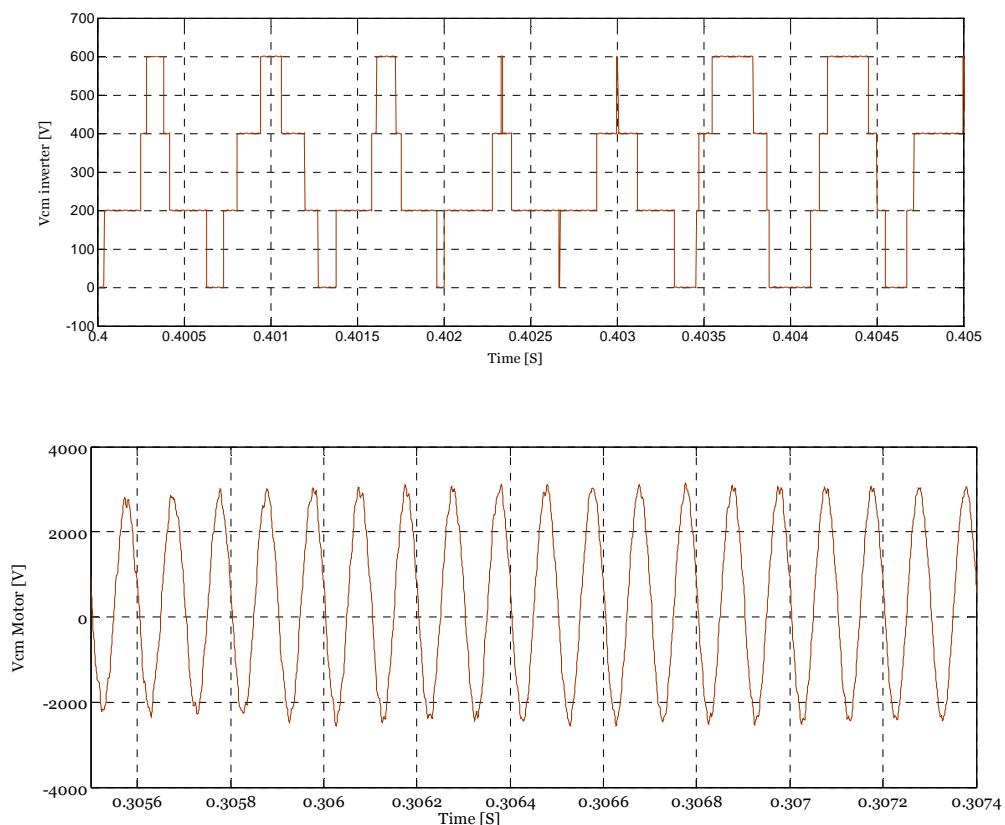


Figure A. 31 For 100 m  $V_{cm}$  inverter and motor terminal vs time with calculated  $R_L L_f C_f$  split filter

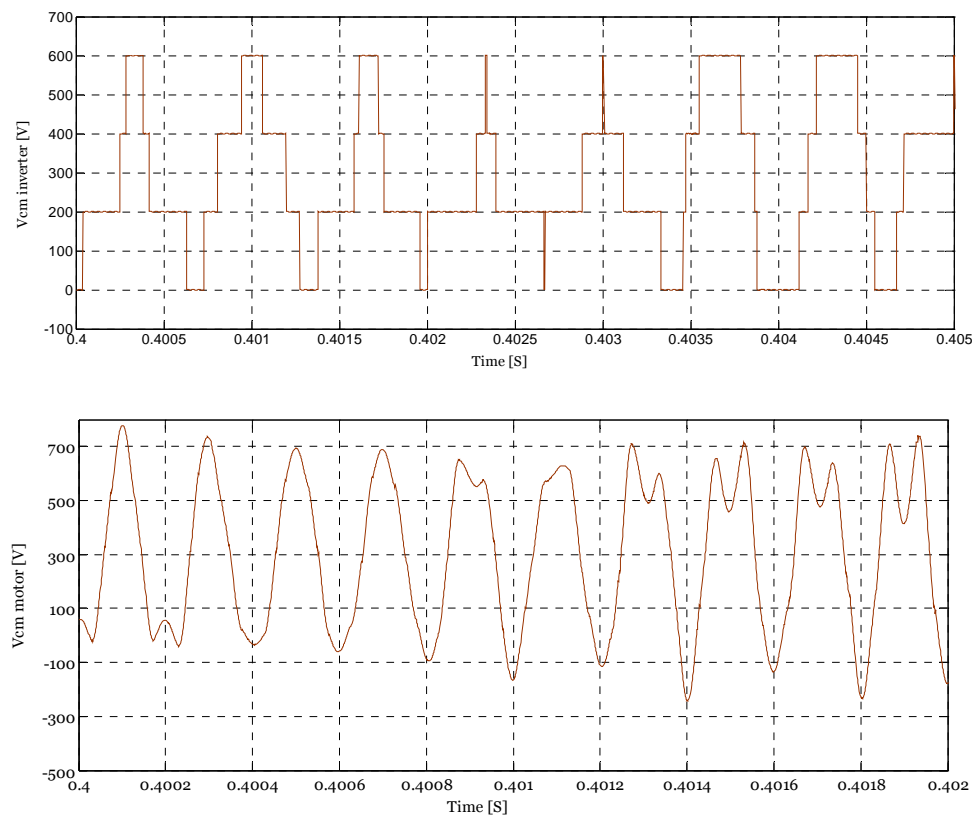


Figure A. 32 For 300 m  $V_{cm}$  inverter and motor terminal vs time with calculated  $R_L L_f C_f$  split filter

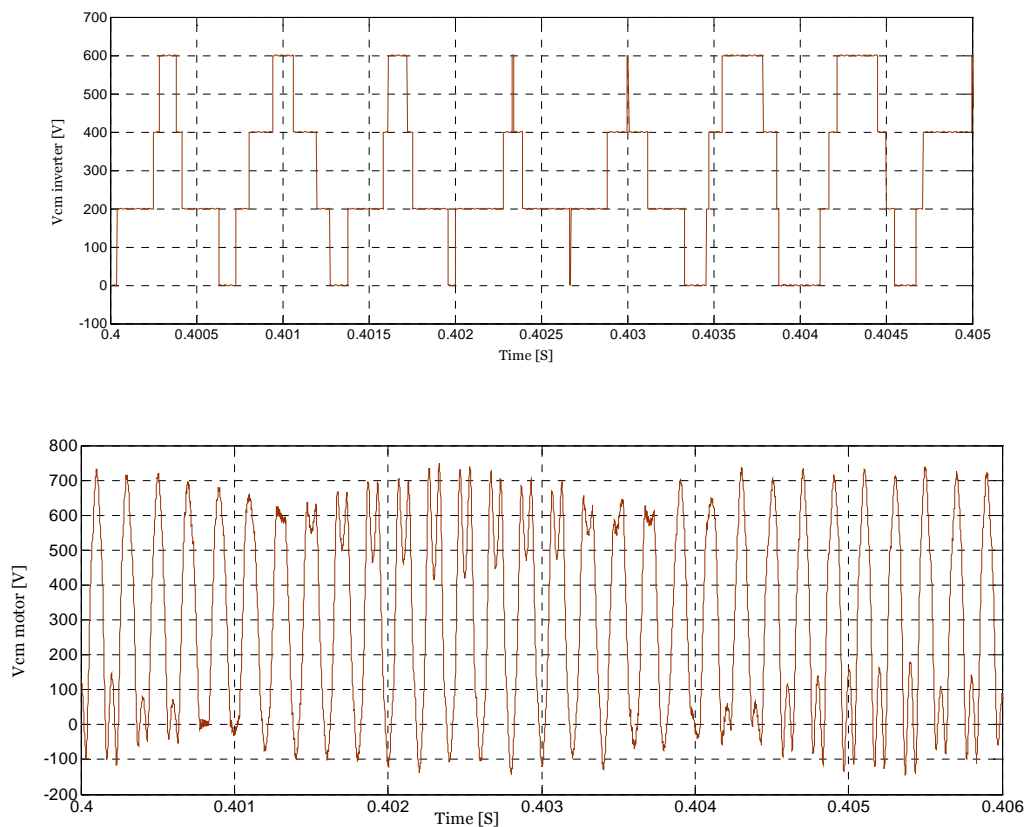


Figure A. 33 For 600 m  $V_{cm}$  inverter and motor terminal vs time with calculated  $R_fL_fC_f$  split filter

### A7 CM noise voltage at inverter and motor terminals using $L_fC_f$ filter

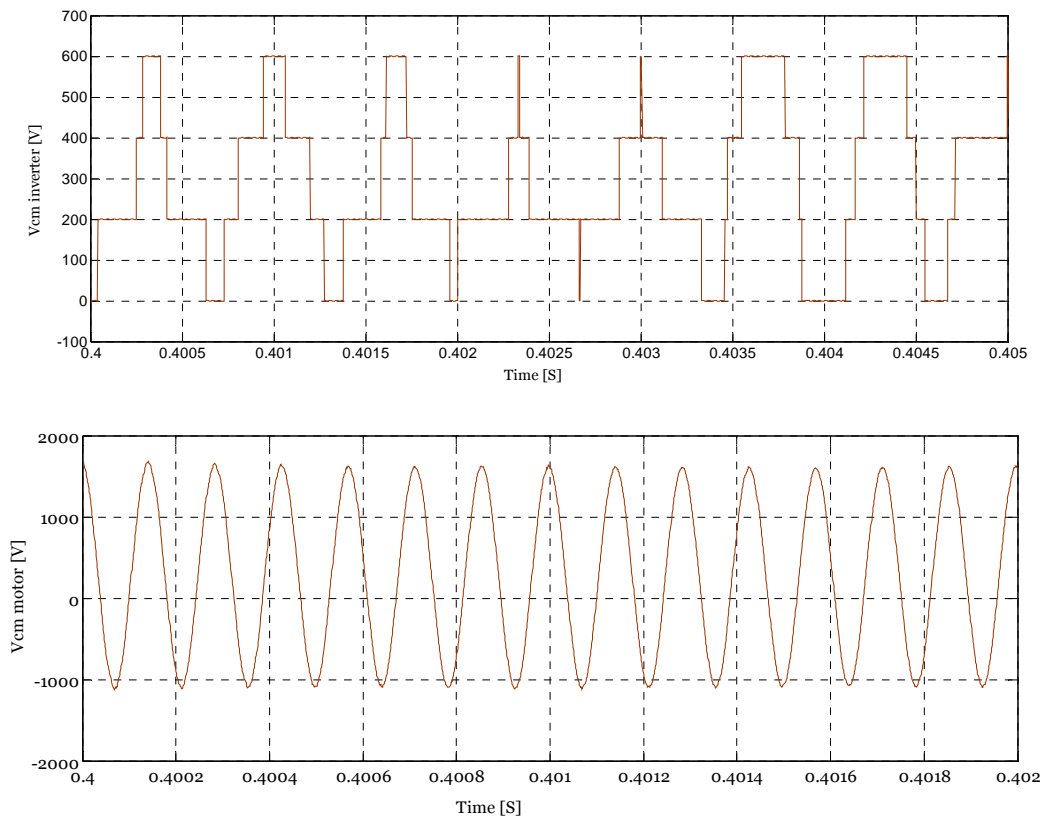


Figure A. 34 For 600 m  $V_{cm}$  inverter and motor terminal vs time with calculated  $L_fC_f$  filter

## B Matlab GUI code

```

function varargout = GUI_dvdtFilterDesign(varargin)
% GUI_DVDTFILTERDESIGN MATLAB code for GUI_dvdtFilterDesign.fig
%     GUI_DVDTFILTERDESIGN, by itself, creates a new GUI_DVDTFILTERDESIGN
or raises the existing
%     singleton*.
%
%     H = GUI_DVDTFILTERDESIGN returns the handle to a new
GUI_DVDTFILTERDESIGN or the handle to
%     the existing singleton*.
%
%     GUI_DVDTFILTERDESIGN('CALLBACK',hObject,eventData,handles,...) calls
the local
%     function named CALLBACK in GUI_DVDTFILTERDESIGN.M with the given
input arguments.
%
%     GUI_DVDTFILTERDESIGN('Property','Value',...) creates a new
GUI_DVDTFILTERDESIGN or raises the
%     existing singleton*. Starting from the left, property value pairs
are
%     applied to the GUI before GUI_dvdtFilterDesign_OpeningFcn gets
called. An
%     unrecognized property name or invalid value makes property
application
%     stop. All inputs are passed to GUI_dvdtFilterDesign_OpeningFcn via
varargin.
%
%     *See GUI Options on GUIDE's Tools menu. Choose "GUI allows only one
%     instance to run (singleton)".
% See also: GUIDE, GUIDATA, GUIHANDLES
% Edit the above text to modify the response to help GUI_dvdtFilterDesign
% Last Modified by GUIDE v2.5 02-Jul-2012 21:58:33
% Begin initialization code - DO NOT EDIT
gui_Singleton = 1;
gui_State = struct('gui_Name',       mfilename, ...
                  'gui_Singleton',  gui_Singleton, ...
                  'gui_OpeningFcn', @GUI_dvdtFilterDesign_OpeningFcn, ...
                  'gui_OutputFcn',  @GUI_dvdtFilterDesign_OutputFcn, ...
                  'gui_LayoutFcn',  [], ...
                  'gui_Callback',   []);
if nargin && ischar(varargin{1})
    gui_State.gui_Callback = str2func(varargin{1});
end
if nargout
    [varargout{1:nargout}] = gui_mainfcn(gui_State, varargin{:});
else
    gui_mainfcn(gui_State, varargin{:});
end
% End initialization code - DO NOT EDIT
% --- Executes just before GUI_dvdtFilterDesign is made visible.
function GUI_dvdtFilterDesign_OpeningFcn(hObject, eventdata, handles,
varargin)
% This function has no output args, see OutputFcn.
% hObject    handle to figure
% eventdata  reserved - to be defined in a future version of MATLAB
% handles    structure with handles and user data (see GUIDATA)
% varargin   command line arguments to GUI_dvdtFilterDesign (see VARARGIN)
% Choose default command line output for GUI_dvdtFilterDesign

```

```

handles.filename='PM_2L_Drive_long_cableRLC';
handles.filterType=1;
%Cable parametr initial values
set(handles.editRc,'String', num2str(8));
set(handles.editLc,'String', num2str(1e-3));
set(handles.editCc,'String', num2str(0.137e-6));
set(handles.editCableLength,'String', num2str(0.2));
set(handles.editVn,'String', num2str(200));
set(handles.editIn,'String', num2str(20));
set(handles.editfn,'String', num2str(50));
set(handles.editpolepair,'String', num2str(4));
set(handles.editrS,'String', num2str(0.2));
set(handles.editxd,'String', num2str(0.2));
set(handles.editxq,'String', num2str(0.2));
set(handles.editpsi_m,'String', num2str(0.9));
set(handles.editSamplingTime,'String', num2str(1/1500));
%Cable parametr initial values

handles.output = hObject;
    % Update handles structure
guidata(hObject, handles);

% UIWAIT makes GUI_dvdtFilterDesign wait for user response (see UIRESUME)
% uiwait(handles.figure1);
    % --- Outputs from this function are returned to the command line.
function varargout = GUI_dvdtFilterDesign_OutputFcn(hObject, eventdata,
handles)
% varargout    cell array for returning output args (see VARARGOUT);
% hObject      handle to figure
% eventdata    reserved - to be defined in a future version of MATLAB
% handles      structure with handles and user data (see GUIDATA)

% Get default command line output from handles structure
varargout{1} = handles.output;
function editvdc_Callback(hObject, eventdata, handles)
% hObject      handle to editvdc (see GCBO)
% eventdata    reserved - to be defined in a future version of MATLAB
% handles      structure with handles and user data (see GUIDATA)

% Hints: get(hObject,'String') returns contents of editvdc as text
%         str2double(get(hObject,'String')) returns contents of editvdc as a
double
    % --- Executes during object creation, after setting all properties.
function editvdc_CreateFcn(hObject, eventdata, handles)
% hObject      handle to editvdc (see GCBO)
% eventdata    reserved - to be defined in a future version of MATLAB
% handles      empty - handles not created until after all CreateFcns called
    % Hint: edit controls usually have a white background on Windows.
    %         See ISPC and COMPUTER.
if ispc && isequal(get(hObject,'BackgroundColor'),
get(0,'defaultUiControlBackgroundColor'))
    set(hObject,'BackgroundColor','white');
end
    % --- Executes on button press in pbFilterDesign.
function pbFilterDesign_Callback(hObject, eventdata, handles)
% hObject      handle to pbFilterDesign (see GCBO)
% eventdata    reserved - to be defined in a future version of MATLAB
% handles      structure with handles and user data (see GUIDATA)
    %Read cable parameters
length=str2double(get(handles.editCableLength,'String'));
Rc=str2double(get(handles.editRc,'String'));

```

```

Cc=str2double(get(handles.editCc, 'String'));
Lc=str2double(get(handles.editLc, 'String'));
%Read Inverter parameters
% Vdc=str2double(get(handles.editvdc, 'String'));
% ma=str2double(get(handles.editModulationIndex, 'String'));

% filter design calculation RLC
if(handles.filterType==1)

    zeta=str2double(get(handles.editZeta, 'String'));
    Rf=0.5*sqrt(Lc/Cc);
    fco=1/(27*length*sqrt(Lc*Cc));

    Cf=2*sqrt(1+2*zeta^2+sqrt((1+2*zeta^2)+1))/(pi*Rf*fco);
    Lf=Cf*(Rf/4)*(Rf/4);
    set(handles.editRf, 'String', num2str(Rf));
    set(handles.editCf, 'String', num2str(Cf));
    set(handles.editLf, 'String', num2str(Lf));
    set(handles.editfco, 'String', num2str(fco));
end

%filter design calculation RC
if(handles.filterType==2)
    Rf=sqrt(Lc/Cc);
    Cf=Lc*Cc/0.22314;
    set(handles.editRf, 'String', num2str(Rf));
    set(handles.editCf, 'String', num2str(Cf));
    set(handles.editLf, 'String', '-');
    set(handles.editfco, 'String', '-');
end

if(handles.filterType==3)
    Lf=200*8/(20*2*pi*60*sqrt(3)*100);
    set(handles.editRf, 'String', '-');
    set(handles.editCf, 'String', '-');
    set(handles.editLf, 'String', num2str(Lf));
    set(handles.editfco, 'String', '-');
end

if(handles.filterType==4)
    set(handles.editRf, 'String', '-');
    set(handles.editCf, 'String', '-');
    set(handles.editLf, 'String', '-');
    set(handles.editfco, 'String', '-');
end

open(handles.filename);
set_param([handles.filename '/U_dc1'], 'Amplitude',
get(handles.editvdc, 'String'));
%Filter parameters
if(handles.filterType==1)
    set_param([handles.filename '/RC'], 'Resistance', num2str(Rf));
    set_param([handles.filename '/RC'], 'Capacitance', num2str(Cf));
    set_param([handles.filename '/L'], 'Inductance', num2str(Lf));
end
if(handles.filterType==2)
    set_param([handles.filename '/RC'], 'Resistance', num2str(Rf));
    set_param([handles.filename '/RC'], 'Capacitance', num2str(Cf));
end
if(handles.filterType==3)
    set_param([handles.filename '/L'], 'Inductance', num2str(Lf));
end
%cable parameters
%[R1 R0]

```

```

Resistance= ['[' get(handles.editRc, 'String') ' ' num2str(Rc+3*(2.5*Rc))
']']
set_param([handles.filename '/Cable'],'Resistance',Resistance);

    %[L1 L0]
Inductance= ['[' get(handles.editLc, 'String') ' ' num2str(Lc+3*Lc) ']]
set_param([handles.filename '/Cable'],'Inductance',Inductance);
    %[C1 C0]
Capacitance= ['[' get(handles.editCc, 'String') ' ' num2str(0.75*Cc) ']]
set_param([handles.filename '/Cable'],'Capacitance', Capacitance );
    set_param([handles.filename '/Cable'],'Length',
get(handles.editCableLength, 'String'));
% Generator parameters
Vn=str2double(get(handles.editVn, 'String'));
In=str2double(get(handles.editIn, 'String'));
Rs=str2double(get(handles.editrs, 'String'));
Lq=str2double(get(handles.editxq, 'String'));
Ld=str2double(get(handles.editxd, 'String'));
fn=str2double(get(handles.editfn, 'String'));
p=str2double(get(handles.editpolepair, 'String'));
VsN=str2double(get(handles.editVn, 'String'));
IsN=str2double(get(handles.editIn, 'String'));
xd=str2double(get(handles.editxd, 'String'));
xq=str2double(get(handles.editxq, 'String'));
% set parameters to Simulink machine parameters
set_param([handles.filename '/PMMachine'],'UsN',get(handles.editVn,
'String'));
set_param([handles.filename '/PMMachine'],'IsN',get(handles.editIn,
'String'));
set_param([handles.filename '/PMMachine'],'fn',get(handles.editfn,
'String'));
set_param([handles.filename '/PMMachine'],'p',get(handles.editpolepair,
'String'));
set_param([handles.filename '/PMMachine'],'r_s',get(handles.editrs,
'String'));
set_param([handles.filename '/PMMachine'],'x_d',get(handles.editxd,
'String'));
set_param([handles.filename '/PMMachine'],'x_q',get(handles.editxq,
'String'));
set_param([handles.filename '/PMMachine'],'psi_M',get(handles.editpsi_m,
'String'));
% set parameters to Simulink control parameters
set_param([handles.filename '/PMMControl'],'UsN',get(handles.editVn,
'String'));
set_param([handles.filename '/PMMControl'],'IsN',get(handles.editIn,
'String'));
set_param([handles.filename '/PMMControl'],'fn',get(handles.editfn,
'String'));
set_param([handles.filename
'/PMMControl'],'polepairs',get(handles.editpolepair, 'String'));
set_param([handles.filename '/PMMControl'],'r_s',get(handles.editrs,
'String'));
set_param([handles.filename '/PMMControl'],'x_d',get(handles.editxd,
'String'));
set_param([handles.filename '/PMMControl'],'x_q',get(handles.editxq,
'String'));
set_param([handles.filename '/PMMControl'],'psi_s0',get(handles.editpsi_m,
'String'));
set_param([handles.filename
'/PMMControl'],'Tsamp',get(handles.editSamplingTime, 'String'));
switch get(handles.popupmenuControlMode, 'Value')

```



```

    case 1
        control_mode=0;
    case 2
        control_mode=1;
end

set_param([handles.filename
'/PMMControl'],'Speed_Controlled',num2str(control_mode));
% set parameters to Simulink Simulation parameters
set_param(handles.filename,
'StopTime',get(handles.editSimulationTime,'String'));
set(handles.pbRunSimulation,'Enable','on');
guidata(hObject,handles)
% --- Executes on button press in pbRunSimulation.
function pbRunSimulation_Callback(hObject, eventdata, handles)
% hObject    handle to pbRunSimulation (see GCBO)
% eventdata  reserved - to be defined in a future version of MATLAB
% handles    structure with handles and user data (see GUIDATA)
%cellstr
%contents=get(handles.popupmenuInverterType,'String');
%val=get(handles.popupmenuInverterType,'Value');
[handles.timeVector,handles.stateVector,handles.outputVector]
=sim(handles.filename);
set(handles.pbPlotResult,'Enable','on');

guidata(hObject,handles)
% --- Executes on button press in pbPlotResult.
function pbPlotResult_Callback(hObject, eventdata, handles)
% hObject    handle to pbPlotResult (see GCBO)
% eventdata  reserved - to be defined in a future version of MATLAB
% handles    structure with handles and user data (see GUIDATA)
if(get(handles.checkboxInverter,'Value' ))
    figure('Name','Inverter ouput voltage');
    plot(handles.timeVector,handles.outputVector(:,1));
    xlabel('Time [s]');
    ylabel('Vab Inverter [V]');
    grid;
end
if (get(handles.checkboxFilter,'Value' ))
    figure('Name','Filter ouput voltage');
    plot(handles.timeVector,handles.outputVector(:,2));
    xlabel('Time [s]');
    ylabel('Vab Filter [V]');
    grid;
end
if(get(handles.checkboxMotor,'Value' ))
    figure('Name','Motor terminal voltage');
    plot(handles.timeVector,handles.outputVector(:,3));
    xlabel('Time [s]');
    ylabel('Vab motor [V]');
    grid;
end
if(get(handles.checkboxCMVoltage,'Value'))
    figure('Name','Common Mode voltage');
    subplot(2,1,1)
    plot(handles.timeVector,handles.outputVector(:,4));
    xlabel('Time [s]');
    ylabel('VCM Inverter [V]');
    grid;
    subplot(2,1,2)
    plot(handles.timeVector,handles.outputVector(:,5));

```

```

        xlabel('Time [s]');
        ylabel('VCM Motor [V]');
        grid;
end
if(get(handles.checkboxFFT, 'Value'))
    figure('Name', 'FFT');
        subplot(3,1,1)
        fft(handles.outputVector(:,1));
        xlabel('Frequency [Hz]');
        ylabel('Inverter Voltage [V]');
        grid;
        subplot(3,1,2)
        fft(handles.outputVector(:,2));
        xlabel('Frequency [Hz]');
        ylabel('Filter Voltage [V]');
        grid;
        subplot(3,1,3)
        fft(handles.outputVector(:,2));
        xlabel('Frequency [Hz]');
        ylabel('Motor Voltage [V]');
        grid;
        handles.timeVector
        length(handles.timeVector)
end
function editRf_Callback(hObject, eventdata, handles)
% hObject    handle to editRf (see GCBO)
% eventdata  reserved - to be defined in a future version of MATLAB
% handles    structure with handles and user data (see GUIDATA)

% Hints: get(hObject,'String') returns contents of editRf as text
%        str2double(get(hObject,'String')) returns contents of editRf as a
double
% --- Executes during object creation, after setting all properties.
function editRf_CreateFcn(hObject, eventdata, handles)
% hObject    handle to editRf (see GCBO)
% eventdata  reserved - to be defined in a future version of MATLAB
% handles    empty - handles not created until after all CreateFcns called

% Hint: edit controls usually have a white background on Windows.
%        See ISPC and COMPUTER.
if ispc && isequal(get(hObject,'BackgroundColor'),
get(0,'defaultUicontrolBackgroundColor'))
    set(hObject,'BackgroundColor','white');
end
function editfco_Callback(hObject, eventdata, handles)
% hObject    handle to editfco (see GCBO)
% eventdata  reserved - to be defined in a future version of MATLAB
% handles    structure with handles and user data (see GUIDATA)

% Hints: get(hObject,'String') returns contents of editfco as text
%        str2double(get(hObject,'String')) returns contents of editfco as a
double

% --- Executes during object creation, after setting all properties.
function editfco_CreateFcn(hObject, eventdata, handles)
% hObject    handle to editfco (see GCBO)
% eventdata  reserved - to be defined in a future version of MATLAB
% handles    empty - handles not created until after all CreateFcns called
% Hint: edit controls usually have a white background on Windows.
%        See ISPC and COMPUTER.

```

```

if ispc && isequal(get(hObject,'BackgroundColor'),
get(0,'defaultUiControlBackgroundColor'))
    set(hObject,'BackgroundColor','white');
end
function editCf_Callback(hObject, eventdata, handles)
% hObject      handle to editCf (see GCBO)
% eventdata    reserved - to be defined in a future version of MATLAB
% handles      structure with handles and user data (see GUIDATA)
% Hints: get(hObject,'String') returns contents of editCf as text
%          str2double(get(hObject,'String')) returns contents of editCf as a
double
% --- Executes during object creation, after setting all properties.
function editCf_CreateFcn(hObject, eventdata, handles)
% hObject      handle to editCf (see GCBO)
% eventdata    reserved - to be defined in a future version of MATLAB
% handles      empty - handles not created until after all CreateFcns called
% Hint: edit controls usually have a white background on Windows.
%          See ISPC and COMPUTER.
if ispc && isequal(get(hObject,'BackgroundColor'),
get(0,'defaultUiControlBackgroundColor'))
    set(hObject,'BackgroundColor','white');
end
function editLf_Callback(hObject, eventdata, handles)
% hObject      handle to editLf (see GCBO)
% eventdata    reserved - to be defined in a future version of MATLAB
% handles      structure with handles and user data (see GUIDATA)

% Hints: get(hObject,'String') returns contents of editLf as text
%          str2double(get(hObject,'String')) returns contents of editLf as a
double
% --- Executes during object creation, after setting all properties.
function editLf_CreateFcn(hObject, eventdata, handles)
% hObject      handle to editLf (see GCBO)
% eventdata    reserved - to be defined in a future version of MATLAB
% handles      empty - handles not created until after all CreateFcns called

% Hint: edit controls usually have a white background on Windows.
%          See ISPC and COMPUTER.
if ispc && isequal(get(hObject,'BackgroundColor'),
get(0,'defaultUiControlBackgroundColor'))
    set(hObject,'BackgroundColor','white');
end
function editRc_Callback(hObject, eventdata, handles)
% hObject      handle to editRc (see GCBO)
% eventdata    reserved - to be defined in a future version of MATLAB
% handles      structure with handles and user data (see GUIDATA)
% Hints: get(hObject,'String') returns contents of editRc as text
%          str2double(get(hObject,'String')) returns contents of editRc as a
double
% Rc=str2double(get(hObject,'String'));
% --- Executes during object creation, after setting all properties.
function editRc_CreateFcn(hObject, eventdata, handles)
% hObject      handle to editRc (see GCBO)
% eventdata    reserved - to be defined in a future version of MATLAB
% handles      empty - handles not created until after all CreateFcns called
% Hint: edit controls usually have a white background on Windows.
%          See ISPC and COMPUTER.
if ispc && isequal(get(hObject,'BackgroundColor'),
get(0,'defaultUiControlBackgroundColor'))
    set(hObject,'BackgroundColor','white');
end

```

---

```

function editCc_Callback(hObject, eventdata, handles)
% hObject    handle to editCc (see GCBO)
% eventdata  reserved - to be defined in a future version of MATLAB
% handles    structure with handles and user data (see GUIDATA)
% Hints: get(hObject,'String') returns contents of editCc as text
%         str2double(get(hObject,'String')) returns contents of editCc as a
double
% Cc=str2double(get(hObject,'String'));

% --- Executes during object creation, after setting all properties.
function editCc_CreateFcn(hObject, eventdata, handles)
% hObject    handle to editCc (see GCBO)
% eventdata  reserved - to be defined in a future version of MATLAB
% handles    empty - handles not created until after all CreateFcns called
% Hint: edit controls usually have a white background on Windows.
%         See ISPC and COMPUTER.
if ispc && isequal(get(hObject,'BackgroundColor'),
get(0,'defaultUiControlBackgroundColor'))
    set(hObject,'BackgroundColor','white');
end
function editLc_Callback(hObject, eventdata, handles)
% hObject    handle to editLc (see GCBO)
% eventdata  reserved - to be defined in a future version of MATLAB
% handles    structure with handles and user data (see GUIDATA)

% Hints: get(hObject,'String') returns contents of editLc as text
%         str2double(get(hObject,'String')) returns contents of editLc as a
double
% Lc=str2double(get(handles.editLc,'String'));
% --- Executes during object creation, after setting all properties.
function editLc_CreateFcn(hObject, eventdata, handles)
% hObject    handle to editLc (see GCBO)
% eventdata  reserved - to be defined in a future version of MATLAB
% handles    empty - handles not created until after all CreateFcns called

% Hint: edit controls usually have a white background on Windows.
%         See ISPC and COMPUTER.
if ispc && isequal(get(hObject,'BackgroundColor'),
get(0,'defaultUiControlBackgroundColor'))
    set(hObject,'BackgroundColor','white');
end

function editSimulationTime_Callback(hObject, eventdata, handles)
% hObject    handle to editSimulationTime (see GCBO)
% eventdata  reserved - to be defined in a future version of MATLAB
% handles    structure with handles and user data (see GUIDATA)

% Hints: get(hObject,'String') returns contents of editSimulationTime as
text
%         str2double(get(hObject,'String')) returns contents of
editSimulationTime as a double

%Tsimulation=str2double(get(hObject,'String'));

% --- Executes during object creation, after setting all properties.
function editSimulationTime_CreateFcn(hObject, eventdata, handles)
% hObject    handle to editSimulationTime (see GCBO)
% eventdata  reserved - to be defined in a future version of MATLAB
% handles    empty - handles not created until after all CreateFcns called

```

```

% Hint: edit controls usually have a white background on Windows.
%     See ISPC and COMPUTER.
if ispc && isequal(get(hObject,'BackgroundColor'),
get(0,'defaultUiControlBackgroundColor'))
    set(hObject,'BackgroundColor','white');
end
% --- Executes on button press in pbReset.
function pbReset_Callback(hObject, eventdata, handles)
% hObject     handle to pbReset (see GCBO)
% eventdata   reserved - to be defined in a future version of MATLAB
% handles     structure with handles and user data (see GUIDATA)
set(handles.editRc,'String',[]);
set(handles.editLc,'String',[]);
set(handles.editCc,'String',[]);
set(handles.editCableLength,'String',[]);
set(handles.editfco,'String',[]);
set(handles.edittvdc,'String',[]);
set(handles.editModulationIndex,'String',[]);
set(handles.editSimulationTime,'String',' ');
%Generstor parameter
set(handles.editVn, 'String',[] );
set(handles.editIn, 'String',[] );
set(handles.editrS, 'String',[] );
set(handles.editxd, 'String',[] );
set(handles.editxq, 'String',[] );
set(handles.editfn, 'String',[] );
set(handles.editpolepair, 'String',[] );
set(handles.editfop, 'String',[] );
    set(handles.editRf,'String',[]);
set(handles.editLf,'String',[]);
set(handles.editCf,'String',[]);
    set(handles.pbRunSimulation,'Enable','off');
set(handles.pbPlotResult,'Enable','off');

set(handles.checkboxInverter,'Value',0);
set(handles.checkboxFilter,'Value',0);
set(handles.checkboxMotor,'Value',0);
% --- Executes on button press in pbClose.
function pbClose_Callback(hObject, eventdata, handles)
% hObject     handle to pbClose (see GCBO)
% eventdata   reserved - to be defined in a future version of MATLAB
% handles     structure with handles and user data (see GUIDATA)

close();
% --- Executes on selection change in popupmenuInverterType.
function popupmenuInverterType_Callback(hObject, eventdata, handles)
% hObject     handle to popupmenuInverterType (see GCBO)
% eventdata   reserved - to be defined in a future version of MATLAB
% handles     structure with handles and user data (see GUIDATA)

% Hints: contents = cellstr(get(hObject,'String')) returns
popupmenuInverterType contents as cell array
%     contents{get(hObject,'Value')} returns selected item from
popupmenuInverterType
switch get(hObject,'Value')
    case 1
        open('\windgen2level_tg');
    case 2
        open('\windgen3level_tg');
end
--- Executes during object creation, after setting all properties.

```

```

function popupmenuInverterType_CreateFcn(hObject, eventdata, handles)
% hObject    handle to popupmenuInverterType (see GCBO)
% eventdata  reserved - to be defined in a future version of MATLAB
% handles    empty - handles not created until after all CreateFcns called

% Hint: popupmenu controls usually have a white background on Windows.
%       See ISPC and COMPUTER.
if ispc && isequal(get(hObject,'BackgroundColor'),
get(0,'defaultUiControlBackgroundColor'))
    set(hObject,'BackgroundColor','white');
end
function editModulationIndex_Callback(hObject, eventdata, handles)
% hObject    handle to editModulationIndex (see GCBO)
% eventdata  reserved - to be defined in a future version of MATLAB
% handles    structure with handles and user data (see GUIDATA)

% Hints: get(hObject,'String') returns contents of editModulationIndex as
text
%       str2double(get(hObject,'String')) returns contents of
editModulationIndex as a double
% --- Executes during object creation, after setting all properties.
function editModulationIndex_CreateFcn(hObject, eventdata, handles)
% hObject    handle to editModulationIndex (see GCBO)
% eventdata  reserved - to be defined in a future version of MATLAB
% handles    empty - handles not created until after all CreateFcns called

% Hint: edit controls usually have a white background on Windows.
%       See ISPC and COMPUTER.
if ispc && isequal(get(hObject,'BackgroundColor'),
get(0,'defaultUiControlBackgroundColor'))
    set(hObject,'BackgroundColor','white');
end
function editCableLength_Callback(hObject, eventdata, handles)
% hObject    handle to editCableLength (see GCBO)
% eventdata  reserved - to be defined in a future version of MATLAB
% handles    structure with handles and user data (see GUIDATA)

% Hints: get(hObject,'String') returns contents of editCableLength as text
%       str2double(get(hObject,'String')) returns contents of
editCableLength as a double
% --- Executes during object creation, after setting all properties.
function editCableLength_CreateFcn(hObject, eventdata, handles)
% hObject    handle to editCableLength (see GCBO)
% eventdata  reserved - to be defined in a future version of MATLAB
% handles    empty - handles not created until after all CreateFcns called

% Hint: edit controls usually have a white background on Windows.
%       See ISPC and COMPUTER.
if ispc && isequal(get(hObject,'BackgroundColor'),
get(0,'defaultUiControlBackgroundColor'))
    set(hObject,'BackgroundColor','white');
end
% --- Executes on button press in checkboxCMVoltage.
function checkboxCMVoltage_Callback(hObject, eventdata, handles)
% hObject    handle to checkboxCMVoltage (see GCBO)
% eventdata  reserved - to be defined in a future version of MATLAB
% handles    structure with handles and user data (see GUIDATA)

% Hint: get(hObject,'Value') returns toggle state of checkboxCMVoltage
% --- Executes on button press in checkboxInverter.

```

---

```

function checkboxInverter_Callback(hObject, eventdata, handles)
% hObject      handle to checkboxInverter (see GCBO)
% eventdata    reserved - to be defined in a future version of MATLAB
% handles      structure with handles and user data (see GUIDATA)

% Hint: get(hObject,'Value') returns toggle state of checkboxInverter
% --- Executes on button press in checkboxFilter.
function checkboxFilter_Callback(hObject, eventdata, handles)
% hObject      handle to checkboxFilter (see GCBO)
% eventdata    reserved - to be defined in a future version of MATLAB
% handles      structure with handles and user data (see GUIDATA)

% Hint: get(hObject,'Value') returns toggle state of checkboxFilter
% --- Executes on button press in checkboxMotor.
function checkboxMotor_Callback(hObject, eventdata, handles)
% hObject      handle to checkboxMotor (see GCBO)
% eventdata    reserved - to be defined in a future version of MATLAB
% handles      structure with handles and user data (see GUIDATA)

% Hint: get(hObject,'Value') returns toggle state of checkboxMotor
function editxq_Callback(hObject, eventdata, handles)
% hObject      handle to editxq (see GCBO)
% eventdata    reserved - to be defined in a future version of MATLAB
% handles      structure with handles and user data (see GUIDATA)

% Hints: get(hObject,'String') returns contents of editxq as text
%        str2double(get(hObject,'String')) returns contents of editxq as a
double
% --- Executes during object creation, after setting all properties.
function editxq_CreateFcn(hObject, eventdata, handles)
% hObject      handle to editxq (see GCBO)
% eventdata    reserved - to be defined in a future version of MATLAB
% handles      empty - handles not created until after all CreateFcns called

% Hint: edit controls usually have a white background on Windows.
%        See ISPC and COMPUTER.
if ispc && isequal(get(hObject,'BackgroundColor'),
get(0,'defaultUiControlBackgroundColor'))
    set(hObject,'BackgroundColor','white');
end
function editrs_Callback(hObject, eventdata, handles)
% hObject      handle to editrs (see GCBO)
% eventdata    reserved - to be defined in a future version of MATLAB
% handles      structure with handles and user data (see GUIDATA)

% Hints: get(hObject,'String') returns contents of editrs as text
%        str2double(get(hObject,'String')) returns contents of editrs as a
double
% --- Executes during object creation, after setting all properties.
function editrs_CreateFcn(hObject, eventdata, handles)
% hObject      handle to editrs (see GCBO)
% eventdata    reserved - to be defined in a future version of MATLAB
% handles      empty - handles not created until after all CreateFcns called

% Hint: edit controls usually have a white background on Windows.
%        See ISPC and COMPUTER.
if ispc && isequal(get(hObject,'BackgroundColor'),
get(0,'defaultUiControlBackgroundColor'))
    set(hObject,'BackgroundColor','white');
end

```

---

```

function editfn_Callback(hObject, eventdata, handles)
% hObject    handle to editfn (see GCBO)
% eventdata  reserved - to be defined in a future version of MATLAB
% handles    structure with handles and user data (see GUIDATA)

% Hints: get(hObject,'String') returns contents of editfn as text
%        str2double(get(hObject,'String')) returns contents of editfn as a
double
% --- Executes during object creation, after setting all properties.
function editfn_CreateFcn(hObject, eventdata, handles)
% hObject    handle to editfn (see GCBO)
% eventdata  reserved - to be defined in a future version of MATLAB
% handles    empty - handles not created until after all CreateFcns called

% Hint: edit controls usually have a white background on Windows.
%        See ISPC and COMPUTER.
if ispc && isequal(get(hObject,'BackgroundColor'),
get(0,'defaultUicontrolBackgroundColor'))
    set(hObject,'BackgroundColor','white');
end
function editpolepair_Callback(hObject, eventdata, handles)
% hObject    handle to editpolepair (see GCBO)
% eventdata  reserved - to be defined in a future version of MATLAB
% handles    structure with handles and user data (see GUIDATA)

% Hints: get(hObject,'String') returns contents of editpolepair as text
%        str2double(get(hObject,'String')) returns contents of editpolepair
as a double
% --- Executes during object creation, after setting all properties.
function editpolepair_CreateFcn(hObject, eventdata, handles)
% hObject    handle to editpolepair (see GCBO)
% eventdata  reserved - to be defined in a future version of MATLAB
% handles    empty - handles not created until after all CreateFcns called

% Hint: edit controls usually have a white background on Windows.
%        See ISPC and COMPUTER.
if ispc && isequal(get(hObject,'BackgroundColor'),
get(0,'defaultUicontrolBackgroundColor'))
    set(hObject,'BackgroundColor','white');
end
function editfop_Callback(hObject, eventdata, handles)
% hObject    handle to editfop (see GCBO)
% eventdata  reserved - to be defined in a future version of MATLAB
% handles    structure with handles and user data (see GUIDATA)

% Hints: get(hObject,'String') returns contents of editfop as text
%        str2double(get(hObject,'String')) returns contents of editfop as a
double
% --- Executes during object creation, after setting all properties.
function editfop_CreateFcn(hObject, eventdata, handles)
% hObject    handle to editfop (see GCBO)
% eventdata  reserved - to be defined in a future version of MATLAB
% handles    empty - handles not created until after all CreateFcns called

% Hint: edit controls usually have a white background on Windows.
%        See ISPC and COMPUTER.
if ispc && isequal(get(hObject,'BackgroundColor'),
get(0,'defaultUicontrolBackgroundColor'))
    set(hObject,'BackgroundColor','white');
end

```



---

```

function editVn_Callback(hObject, eventdata, handles)
% hObject      handle to editVn (see GCBO)
% eventdata    reserved - to be defined in a future version of MATLAB
% handles      structure with handles and user data (see GUIDATA)

% Hints: get(hObject,'String') returns contents of editVn as text
%         str2double(get(hObject,'String')) returns contents of editVn as a
double
% --- Executes during object creation, after setting all properties.
function editVn_CreateFcn(hObject, eventdata, handles)
% hObject      handle to editVn (see GCBO)
% eventdata    reserved - to be defined in a future version of MATLAB
% handles      empty - handles not created until after all CreateFcns called

% Hint: edit controls usually have a white background on Windows.
%         See ISPC and COMPUTER.
if ispc && isequal(get(hObject,'BackgroundColor'),
get(0,'defaultUicontrolBackgroundColor'))
    set(hObject,'BackgroundColor','white');
end
function editIn_Callback(hObject, eventdata, handles)
% hObject      handle to editIn (see GCBO)
% eventdata    reserved - to be defined in a future version of MATLAB
% handles      structure with handles and user data (see GUIDATA)

% Hints: get(hObject,'String') returns contents of editIn as text
%         str2double(get(hObject,'String')) returns contents of editIn as a
double
% --- Executes during object creation, after setting all properties.
function editIn_CreateFcn(hObject, eventdata, handles)
% hObject      handle to editIn (see GCBO)
% eventdata    reserved - to be defined in a future version of MATLAB
% handles      empty - handles not created until after all CreateFcns called

% Hint: edit controls usually have a white background on Windows.
%         See ISPC and COMPUTER.
if ispc && isequal(get(hObject,'BackgroundColor'),
get(0,'defaultUicontrolBackgroundColor'))
    set(hObject,'BackgroundColor','white');
end
function editxd_Callback(hObject, eventdata, handles)
% hObject      handle to editxd (see GCBO)
% eventdata    reserved - to be defined in a future version of MATLAB
% handles      structure with handles and user data (see GUIDATA)

% Hints: get(hObject,'String') returns contents of editxd as text
%         str2double(get(hObject,'String')) returns contents of editxd as a
double
% --- Executes during object creation, after setting all properties.
function editxd_CreateFcn(hObject, eventdata, handles)
% hObject      handle to editxd (see GCBO)
% eventdata    reserved - to be defined in a future version of MATLAB
% handles      empty - handles not created until after all CreateFcns called

% Hint: edit controls usually have a white background on Windows.
%         See ISPC and COMPUTER.
if ispc && isequal(get(hObject,'BackgroundColor'),
get(0,'defaultUicontrolBackgroundColor'))
    set(hObject,'BackgroundColor','white');
end

```

```

% --- Executes on button press in radiobuttonRLC.
function radiobuttonRLC_Callback(hObject, eventdata, handles)
% hObject    handle to radiobuttonRLC (see GCBO)
% eventdata  reserved - to be defined in a future version of MATLAB
% handles    structure with handles and user data (see GUIDATA)

% Hint: get(hObject,'Value') returns toggle state of radiobuttonRLC
% --- Executes on button press in radiobuttonRC.
function radiobuttonRC_Callback(hObject, eventdata, handles)
% hObject    handle to radiobuttonRC (see GCBO)
% eventdata  reserved - to be defined in a future version of MATLAB
% handles    structure with handles and user data (see GUIDATA)

% Hint: get(hObject,'Value') returns toggle state of radiobuttonRC
% --- Executes on button press in radiobuttonL.
function radiobuttonL_Callback(hObject, eventdata, handles)
% hObject    handle to radiobuttonL (see GCBO)
% eventdata  reserved - to be defined in a future version of MATLAB
% handles    structure with handles and user data (see GUIDATA)

% Hint: get(hObject,'Value') returns toggle state of radiobuttonL
% --- Executes on button press in radiobuttonNo.
function radiobuttonNo_Callback(hObject, eventdata, handles)
% hObject    handle to radiobuttonNo (see GCBO)
% eventdata  reserved - to be defined in a future version of MATLAB
% handles    structure with handles and user data (see GUIDATA)

% Hint: get(hObject,'Value') returns toggle state of radiobuttonNo
function editSamplingTime_Callback(hObject, eventdata, handles)
% hObject    handle to editSamplingTime (see GCBO)
% eventdata  reserved - to be defined in a future version of MATLAB
% handles    structure with handles and user data (see GUIDATA)

% Hints: get(hObject,'String') returns contents of editSamplingTime as text
%        str2double(get(hObject,'String')) returns contents of
editSamplingTime as a double
% --- Executes during object creation, after setting all properties.
function editSamplingTime_CreateFcn(hObject, eventdata, handles)
% hObject    handle to editSamplingTime (see GCBO)
% eventdata  reserved - to be defined in a future version of MATLAB
% handles    empty - handles not created until after all CreateFcns called
% Hint: edit controls usually have a white background on Windows.
%         See ISPC and COMPUTER.
if ispc && isequal(get(hObject,'BackgroundColor'),
get(0,'defaultUicontrolBackgroundColor'))
    set(hObject,'BackgroundColor','white');
end
% --- Executes on selection change in popupmenuControlMode.
function popupmenuControlMode_Callback(hObject, eventdata, handles)
% hObject    handle to popupmenuControlMode (see GCBO)
% eventdata  reserved - to be defined in a future version of MATLAB
% handles    structure with handles and user data (see GUIDATA)
% Hints: contents = cellstr(get(hObject,'String')) returns
popupmenuControlMode contents as cell array
%        contents{get(hObject,'Value')} returns selected item from
popupmenuControlMode
% --- Executes during object creation, after setting all properties.
function popupmenuControlMode_CreateFcn(hObject, eventdata, handles)
% hObject    handle to popupmenuControlMode (see GCBO)
% eventdata  reserved - to be defined in a future version of MATLAB

```

```

% handles    empty - handles not created until after all CreateFcns called
% Hint: popupmenu controls usually have a white background on Windows.
%         See ISPC and COMPUTER.
if ispc && isequal(get(hObject,'BackgroundColor'),
get(0,'defaultUiControlBackgroundColor'))
    set(hObject,'BackgroundColor','white');
end
% --- Executes on button press in checkboxFFT.
function checkboxFFT_Callback(hObject, eventdata, handles)
% hObject    handle to checkboxFFT (see GCBO)
% eventdata  reserved - to be defined in a future version of MATLAB
% handles    structure with handles and user data (see GUIDATA)

% Hint: get(hObject,'Value') returns toggle state of checkboxFFT
function editpsi_m_Callback(hObject, eventdata, handles)
% hObject    handle to editpsi_m (see GCBO)
% eventdata  reserved - to be defined in a future version of MATLAB
% handles    structure with handles and user data (see GUIDATA)
% Hints: get(hObject,'String') returns contents of editpsi_m as text
%        str2double(get(hObject,'String')) returns contents of editpsi_m as
a double
% --- Executes during object creation, after setting all properties.
function editpsi_m_CreateFcn(hObject, eventdata, handles)
% hObject    handle to editpsi_m (see GCBO)
% eventdata  reserved - to be defined in a future version of MATLAB
% handles    empty - handles not created until after all CreateFcns called

% Hint: edit controls usually have a white background on Windows.
%         See ISPC and COMPUTER.
if ispc && isequal(get(hObject,'BackgroundColor'),
get(0,'defaultUiControlBackgroundColor'))
    set(hObject,'BackgroundColor','white');
end
% --- Executes when selected object is changed in uipanelFilterType.
function uipanelFilterType_SelectionChangeFcn(hObject, eventdata, handles)
% hObject    handle to the selected object in uipanelFilterType
% eventdata  structure with the following fields (see UIBUTTONGROUP)
%   EventName: string 'SelectionChanged' (read only)
%   OldValue: handle of the previously selected object or empty if none was
selected
%   NewValue: handle of the currently selected object
% handles    structure with handles and user data (see GUIDATA)

switch get(eventdata.NewValue,'Tag') % Get Tag of selected object.
case 'radiobuttonRLC'
    % Code for when radiobutton1 is selected.
    handles.filename='PM_2L_Drive_long_cableRLC';
    handles.filterType=1;
case 'radiobuttonRC'
    % Code for when radiobutton2 is selected.
    handles.filename='PM_2L_Drive_long_cableRC';
    handles.filterType=2;

case 'radiobuttonL'
    % Code for when togglebutton1 is selected.
    handles.filename='PM_2L_Drive_long_cableL';
    handles.filterType=3;
otherwise
    % Code for when there is no match.
    handles.filename='PM_2L_Drive_long_cablewithoutfilter';

```

```
        handles.filterType=4;
end

if handles.filterType==1
    set(handles.editZeta,'Visible','on');
else
    set(handles.editZeta,'Visible','off');
end
guidata(hObject,handles)
function editZeta_Callback(hObject, eventdata, handles)
% hObject    handle to editZeta (see GCBO)
% eventdata  reserved - to be defined in a future version of MATLAB
% handles    structure with handles and user data (see GUIDATA)

% Hints: get(hObject,'String') returns contents of editZeta as text
%        str2double(get(hObject,'String')) returns contents of editZeta as
a double
if handles.filterType==1
    set(hObject,'Visible','on');
else
    set(hObject,'Visible','off');
end
guidata(hObject,handles)
% --- Executes during object creation, after setting all properties.
function editZeta_CreateFcn(hObject, eventdata, handles)
% hObject    handle to editZeta (see GCBO)
% eventdata  reserved - to be defined in a future version of MATLAB
% handles    empty - handles not created until after all CreateFcns called

% Hint: edit controls usually have a white background on Windows.
%       See ISPC and COMPUTER.
if ispc && isequal(get(hObject,'BackgroundColor'),
get(0,'defaultUiControlBackgroundColor'))
    set(hObject,'BackgroundColor','white');
end
```

## C Specification of instruments

Table C. 1 Key Features & specifications for N9000A series CXA signal analyzer

Functionality	Performance	Measurement Application & Software	Automation & Communication Interface
9 kHz to 3 or 7.5 GHz; internal preamplifier options up to 7.5 GHz	$\pm 0.5$ dB absolute amplitude accuracy	CXA supports over 25 measurement applications, covering cellular communication, wireless connectivity, digital video, and general purpose	USB 2.0, 1000 Base-T LAN, GPIB
Optional built-in tracking generator 3 or 6 GHz	+17 dBm third order intercept (TOI)	Advanced analysis of up to 70 signal formats, software runs inside the CXA	Programming remote language compatibility with ESA and other X-Series
10 MHz (standard), 25 MHz (optional) analysis bandwidth	-163 dBm displayed average noise level (DANL)		Common X-Series user interface / Open Windows® XP operating system

Table C. 2 Key Features & specifications Agilent 41800A series active Probe

Functionality	Frequency response:	Allowable input (DC + AC) and connector
Bandwidth: 5 Hz to 500 MHz	relative to 50 MHz: +1/-2 dB @ < 50 Hz	Maximum allowable input (DC + AC): $\pm 40$ V
Probe gain: 0 dB $\pm$ 0.5 dB @ 50 MHz	$\pm 1$ dB @ 50 Hz to 200 MHz	Output connector: 50 W type-N male
	+1.5/-2 dB @ > 200 MHz	

Table C. 3 Key Features &amp; specifications PEARSON current probe model 110

<b>Functionality</b>
Sensitivity 0.1 Volt/Ampere +1/-0%
Output resistance 50 ohms
Maximum peak current 5000 Amperes
Maximum rms current 65 Amperes
Low frequency 3dB cut-off 1 Hz (approximate)
High frequency 3dB cut-off 20 MHz (approximate)
Output connector BNC (UG-290A/U)
Operating temperature 0 to 65oC

Table C. 4 Key Features &amp; Specifications of FCC-LISN-50-50-4

<b>Functionality</b>
Maximum frequency (MHz):0.15-30MHz
Network inductance: 50ohm/50μH
Maximum current: 50A
Standard maximum voltage: 240V

## D Pictures of laboratory test setup

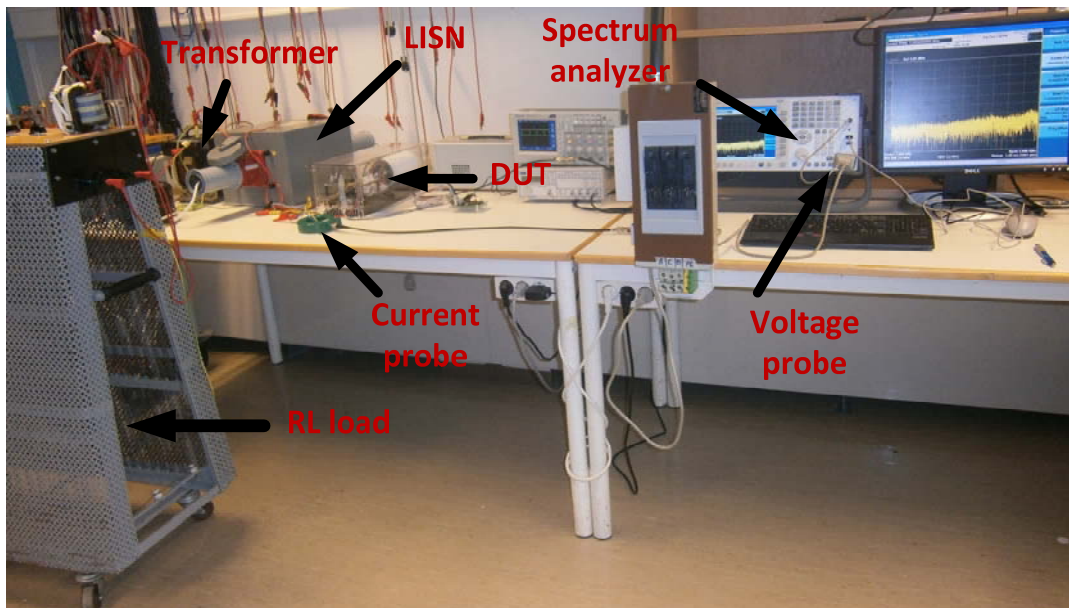


Figure D.1 EMI measurement laboratory setup for the chopper test circuit

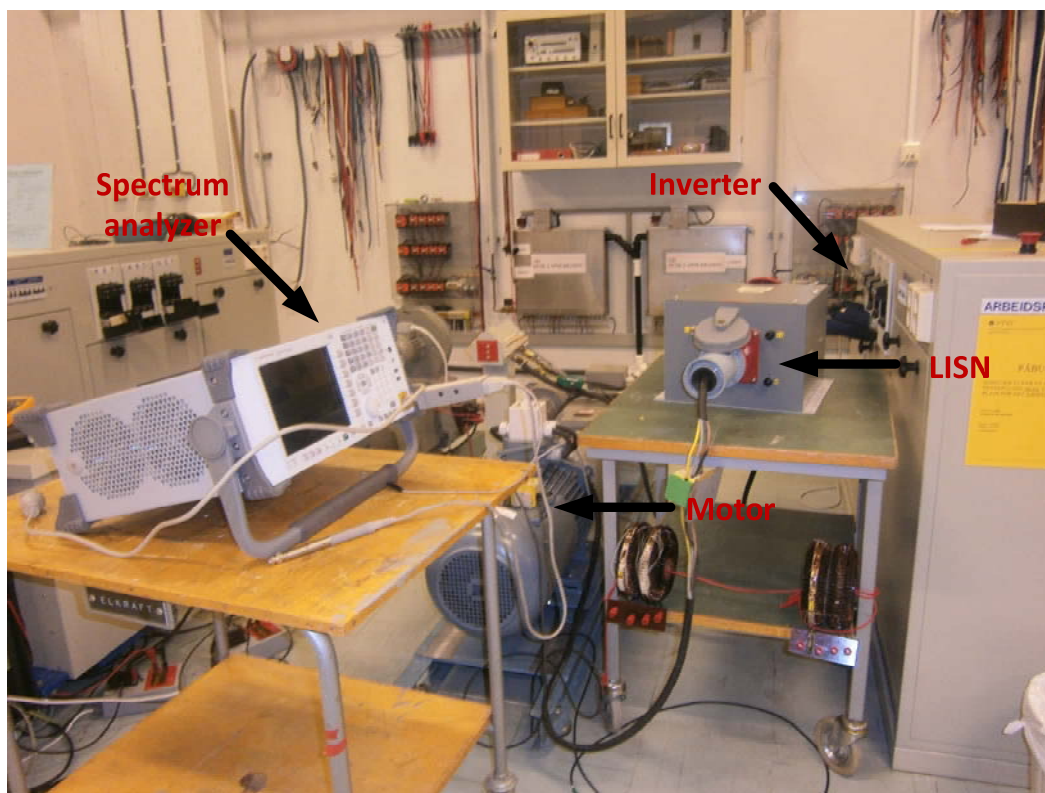


Figure D.2 EMI measurement lab setup when LISN filter between the inverter & motor terminal

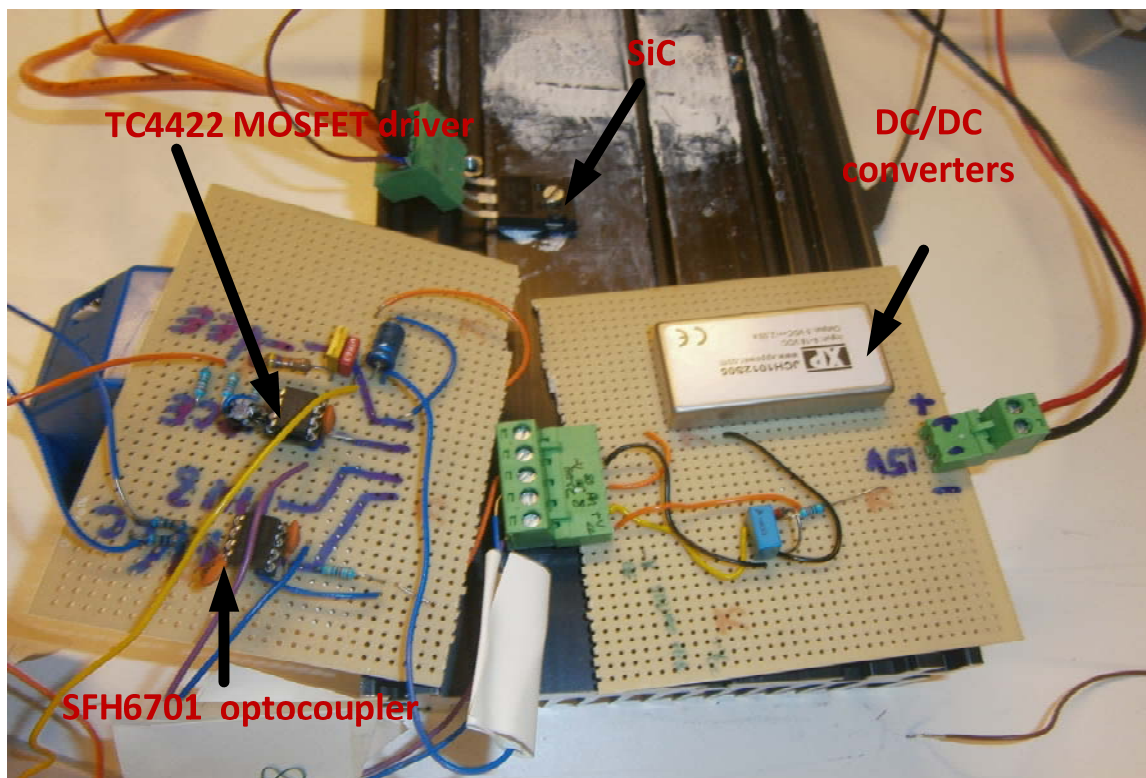


Figure D.3 SiC test drive circuit